Dissertation
submitted to the
Combined Faculties for the Natural Sciences and for Mathematics
of the Ruperto-Carola University of Heidelberg, Germany
for the degree of
Doctor of Natural Sciences

presented by

Diplom-Biotechnologin Anja Schillert
born in: Aschersleben / Germany
Oral-examination: 24.09.2012

Identification and functional analysis of slowly cycling cells in colorectal cancer

Referees: Prof. Dr. Andreas Trumpp

Prof Dr. Petra Boukamp

1. Table of Contents

2. Summary

Colorectal cancer is the third most common visceral malignancy and remains one of the leading causes of cancer-related deaths due to late diagnosis and therapy resistance. Even many years after initially successful treatment, the disease recurs in many patients and frequently spreads to distant organs. It is currently hypothesized that relapse may at least partially, be caused by a small population of dormant- or slowly cycling tumor cells. Presumably these cells are more resistant to the effects of DNA-damaging agents such as chemotherapy and irradiation than cycling cells. Such dormant cells have already been identified in the stem cell compartments of many tissues of the body, for instance in the skin, the hematopoietic system and the intestine. In parallel, it has been proposed that tumors arise from cancer stem cells, which might share common features with normal tissue stem cells, such as the ability to remain dormant. However, there is so far very little experimental evidence for the existence of dormant- or slow-cycling cells in cancer.

In order to study the occurrence of dormancy in colorectal cancer, primary tumor models were used. Primary colorectal cancer cell lines were labeled with a tetracycline-inducible H2B-GFP reporter that enables the detection and *in vivo* isolation of label-retaining cells.

Slowly cycling cells were identified *in vitro* and *in vivo.* Cell cycle analyses demonstrated a correlation between label-retention and cell cycle activation, suggesting the presence of quiescent tumor cells. The properties and hierarchical relation of label-retaining and non-label retaining cells were compared. Sorting into fast-, medium- and slowly cycling cell populations and subsequent tracing demonstrated that the initial phenotypes were preserved over several days *in vitro*. However, all three populations were capable of generating label-retaining cells as well as fast cycling cells, suggesting a dynamic switch between the different proliferative phenotypes. Furthermore, slowly cycling cells showed an enhanced resistance to standard chemotherapy.

These findings suggest that label-retaining cells exist within at least some colorectal tumors and that they can switch from a dormant to an active proliferative state, suggesting a possible role in tumor-recurrence after therapy.

3. Zusammenfassung

Darmkrebs ist eine der häufigsten krebsbedingten Todesursachen in der westlichen Welt, verursacht durch eine oftmals verspätete Erstdiagnose und Entwicklung von Resistenzen gegenüber Standardtherapien. In einigen Fällen sind Spätrezidive bekannt, bei denen Tumorzellen bereits in verschiedene Organe des Körpers disseminiert sind. Diese Rezidive werden möglicherweise von einer kleinen Tumorzellpopulation verursacht, die sich in einem so genannten Ruhezustand befindet oder sich nur langsam teilt. Diese Zellen sind vermutlich resistenter gegenüber DNA-schädigenden Therapien, wie der Chemotherapie oder Bestrahlung. Ruhende Zellen wurden bereits in verschiedenen Geweben des Körpers identifiziert, wie zum Beispiel in der Haut, im hämatopoetischen System und im Darm. Es wurde gezeigt, dass diese ruhenden Zellen Behandlungen mit Bestrahlung besser überleben und zerstörte Gewebe wiederherstellen können. Es wird ferner spekuliert, dass Tumore aus Krebsstammzellen entstehen können, die gemeinsame Eigenschaften mit normalen Stammzellen teilen. Dazu gehört die Fähigkeit zur Selbsterneuerung sowie Differenzierung und die Möglichkeit in einem Ruhezustand zu verharren. Um ruhende Tumorzellen im Darmkrebs zu untersuchen wurden geeignete Tumormodelle generiert. Primäre Darmkrebszelllinien wurden mit einem Tetrazyklin-induzierbaren H2B-GFP-Reporter markiert, welcher die Detektion und *in vivo* Isolation von sich langsam teilenden- oder ruhenden Tumorzellen ermöglicht. Ruhende Tumorzellen behalten diese Markierung, während sich schnell teilende Zellen diese mit zunehmenden Zellteilungen verlieren. Sich langsam teilende Tumorzellen wurden *in vitro* und *in vivo* identifiziert. Zellzyklusanalysen zeigten, dass eine Beibehaltung der H2B-GFP Markierung mit der Zellzyklusaktivität und einer möglichen ruhenden Tumorzellpopulation korreliert. Die Tumorzellen wurden in drei Populationen eingeteilt: schnell-, mittel- und langsam proliferierende Zellen. Die verschiedenen Zellpopulationen wurden mittels eines Durchflusszytometers separiert, um funktionelle Unterschiede der Populationen zu analysieren. Der ursprüngliche Phänotyp der Tumorzellen blieb über mehrere Tage *in vitro* erhalten. Interessanterweise waren alle drei Populationen dazu in der Lage wieder schnell proliferierende- und auch langsam proliferierende Zellen zu generieren, was auf einen dynamischen Prozess zwischen den verschiedenen Phänotypen schließen lässt. Des Weiteren zeigen die langsam teilenden Tumorzellen eine erhöhte Resistenz gegenüber einer Standardchemotherapie des Kolonkarzinoms. Diese Ergebnisse deuten darauf hin, dass ruhende Tumorzellen in einen aktiv

proliferierenden Zustand wechseln können und damit möglicherweise eine Rolle bei der Rezidivbildung nach der Therapie spielen.

4. Introduction

4.1. Cancer: a global disease

Cancer is the leading cause of death in economically developed countries (WHO, 2004). The global burden of cancer continuously increases due to growth of the world population, aging and an increasing change of lifestyle that favors cancer development. This includes smoking, physical inactivity and specific diets. About 12.7 million cancer cases (Fig. 1) and 7.6 million cancer deaths are estimated to have occurred worldwide in 2008. Of these, more than half of the deaths occurred in the economically developing world (Ferlay et al., 2011; Jemal et al., 2011).

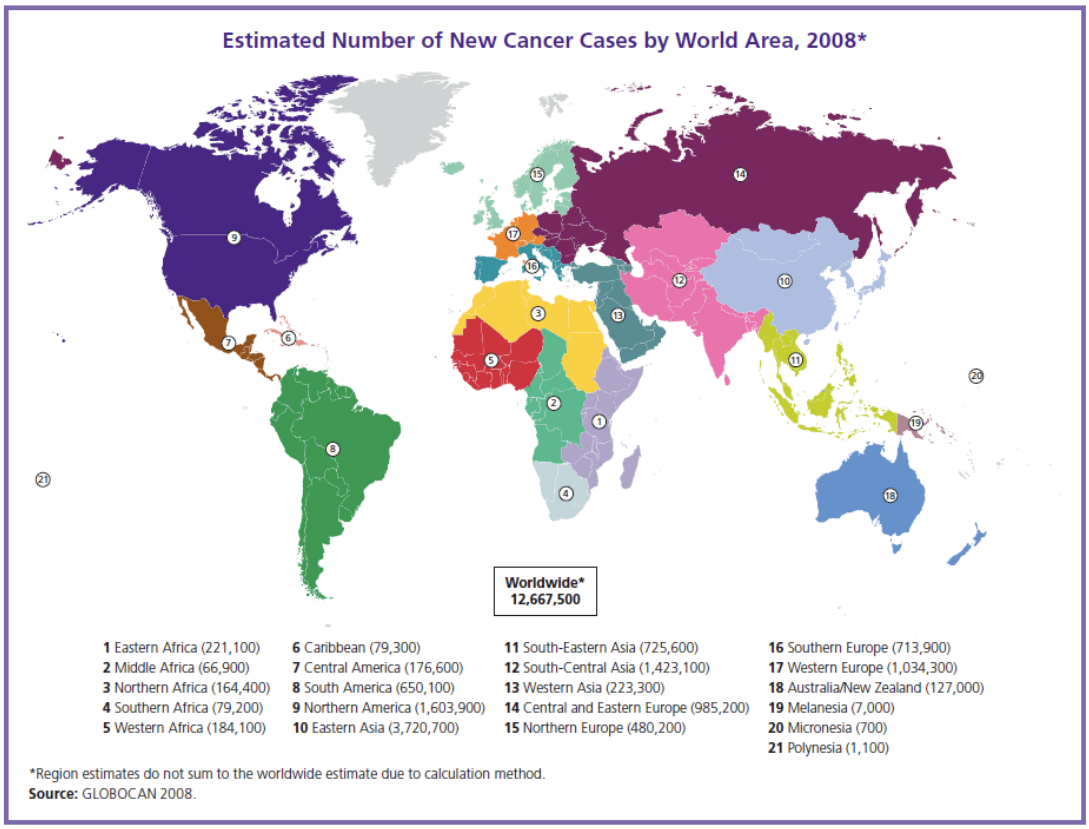

Fig. 1: Estimated number of new cancer cases by World Area. *(adapted from American Cancer Society. Global Cancer Facts & Figures 2nd Edition. Atlanta: American Cancer Society; 2011)*

Even though cancer is an increasing global health problem, the disease is still poorly understood. One major reason is the enormous complexity of the neoplastic disease. Cancer has been described as a multistep disease where normal cells acquire certain functional capabilities, also referred to as “hallmarks” that enable the cells to become tumorigenic and finally malignant (Fig.2) (Hanahan and Weinberg, 2000). Hanahan and Weinberg proposed six hallmarks of cancer that describe an organizing principle in order to better understand the complexity of the disease.

These hallmarks include sustaining proliferative signaling, evading growth suppressors, activating invasion and metastasis, enabling replicative immortality, inducing angiogenesis and resisting cell death (Hanahan and Weinberg, 2000). New insights into the development of cancer have been gained since then and the hallmarks of cancer have been extended and revised (Fig. 2). Genomic instability and tumor-promoting inflammation have been added as enabling characteristics of tumor cells. Moreover, two additional emerging hallmarks, such as reprogramming of cellular energy metabolism and the evasion of cancer cells from the attack and elimination by immune cells have been suggested to play an important role in tumor development and progression (Hanahan and Weinberg, 2011).

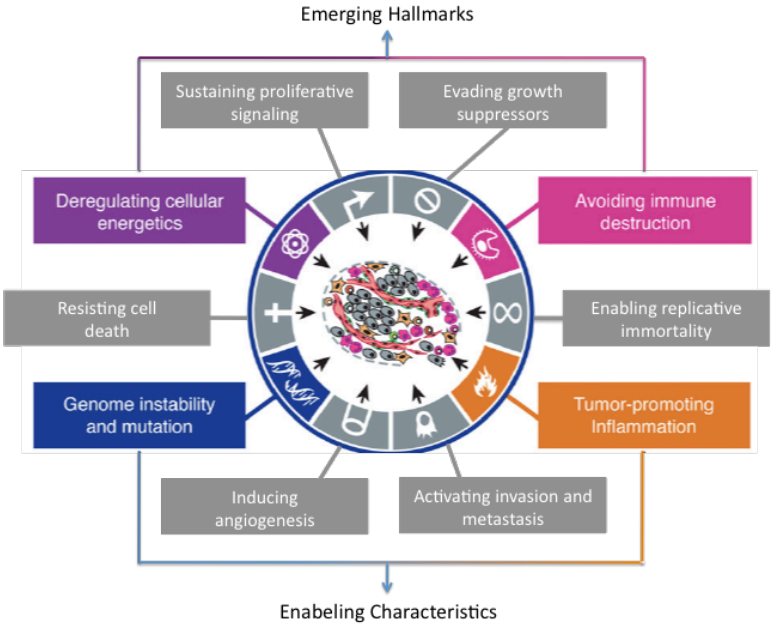

Fig. 2: The hallmarks of cancer - revised and extended version. The six hallmarks of cancer proposed by Hanahan and Weinberg are depicted in grey. These hallmarks have been extended including emerging and enabling characteristics of cancer cells (depicted in color). Some, or possibly all, tumor cells are able to deregulate the cellular energy metabolism in order to support cell growth and proliferation. Moreover, the cancer cells are able to evade the immune system. Genomic instability enables the acquisition of mutations that favor tumor progression and development. Additionally, inflammation and thus immune cells can promote tumor progression. *Modified and adapted from Hanahan and Weinberg (Hanahan and Weinberg, 2000, 2011).*

Tumors can be considered as complex tissues containing several different cell types that interact with each other in a specific “tumor microenvironment” (Hanahan and Weinberg, 2011). The cancer cells need to acquire a certain amount of the described hallmarks to become tumorigenic. A few of these hallmarks will be discussed in the next chapters in the context of colorectal cancer.

4.2. Colorectal cancer, mutations and genomic instability

Colorectal cancer (CRC) is the second most commonly diagnosed cancer in females and the third in males. In 2008, over 1.2 million new CRC cases and 608700 deaths were estimated to have occurred worldwide (Jemal et al., 2011). The incidence of CRC increases with age or in individuals that harbor a genetic predisposition. These inherited predispositions can cause familial adenomatous polyposis (FAP) or hereditary nonpolyposis colorectal cancer (HNPCC, also referred to as Lynch syndrome) (see chapter 4.3.). However the majority of CRCs arise from somatic mutations that accumulate over time.

During the last decades there has been significant progress in investigating specific genetic defects in CRC. A model of successive accumulations of genetic changes proposed by Fearon and Vogelstein has long been regarded as the paradigm for the development of colorectal cancer (Fearon and Vogelstein, 1990). The authors have shown that the progression from aberrant crypt foci (ACF) to malignant carcinoma is a multistep process and requires at least seven genetic events for completion (Fig. 3). The molecular defects, resulting in CRC are either alterations that lead to novel or increased functions of oncogenes or loss of function of tumor-suppressor genes (Fearon, 2011). The most common oncogenes or tumor-suppressor genes that are mutated in CRC are adenopolyposis coli (*APC*), *KRAS*, *TP53* and SMAD family member 4 (*SMAD4*) (Fearon and Vogelstein, 1990).

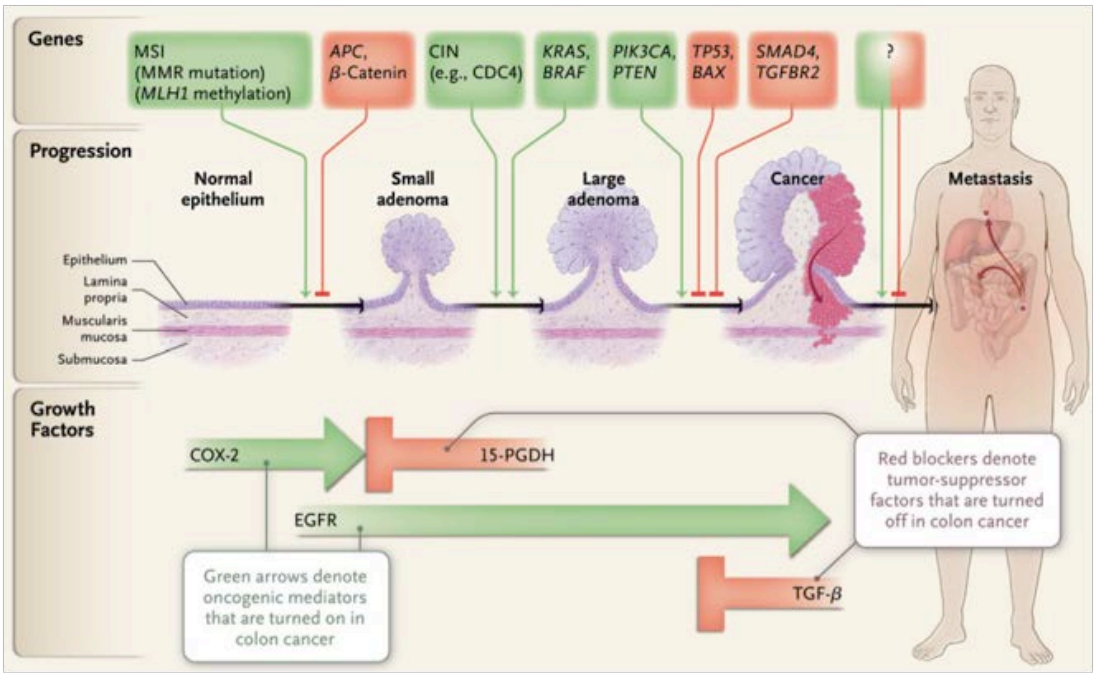

Fig. 3: Genetic changes and growth factors associated with colorectal tumorigenesis. At the top of the diagram are the genes depicted that are altered during CRC progression. APC mutations initiate the tumor formation. The progression to malignant CRC results from mutations in other genes indicated in the scheme. Moreover, microsatellite instability (MSI) and mutations in the Mismatch Repair genes (MMR) accelerate the cancer development. Genetic- or epigenetic changes that might be involved in metastasis still need to be identified. Growth-factor pathways that are mainly altered during CRC progression are depicted at the bottom of the scheme. *Adapted from Markowitz and Bertagnolli (Markowitz and Bertagnolli, 2009).*

Furthermore, aberrant DNA-methylation and chromatin-structure changes, together with mutational changes orchestrate a deregulation of signaling pathways that are involved in proliferation, cellular metabolism, differentiation and survival (Fearon, 2011). At least four types of genomic or epigenetic instabilities can be found in CRC: chromosomal instability (CIN), microsatellite instability (MSI), CpG island methylator phenotype (CIMP) and global DNA hypomethylation (Pritchard and Grady, 2011).

CIN is the most common form of genomic instability that can be found in 85% of CRCs (Grady and Carethers, 2008; Lengauer et al., 1998). CIN causes various changes in chromosomal copy number and structure that can be recognized by the presence of aneuploidy (Lengauer et al., 1998; Miyazaki et al., 1999; Walther et al., 2008). Moreover, there is some evidence from large meta-analysis that CIN is a marker of poor prognosis in CRCs (Popat and Houlston, 2005; Walther et al., 2008).

MSI is defined as insertion or deletion of repeating units in a microsatellite within a tumor that lead to a change of length in comparison to normal tissue (Boland et al., 1998). Patients with MSI have been shown to have a better prognosis in comparison to patients with CIN tumors (Popat et al., 2005; Walther et al., 2008). The mechanisms underlying MSI are well understood. The presence of MSI was

associated with loss of function of the DNA mismatch repair system (MMR), which was first investigated in bacteria and yeast (Boland et al., 2008; Fishel and Kolodner, 1995). MSI occurs in 15-20% of sporadic CRCs whereas 95% of patients with Lynch syndrome display MSI (Grady and Carethers, 2008).

The clinical relevance of CIMP and global DNA hypomethylation is not yet clear. CIMP is defined as hypermethylation of gene promoters that contain CpG islands and is associated with *BRAF V600E* mutations (Barault et al., 2008; Weisenberger et al., 2006). Furthermore, a global decrease in methylation has been identified in many CRCs (Matsuzaki et al., 2005; Rodriguez et al., 2006).

4.3. Hereditary Colorectal Cancer

Approximately 15-25% of CRCs have been estimated to occur in dominantly inherited patterns including first- to third degree relatives (Cannon-Albright et al., 1988; Kerber et al., 2005; Taylor et al., 2010). Two major hereditary diseases that can cause CRC are well studied: Familial Adenomatous Polyposis (FAP) and Hereditary Nonpolyposis Colorectal Cancer (HNPCC, also referred to as Lynch syndrome).

The mechanisms responsible for the development of HNPCC are different from FAP. The defect in HNPCC mainly affects tumor progression via germline defects in MMR genes such as *MLH1* and *MSH2* (Bronner et al., 1994; Fishel et al., 1993). Patients with HNPCC have a lifetime risk of about 80% to develop colorectal cancer on average by the age of 45 years while the average age for the onset of sporadic CRC is 65 years (Hampel et al., 2005; Lynch et al., 2008). The loss of MMR genes in patients with HNPCC is not only due to germline mutations but also to somatic inactivation of the wild-type (wt) parental allele (Boland et al., 2008). This MMR deficiency causes genomic instability and therefore highly increases the development of CRC in HNPCC-patients. Mutation rates in tumor cells with MMR deficiency are two to three orders of magnitude higher than in normal cells (Bhattacharyya et al., 1994; Eshleman et al., 1995; Shibata et al., 1994). The impaired MMR function is associated with MSI leading to mutations at the nucleotide level with changes in repeat length or minor changes of typically two base pairs (Ionov et al., 1993; Thibodeau et al., 1993). HNPCC accounts for 2 to 4% of the total CRC cases in the western world (Lynch et al., 1996). Another 13% of the total CRCs account for microsatellite instability in sporadic tumors (Aaltonen et al., 1993; Ionov et al., 1993; Thibodeau et al., 1993).

FAP is an autosomal, dominantly inherited disease that is caused by germline mutations in the *APC* gene. The *APC* gene is regarded as the „gatekeeper“ for colorectal tumor initiation (Kinzler and Vogelstein, 1996). This gene is located on chromosome 5q21 and consists of 15 exons (Nakamura, 1993). Patients with FAP develop hundreds to thousands benign colorectal tumors during their second or third decades of life. Even though these tumors are benign, the likelihood that some of these tumors will develop into malignant carcinomas is very high due to a genetic predisposition (Kinzler and Vogelstein, 1996). However, additional mutations are required for the progression of the disease (Fig. 3).

Since germline mutations of the *APC* gene have been discovered to cause FAP, several studies reported that somatic mutations of the same gene occur in more than 80% of sporadic (non-familial) colorectal cancers (Miyoshi et al., 1992; Powell et al., 1992; Smith et al., 1993). This shows that the *APC* gene is a key player in CRC initiation.

4.4. Functions of key molecules involved in CRC development

APC and canonical Wnt signaling

APC is a tumor-suppressor gene, which was identified by positional cloning of the FAP locus (Groden et al., 1991; Kinzler et al., 1991). Subsequently, sporadic colorectal tumors were analyzed and have been found to display mutations in both alleles of the *APC* gene (Nagase and Nakamura, 1993). Mutations in the *APC* gene are the earliest genetic alterations in the process of colorectal tumor development and have been identified in very early stages of neoplasia (Jen et al., 1994; Kinzler and Vogelstein, 1996; Smith et al., 1994a; Vogelstein et al., 1988). *APC* encodes for a multifunctional 312 kDa protein that may be involved in the regulation of cell-cell adhesion, cell migration, chromosomal segregation and apoptosis (Aoki and Taketo, 2007; Fodde et al., 2001; Polakis, 2007). These are all important cellular processes that may lead to cancer development but the major role of APC seems to be the proper interaction and regulation of intracellular ß-catenin, which is a key molecule in the canonical Wnt signaling pathway (Korinek et al., 1997; Morin et al., 1997; Munemitsu et al., 1995; Smits et al., 1999). Even though the vast majority of CRC patients carry *APC* mutations, those with an active *APC* gene display activating mutations in ß-catenin that alter the important phosphorylation sites and protect the protein from APC-mediated degradation (Morin et al., 1997; Sparks et al., 1998). Therefore it seems that the canonical Wnt signaling pathway plays an important role in cancer development. More evidence is provided by the fact that additional

members of the Wnt pathway can be mutated in rare cases of CRC, such as TCF-4 and axin (Duval et al., 2000; Liu et al., 2000).

In the absence of Wnt ligands, ß-catenin is recruited to the destruction complex that contains APC, axin/conductin and glycogen synthase kinase 3ß (GSK3ß) (Behrens et al., 1998; Fagotto et al., 1999; Hart et al., 1998; Kishida et al., 1999). Following N-terminal phosphorylation of ß-catenin via GSK3ß and casein kinase 1α (CK1α) (Ikeda et al., 2000), ß-catenin is targeted for ubiquitylation by an SCF-complex that contains the f-box protein ßTrCP and is proteosomally degraded (Jiang and Struhl, 1998; Marikawa and Elinson, 1998), leading to low cytoplasmic levels of ß-catenin. Moreover, the co-repressor Groucho is recruited to the LEF (lymphoid enhancer factor)-TCF (T-cell factor) transcription factors (TFs) in order to repress Wnt signaling (Cavallo et al., 1998; Roose et al., 1998) (Fig. 4a).

In the presence of Wnt ligands, Frizzled receptors are activated and form a complex with low-density lipoprotein-related receptor protein 5 and 6 (LRP5 and LRP6). The LRP5-LRP6 complex is phosphorylated by GSK3ß and CK1α. Dishevelled (DVL) proteins are recruited to the plasma membrane to interact with the intracellular domain of Frizzled receptors (Bilic et al., 2007; Schwarz-Romond et al., 2007). The phosphorylated LRP5 or LRP6 molecule and Dishevelled interact with axin and lead to the inactivation of the destruction complex and subsequent stabilization of ß-catenin. The exact mechanisms for inactivation of the destruction complex are not yet completely understood. Finally, ß-catenin translocates to the nucleus where it forms a transcriptionally active complex with LEF and TCF TFs by displacing Grouchos and interaction with co-activators (Fig. 4b) (Behrens et al., 1996; Huber et al., 1996; Molenaar et al., 1996), such as BCL9 (Kramps et al., 2002), Pygopus (Belenkaya et al., 2002), CREB-binding protein (CBP) (Hecht et al., 2000) or Hyrax (Mosimann et al., 2006).

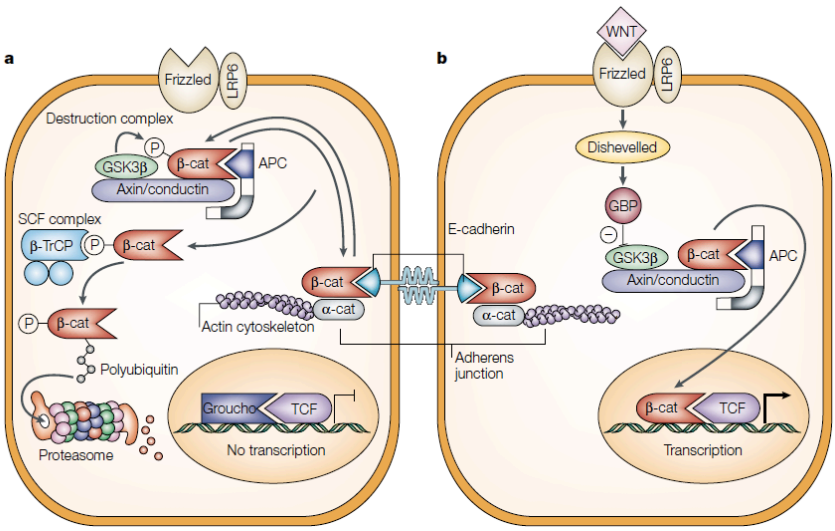

Fig. 4: The role of APC in canonical Wnt signaling. a) In the absence of Wnt ligands, ß-catenin is recruited to the destruction complex and phosphorylated at the amino-terminus via GSK3ß. The phosphorylated ß-catenin is targeted for proteasome-dependent degradation that involves an interaction with ß-TrCP (ß-transducin repeat-containing protein). Cytoplasmic ß-catenin levels are low and LEF and TCF that are located in the nucleus interact with Grouchos in order to repress transcription of Wnt-specific target genes. b) In the presence of Wnt ligands, LRP6 is phosphorylated via GSK3ß and forms a complex with Frizzled. Dishevelled is recruited to the plasma membrane where it interacts with Frizzled receptors. This leads to an inactiavation of the destruction complex and ß-catenin is stabilized. The stabilized ß-catenin translocates to the nucleus where it binds to LEF and TCF and acts as a co-activator for the transcription of Wnt target genes. *Adapted from Fodde (Fodde et al., 2001).*

Taken together, the Wnt signaling pathway is deregulated in the majority of CRCs. Important downstream targets of the APC/ß-catenin pathway are *c-Myc* and *cyclin D1 (CCND1)* that are relevant in tumor formation, due to their role in proliferation, apoptosis and cell cycle progression (He et al., 1998; Shtutman et al., 1999; Tetsu and McCormick, 1999). Furthermore, Wnt target genes such as *metalloproteinase matrilysin* (*MMP-7*) (Brabletz et al., 1999; Crawford et al., 1999), *CD44* (Wielenga et al., 1999) and *urokinase-type plasminogen activator receptor* (*uPAR*) (Mann et al., 1999) seem to be involved in tumor progression. However, not all CRC tumors that harbor *APC* mutations contain active Wnt signaling. Immunohistochemistry studies showed that nuclear ß-catenin expression is heterogeneously distributed among CRC cells (Brabletz et al., 2001). This phenomenon is also referred to as ß-catenin paradox, indicating that different subsets of tumor cells exist with different tumorigenic capacities (Fodde and Brabletz, 2007; Vermeulen et al., 2008a). Furthermore, Vermeulen and colleagues provide some evidence that Wnt signaling activity in CRC is partially regulated by the microenvironment (Vermeulen et al., 2010).

Impact of *APC*-mutations

APC encodes for a multi-domain protein that consists of 2843 amino acids. The protein contains numerous protein binding sites, including microtubules (Munemitsu et al., 1994; Smith et al., 1994b), ß-catenin and axin (Rubinfeld et al., 1993; Su et al., 1993), cytoskeleton regulators EB1 and dDlg (human homolog of the Drosophila Disc large tumor suppressor gene) (Matsumine et al., 1996; Su et al., 1995), and the Rac guanine-nucleotide-exchange factor (GEF) Asef1 (Kawasaki et al., 2003; Kawasaki et al., 2000) (Fig. 5a).

The most common identified *APC* mutations are frameshift, nonsense or splice-site mutations, which result in truncations of the APC protein (Kinzler and Vogelstein, 1996; Klaus and Birchmeier, 2008; Polakis, 2000). In FAP patients and in sporadic cancers virtually all mutations lead to C-terminally truncated proteins (Miyoshi et al., 1992; Nagase and Nakamura, 1993; Powell et al., 1992).

Germline mutations are scattered throughout the 5′ half of the gene, with two hot spot codons identified at positions 1061 and 1309 (Fig. 5b). However, patients harboring germline mutations in the *APC* gene do not necessarily develop CRCs, as additional genetic alterations of the wt allele inherited from the unaffected parent are required (Ichii et al., 1992; Kinzler and Vogelstein, 1996; Levy et al., 1994; Luongo et al., 1994). In contrast to germline mutations, 60% of the somatic mutations are concentrated in a mutation cluster region (MCR), with two hot spots occurring at the codon positions 1309 and 1450 (Fig. 5c) (Beroud and Soussi, 1996). This MCR is located in the central third of the protein among several independent 20 amino acid repeats, which are involved in ß-catenin binding (Fig. 5). In contrast to the *APC* mouse model, where all the 20-amino acid repeats are truncated and ß-catenin degradation is completely inactivated (Smits et al., 2000), in most CRC patients one or two of these repeats are retained (Albuquerque et al., 2002). Recent studies have shown that there is an active selection process for tumors that still maintain 20-amino acid repeats. The genotypes still providing a specific level of downregulation activation of ß-catenin signaling have a selection advantage over tumor cells that completely lost this regulatory function. This selection process is termed as the “just right signaling model” (Albuquerque et al., 2002). Additionally Kim and colleagues could show that excessive ß-catenin accumulation in the nucleus leads to programmed cell death (Kim et al., 2000). Thus tumors that retain their ß-catenin downregulation activity to some degree have an advantage in tumor formation.

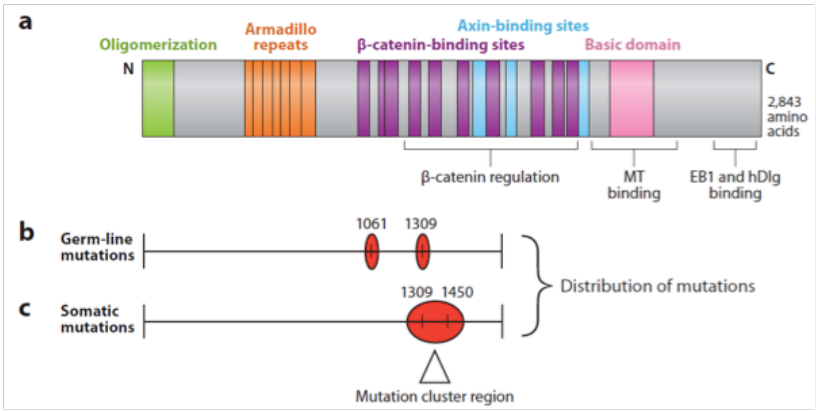

Fig. 5: Schematic representation of the APC protein and its mutation sites. a) The APC protein consists of 2843 amino acids and contains several protein binding sites. The N-terminal region regulates APC oligomerization (green). In the first third of the amino-terminus are the Armadillo repeats located (orange). In the central third of the APC protein, several independent 20 amino acid repeats that are involved in ß-catenin binding can be found (violet). Furthermore numerous SAMP repeats, that are binding sites for the axin protein, are located among the ß-catenin binding sites (blue). The C-terminal part of the protein contains a microtubule (MT) binding site (pink) and a region involved in the binding of EB1 and hDlg. Schematic representation of hot spot codons that are frequently mutated in b) the germline or c) sporadic. *Adapted from Fearon (Fearon, 2011).*

Moreover, truncations in the APC protein have been shown to have a major impact on Wnt signaling (see chapter 4.4.). However, these are not the only effects. Furthermore, these truncating mutations play an important role in chromosome segregation and can contribute to CIN, which has been reported to occur for the majority of CRCs (see chapter 4.2.). It has been shown that APC localizes to kinetochores, spindles and centrosomes during mitosis, where it contributes to the regulation of the cytoskeleton function and to the stabilization of the microtubules (Dikovskaya et al., 2004; Kaplan et al., 2001; Louie et al., 2004; Olmeda et al., 2003). Thus the impact of APC truncating mutations on Wnt signaling and chromosome segregation is of major importance for tumor progression.

The role of KRAS on colorectal cancer development

Numerous oncogenes play important roles in the promotion of CRC progression (Fig. 3). Fearon and Vogelstein identified KRAS as being involved in the transition from small adenomas to larger more dysplastic ones (Fearon and Vogelstein, 1990). The RAS family of small-G-proteins comprises over 150 human members (Malumbres and Barbacid, 2003; Wennerberg et al., 2005). Somatic mutations in three of the various RAS familiy members namely HRAS, NRAS and KRAS have been frequently identified in many human cancers (Malumbres and Barbacid, 2003). In 40-50% of CRCs, point mutations in the coding sequence of *KRAS* are prevalent

(Bos et al., 1987; Forrester et al., 1987). The majority of these mutations occur in the codons 12 and 13 of the *KRAS* gene and the remaining mutations occur in codon 61. These common mutation sites are also referred to as “hotspot codons” (Bos et al., 1987; Smith et al., 2010). Furthermore, a few other less frequent apparent mutational sites have been identified at codons 19, 22 and 146 (Akagi et al., 2007; Miyakura et al., 2002; Orita et al., 1991; Smith et al., 2010).

Most of these mutations lead to constitutive activation of RAS signaling via impaired GTPase activity. GTPase-activating proteins (GAPs) are prevented from hydrolysis of GTP to GDP and therefore cause RAS to accumulate in the GTP-bound, active form (Downward, 2003). RAS proteins serve as signaling nodes that bind and activate numerous effector enzymes, which regulate cell proliferation, differentiation and survival (Shields et al., 2000; Wennerberg et al., 2005). RAF was the first identified mammalian effector (Leevers et al., 1994; Marais et al., 1995), which belongs to the family of serine/threonine kinases and exists in three forms: RAF-1, ARAF and BRAF (Daum et al., 1994). The KRAS protein signals through BRAF to activate the mitogen-activated protein kinase (MAPK) pathway and thus promotes cell growth and survival (Pritchard and Grady, 2011).

RAS can also activate additional effectors such as Phosphoinositide 3-kinases (PI3Ks), which in turn are involved in the activation of AKT/PKB (protein kinase B) and therefore contribute to cell survival (Brazil et al., 2004; Datta et al., 1999; Franke et al., 1995; Klippel et al., 1996). AKT regulates cell survival either directly by phosphorylating components of the apoptotic machinery or indirectly by altering the expression level of genes encoding for components of the cell survival pathway, such as Bad, caspase 9, the Forkhead family of transcription factors (FOXO) and inhibitor of nuclear factor kappa-B kinase-ß (IKK-ß) (Datta et al., 1999).

KRAS is a major downstream target of the epidermal growth factor receptor (EGFR = HER1 = ERBB-1), a transmembrane glycoprotein that belongs to the receptor tyrosine kinase family (RTKs). The EGFR dimerizes and is autophosphorylated upon ligand binding which results in the activation of a signaling cascade triggering many cellular processes such as proliferation, prevention of apoptosis, promotion of invasion, metastasis and neovascularization (Carpenter, 1987; Carpenter and Cohen, 1990; Hynes and Lane, 2005). In CRCs, this receptor is overexpressed in approximately 80% of the patients (Spano et al., 2005). The EGFR can be targeted either via monoclonal antibodies that are directed against the extracellular domain (e.g. cetuximab) of the receptor or via small molecules that act as tyrosine kinase (TK) inhibitors in a competitive manner (e.g. erlotinib and gefitinib) (Croce, 2008). The treatment response of patients is dependent on specific mutations in

oncogenes. *KRAS* is one of the most important predictors of resistance to targeted therapy because its mutation causes EGFR independent signaling (Uberall et al., 2008). It has been shown that CRC patients that harbor activating mutations in the *KRAS* gene did not benefit from therapy with EGFR-TK inhibitors (Lievre et al., 2008; Massarelli et al., 2007).

The complex functions of p53 in colorectal cancer

Loss of chromosome 17p has been found in approximately 75% of CRCs (Vogelstein, 1990). This region harbors the gene *TP53*, which encodes for p53. It has been shown that this chromosomal loss is often associated with the presence of missense mutations in the remaining *TP53* allele (Baker et al., 1989). *TP53* is mutated in 40-50% of all CRCs (Hollstein et al., 1991; Olivier et al., 2002; Vogelstein, 1990). P53 is a stress-response protein that acts as a tetrameric TF, regulating a large number of genes involved in cell cycle control, apoptosis, and senescence. Several other functions have been described such as regulations of DNA metabolism, angiogenesis, cellular differentiation and immune response (Vousden and Prives, 2009). The extend of the stress level that influences the tumor cells may trigger the decision between cell death or cell cycle arrest. Vousden and Prives suggested that low levels of DNA damage induce repair and survival responses whereas high levels of DNA damage that cannot be repaired subsequently lead to apoptosis or senescence (Vousden and Prives, 2009).

Germline mutations of *TP53* cause the Li-Fraumeni syndrome, a hereditary predisposition for various types of cancer (Li and Fraumeni, 1969a, b). Patients that harbor these germline mutations have an increased susceptibility to CRCs and develop the disease several decades earlier compared to the general population (Wong et al., 2006).

43% of all somatic *TP53* mutations in CRC occur mainly in five hotspot codons, such as 175, 245, 248, 273 and 282 (Greenblatt et al., 1994; Nigro et al., 1989; Soong et al., 2000). These codons are located in the conserved region of *TP53* that is important for the transcriptional activity of the protein (Fig. 6). Due to the mutations, the specific DNA binding capacity of p53 is abrogated, which results in a transition of large adenomas into invasive carcinomas (Baker et al., 1990; Vogelstein et al., 1988). Moreover, some mutations can also induce local or global conformational distortions (Brosh and Rotter, 2009).

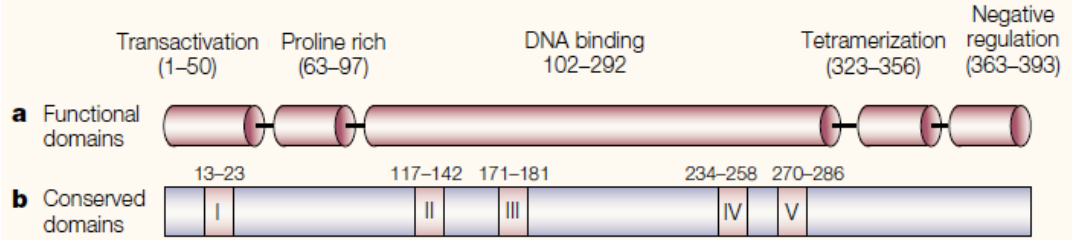

Fig. 6: Schematic representation of the p53 protein. a) Depicted are the functional domains of p53. b) The areas of the conserved sequences are shown in orange (I-V). *Adapted from Soussi and Beroud (Soussi and Beroud, 2001).*

However, it has been shown that mutations occurring in *TP53* are heterogeneous and may have different prognostic significance dependent on the ethnic group (Manne et al., 1998), site of tumor origin (Diez et al., 2000; Manne et al., 1998; Samowitz et al., 2002; Soong et al., 1997; Sun et al., 1996) and stage of the disease (Adrover et al., 1999; Ahnen et al., 1998; Soong et al., 1997). It became also evident that different *TP53* mutant forms exist harboring properties such as loss of the tumor suppressor function, dominant negative activity over the remaining wt-allele (Milner and Medcalf, 1991; Milner et al., 1991; Sigal and Rotter, 2000) and gain of new oncogenic properties (Blandino et al., 1999; Dittmer et al., 1993; Li et al., 1998; Wolf et al., 1984).

Smad4 and TGFß signaling

Smad4 is a tumor suppressor gene and belongs to the Smad family, which plays a major role in transforming growth factor-ß (TGFß) signaling. Eight Smads have been identified in mammals: receptor-regulated Smads (R-Smads: Smad 2 and 3 that mediate TGFß signaling and Smad 1, 5 and 8 that transduce BMP signaling), one co-mediator Smad (Co-Smad: Smad 4) and two inhibitory Smads (I-Smads: Smad 6 and 7) (Shi and Massague, 2003).

Smad4 was first identified in pancreatic cancer by Hahn and colleagues. Approximately 90% of pancreatic cancers show loss of herterozygosity (LOH) at chromosome 18q, in which the candidate tumor suppressor gene *Smad4* (also called *DPC4*, deleted in pancreatic carcinoma, locus 4) is located (Hahn et al., 1996). This LOH of chromosome 18q was also found in 70% of colorectal cancers, of which 50% were late stage adenomas and about 10% were early stage adenomas (Fearon and Vogelstein, 1990; Vogelstein et al., 1988). Two additional Smad family members, namely Smad2 and Smad7 are also located on chromosome 18q, suggesting that LOH of chromosome 18q promotes tumorigenesis at least partially via the TGFß pathway (Nakao et al., 1997; Pritchard and Grady, 2011; Roijer et al., 1998). This signaling pathway can be transduced in two different ways, either independent of

Smads or through Smads (Fig. 7). Both signaling pathways are mediated via TGFß ligands that bind to TGFß type 2 receptor (TGFßR2). The TGFßR2 forms a heterotetrameric receptor complex together with TGFß type 1 receptor (TGFßR1). This complex formation leads to the phosphorylation and activation of TGFßR1 (Annes et al., 2003; Feng and Derynck, 2005; Heldin et al., 1997; Shi and Massague, 2003; Wrana et al., 1994). The activated receptor complex can regulate non-Smad pathways, including extracellular signal-regulated kinase (ERK), p38 MAPK, JUN N-terminal kinase (JNK), PI3K-AKT and small GTPases, as well as Smad mediated pathways (Moustakas and Heldin, 2005; Zhang, 2009).

The Smad mediated pathway is transduced via recruitment of Smad2 and 3 to TGFß1R. The two activated R-Smads form a heteromeric complex with Smad4 and translocate to the nucleus (Shi and Massague, 2003). This complex binds directly to the DNA or indirectly through other DNA binding proteins and regulates the transcription of target genes involved the regulation of proliferation and invasion. TGFß signaling mediates many cellular processes in a context dependent manner (Ikushima and Miyazono, 2010a). The activated Smad pool is shared among many competing interaction partners such as co-activators or co-repressors, which in the end determine whether a target gene is activated or repressed (Chen et al., 2002; Feng et al., 1998; Ikushima and Miyazono, 2010a; Janknecht et al., 1998). Distinct repertoires of transcription partners of the Smad complex are expressed dependent on the cell type or the conditions the cells are exposed to (Ikushima and Miyazono, 2010a).

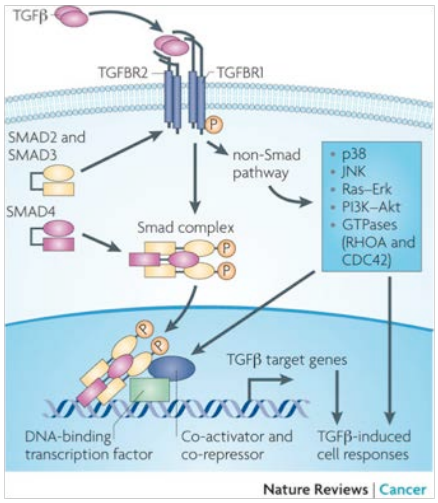

Fig. 7: Schematic representation of the TGFß signaling pathway. The TGFß signaling pathway is mediated upon ligand binding to the TGFßR2, which subsequently forms a complex with TGFßR1. This results in the phosphorylation of TGFßR1 that in turn recruits and phosphorylates Smad2 and 3. The activated R-Smads form a complex with Smad4 and translocate to the nucleus where they regulate the transcription of TGFß target genes in association with co-activators or co-repressors. The TGFß signaling pathway can be mediated in a Smad independent way as well. *Adapted from Ikushima and Miyazono (Ikushima and Miyazono, 2010b).*

Perturbations of the TGFß signaling pathway via mutations in proteins involved in the regulation of this pathway play a central role in tumorigenesis and tumor progression. Homozygous deletions and/or mutations were identified in colorectal cancer at frequencies from 10 to 35% (Koyama et al., 1999; MacGrogan et al., 1997; Takagi et al., 1996). Miyaki and colleagues showed that the frequency of *Smad4* mutations increases with tumor progression with the highest mutation frequency in patients that developed distal metastasis (Maitra et al., 2000; Miyaki et al., 1999). These *Smad4* gene mutations occur in more than 80% of the cases at the Mad homology 2 (MH2) region. This is one of the evolutionary conserved regions, which is responsible for heteromerization and transactivation function of the Smad proteins (Dai et al., 1998; Liu et al., 1996; Shi et al., 1997). This region also partially interferes with the DNA binding function of the Mad homology 1 (MH1) region (Dai et al., 1998; Hata et al., 1997; Kim et al., 1997; Zawel et al., 1998), the second conserved region in the Smad proteins. The mutations include frameshift, nonsense and missense mutations, with a hot spot missense mutation in codon 361. These mutations lead to a deregulation of several target genes that play critical roles in tumor progression and invasion.

All of the key molecules described in this chapter contribute to colorectal cancer development and progression via different mechanisms. Thereby the above named molecules functionally interact via cross-regulating activities with each other.

For instance, it has been reported that the Wnt- and the TGF-ß signaling pathway converge on p27, a tumor suppressor that acts as cell cycle inhibitor (Arends, 2000). The disrupted TGF-ß pathway and elevated c-Myc levels, resulting from mutations in Wnt signaling, cooperatively increase the proteasomal degradation of p27, which is associated with more aggressive CRCs (Kawada et al., 1997; Loda et al., 1997).

Genomic instability, inactivation of tumor-suppressor genes or activation of oncogene pathways can lead to sustained proliferation and evasion of apoptosis, which are crucial hallmarks of cancer (Fig. 2). These hallmarks are acquired by tumor cells in order to progress to a malignant disease as described by Hanahan and Weinberg (Hanahan and Weinberg, 2000, 2011). Furthermore, the tumor cells evolve and gain invasive and metastatic capabilities. This additional hallmark represents the last step in tumor progression and will be described in the next chapter.

4.5. Metastasis - a multi step process

Metastasis is a multi step process where tumor cells acquire certain abilities to overcome several barriers, as well as produce and respond to various growth factors and cytokines. As a first step, the tumor cells separate from the primary tumor and breach surrounding tissues and basement membranes, in order to access the circulation, the lymphatics or the peritoneal space. On their way to the secondary site, the tumor cells are exposed to numerous stresses, such as mechanical forces caused by the circulation and cell destruction mediated by the immune system (Chambers et al., 2001; Fidler, 1990; Mehlen and Puisieux, 2006; Weiss et al., 1992). This seeding process is followed by an extravasation into the foreign microenvironment of the target organ where the tumor cells proliferate and constitute a metastasis (Fig. 8) (Hunter et al., 2008; Welch, 2006). Every single step is rate-limiting for a tumor cell to develop into overt metastasis (Fidler, 2002; Poste and Fidler, 1980), which explains the low efficiency of the metastatic process overall (Weiss, 1990). Fidler and colleagues analyzed the metastatic ability of radioactively labeled tumor cells in the circulation of animal models. Their studies showed that less than 0.1% of tumor cells were still alive after 24 hours and less than 0.01% of these cells were able to develop into metastasis (Fidler, 1970), suggesting that not every tumor cells is able to successfully metastasize and that tumors are heterogeneous consistent of different subpopulations of cells with distinct biological characteristics .

Even though metastasis formation is such an inefficient process, it presents one of the most challenging problems in cancer patients. In order to tackle this problem, the underlying mechanisms of metastasis need to be uncovered. One important aspect is the time point of the metastatic spread to distant organs, which would bring new insights into treatment strategies and would help to predict responses to adjuvant therapies. Two fundamental models of metastasis are currently discussed in the field, namely the linear- and parallel-progression model, reviewed by Klein (Klein, 2009).

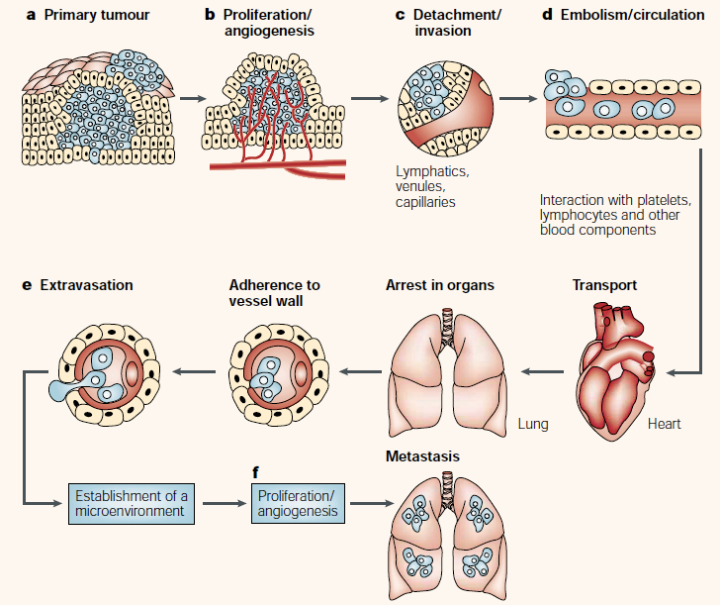

Fig. 8: Necessary steps for metastasis formation. a) Transformation of normal cells into tumor cells. b) Increasing tumor mass that needs to be vascularized in order to gain access to nutrition. Angiogenic factors are secreted to establish a capillary network. c) Tumor cells separate from the primary tumor and invade the surrounding host tissue and breach basement membranes d) to enter the vasculature, the lymphatics or the peritoneal cavity. In the circulation, tumor cells are exposed to the immune system of the host and they need to survive mechanical stresses. Tumor cells that survived in the circulation and reached the target organs e) need to extravasate and adapt to the new microenvironment. f) As the last step in order to grow successfully into an overt metastasis, the tumor cells need to proliferate and survive the host defense mechanisms. New vasculature needs to be formed to allow sufficient nutrition supply. *Adapted from Fidler (Fidler, 2003).*

4.6. The Linear- and parallel-progression model of metastasis

The linear progression model

The linear progression model supports the hypothesis that cells present in a primary tumor acquire multiple genetic and epigenetic alterations prior to dissemination (Klein, 2009). This indicates that tumor cell dissemination is a rather late event in tumor progression (Fig. 9). Furthermore, this model suggests that primary metastasis that have adapted to the new microenvironment have the potential to propagate a whole series of additional metastasis, a so called “metastatic shower” (Weinberg, 2008). These cells have already acquired all the genetic alterations needed to become a successful metastasis.

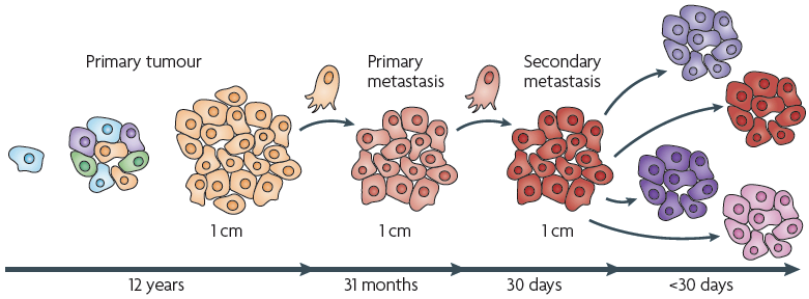

Fig. 9: The linear progression model. The primary tumor develops for several years and accumulates a set of genetic alterations prior to metastasis formation. The metastases are able to generate further metastatic foci. This model suggests that metastasis is a late event in tumor progression. *Adapted from Klein (Klein, 2009).*

These observations represent the basis for the international tumor, node, metastasis (TNM) classification system. This system associates larger tumors with higher frequencies of metastasis.

Moreover, the linear progression model is in line with the genetic model for colorectal cancer progression proposed by Fearon and colleagues (Fearon and Vogelstein, 1990) where specific genetic alterations are needed for the transition from hyperplasia to an invasive carcinoma. Jones and colleagues performed comparative lesion sequencing analysis, which allowed the direct comparison of different mutations within the late stage primary tumor and the metastasis from the same patient. The authors could show that it takes approximately 17 years for a large adenoma to develop into an advanced carcinoma but it takes less than two years for the generation of metastasis. Furthermore, Jones and colleagues identified only very few additional alterations in metastases in comparison to advanced carcinomas (Jones et al., 2008), indicating that metastasis formation is a late event in colorectal cancer development. A similar finding was reported for the progression of pancreatic cancer. Sequencing data of metastasis from pancreatic cancer patients revealed that the progression of the disease takes at least 15 years until the tumor cells have acquired their metastatic potential (Yachida et al., 2010), supporting the hypothesis that metastasis arise from clones disseminated at late stages during tumor progression.

The parallel progression model

In contrast to the linear progression model, the parallel progression model supports the idea that the process of metastasis is an early event in tumor progression. Tumor cells disseminate before the primary lesion reaches a fully malignant phenotype, leading to a divergent development of metastasis and primary tumor (Klein, 2009). Moreover, this model suggests that dissemination of tumor cells to distinct target organs can occur in parallel and that these cells adapt to the different features of the foreign microenvironment (Fig. 10). This might also be a selection process for tumors cells that are able to survive in distant organs (Scheel et al., 2007), implying that the different metastasis also harbor distinct alterations when compared to each other. Furthermore, the disseminated tumor cells may remain in a dormant state after their departure from the primary tumor until they have acquired all the alterations needed for a successful colonization at the distant site, explaining the fact these cells remain undetected at the time point of diagnosis.

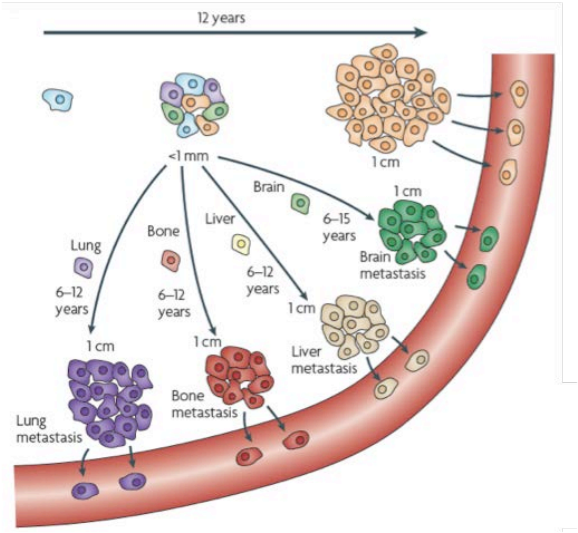

Fig. 10: The parallel progression model. Tumor cells disseminate from the primary tumor in early stages of tumor progression. These disseminating tumor cells depart in parallel from the primary tumor to different metastatic sites and adapt to the foreign microenvironment. The primary tumor and the metastasis develop divergent genetic alterations. *Adapted from Klein (Klein, 2009).*

Studies of various types of cancer provide some evidence for the parallel progression model. The fact that disseminated tumor cells were observed in the bone marrow of cancer patients even in the absence of lymph node metastasis or clinical signs of overt metastasis supports the model of an early dissemination (Braun et al., 2000; Husemann et al., 2008; Lindemann et al., 1992; Pantel et al., 1996). Furthermore, Klein and colleagues performed comparative genomic hybridization (CGH) of single disseminated tumor cells that were detected in the

bone marrow of breast cancer patients. The authors showed that there is genetic heterogeneity among these early-disseminated tumor cells (Klein et al., 2002). In addition, tumor cells present in the bone marrow and their matched primary tumors harbored very divergent genetic alterations (Schmidt-Kittler et al., 2003), indicating that the tumor cells have spread already early during tumor progression. However, it has never been shown yet whether the tumor cells detected in the bone marrow of cancer patients will ever develop into overt metastasis and are therefore functionally relevant. Even though some studies indicate that the existence of disseminated tumor cells in the bone marrow is associated with unfavorable prognosis (Braun et al., 2005; Slade and Coombes, 2007).

Both metastasis progression models may be valid and several studies provide evidence for each of the model systems. However, as tumors are very heterogeneous and every tumor type displays different genetic features, either of the two models may apply dependent on the tumor type.

4.7. Regulation of metastasis via the microenvironment

The “seed and soil” hypothesis proposed by Steven Paget opened a whole new field of research. The concept that malignant cells need a receptive microenvironment in order to engraft and to develop into overt metastasis in distant tissues has emerged. Paget suggested that certain organs were especially receptive to metastases, such as the liver in CRC or the lung in breast cancer (Paget, 1989). Since then, numerous studies have been performed and much more attention has been given to the interactions of tumor cells with their surrounding microenvironment. Tumors are considered as complex tissues consistent of many different cell types such as endothelial cells, stromal fibroblasts and various bone marrow-derived cells (BMDCs) (Fig. 11) (Joyce and Pollard, 2009). It has been proposed that a specific “invasive niche” may exist within the primary tumor. This invasive niche is composed of a dense accumulation of all these different cell types that form a complex signaling network, resulting in an enhanced invasive and metastatic capacity of the cancer cells. This complex network forms a so-called tumor microenvironment of metastasis (TMEM) (Robinson et al., 2009).

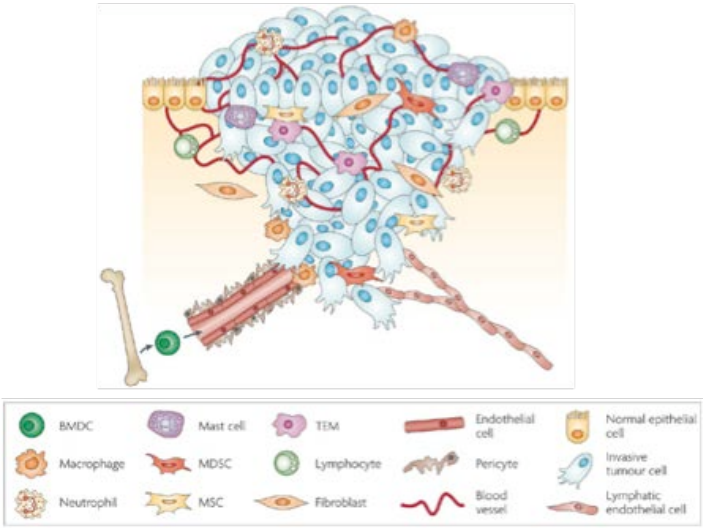

Fig. 11: A tumor is a complex tissue. Tumor cells form complex cellular networks with their surrounding microenvironment. The tumor microenvironment consists of various cell types, such as endothelial cells, stromal fibroblasts and bone marrow-derived cells, including macrophages, mesenchymal stem cells (MSCs), myeloid-derived suppressor cells (MDSCs) and TIE2-expressing monocytes (TEMs). *Adapted from Joyce and Pollard (Joyce and Pollard, 2009).*

Priming of the "foreign soil"

Recent studies provide some evidence that growth factors secreted by the primary tumor prime metastatic target tissues and thus facilitate the engraftment of the cancer cells (Hiratsuka et al., 2006; Hiratsuka et al., 2008; Kaplan et al., 2005). Subsequently, bone marrow-derived hematopoietic progenitor cells and macrophages are recruited to these tissues, creating a so-called "pre-metastatic niche" that is permissive for metastatic tumor cells (Hiratsuka et al., 2006; Kaplan et al., 2005). These bone marrow-derived cells (BMDCs) have been suggested to increase fibronectin deposition. Fibronectin is an important component of the extracellular matrix (ECM) and its accumulation facilitates the extravasation of metastatic tumor cells that interact with ECM components via cell adhesion molecules (Kaplan et al., 2005).

Chemoattractants in the "soil" pave the way for tumor cells

Tumor cells, pericytes, platelets and fibroblasts synthesize for instance stromal cell-derived factor 1 (SDF1). SDF1 is a chemokine that interacts with C-X-C chemokine receptor type 4- (CXCR4) expressing tumor cells and thus favors their interaction with the above mentioned cell types (Jin et al., 2006). Platelets for example express numerous pro- and anti-angiogenic factors (Massberg et al., 2006). Moreover, they form clots with circulating tumor cells in order to protect them against host-immune

cells, which in turn supports the invasive potential of the cancer cells (Samak and Israel, 1982). Furthermore, bone marrow stroma is a source of SDF1 and may influence the ability of cancer cells to home to the bone marrow. The bone marrow has been shown to provide a niche for disseminated breast cancer cells that express high levels of CXCR4 (Muller et al., 2001). In CRC, tumor cells often migrate to the liver and the lymph nodes. The liver and lymph endothelial cells express C-X-C motif chemokine 13 (CXCL13), which is the ligand for C-X-C chemokine receptor type 5 (CXCR5) that is expressed in many colorectal cancer cells. CXCL13 may act as potential chemoattractant and possibly directs tumor cells via the lymphatics to their target organs (Meijer et al., 2006). This would support the hypothesis that tumor cells have a specific tissue tropism and seed only to a specific “soil” that promotes their outgrowth.

However, the interactions of the microenvironment with tumor cells at secondary sites are less well studied than the interactions within the primary tumor.

The role of macrophages within the primary tumor

In the primary tumor, the recruited macrophages have been suggested to play a role in chronic inflammation, matrix remodeling, tumor cell invasion, intravasation and angiogenesis (Condeelis and Pollard, 2006). Tumor associated macrophages (TAMs) have been shown to secrete vascular endothelial cell growth factor A (VEGFA) and therefore favor metastasis by the promotion of angiogenesis (Barbera-Guillem et al., 2002). In addition, macrophages as well as primary tumors produce tumor necrosis factor α (TNFα). TNFα mediates an upregulation of adhesion molecules in endothelial cells, such as E-selectin, P-selectin and vascular cell adhesion protein 1 (VCAM1), which in turn promote tumor cell migration and extravasation (Mannel et al., 1994; Stoelcker et al., 1995).

Hafner and colleagues proposed that TNFα impairs natural killer (NK) cell activity and protects tumors cells from NK cell attacks (Hafner et al., 1996).

Several studies using mouse models demonstrated that macrophages mediate tumor growth. Mice deficient in macrophage function showed decreased levels of macrophage infiltration into the tumor surroundings, leading to an inhibition of tumor angiogenesis, metastasis and tumor growth (Hiraoka et al., 2008; Lin et al., 2006; Lin et al., 2001; Miselis et al., 2008; Zeisberger et al., 2006).

The role of fibroblasts within the primary tumor

Stromal fibroblasts present in the primary tumor are referred to as carcinoma-associated fibroblasts (CAFs) or myofibroblasts. These fibroblasts constitute a source of matrix metalloproteinases (MMPs) that degrade matrix components and thereby support tumor cell invasion into the surrounding tissue (Afzal et al., 1998; Noel et al., 1998). Rabinovitz and colleagues showed that laminin-1 is released upon MMP degradation of the ECM and subsequently promotes cell migration of integrin α6ß4 expressing colorectal tumor cells (Rabinovitz and Mercurio, 1997).
Additionally, Vermeulen et al. suggest that myofibroblasts located at the invasive front of the tumor, maintain high Wnt activity in putative colorectal cancer stem cells (CSCs) via hepatocyte growth factor (HGF) production (CSCs see chapter 4.10.1). These myofibroblasts are able to activate Wnt signaling in more differentiated tumor cells and thereby restore their tumorigenic capabilities (Vermeulen et al., 2010).

Taken together, it is clear that various cell types play a role in both, the primary tumor and the metastatic sites. This complex network of diverse cellular interactions poses a big challenge for cancer treatment but also opens many new avenues for the development of novel therapeutics.

4.8. Current treatment methods of metastatic colorectal cancer

Colorectal cancer is still one of the leading causes of cancer-related death (Jemal et al., 2011), even though the death rates have been decreasing in the Western countries due to improved treatment and a frequent use of early detection methods (Chu et al., 1994; Edwards et al., 2010; Mitry et al., 2002; Sant et al., 2001). The major cause of death is the development of metastasis. Approximately 70% of the colorectal cancer patients develop metastasis (Wanebo et al., 1978; Welch and Donaldson, 1979). The liver is the most common site of metastasis and the median survival without treatment is between 6 and 9 months (Simmonds, 2000). Hepatic resection is the gold standard in treatment of metastatic CRC patients and the only curative treatment for some patients (Rothbarth and van de Velde, 2005), with 5-year survival rates ranging from 25 to 39% (Adson et al., 1984; Hughes et al., 1986; Scheele et al., 1995). The tumor cells mainly spread via the portal vein to the liver. In advanced stages of the disease, metastases are also found in the lungs, the lymph nodes or the peritoneal cavity. Weiss and colleagues analyzed autopsy data from 1541 CRC patients and showed that metastases followed a sequential pattern of first liver, then lung and then other organs (Weiss et al., 1986). These data support the

linear progression model (see chapter 4.6.), which suggests that primary metastases are able to generate additional metastases in a sequential manner. Furthermore, some patients harbor bone metastases that are usually associated with widely disseminated CRC (Leinung et al., 2000).

In addition to surgery, patients with metastatic CRC are treated with radio- and/or chemotherapy such as 5-Fluorouracil (5-FU) alone or in combination with Oxaliplatin or Irinotecan (Pasetto et al., 2005). These three compounds have different modes of action. 5-FU is a nucleoside analog that blocks the enzyme thymidylate synthase and thus disrupts the synthesis of thymine nucleotides that are needed for DNA replication (Segal and Saltz, 2009). Oxaliplatin is a platinum-based compound that prevents DNA replication and transcription via the formation of cross-linking DNA adducts (Woynarowski et al., 1998). Irinotecan inhibits the nuclear enzyme topoisomerase I, which enables the uncoiling of the DNA during replication (Hsiang et al., 1985).

The combinatorial treatment, usually administered as FOLFOX (5-FU / Leucovorin / Oxaliplatin) or FOLFRI (5-FU / Leucovorin / Irinotecan), has improved the response-rates for advanced CRC from 10-20% to 40-50% (Douillard et al., 2000; Giacchetti et al., 2000; Raymond et al., 1998). Furthermore, novel targeted therapies have been developed, including monoclonal antibodies and small molecule inhibitors directed against the vascular endothelial growth factor (VEGF), or epidermal growth factor receptor (EGFR). Anti-VEGF therapy targets the vasculature by blocking the VEGF function. Numerous small molecule tyrosine kinase inhibitors have been developed that compete with ATP for the binding to the EGFR and thereby disable ligand-induced responses (Chen et al., 1987; Honegger et al., 1987a; Honegger et al., 1987b).

Even though therapies against CRC and the understanding of the disease improved in the past years, resistance to chemotherapy limits the success of treatment and many patients develop recurrent metastatic disease, dependent on the stage of the disease. Approximately 95% of these patients relapse within 5 years after treatment (Kobayashi et al., 2007). The tumor cells that have shed to distant organs might persist in a dormant state, meaning that they do not divide and show low metabolic activity (Aguirre-Ghiso, 2007). As chemotherapy regimens target proliferating cells, the dormant cells with an altered regulation of the cell cycle may survive these treatments. Many studies have started to implement the concept of dormancy and try to unravel its role in adult stem cells and cancers.

4.9. The concept of dormancy

The term “tumor dormancy” originates from clinical observations in cancer patients that relapse years to decades after apparently successful treatment. During this time period, tumor cells remain in the body of the patient either at the primary site or as distant metastasis. This phenomenon is also referred to as minimal residual disease (MRD). The remnant tumor cells are below the detection threshold and therefore remain unnoticed (Hedley and Chambers, 2009).

Breast cancer is one of the most frequent types of solid cancers where dormancy has been observed. Demicheli and colleagues for example analyzed the recurrence speed in a cohort of 1173 breast cancer patients who had undergone mastectomy. Around 50% of the patients suffered from relapse within 15 years (Demicheli et al., 1996). The time from first-line therapy to recurrence of the disease can take up to 25 years (Meltzer, 1990) and the relapse rate after more than 5 years is 20% (Marches et al., 2006).

One reasonable hypothesis explaining the long latency period between removal of the primary tumor and recurrence is tumor dormancy (Fig. 12). Demicheli and colleagues suggested that tumor growth occurs rather rapidly after a period of dormancy (Demicheli et al., 1994) and that the activation of the dormant cells may be induced via tumor- or microenvironment changes (Demicheli et al., 1996).

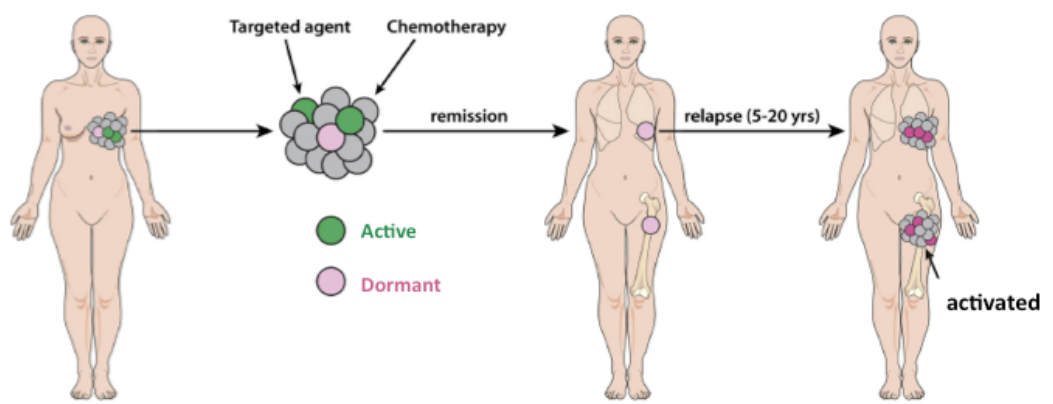

Fig. 12: Scheme of possible cancer relapse mechanisms. Tumor cells that have shed to distant organs are resistant to chemotherapy and/or targeted agents due to the acquisition of a dormant state. These dormant tumor cells are activated years to decades after treatment and will develop into overt metastasis. *Adapted and modified from Visvader and Lindemann (Visvader and Lindemann, 2012).*

Folkman and colleagues provided further evidence of the existence of tumor dormancy, where autopsies performed on individuals that died of trauma often revealed *in situ* carcinomas, even though they did not have cancer-related disease (Folkman and Kalluri, 2004). This finding indicates that many more individuals than

expected harbor tumors that may be in a dormant state for their entire lifetime. The following questions arise upon these observations: what keeps certain tumor cells in a dormant state and what are the mechanisms leading to their activation and growth. The answer to these questions is the key to better understand the process of metastasis and relapse. Currently there is no direct evidence of the existence of such dormant cells and there are no available markers characterizing them. Indeed, the study of tumor dormancy is difficult due to detection limitations and the lack of suitable model systems. In order to unravel the process of tumor dormancy, the term needs to be properly defined because there may be several independent mechanisms leading to this phenomenon. Two major definitions that are used in the field should not be confused: tumor mass- and cellular dormancy. Tumor mass dormancy refers to a state where proliferation is counterbalanced by apoptosis. The tumor cells still actively divide but the tumor mass does not increase. Contrarily, tumor cells that are in a state of cellular dormancy show low metabolic activity and enter a G0-G1 arrest, also referred to as quiescence. The cellular characteristics of one or the other mechanism may be completely different. A transition between the two states of dormancy may be possible as well. In the following chapters the current knowledge on cellular dormancy and the future impact on cancer patients will be discussed.

Quiescence as a feature of adult stem cells

Multipotent stem cells are crucial to maintain regenerative tissues in the body such as the skin, the hematopoietic system and the gut. These cells undergo life-long self-renewal and have the capacity to generate all different cell types of each lineage (Weissman, 2000). Populations of adult stem cells have been identified in several tissues of the body, including the skin (Clayton et al., 2007; Cotsarelis et al., 1990; Lyle et al., 1998; Snippert et al., 2010), the intestine (Barker et al., 2007; Bjerknes and Cheng, 1999; Cheng and Leblond, 1974; Potten et al., 1992; Potten et al., 1974; Sangiorgi and Capecchi, 2008), the mammary glands (Shackleton et al., 2006; Welm et al., 2002), the brain (Uchida et al., 2000), the prostate (Leong et al., 2008) and the hematopoietic system (Morrison and Weissman, 1994; Osawa et al., 1996). It has been suggested that infrequent cell division or quiescence might play an important role in adult stem cell pool maintenance of some tissues (Orford and Scadden, 2008). In addition, quiescence may limit the accumulation of mutations during numerous rounds of DNA synthesis (Coller et al., 2006; Sang et al., 2008; Viatour et al., 2008) and therefore prevent a malignant transformation to putative cancer stem cells (CSCs) (Lobo et al., 2007; Park and Gerson, 2005; Wang and Dick, 2005).

The mouse hematopoietic stem cells (HSCs) are the best-characterized adult stem cells. Slowly cycling HSCs have been identified in several studies (Cheshier et al., 1999; Foudi et al., 2009; Morrison and Weissman, 1994; Passegue et al., 2005; Yoshihara et al., 2007) and the existence of a highly dormant population of functional HSCs has been described in mice. These highly dormant cells divide only five times during the remaining lifespan of the organism and can be activated in response to bone marrow injury. After re-establishment of homeostasis, the activated cells may reenter a dormant state (Wilson et al., 2008). Furthermore, it is discussed whether different subsets of HSCs may co-exist: dormant- and homeostatic HSCs. The dormant cells may represent a reserve stem cell pool that harbors long-term reconstitution abilities whereas the homeostatic HSCs cycle more actively and therefore support the daily production of new blood cells (Abkowitz et al., 1990; Haug et al., 2008; Wilson et al., 2008).

The intestinal stem cell: a complex and heterogeneous system

In the intestine, the identity of the stem cell is still under debate. Two different models were proposed so far: The +4 model and the stem cell zone model. In the +4 model, cell-tracking experiments predicted a common cell of origin at position 4-5 in the crypt just above the Paneth cells (Fig. 13) (Cairnie et al., 1965; Potten, 1977; Potten et al., 1974). The +4 cells retain DNA labels for long time periods suggesting that these cells are having quiescent features (Potten, 1977; Potten et al., 1974). The polycomb group protein Bmi1, marks intestinal stem cells (ISCs) at the +4 position that are able to give rise to all four epithelial lineages (Sangiorgi and Capecchi, 2008).

In contrast to the +4 model, the stem cell zone model proposes that crypt-based columnar cells (CBCs) located among Paneth cells at the crypt bottom represent the intestinal stem cells (Fig. 13) (Bjerknes and Cheng, 1999; Cheng and Leblond, 1974). Barker and colleagues identified leucine-rich-repeat containing G-protein-coupled receptor 5 (Lgr5) as a marker for the corresponding murine ISCs. These Lgr5 positive CBC cells are actively cycling and have the capacity to generate all epithelial lineages similar to the Bmi1 expressing cells (Barker et al., 2007).

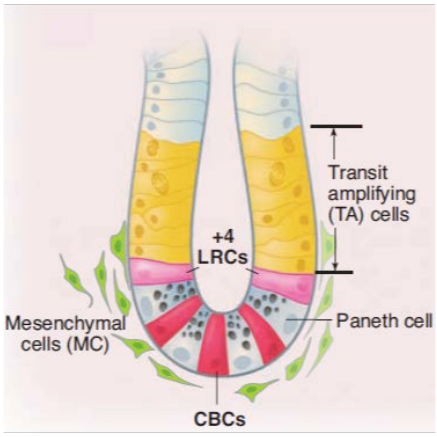

Fig. 13: Schematic representation of the intestinal crypt structure. The intestinal crypt is composed of actively dividing CBC cells ($Lgr5^+$) located at the bottom of the crypt and LRCs cells ($Bmi1^+$) at the +4 position. Transit amplifying cells produced by the stem cells migrate up the crypt where they differentiate into distinct functional epithelial lineages, such as enterocytes, goblet cells and enteroendocrine cells. *Adapted from Li and Clevers (Li and Clevers, 2010).*

However, the relationship between the two intestinal stem cell types is still poorly understood. It has been recently proposed that quiescent and active ISCs coexist in two different zones within the crypt: a quiescent- and an active stem cell zone (Li and Clevers, 2010; Scoville et al., 2008). The stem cells are stimulated or inhibited via the microenvironment. The microenvironment surrounding the crypt bottom, where the Lgr5 positive cells are located, has high Wnt activity (Barker et al., 2007) and inhibited bone morphogenetic protein (BMP) signaling (He et al., 2004; Kosinski et al., 2007). Contrarily, the stem cells at the +4 position are exposed to BMP4 and the Wnt inhibitor secreted frizzled-related protein 5 (sFRP5) (Gregorieff and Clevers, 2005; He et al., 2004). Wnt signaling is involved in the activation of the intestinal stem cells whereas BMP signaling was suggested to antagonize crypt formation and ISC self-renewal (Haramis et al., 2004; He et al., 2004).

Greco at al. proposed that the balance between quiescent and actively dividing stem cells might be organized via compartmentalization of the stem cell niche. The authors suggested that the stem cells might work cooperatively, where one compartment is maintained as a stem cell pool and the other one is engaged in immediate and rapid new growth. Recent studies indicate that there may be an interconversion between the identified stem cell populations. Tian and colleagues suggested that Bmi1 positive cells might serve as reserve stem cell pool. In case of injury and elimination of Lgr5 positive cells, these cells are able to give rise to Lgr5 positive cells (Tian et al., 2011). Moreover, the atypical homeobox gene (*Hopx*) has been shown to co-localize with the quiescent ISC population at the +4 position. These *Hopx* expressing cells can give rise to Lgr5-expressing CBC cells and the other way around (Takeda et al., 2011), suggesting an interplay between the two cell types. Additionally, Montgomery and colleagues identified mouse telomerase reverse transcriptase (mTERT) as a marker for slowly cycling intestinal stem cells (Montgomery et al., 2011). mTERT expressing cells give rise to all differentiated cell

types present in the intestine. Like the Bmi1 positive cells, these cells are resistant to radiation and can give rise to Lgr5 positive cells upon injury (Montgomery et al., 2011; Yan et al., 2012). Yan et al. demonstrated that Bmi1- and Lgr5 positive cells are two functionally distinct but cooperative populations. The authors showed that Bmi1 positive ISCs represent a quiescent and injury-inducible reserve ISC pool whereas Lgr5 positive cells contribute to homeostasis of the small intestine (Yan et al., 2012).

Recently leucine-rich repeats and immunoglobulin-like domains 1 (Lrig1) have been identified as a new ISC marker via gene expression profiling of CD24-purified mouse colonic epithelial progenitor cells (Akashi et al., 1994; Gracz et al., 2010; Powell et al., 2012; von Furstenberg et al., 2011). Lrig1 has been described as a negative feedback inhibitor of ErbB signaling (Laederich et al., 2004) that marks predominantly non-cycling, long-lived stem cells. Powell and colleagues proposed that Lrig1 positive cells are downstream of the quiescent Bmi1- or mTERT positive stem cells giving rise to transient amplifying (TA) cells and/or Lgr5 positive cells. The authors showed that most crypt cells express either Lgr5 or Lrig1, however, in rare cases colocalization of the two markers occurred in the same cells (Powell et al., 2012). This is in line with the finding of Itzokoviz and colleagues who investigated an overlapping expression of several ISC markers such as Lgr5, Bmi1 and mTert, in crypt base cells (Itzkovitz et al., 2012).

Most of the described studies indicate that several pools of intestinal stem cells might coexist. Actively cycling cells that may be important for the homeostasis of the regenerative tissue whereas the quiescent SC population may serve as a reserve pool that can be activated in cases of injury or stress. The SC function might be triggered partially by the microenvironment leading to the presence of heterogeneous cellular stem cell states that might transition among each other. Further investigations need to be performed to unravel the complex mechanisms of ISCs.

4.10. Cancer, cancer stem cells and quiescence: Plasticity vs. Stability

Cancer stem cells in colorectal cancer

Due to the observation of a cellular hierarchy within several cancer entities (Al-Hajj et al., 2003a; Bonnet and Dick, 1997), a parallel has been made between the cellular organization of adult tissues and those of tumors. This parallel lead to the formulation of the cancer stem cell hypothesis (Reya et al., 2001). According to this hypothesis, so called cancer stem cells (CSCs) or tumor initiating cells (TICs)

represent a subpopulation within the bulk of the tumor (Lobo et al., 2007; Trumpp and Wiestler, 2008) that have the capacity to self-renew as well as to generate all the diverse cellular phenotypes of the tumor (Vermeulen et al., 2008a). The current standard to test a prospective cell population for those abilities is the xenotransplantation into immunocompromised mice. Only cancer stem cells should be able to regenerate a heterogeneous tumor with similar properties of the primary tumor. In addition, the xenograft must be serially transplantable into new recipient mice, which is an indication for long-term self-renewal capacity of the stem cell (Vermeulen et al., 2008a) (Fig. 14).

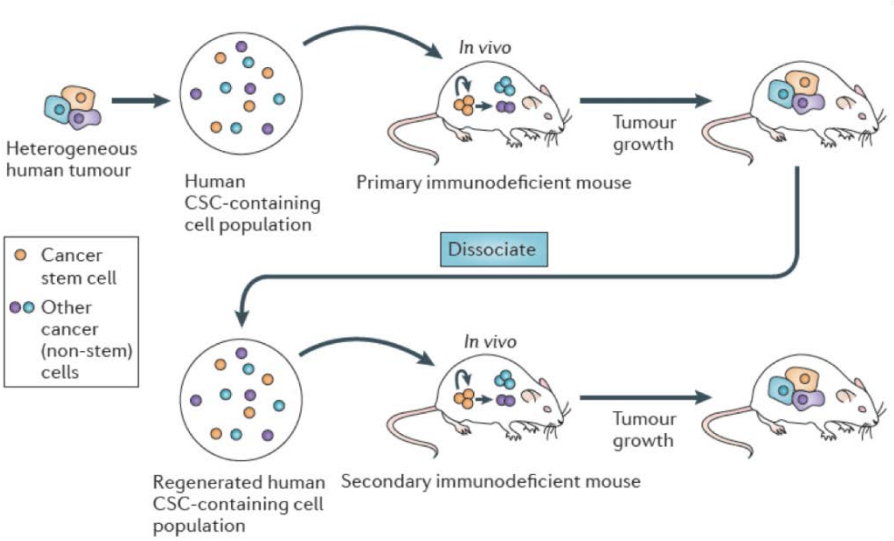

Fig. 14: *In vivo* CSC assay. CSCs have been defined as a subpopulation of tumor cells, able to self-renew and to generate all various cell types present in the original tumor. In order to test these CSC functions, diverse tumor cell populations are sorted and transplanted into immunodeficient mice, usually at limiting-dilutions. Only if CSCs are present, a heterogeneous tumor, resembling the original tumor will develop. Furthermore, primary xenografts are dissociated and further transplanted into secondary recipients in order to show the long-term self-renewal capacity of the tumor cells. *Adapted from Nguyen (Nguyen et al., 2012)*

Many studies were performed in order to identify potential CSC markers in CRCs. Most of these studies screened for differentially expressed cell surface markers, sorted marker-positive and -negative subpopulations and performed transplantation assays to functionally validate these markers as described above.

In 2007, two groups proposed that CD133 might be a potential marker for CRC stem cells (O'Brien et al., 2007; Ricci-Vitiani et al., 2007). CD133, also referred to as Prominin-1, has been described as a marker for primitive hematopoietic- and neural stem cells (Uchida et al., 2000; Yin et al., 1997). CD133 is a pentaspan membrane protein that contains two glycosylated extracellular loops (Corbeil et al., 2001). Even though this marker has been described for many years, the function of CD133 is still relatively unclear.

O'Brien and colleagues sorted CD133 positive and -negative CRC tumor cells and performed limiting dilution assays in immunodeficient mice. The authors demonstrated that the CD133 positive cell population was highly enriched for tumor initiating cells (O'Brien et al., 2007). Similarly Ricci-Vitiani et al. showed that only CD133 positive cells give rise to tumors whereas the CD133 negative cell population did not develop into tumors after subcutaneous transplantation (Ricci-Vitiani et al., 2007).

However, a recent study from Shmelkov and colleagues challenges this finding. Here, the authors analyzed the expression pattern of CD133 in CRCs and normal murine epithelium using a genetic mouse model harboring the *lacZ* reporter gene in the CD133 locus. The marker expression was detected in a broad spectrum of differentiated and undifferentiated epithelial cells, including the colon. This finding indicates that CD133 expression is not restricted to the stem cell compartment. Furthermore the authors demonstrated that epithelial cell adhesion molecule (EpCAM) positive/CD133 negative cells were able to generate tumors in immunodeficient nonobese diabetic/severe combined immunodeficiency disease (NOD/SCID) mice over serial passages. Surprisingly, the CD133 negative population resulted in more aggressive tumors than the ones generated by CD133 positive tumor cells (Shmelkov et al., 2008). Nevertheless, CD133 expression has been described to correlate with poor prognosis (Horst et al., 2008) and low levels of this marker result in a longer relapse-free interval in CRC patients (Artells et al., 2010). Taken together these data suggest that CD133 might not be a specific CSC marker for CRCs.

Further investigations have identified novel CSC markers. Dalerba and colleagues suggested that $EpCAM^{high}CD44^{+}$ tumor cells were able to engraft in immunodeficient mice whereas $EpCAM^{low}CD44^{-}$ populations did not induce the development of tumors. The authors also identified CD166 as a co-CSC marker that was independent and synergistic with regard to CD44 (Dalerba et al., 2007).

CD44 has been described as CSC marker in prostate- (Collins et al., 2005; Patrawala et al., 2006), pancreatic- (Li et al., 2007) and breast cancer (Al-Hajj et al., 2003a). The hyaluronic acid receptor CD44 is a transmembrane glycoprotein that plays a role in many cellular processes such as cell growth, survival, differentiation and motility (Aruffo et al., 1990; Cheng and Sharp, 2006; Nagano and Saya, 2004; Vigetti et al., 2008). Moreover, CD166 also referred to as activated leucocyte cell adhesion molecule (ALCAM), has been described as mesenchymal stem cell marker in melanoma (van Kempen et al., 2000). In addition, CD166 is highly expressed within the endogenous intestinal stem cell niche (Levin et al., 2010). Weichert and

colleagues report a shortened survival for CRC patients that have an altered CD166 expression (Weichert et al., 2004).

Recently, the aldehyde dehydrogenase 1 (ALDH1) has also been suggested to mark CRC stem cells. Huang and colleagues identified ALDH1 expression in the bottom of the crypts where the ISCs are located. Furthermore transplantation assays revealed that only ALDH1 positive cells were able to develop into a tumor, whereas ALDH1 negative cells failed (Huang et al., 2009).

In summary, many distinct markers have been proposed as putative CSC markers for CRCs. However, the overlap between the different CSC populations described in these different studies still remains to be investigated. Furthermore, the specificity of these markers is still under debate. Many of these markers are not restricted to the stem cell compartment and are expressed in various tissues and cell types. Moreover, the function of most of these markers in regard to CSCs is still not fully understood.

An explanation for the discrepancy between the different reported CRC stem cell populations might be found among the increasing evidence on the highly plastic and dynamic features of CSCs. Indeed, it has been shown that the phenotype of CSCs may vary between individual patients and that several CSC clones may coexist within the tumor of an individual patient (Anderson et al., 2011; Notta et al., 2011). Adding to this complexity, it has also been reported in CRC that non-CSCs might be able to acquire CSC function when placed in the right microenvironment (Vermeulen et al., 2010).

4.11. Quiescence in cancer

Relatively few studies have been performed to study quiescence in cancer compared to adult tissues. This is most probably due to the lack of appropriate model systems. However, there is some evidence that quiescence might play an important role in at least some tumor entities.

Gao et al. reported that CD24 positive primary ovarian tumor cells proliferate slower than the CD24 negative cell population. CD24 positive cancer cells were more tumorigenic and expressed stem cell-associated genes such as *nestin*, *oct4* and *notch-1* and *-4.* Furthermore, the slowly cycling CD24 positive cell population was more resistant to cisplatin and expressed higher levels of ATP-binding cassette sub-family G member 2 (ABCG2) transporters that are involved in drug-efflux (Gao et al., 2010). This study suggests that the cell cycle of cancer cells may be linked to cancer stem cell properties, such as higher tumorigenic capacities, quiescence and drug

resistance. However, the CD24 positive cell population was enriched in S phase, which contradicts the finding of a slowly cycling phenotype. Moreover, quiescent cells have been identified in spheroids isolated from ascites of ovarian cancer patients. These quiescent cells were able reinitiate cell division upon attachment to a favorable environment in an AKT-dependent manner (Correa et al., 2012). To date, it is still unclear whether cancer stem cells relate to specific cell cycle distributions. Studies performed in breast- and pancreatic cancer did not find any correlation between CSCs and a particular cell cycle state (Al-Hajj et al., 2003b; Li et al., 2007). Possibly quiescent cells represent a very small subpopulation of the putative identified CSC populations in some tumor entities, that a difference in cell cycle state is not detectable when analyzing the whole CSC population. To overcome these limitations, quiescent cells need to be specifically labeled prior to analysis.

Moore et al. used Carboxyfluorescein succinimidyl ester (CFSE) to label commonly used breast (MDA.MB.231)- and colon (HCT116) cancer cell lines, as well as primary human breast tumor cells. They identified a small subpopulation of slowly cycling cells that was more resistant to chemotherapy and retained the capacity to proliferate after chemotherapy withdrawal (Moore et al., 2011). Their finding suggests that slowly cycling cells may be responsible for relapse at least in some cancer patients.

Pece and colleges labeled mammospheres isolated from human normal mammary stem cells (hNMSCs) with PKH, a lipophilic dye that is retained in quiescent cells. The transcriptional profile of label retaining mammospheres was generated and could be used to predict biological and molecular features of breast cancers. In addition the authors analyzed mammospheres generated from grade 1 and grade 3 tumors for label retaining cells (LRCs) and found that grade 3 tumors had higher percentages of LRCs suggesting an increase in putative cancer stem cells as the tumor progresses (Pece et al., 2010). This study indicates that LRCs may be associated with the CSC population.

Roesch and colleagues identified the histone demethylase JARID1B as a novel biomarker for slowly cycling melanoma cells. JARID1B was dispensable for tumor initiation but necessary for long-term tumor maintenance, suggesting that JARID1B is not a classical CSC marker. The fact that JARID1B negative cells are able to generate JARID1B positive cells indicates that the JARID1B phenotype is dynamic. The authors suggest that cancer cells are able to transiently acquire stemness properties and thereby support the model of dynamic stemness (Roesch et al., 2010).

Dembinski and Krauss used the lipophilic labeling dye DiI to detect slowly cycling cells in pancreatic cancer cell lines. The slowly cycling cell population showed an increased presence of the pancreatic CSC markers CD24/CD44 and CD133. Furthermore, the slowly cycling cells displayed the morphological and genetic fingerprint of epithelial-mesenchymal transition (EMT) including increased invasiveness, tumor initiating potential and a shift in sensitivity to chemotherapy (Dembinski and Krauss, 2009). In line with Roesch et al. is the finding that the DiI negative population is able to generate DiI positive cells supporting a dynamic model with bidirectional potential in both, subpopulation- and bulk cells. Moreover, data from Sharma and colleagues support a dynamic model regarding treatment sensitivity. The authors suggest a dynamic survival strategy where human cancer cells transiently acquire a drug-tolerant state (Sharma et al., 2010).

The labeling techniques with lipophilic dyes give a first hint whether slowly cycling cells exist in primary tumors. However these dyes have a short half-life and enable studies only over short time periods. Thus to study label retention in more detail long-term inducible labeling methods for *in vivo* experiments are needed. Additionally, the microenvironment might play a very important role as well. Exogenous stimuli and signaling molecules might be involved in the interplay between LRCs and fast cycling cells and they may even trigger a switch between the two cycling states. Some of these studies hint already towards a more dynamic system at least in some tumor entities making it more complex to develop specific treatment strategies.

Moreover, all the studies performed in order to identify and functionally characterize LRCs in solid tumors have been performed with the help of cell lines or primary human cells that were expanded *in vitro* and in xenograft models. Whether the expansion of dormant tumor cells in any of the model system still preserves the phenotype of quiescent cells is still under debate but is to date the only possibility to gain insight into possible mechanisms underlying cellular dormancy (Vessella et al., 2007).

A huge amount of effort has been made to overcome these hurdles and numerous studies in cancer patients have been performed, mainly on disseminating tumor cells (DgTCs) detected in the bone marrow.

Clinical relevance of quiescent cancer cells

Many cancer patients that do not show any sign of metastasis either at the time point of prognosis or surgery harbor tumor cells in their bone marrow. The presence of these disseminating cells (DgTCs) was associated with poor prognosis in breast-

(Braun et al., 2005; Pantel and Woelfle, 2005), prostate- (Morgan et al., 2009) and colorectal cancer patients (Leinung et al., 2000).

These analyses are of great clinical importance and may predict treatment success and possible relapse in cancer patients. However further investigations that unravel the molecular mechanisms of DgTCs are indispensible. Pantel and colleagues performed immunocytochemical analysis on bone marrow aspirates of breast cancer patients using monoclonal antibodies directed against cytokeratins in combination with antibodies against nuclear proliferation markers, such as Ki-67 and p120. The authors showed that the majority of DgTCs are in a quiescent state, one of the hallmark features of stem cells (Pantel et al., 1993). This is in line with the finding that tumor relapse occurs in some patients even decades after apparently successful treatment, indicating that DgTCs may be the source for later developing metastasis.

Furthermore, two independent studies on breast- and ovarian cancer suggest that DgTCs are more resistant to standard chemotherapy treatment (Naumov et al., 2003; Wimberger et al., 2007). Wimberger et al demonstrated that half of the patients harbored remaining DgTCs after first-line therapy (Wimberger et al., 2007).

In conclusion, these findings suggest that DgTCs may be of clinical relevance. DgTCs seem to be in a quiescent state, which might help them to survive standard chemotherapy regimens and finally progress into overt metastasis after a certain period of time. However, these studies are all descriptive without any functional proof that the detected DgTCs are indeed the root of metastasis. Additional studies and functional assays are needed to further analyze these cells and to develop novel treatment strategies.

4.12. Future perspectives

The existence of slowly cycling cells has been demonstrated in several adult stem cells and only a few studies also report evidence for the presence of such cells in the context of cancer.

These quiescent or slowly cycling cell populations seem to be heterogeneous and may have different functions. In the hematopoietic system, long-term and short-term LRCs exist. Both populations are able to reconstitute the hematopoietic system. However, only long-term LRCs retain the capability to reconstitute the blood system in serial transplantation assays, suggesting a co-existence of different stem cell populations possibly fulfilling different functions (see chapter 4.9). Moreover, there is some evidence that these highly dormant HSCs can be activated upon stress induction, such as injury. In order to retain the backup population of stem cells, the activated HSCs may reenter in a dormant state after replenishing the destroyed cells

(Essers et al., 2009; Foudi et al., 2009; Wilson et al., 2008). This dynamic switch between quiescent- and actively dividing cells may be also true for several other tissue stem cells.

In the context of cancer, slowly cycling cells may have the capability to better survive chemotherapy compared to fast cycling tumor cells. In contrast to adult stem cells, the presence of long-term LRCs in tumors has not been described yet experimentally. It is of importance to distinguish between long-term LRCs and slowly cycling cells. These different cycling cell populations may have distinct functions and underlying mechanisms. In tumors, it might be unlikely to detect long-term LRCs, due to mutations in oncogenes and/or tumor suppressor genes that generally support sustained proliferation capacities (Hanahan and Weinberg, 2000, 2011). However, there are several indications that slowly cycling cells exist within a primary tumor. As described for HSCs, it seems that tumor cells are able to switch between different cycling phenotypes. Slowly cycling tumor cells may survive treatment but still retain the potential to proliferate upon so far unknown stimuli and thereby cause recurrence. A better understanding of the underlying mechanisms responsible for the phenotypic switch or for the maintenance of quiescence will open many new avenues for the development of novel therapies.

5. Aim of the thesis

The first goal of this PhD work was to test whether dormant or slowly cycling cells exist within colorectal tumors. To reach this goal, a suitable *in vitro* and *in vivo* model was required that fully recapitulated the human disease. In addition, a suitable cellular tracking system was required in order to detect slowly cycling cells for long time periods *in vitro* and *in vivo*.

If dormant or slowly cycling cells were identified within colorectal tumors, the second goal of this PhD work was to characterize the cellular phenotype and to test whether these cells had any similarities with the previously identified putative colorectal CSCs.

Finally, if dormant or slowly cycling cells could be detected, the third goal of this PhD work was to functionally characterize dormant or slowly cycling colorectal tumor cells by investigating their potential role during tumor progression, metastasis and chemotherapy resistance.

6. Results

6.1. Establishment of a suitable *in vivo* system to study human colon cancer development

In order to study human colorectal cancer (CRC), a suitable model system is needed that fully recapitulates the disease. A good model system is an orthotopic one that preserves the initial microenvironment of the tumor cells. However, injections of primary human tumor cells into the thin colon wall of a mouse are difficult and carry the risk of leakage and intraluminal injection (Tseng et al., 2007) and thus may lead to less reproducible results.

To date, two common methods are widely used for xenotransplantations of colon cancer cells: subcutaneous injections (s.c.) (Ricci-Vitiani et al., 2007; Todaro et al., 2007) or injections into the renal capsule (O'Brien et al., 2007). The renal capsule is used as a transplantation site due to high vascularization that allows a sufficient nutrition supply for the tumor cells.

Both methods were adapted in the following experiments for the xenotransplantations of human colorectal tumor cells. The subcutaneous model was used for the expansion of tumor pieces to increase the limited amount of the primary material. Renal capsule injections were chosen for the transplantation of cancer cells either from primary cancer cell cultures, that are enriched for putative cancer stem cells or from cell suspensions directly derived from primary tumor digests.

Furthermore, the choice of an adequate mouse model is crucial. As reported by Quintana and colleagues, the frequency of cancer initiating cells in melanoma is increased in NOD/SCID interleukin-2 receptor gamma chain null mice (NSG) compared to nonobese diabetic/severe combined immunodeficiency (NOD/SCID) mice (Quintana et al., 2008). NOD/SCID mice have an impaired B- and T cell lymphocyte development, while NSG mice additionally lack functional NK cells and thereby are even more permissive to xenotransplants (Ito et al., 2002; Morton and Houghton, 2007; Richmond and Su, 2008). In order to achieve a high engraftment rate, the NSG mouse model was chosen for the xenotransplantation assays, in knowledge of the limitations due to the partial absence of the immune system that also plays an important role in tumor development.

Expansion of patient tumor specimen in vivo

Freshly collected tumor pieces were isolated from colon cancer patients. In order to expand the primary material, the tumor pieces were expanded *in vivo* in NSG mice. Therefore small pieces were transplanted s.c. into NSG mice. After reaching a tumor size of max. 1.5 cm x 1.5 cm, the tumors were harvested. To investigate whether the xenografts were of epithelial human origin, they were digested using collagenase and DNase and further analyzed using flow cytometry and immunohistochemistry (Fig. 15).

For flow cytometry analysis, HLA (human leucocyte antigen) was chosen as a marker to confirm that the cells are of human origin. HLA is the major histocompatibility complex class I, which is expressed on most nucleated cells of the human body. The mouse counterpart of this protein is H2kD that was chosen to exclude mouse cells from the analysis (Steinmetz and Hood, 1983). Additionally, a human specific anti-EpCAM antibody was used for the staining of the tumor cells. EpCAM is a homophilic cell-to-cell adhesion molecule (Litvinov et al., 1994) that is expressed on the basolateral surfaces of most epithelial cells and is overexpressed in many cancers (Balzar et al., 1999; Litvinov et al., 1997; Munz et al., 2004). An anti-human CD45 antibody was also included in the analysis in order to exclude human hematopoietic cells (Hermiston et al., 2003). This is of great importance as it has been demonstrated that human hematopoietic cells are also able to expand in highly immunocompromized mice (own observations, data not shown) (Chen et al., 2012; Simpson-Abelson et al., 2008).

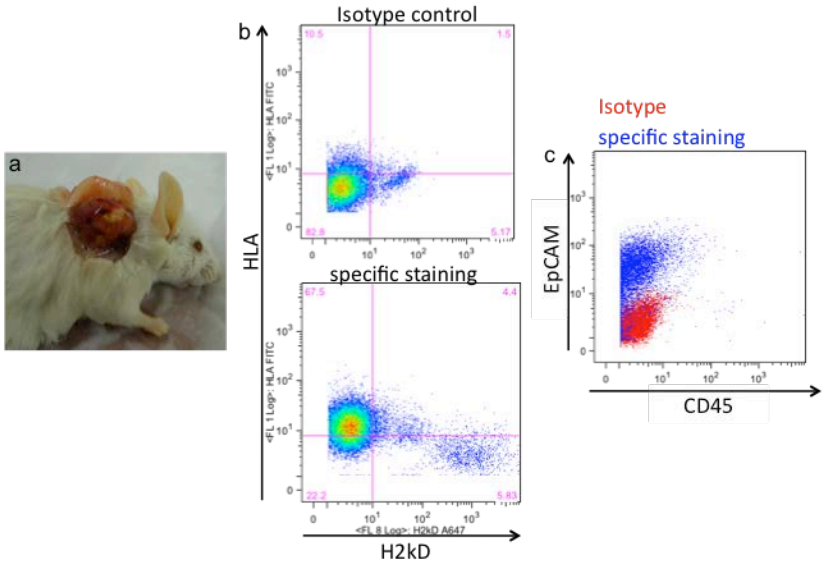

Fig. 15: Xenograft tumors are of human epithelial origin. (a) Expansion of tumor pieces transplanted s.c. into NSG mice. Flow cytometry analysis of tumor cells for (b) HLA- and H2kD expression and (c) EpCAM and CD45 expression (blue = specific staining; red = isotype control).

The cells isolated from s.c. expanded tumors were HLA+ and EpCAM+ (Fig. 15b and c), verifying their human epithelial origin. A few infiltrating mouse cells were identified among the tumor cells via the H2kD antibody staining (Fig. 15b). These cells may be stromal cells or macrophages of the mouse host.

To determine whether the xenografts show a similar morphology to the patient tumor, immunohistochemistry analyses were performed (Fig. 16). The tumors were well differentiated and contained mucin producing cells demonstrated by Periodic acid shiff (PAS) stainings (Fig. 16a). Atypical epithelial cells forming glandular structures could be observed (Fig. 16b and c, black arrows).

This shows that the tumor material can be propagated *in vivo* without loss of morphological heterogeneity and that the model is suitable to study colorectal cancer.

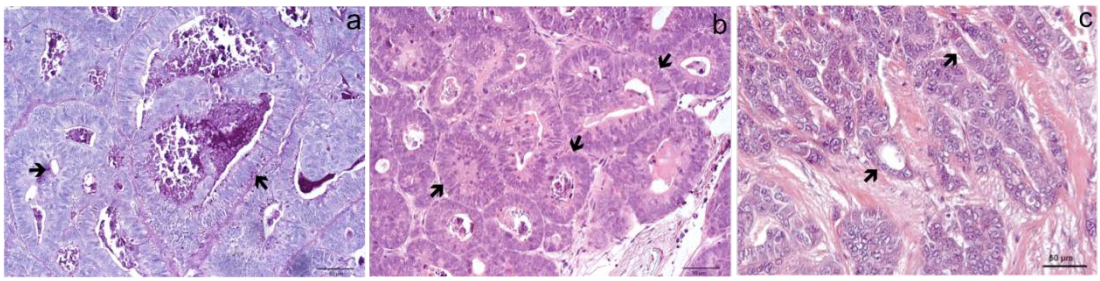

Fig. 16: Immunohistochemistry of xenografts. (a) Periodic acid schiff (PAS) staining which shows mucin and mucin producing cells (pink staining; black arrows), (b) H & E staining of the xenograft, (c) H & E staining of the patient tumor. (b and c) Black arrows mark glandular structures (scale bar 50 µm).

6.2. Establishment of a suitable *in vitro* system to study human colon cancer development

The *in vivo* propagation of the tumor material is a common method to avoid selection pressure due to culturing methods. Important interactions between the microenvironment and the tumor cells are retained *in vivo,* except for large parts of the immune system, which is impaired in the NSG xenograft model. Nevertheless, cell culture is necessary to manipulate the cells and to study cellular mechanisms in detail. Up to now, most cell culture media contained fetal calf serum (FCS). It was reported that these conditions induce a more differentiated phenotype in the tumor cells with less tumor-initiating potential when transplanted into immunocompromized mice (Dalerba et al., 2007). Lee and colleges demonstrated that primary human glioma cells cultured as spheres under serum-free conditions closely preserve the genotype, the gene expression profile and biology of their parental primary tumors (Lee et al., 2006). Therefore, serum-free culture conditions were chosen for the establishment of primary human colorectal cancer cell lines.

Establishment of the colon cancer cell line HD1858 under serum-free conditions

A tumor piece obtained from a resection of a liver metastasis of a late-stage colorectal cancer patient was processed. The freshly isolated tumor piece was enzymatically digested with collagenase and DNase to obtain a single cell suspension (Appendix 9.14.). The tumor cells were cultured under serum-free conditions in cancer stem cell medium (CSC medium, see material and methods) and could be successfully maintained and expanded as spheroid cultures (Fig. 17a). Furthermore, the tumor cells could be cultured and propagated under adherent conditions on collagen I coated plates (Fig. 17b). In contrast to conventional tumor cell culture methods, the adherent cells were still maintained in serum-free cancer stem cell medium, which preserved the CSC marker expression of the cells, while some adhesion molecules showed an altered expression (Appendix 9.15). Moreover, adherent cultures facilitate cell dissociation compared to sphere cultures, making it easier to count the cells, to sort them or to manipulate them with viruses. Therefore, many assays have been performed under adherent conditions.

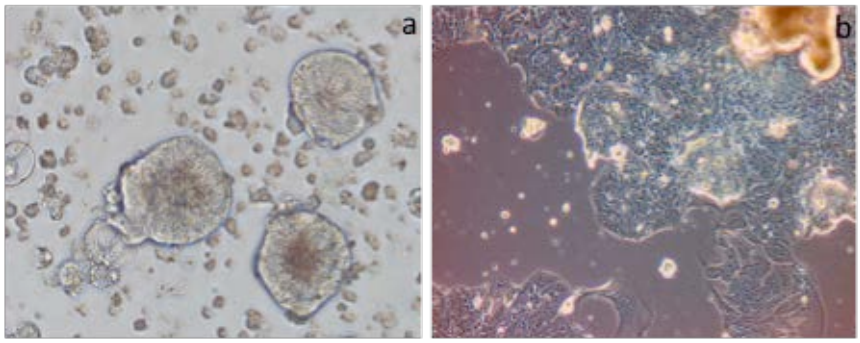

Fig. 17: Colon cancer cultures grown under serum-free conditions. The cells can be maintained as spheres (a) or grown adherent on collagen I coated plates in serum-free cancer stem cell medium (b).

6.3. Characterization of sphere cultures

The colon cancer spheres are tumorigenic *in vivo*

As shown in the previous chapter, primary colorectal tumor cells could be successfully maintained in cultures. To test whether these cells were still tumorigenic, cultured spheres were dissociated with Accutase (Appendix 9.13) and $5x10^5$ cells were transplanted into the kidney capsule of NSG mice. The mice developed tumors two months after transplantation with cellular atypia and tumor architecture similar to the patient tumor (Fig. 18).

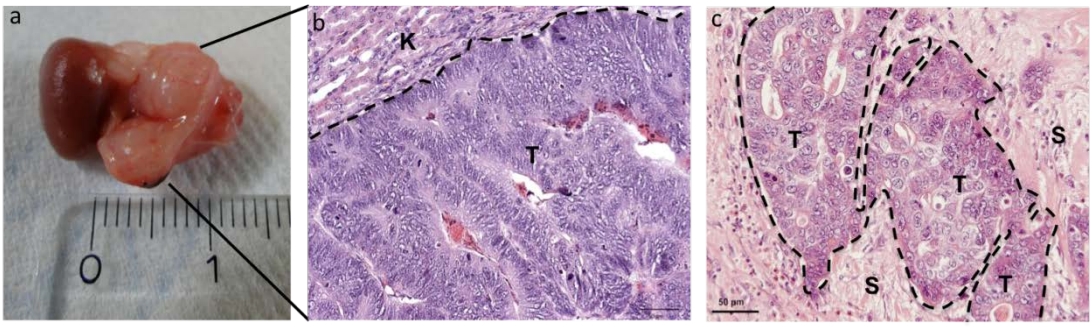

Fig. 18: Colon tumor spheres are tumorigenic. (a) Gross morphology of the tumor invading the kidney capsule. (b) H&E staining of the xenograft. (c) H&E staining of the primary patient tumor. (b and c) In both sections, atypical ductual structures were observed (T = tumor; S = stroma and/or infiltrating immune cells; K = kidney)(scale bar 50 µm).

In vivo tumorigenicity assay of the established colon cancer cell line

In order to determine the tumorigenic potential of the HD1858 spheres *in vivo,* different amounts of cells, ranging from $5x10^5$ to 10^3, were injected into the kidney capsule of NSG mice. To monitor non-invasively the growth of the tumors in the mice, the tumor cells were transduced with a lentiviral vector containing constitutive activated reporters such as luciferase and venus. After successful transduction, venus positive cells were sorted in order to generate a cell line that was completely positive for tumor cells expressing the two reporters. Tumor growth was monitored weekly via *in vivo* bioluminescence imaging using the Xenogen system (IVIS® 200 series, Caliper) (Fig. 19). The first signal was detected after 7 days for $5x\ 10^5$ and $1x\ 10^5$ cells. Both tumor growth curves show similarities regarding the increase of tumor size. However, only in the group where $5x\ 10^5$ cells were injected, all mice developed tumors. In the group where $1x\ 10^5$ tumor cells were transplanted, only one out of three mice showed tumor growth (Tab. 1). For the groups of mice where lower cell numbers were injected tumor growth could not be detected in the same time frame.

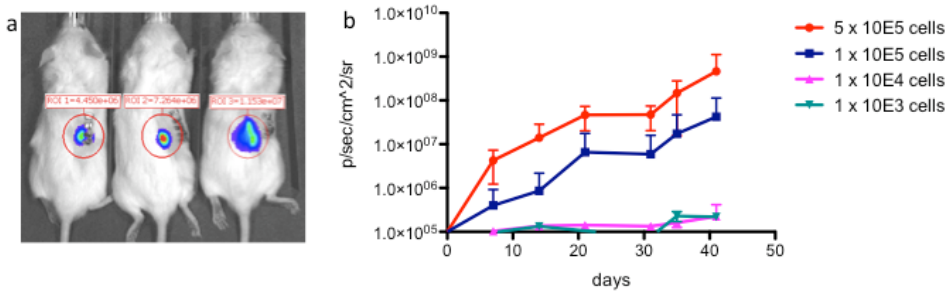

Fig. 19: Tumor growth curve for HD1858 tumor cells. (a) In vivo bioluminescence measurement of tumors using the Xenogen system. (b) In vivo growth curve of tumor cells that were injected under the kidney capsule into NSG mice (n=3 per group).

Tab. 1: Amount of tumor bearing mice. Different amounts of HD1858-luc-venus colorectal tumor cells were injected into the kidney capsule of NSG mice.

cell number	tumor bearing mice / total mice
5 x 10^5	3/3
1 x 10^5	1/3
1 x 10^4	0/3
1 x 10^3	0/3

Cell lines derived from single cell clones are able to generate a differentiated tumor that recapitulates the human primary tumor

In order to test whether the established cell line has the potential to regenerate a whole tumor out of a single cell, luciferase-venus transduced cells were sorted as single cells and expanded *in vitro* as spheres under serum-free conditions. Two sublines derived from single cell clones were generated. The spheres were dissociated and 5 x 10^5 cells were injected into the kidney capsule of NSG-mice. The tumor growth was monitored weekly via the IVIS 200 system (Fig. 20).

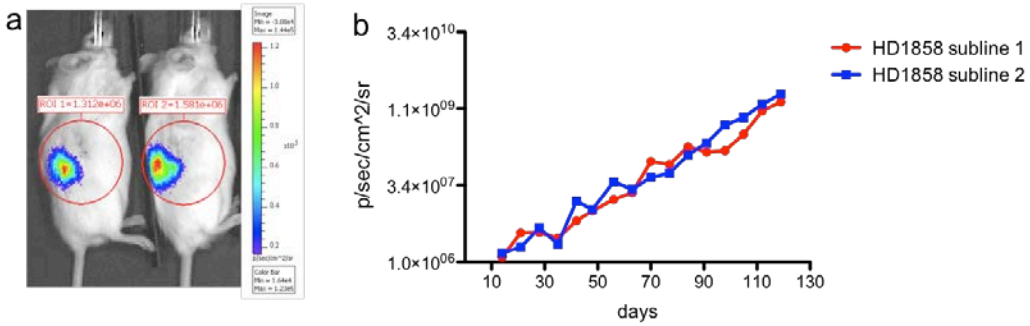

Fig. 20: Cell lines derived from single cell clones generate a tumor in NSG-mice. Tumor growth was monitored weekly via non-invasive bioluminescence measurements using the Xenogen system (a). Tumor growth curve of luciferase transduced HD1858 sublines (n=1/subline) (b).

The tumors grown out of single cell derived tumor cell lines retained their morphological heterogeneity and developed into adenocarcinomas that resembled the patient tumor, consistent of different cell types, including mucin producing goblet cells (Fig. 21). This result suggests that one single cell is capable of generating all the different cell types needed to establish a heterogeneous adenocarcinoma.

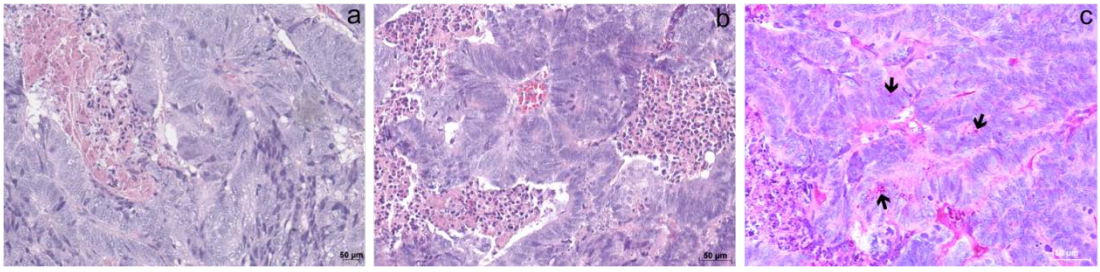

Fig. 21: Tumors grown out of a single cell derived colorectal tumor cell line are heterogeneous and resemble the human primary tumor. H&E staining of xenografts (a and b) and PAS staining (c, goblet cells depicted by black arrows). The origin of the tumor was one single cell that was sorted and expanded *in vitro* into a subline of the parental line.

The colon cancer spheres show nuclear ß-catenin expression

Nuclear ß-catenin localization is a prerequisite and surrogate marker for canonical Wnt signaling. In order to determine whether the Wnt signaling pathway is activated in colon sphere cultures, nuclear ß-catenin expression was measured. Colon spheres were fixed and immunohistochemistry (IHC) stainings for nuclear ß-catenin were performed. Fig. 22a demonstrates that the spheres maintained their heterogeneity regarding Wnt signaling activity and that only a subpopulation of cells showed an accumulation of nuclear ß-catenin similar to the xenograft (Fig. 22b and c, arrows).

This finding suggests that the cultured spheres are suitable to study cancer stem cells *in vitro* as Vermeulen et al. proposed that Wnt signaling activity is a marker for colon cancer stem cells (Vermeulen et al., 2010).

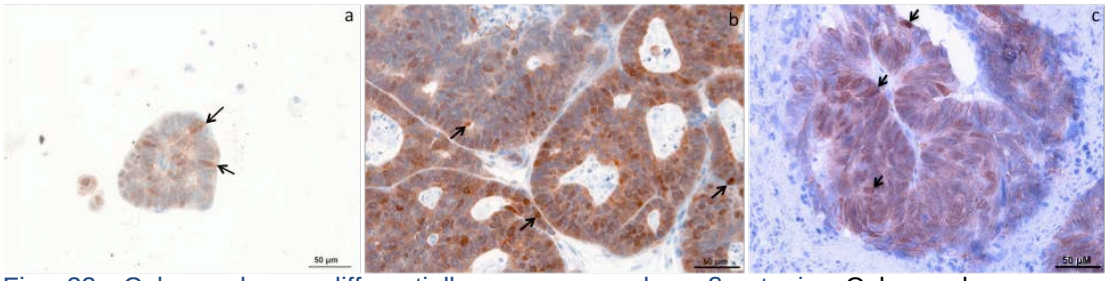

Fig. 22: Colon spheres differentially express nuclear ß-catenin. Colon spheres were embedded in histogel and nuclear ß-catenin staining was performed (brown). (a) Only a few cells within the sphere showed nuclear ß-catenin staining (black arrows) (b) similar to the xenograft originating from tumor pieces implanted s.c. or (c) from spheroid cultures transplanted into the kidney capsule (scale bar 50 µm).

Colorectal cancer sphere cultures express cancer stem cell markers

To investigate whether the cultured colon cancer cells express and preserve the reported cancer stem cell markers *in vitro*, flow cytometry analysis on HD1858 cells was performed. Additionally, a second cell line (G605) described by Vermeulen and colleagues was characterized and used for further experiments (Vermeulen et al., 2010; Vermeulen et al., 2008b).

The marker CD133^{+} (O'Brien et al., 2007; Ricci-Vitiani et al., 2007) or the combination of EpCAM^{high}, CD44^{+} and CD166^{+} (Dalerba et al., 2007) were suggested as potential colorectal CSC markers. Furthermore the marker combination of CD24^{+} and CD44^{+} was analyzed because this combination was described as putative cancer stem cell marker in other types of cancer such as pancreatic- and gastric cancer (Li et al., 2007; Zhang et al., 2011) but not yet for colon cancer.

Both cell lines, HD1858 and G605, were completely positive for EpCAM (data not shown) but differed in their expression pattern of the other described cancer stem cell markers. CD133 was only expressed in G605 cells whereas HD1858 cells were completely negative for this marker (Fig. 23a and d). Both cell lines contained a double positive population of CD44 and CD166 expressing cells (Fig. 23b and e). However this population was smaller in the G605 cells when compared to HD1858 cells (36% vs. 57%). Surprisingly, the broadest expression pattern was observed for the marker combination CD24 and CD44 (Fig. 23c and f). The cell line G605 was almost completely positive for both markers (Fig. 23c) with a broad expression spectrum, while the HD1858 cell line had a double positive population of 22% and a double negative population of 26%. Cells expressing only one of the markers were also present (Fig. 23f).

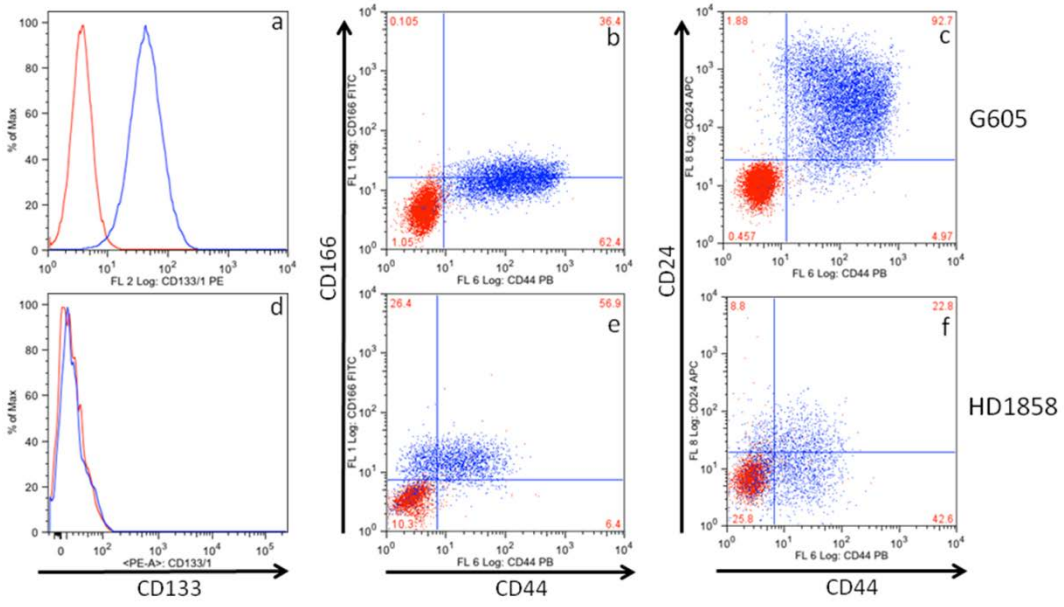

Fig. 23: Colorectal cancer cells express CSC-markers. Doublet- and dead cell exclusion were performed. HD1858 cells were negative for CD133 (d) and the G605 cells were completely positive for CD133 expression (a). In both cell lines, a population of CD44 and CD166 positive cells was present (b and e). The expression pattern for CD24 and CD44 was very heterogeneous (c and f) (red = Isotype control; blue = specific staining).

Colorectal cancer cells differentially express cell surface molecules involved in migration and metastasis

In addition to the classical cancer stem cell markers, cell surface proteins that are involved in migration and adhesion, including c-Met and the different alpha integrins, were analyzed. Most of the HD1858 cells were homogeneous concerning alpha integrin expression (Fig. 24b, c and f). The only two alpha integrins that showed a broader expression pattern were CD49a (integrin alpha 1) and CD49e (integrin alpha 5) (Fig. 24a and e). Moreover, 78 % of the cells were positive for c-Met (Fig. 24g). Similar results were obtained for the G605 cells. In this cell line, CD49c (integrin alpha 3) was differentially expressed in addition to CD49a and CD49e. C-Met was expressed in almost all tumor cells (Appendix 9.3).

This demonstrates that the cells were heterogeneous in regard to some cell surface markers that play a potential role in metastasis, even though they were expanded *in vitro.*

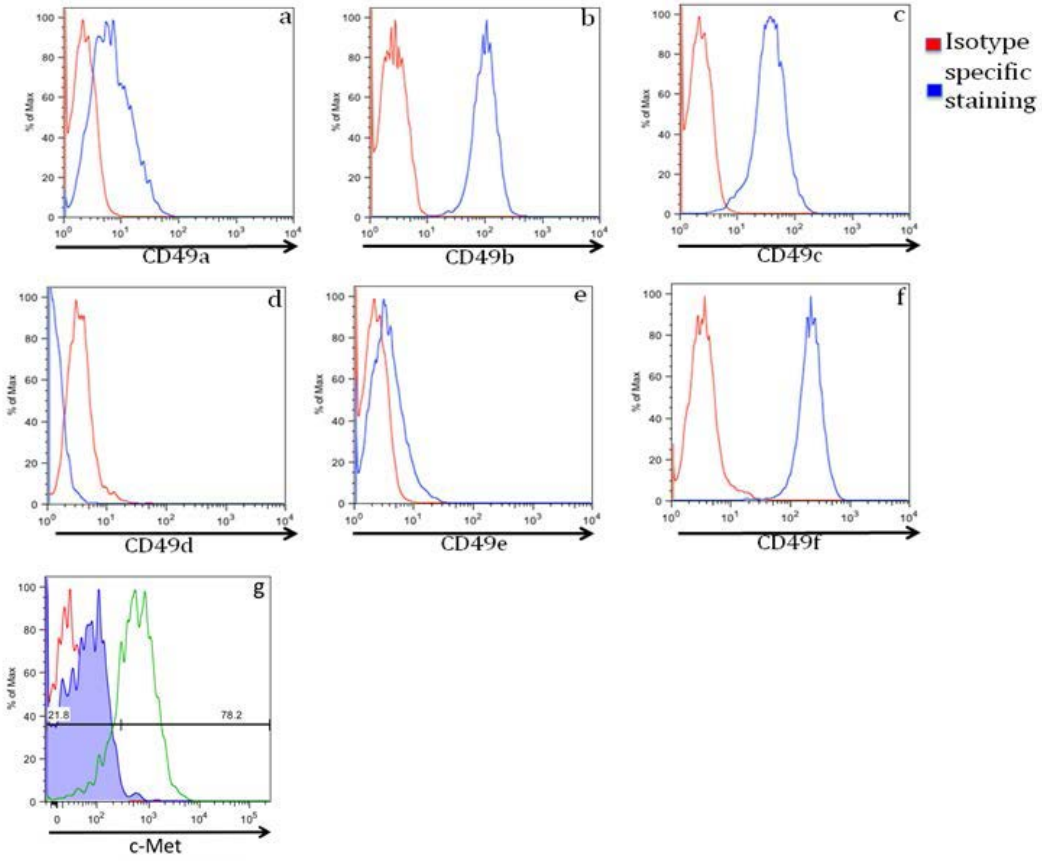

Fig. 24: HD1858 cells differentially express alpha integrins and c-Met. Dead cell exclusion using PI and doublet exclusion were performed. (a) The spheres differentially expressed CD49a, (e) CD49e and (g) c-Met. b) Colorectal cancer cells were completely positive for CD49b and (c) CD49c. (d) The tumor cells did not express CD49d (red = unstained; blue = isotype control; green = specific staining).

6.4. Evaluation of the marker combination CD24/CD44 as putative new cancer stem cell markers in GFP+ G605 colon cancer spheres

As detected in sphere cultures, CD24 and CD44 showed the broadest expression pattern compared to any other marker analyzed in this study. In order to determine whether these two markers show any functional differences *in vivo*, $CD24^{high}/CD44^{high}$ and $CD24^{low}/CD44^{low}$ cell populations were sorted (Fig. 25) and injected into the kidney capsule of NSG mice (40.000 cells/mouse; n=3 per group). For this experiment, the cell line G605 was chosen because it had a higher tumorigenicity than the primary cell line HD1858. In addition, this cell line was able to metastasize to the liver and the lungs whereas no metastases were observed in HD1858 injected mice. Furthermore, G605 cells were transduced with the tetracycline-inducible lentirviral vector expressing the H2B-GFP reporter (vector map see chapter 9.5.) but without repressing the reporter, in attempt to detect micrometastasis in distant organs using flow cytometry.

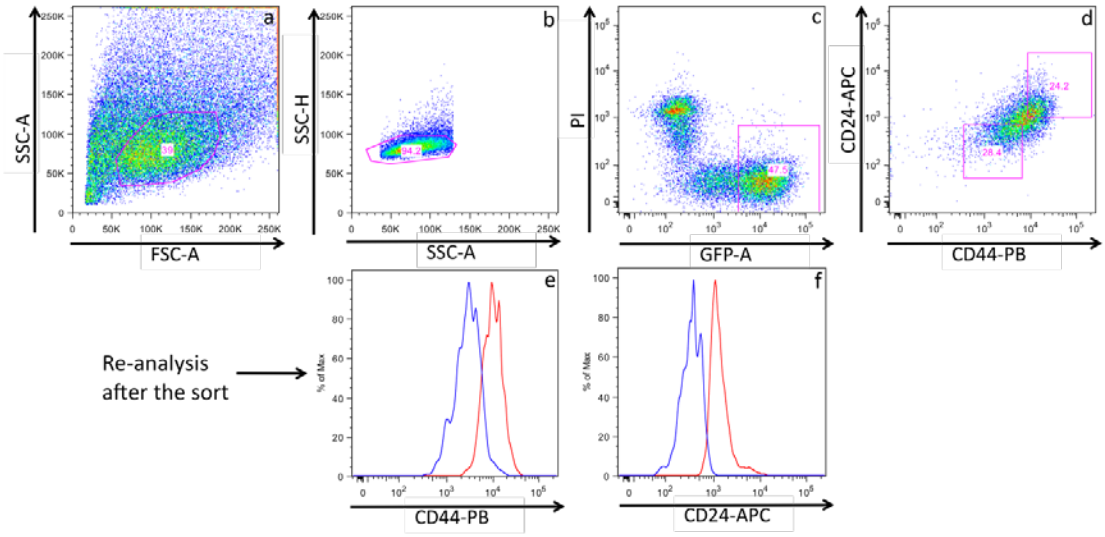

Fig. 25: Gating scheme of sorted H2B-GFP+G605 colon cells. Doublet- (b) and dead cell exclusion (c) were performed. The cells were stained with anti-human CD44-PB and CD24-APC antibodies (d). A re-analysis was performed after the sort (e-f). Both populations have been sufficiently separated (blue = $CD24^{low}/CD44^{low}$; red = $CD24^{high}/CD44^{high}$).

The mice were euthanized 3 months after injection and the tumor volume was analyzed. Tumors grew in all mice independent of the two markers and the tumor size was very variable even within both groups of mice. There was an increase in mean tumor volume in $CD24^{high}/CD44^{high}$ injected mice compared to $CD24^{low}/CD44^{low}$ injected mice. However, the difference between the two groups was not significant (p=0.1998) (Fig. 26). Moreover, the tumor growth was measured only at the end of the experiment. Possibly, the onset of tumor growth between the two groups might differ. Further analysis including *in vivo* bioluminescence measurements need to be

performed to investigate this further. Limiting dilution transplantation assays would provide additional information about the frequency of tumor initiating cells present in each population.

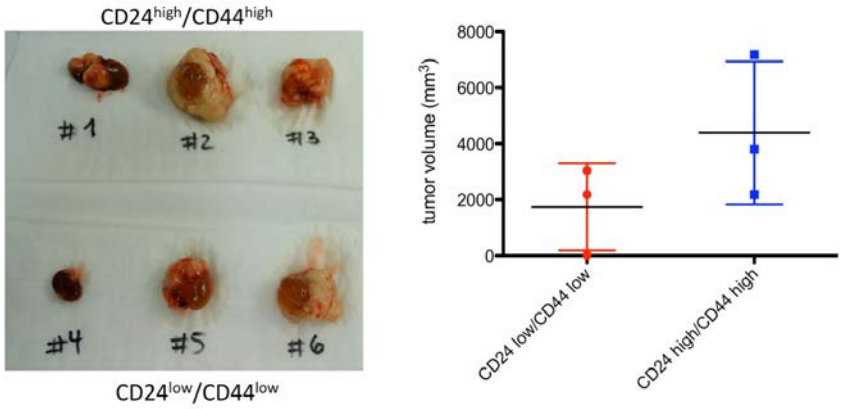

Fig. 26: The tumorigenicity was not significantly different between $CD24^{high}/44^{high}$ and $CD24^{low}/44^{low}$ cells. The tumor volume was estimated via caliper measurements at the endpoint of the experiment. A T-test was performed. Error bars represent 95% confidence intervals (p = 0.1998).

Furthermore, the presence of macrometastasis was evaluated. Only in the mice injected with $CD24^{high}/CD44^{high}$ cells macrometastasis could be observed in the lung (n=1/3) and in the liver (n=2/3) (Tab. 2 and Fig. 27). Mice injected with $CD24^{low}/CD44^{low}$ cells did not display any macro-metastases. Further evaluation of the organs for the presence of H2B-GFP expressing tumor cells using flow cytometry was not feasible due to technical challenges. The lungs could not be properly dissociated, even with the use of various enzymes and the livers contained too many cells, making it difficult to detect the very few tumor cells present (data not shown).

Tab. 2: Evaluation of macro-metastasis after injection of $CD24^{high}/CD44^{high}$ and $CD24^{low}/CD44^{low}$ cells into the kidney capsule of NSG mice.

	$CD44^{high}/CD24^{high}$	$CD44^{low}/CD24^{low}$
lung metastasis	1/3	0/3
liver metastasis	2/3	0/3

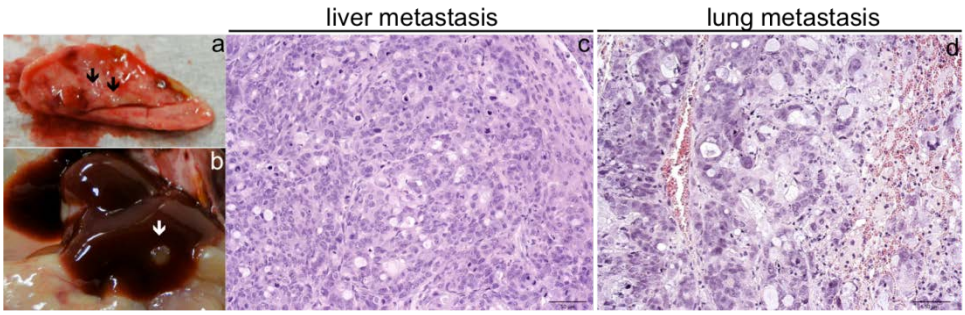

Fig. 27: Development of macrometastasis after injection of $CD24^{high}/CD44^{high}$ tumor cells. Lung (black arrows) (a) and liver metastasis (white arrow) (b) developed. H&E staining of liver- (c) and lung metastasis (d) (scale bar 50 µm).

In brief, the expression of the marker combination $CD24^{high}/CD44^{high}$ does not seem to have a significant impact on tumor growth in this experimental setting but may play a role in metastasis formation. However, the cohort of mice used in this experiment was too small to balance the biological variation of tumor growth between the different mice. Therefore further studies need to be performed to unravel the exact role of this marker combination.

6.5. Functional approach for the identification of putative cancer stem cells

To date, flow cytometry analyses of surface proteins are widely used to identify CSC markers. In most studies, panels of antibodies were screened and the existence of cancer stem cells was validated via xenograft models. While largely successful, this approach also has certain limitations. All of these markers describe only a certain phenotype that does not necessarily accurately define a functional phenotype. Consequently, a functional role for most of these proteins that would exclusively link them to stem cell function has not been demonstrated yet. As most of these proteins are also expressed on a variety of somatic cells, it is unlikely that a single marker alone has precise predictive power.

To overcome these limitations, a novel approach based on a more functional read-out has been developed for the identification of putative cancer- and/or metastasis initiating cells. This approach is based on the assumption that these cells might be in a quiescent state and therefore survive conventional therapies. Therefore novel inducible labeling techniques were used that allow the *in vitro* and *in vivo* tracking of these cells.

Slowly cycling cells can be detected *in vitro* in the CRC cultures

Primary colon cancer cells were transduced with an inducible Tet-off-H2B-GFP lentiviral reporter vector that has been generated for the detection and *in vivo*

isolation of LRCs (Falkowska-Hansen et al., 2010) (vector map see chapter 9.5.). This system allows the tracking of slowly cycling cells via Doxycyclin (Dox) treatment. In the absence of Dox, the transactivator binds to the tet-responsive element (TRE) in the promotor region of H2B-GFP and activates the GFP expression. In the presence of Dox, the transactivator changes its confirmation and does not bind to the TRE anymore. The expression of GFP is blocked. Only the cells that do not divide retain their GFP-label whereas actively dividing cells loose their label after several divisions. This method was used to track slowly cycling colorectal cancer cells *in vitro* and *in vivo*. The cells were treated for different time periods with Dox in order to analyze the growth kinetics of slowly cycling- or label-retaining cells. After specific time points, the cells were analyzed for their GFP expression via flow cytometry (Fig. 28). The signal decreased over time in proliferating cells due to the loss of the histone label. A small percentage of GFP^{high} cells remained detectable even after 10 days of Dox treatment, indicating the presence of slowly cycling cells (Fig. 28c).

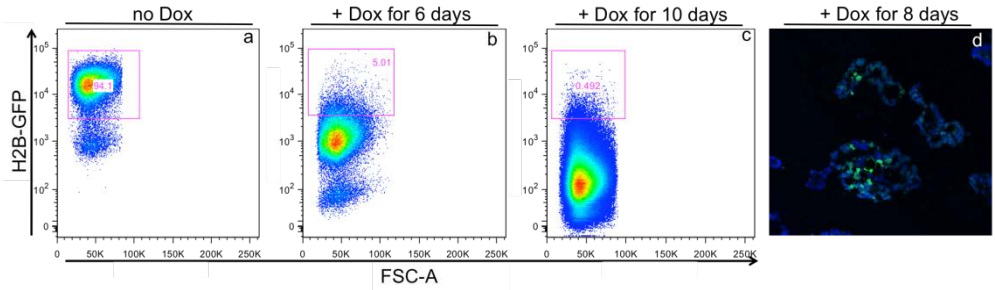

Fig. 28: Slowly cycling cells are present in primary CRC cultures (HD1858). The tumor cells were cultured with Doxycyclin (10 ng/ml) for several days. The amount of LRCs was analyzed via flow cytometry after 6 (b) and 10 days (c) of treatment and compared to controls (a). Cryosections of the spheres after 8 days in culture with Doxycyclin showed label-retaining cells (LRCs in green; Dapi in blue) (d).

A Ki-67/Hoechst staining was performed to analyze the cell cycle of the primary cell lines. Therefore the bulk population was divided into three fractions upon Dox treatment: slowly- (Fig. 29b), medium- (Fig. 29c) and fast cycling cells (Fig. 29d). This division was arbitrarily chosen. The gate for the slowly cycling cell population was defined according to the control cells not treated with Dox (H2B-GFP^{high}). The majority of the untreated cells were located in this gate. A pre-test using Ki-67/Hoechst staining revealed that the medium cycling cell population was directly adjacent to this gate. Furthermore, the fast cycling population was defined as the lower third of the bulk population.

The H2B-GFP^{high} cells (Fig. 29a) were enriched for a cell population that was in G_0 phase (55%) (Fig. 29b), when compared to medium- (44%) and fast cycling cells (31%), confirming that the slowly cycling cells were indeed more quiescent.

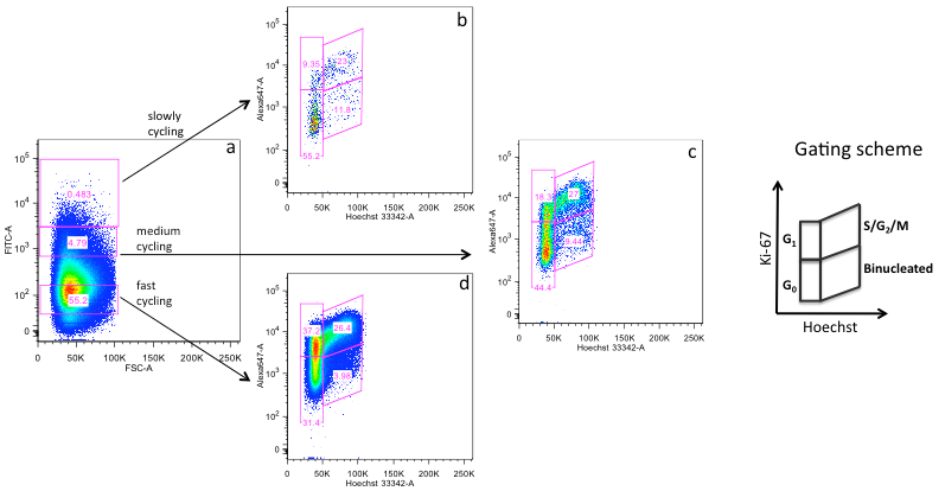

Fig. 29: Slowly cycling tumor cells are more quiescent (HD1858). The cells were treated for 10 days with Doxycycline (10 ng/ml) and a Ki67/Hoechst staining was performed (a). More than half of the slowly cycling cell population was in G_0 phase (55 %) (b), in comparison to the medium cycling population (44 %) (c) and the fast cycling population were only 31 % of the cells were in G_0 phase (d).

Slowly cycling cells are not enriched for CSC markers *in vitro* (G605 H2B/GFP)

In order to investigate whether the reported CSC-markers are enriched in slowly cycling cell populations, G605-H2B-GFP positive cells were cultured for 10 days under serum-free conditions with Dox. Flow cytometry analysis was performed for CD133- (Fig. 30b), EpCAM- (Fig. 30c), CD44- (Fig. 30d) and CD166-expression (Fig. 30e). The gating of the three different cycling populations (Fig. 30a) was performed according to the control cell line that was not treated wit Dox (data not shown).

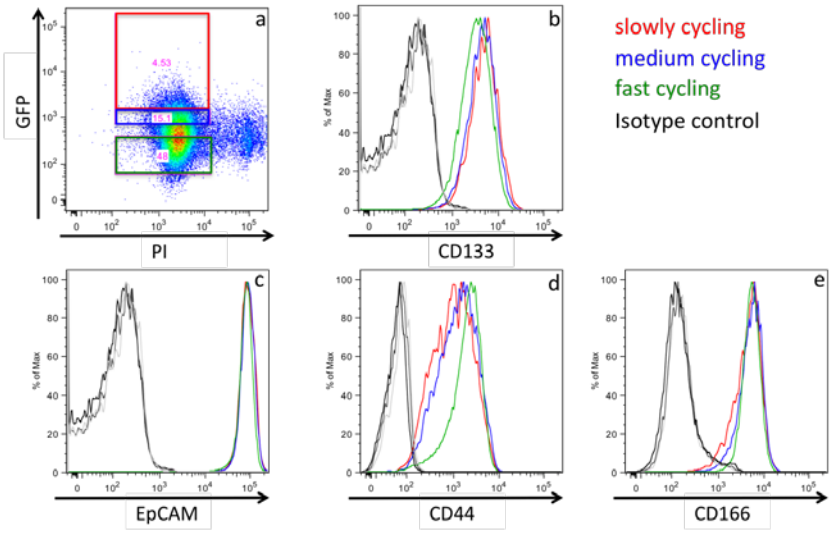

Fig. 30: CSC-markers are not enriched in slowly cycling cells. (a) The cells were treated for 10 days with Dox to separate the cells into the distinct cycling cell populations. Flow cytometry analysis was performed for (b) CD133, (c) EpCAM, (d) CD44, (e) CD166. A doublet- and dead cell exclusion were performed prior to analysis.

None of the reported CSC-markers was enriched in the slowly cycling cell population *in vitro* arguing that these cells are not enriched for phenotypically defined CSCs. A similar result was obtained for the HD1858 cell line (Appendix 9.4.). However, the *in vivo* situation might be different because the cells were cultured under serum-free conditions and the medium contained various growths factors favoring the expansion of cells with a more “stem-cell-like” phenotype. These cultured cells may have already reached the maximum expression of these markers and do not show strong differences anymore.

Slowly cycling cells expand *in vitro* after sorting

To determine the proliferative potential of the three different cycling cell populations, G650-H2B-GFP positive cells were treated with Dox for 10 days. The cells were maintained adherent in serum-free medium. Afterwards, the three cell populations were sorted according to their cell cycle speed and cultured separately under serum-free conditions (Fig. 31).

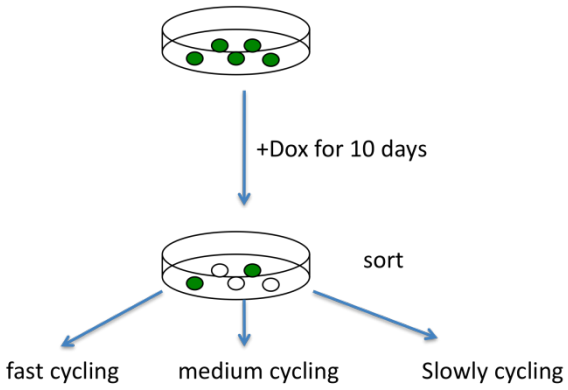

Fig. 31: Experimental set up to isolate slowly cycling cells *in vitro*. Colorectal cancer cells that express H2B-GFP were treated with Dox (10 ng/ml) for 10 days. The cells were separated into three different populations according to their cycling behavior using a cell sorter in order to functionally characterize the distinct populations.

The fast-, medium- and slowly cycling cell populations expanded *in vitro* after the sort (Fig. 32), suggesting that the slowly cycling cells are not permanently in a quiescent state.

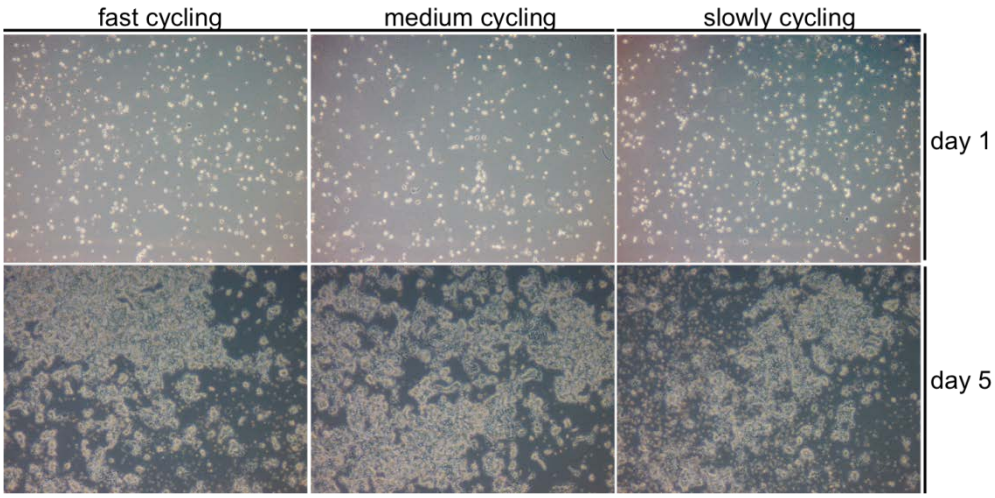

Fig. 32: Slowly cycling cells still expand *in vitro*. Fast-, medium- and slowly cycling cells were sorted after 10 days of Dox treatment and cultured under serum-free conditions. All three populations expanded *in vitro*.

Slowly cycling cells grow slower *in vitro* in comparison to fast cycling cells (G605)

As shown in Fig 29, slowly cycling cells exist *in vitro*. In order to test whether these cells are functionally different from medium- or fast cycling cells, the three distinct proliferating cell populations were sorted and 50.000 cells per population were seeded under serum-free conditions. The cells were grown adherent on collagen I coated plates and dead cells were washed away before counting. After eight days in culture, the cell number was estimated for each population (Fig. 33). The highest cell number was detected in the fast cycling population (app. 2.5 x 10^6). The medium cycling population contained 1.7 x 10^6 cells. The slowly cycling cell population accounted for the lowest cell number with 1.1 x 10^6 cells. This result indicates that the cycling behavior of the cells might be stable for at least eight days *in vitro* after the sort.

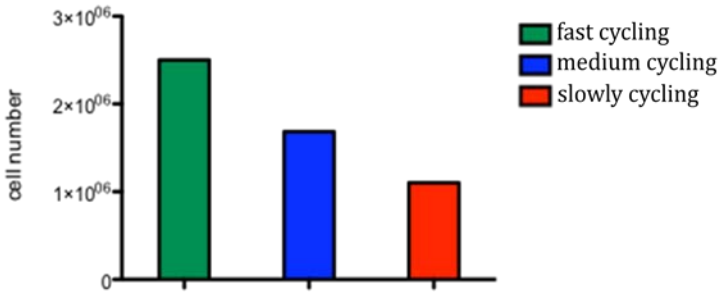

Fig. 33: The different cycling populations retain their initial cycling phenotype for one week *in vitro*. Fast-, medium- and slowly cycling cells were sorted and cultured under serum-free conditions (50.000 cells/well/population). The cell number of each population was determined after eight days in culture (n=1).

Slowly cycling cells are less clonogenic than fast cycling cells *in vitro*

Clonogenicity is a read-out that characterizes the ability of a single cell to grow into a colony (Franken et al., 2006). HD1858-H2B-GFP expressing cells were maintained in adherent serum-free cultures. Fast-, medium- and slowly cycling cells were sorted after 10 days of Dox treatment and 12.000 cells per population were seeded for additional six days on collagen I coated plates. Afterwards, the cells were fixed with glutaraldehyde (6.0% v/v) and stained with crystal violet (0.5% w/v) according to the protocol of Franken and colleagues (Franken et al., 2006) (Fig. 34a-c). In order to determine the colony number and sizes, Image J particle count was used. The fast cycling cell population showed higher clonogenic capacities in comparison to the medium- and slowly cycling population (Fig. 34d). This result is in line with the cell number count of the distinct sorted cell populations of the G605-H2B-GFP cell line depicted in Fig. 33, indicating that the initial cycling behavior is preserved at least over one week in culture.

In addition, the average colony sizes were measured using Image J (Fig. 34e). The average colony sizes were slightly lower in the slowly cycling cell population in comparison to the medium- and fast cycling cell populations. These results suggest that the slowly cycling cells retain their initial phenotype at least for six days *in vitro* after the sort. However, the experiment needs to be repeated, to confirm this result.

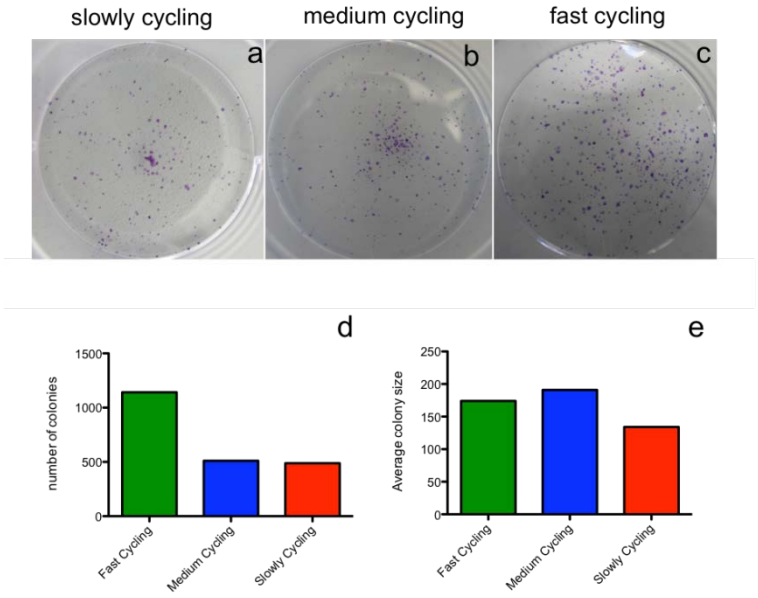

Fig. 34: Slowly cycling cells are less clonogenic *in vitro*. Fast-, medium- and slowly cycling cells were sorted upon 10 days of Dox (10 ng/ml) treatment *in vitro*. The sorted cell populations were reseeded under adherent, serum-free conditions. Six days later the cells were fixed and stained with crystal violet (a-c). The colony numbers (d) and sizes (e) of the different cell populations were estimated via Image J particle count (n=1).

Furthermore, a different assay was performed to assess the clonogenicity of the G605 cells. Therefore different amounts of cells ranging from 1 to 2048 were sorted in 8 technical replicates into 96-well plates (Fig. 35). The cells were separated into fast-, medium- and slowly cycling populations after culturing with Dox for 10 days.

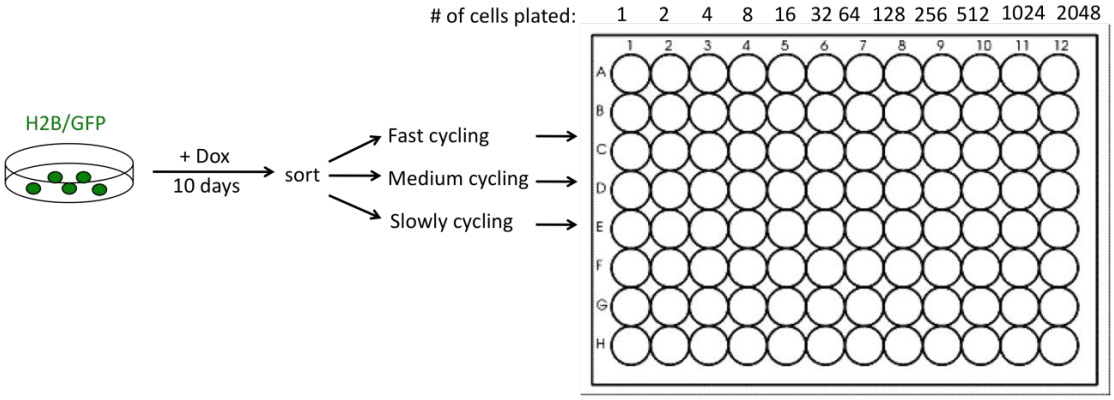

Fig. 35: Experimental set up to determine the *in vitro* clonogenicity of the G605-H2B-GFP cell line. The tumor cells were cultured with Dox for 10 days and sorted for slowly-, medium- and fast cycling cells. Different amounts of cells, ranging from 1 to 2048, were seeded into 96-well plates and the cell growth was monitored microscopically. Eight replicates per cell number were analyzed.

The growth of the sorted cells was monitored via the microscope. Wells containing colonies were counted as positive and wells without growing colonies were counted as negative result. In order to estimate the clonogenicity of the different cell populations, the ELDA-software (Extreme Limiting Dilution Analysis: (http://bioinf.wehi.edu.au/ software/elda/) was applied (Hu and Smyth, 2009).

Tab. 3: Confidence Intervals of 95% for the active cell frequency in each population group. Slowly cycling cells are less clonogenic than medium- and fast cycling cells.

Group	Lower Estimate	Estimate	Upper Estimate
Fast cycling	2.32	1.59	1.22
Medium cycling	2.92	1.97	1.43
Slowly cycling	5.15	3.38	2.30

The ELDA software was used to calculate the active cell frequency in a 95% confidence interval (Tab. 3). The result indicates that the slowly cycling cells are less clonogenic (1 in 3.38 cells) than the medium- (1 in 1.97 cells) or fast cycling cells (1 in 1.59 cells). There was a significant difference between all the groups (p=0.0126). However all three populations were highly clonogenic, which might be due to the culture medium that contained numerous growth factors and therefore enriched already for cancer stem cells. Furthermore, pair wise group differences were

estimated. Slowly cycling cells were significantly different from fast cycling cells (p = 0.00449) in terms of clonogenicity (Tab. 4).

Tab. 4: Pairwise group difference between fast-, medium- and slowly cycling cells.

Group 1	Group 2	Chisq	Pr(>Chisq)
Fast cycling	Medium cycling	0.747	0.387
Fast cycling	Slowly cycling	8.07	0.00449
Medium cycling	Slowly cycling	3.61	0.0574

All cycling cell populations are able to regenerate slowly-, medium- and fast cycling cells *in vitro* (G605)

In order to analyze whether all cells are capable of generating all three different cell types again the following experimental set up was performed:
The colon cancer cell lines were cultured with Dox for 10 days and the different cycling cell populations were sorted according to the established gating scheme (Fig. 29a). After the sort, the different populations were cultured separately without Dox in order to relabel all the cells with H2B-GFP. Afterwards, the cells were treated again with Dox for eight days and the amount of LRCs was analyzed via flow cytometry (Fig. 36).

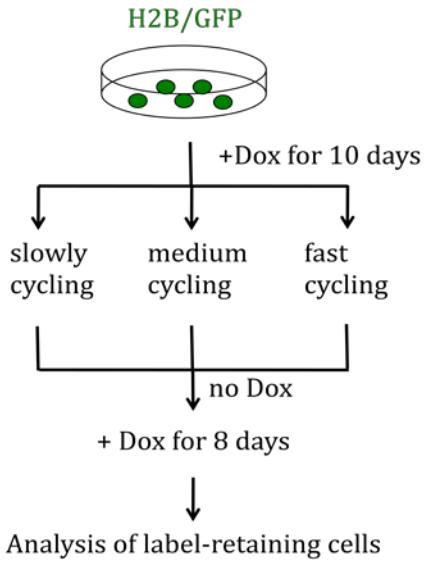

Fig. 36: Experimental set up to analyze the regeneration capacity of the distinct cycling cell populations *in vitro*. Colorectal cancer cells transduced with the inducible tet-Off-H2B-GFP lentiviral vector system were treated with Dox (10 ng/ml) for 10 days. The cells were separated in 3 different populations according to their cycling behavior and reseeded without Dox to relabel all the cells. Afterwards, the cells were treated again with Dox for 8 days and the label-retention was analyzed.

All the three sorted cell populations were able to regenerate fast-, medium- and slowly cycling cells *in vitro* (Fig. 37a-c). However, the sorted slowly- and medium

cycling cells gave rise to approximately 5% of label-retaining cells (Fig. 37a and b) whereas the fast cycling population regenerated only around 2% of label-retaining cells (Fig. 37c).

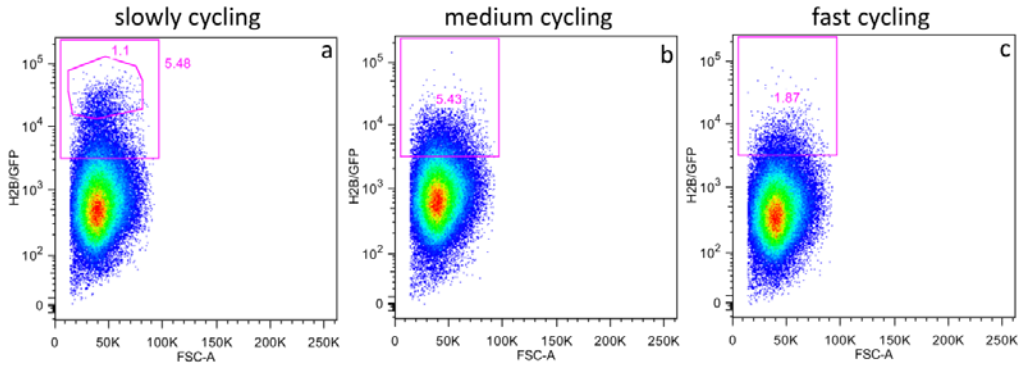

Fig. 37: Fast-, medium- and slowly cycling cells are able to regenerate all distinct cycling populations *in vitro*. The distinct cycling cell populations were sorted upon 10 days of Dox treatment *in vitro* and reseeded without Dox for several days. Dox treatment was reapplied to the cells for 8 days and the amount of LRCs was estimated for each population (a-c). Doublet- and dead cell exclusion were performed (PI) prior to analysis.

This finding indicates that the phenotypic differences regarding cell growth and clonogenicity observed in the previous experiments might only be transient. Slowly cycling cells are able to reenter the cell cycle and fast cycling cells are able to enter a more slowly cycling state suggesting a dynamic switch between the different cell cycle states within each population.

Some LRCs loose their ability to switch off H2B-GFP expression under Dox treatment (G605)

The three sorted cycling cell populations were cultured for 22 days with Dox (10 days Dox before the sort + 12 days Dox after the sort) in order to detect whether long-term LRCs may be present among the slowly cycling cells. Surprisingly, a small population of GFP^{high} expressing cells of around 1% was detected within the slowly cycling cell population (Fig. 38a), while in the other two populations such potential long-term LRCs were not present (Fig. 38b-c).

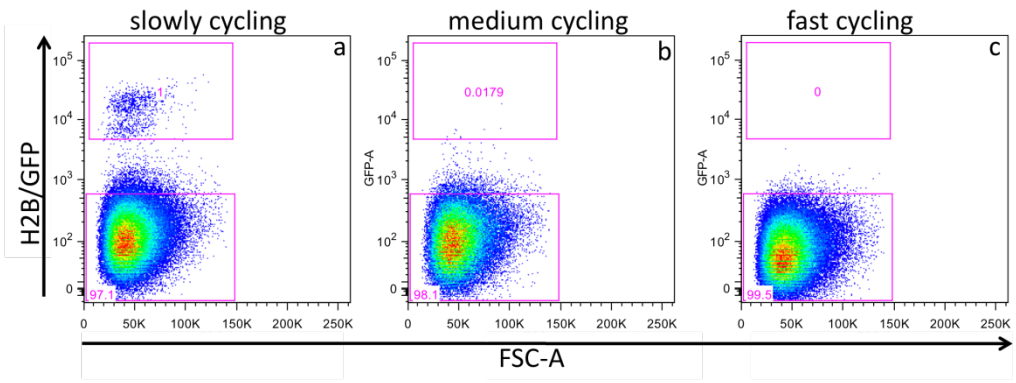

Fig. 38: A small population of slowly cycling cells retains the H2B-GFP label *in vitro*. The distinct cycling cell populations were sorted after 10 days of Dox treatment *in vitro*. The sorted cell populations were reseeded and the amount of LRCs was estimated for each population after additional 12 days of Dox treatment (10 days prior to sort and 12 days post sort) (a-c). Doublet- and dead cell exclusion were performed (PI) prior to analysis.

In order to test whether this small population of GFP^{high} expressing cells is indeed a highly dormant long-term label-retaining population, a cell cycle analysis was performed. The cells were harvested, fixed and stained with a human specific anti-Ki-67 antibody and Hoechst (Fig. 39). There was no difference in cell cycle behavior between cells that have lost their GFP label (Fig. 39c) and GFP^{high} expressing cells (Fig. 39b) upon 22 days of Dox treatment. The putative long-term LRCs were not enriched in G_0-phase indicating that this population presents rather an artifact than a long-term label-retaining population.

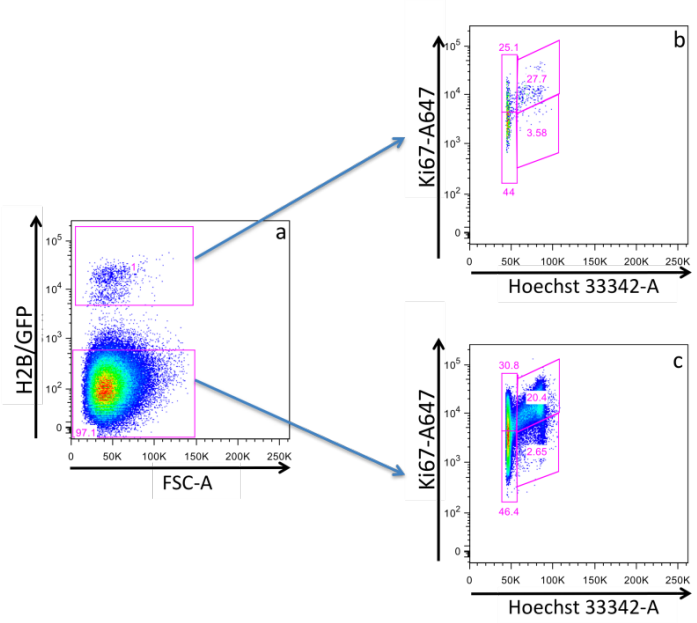

Fig. 39: No difference in cell cycle behavior between slowly cycling cells that retained the GFP-label and slowly cycling cells that actively divided and lost their GFP-label. a) Ki-67/Hochst staining was performed on sorted slowly cycling cells that were cultured with Dox for 22 days (10 days prior to sort and 12 days post sort). b) Putative long-term LRCs and c) initially slowly cycling cells (that lost their GFP label upon long-term Dox treatment), show a similar cell cycle distribution.

In addition to the cell cycle analysis, the putative long-term LRCs were sorted and cultured with Dox (Fig. 40). The cells expanded and still kept their GFP-label. The results from the Ki-67/Hoechst staining and from the sort indicate that fast- and slowly cycling cells are present in the same population.

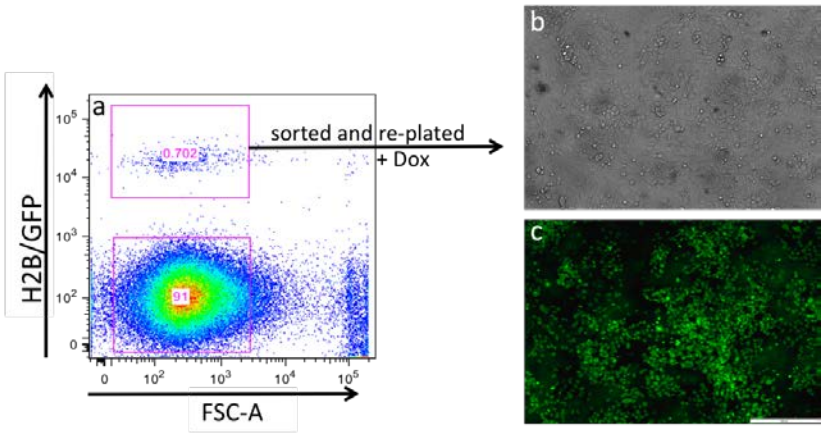

Fig. 40: A small artifact of LRCs is present in the slowly cycling cell population. Long-term label-retaining cells were sorted (a) and re-cultured with Dox. The cells actively divided and still retained their GFP-label (b-c).

However, the cells that constitutively express GFP represent a very small population that appeared only after the first sort of slowly cycling cells. Moreover, this population contaminates the slowly cycling population with cells that do not belong to this population. Therefore it even strengthens the differences observed between the different cycling cell populations.

Generation of sublines derived from single cell clones sorted from fast-, medium- and slowly cycling cells (G605)

To test whether the observed phenotype of the three different cycling cell populations was more stable in cell lines derived from single cell clones, the following experimental set up was performed (Fig. 41):

G605 H2B-GFP expressing cells were maintained for 10 days with Dox *in vitro* under adherent conditions in serum-free medium. Afterwards, fast-, medium- and slowly cycling cells were sorted as single cells into 96-well plates. Each well was analyzed manually using a microscope to verify the presence of a single cell per well (Fig. 42). The single cells were expanded into sublines, which were analyzed afterwards for their capability to regenerate fast-, medium- and slowly cycling cells.

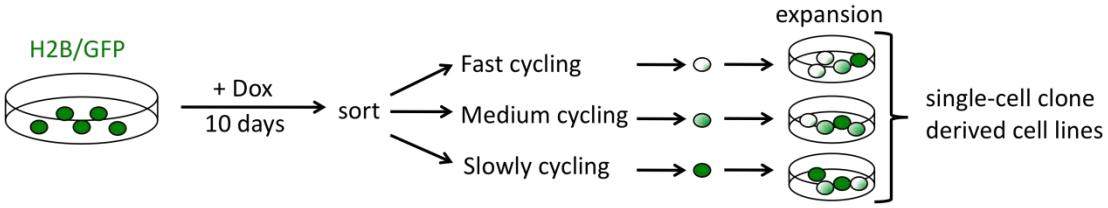

Fig. 41: Experimental set up to analyze the regeneration capacity of single cell clone derived cells *in vitro*. G605 H2B-GFP+ cells were cultured for 10 days with Dox (10 ng/ml). Fast-, medium- and slowly cycling cells were sorted as single cells into 96-well plates. These single cells were expanded into cell lines and afterwards analyzed for their ability to regenerate fast-, medium- and slowly cycling cells.

It was possible to expand single cells derived from each cycling cell population into sublines. However, in the fast cycling population seven out of eight single cells could have been expanded into cell lines whereas only four out of seven single cells were able to expand from slowly cycling cells. Furthermore, the colonies of the fast cycling cell population were much bigger 21 days after the sort than the colonies of the medium- and slowly cycling cells (Fig. 42), indicating again that the initial cycling behavior is retained *in vitro* over a short period of time.

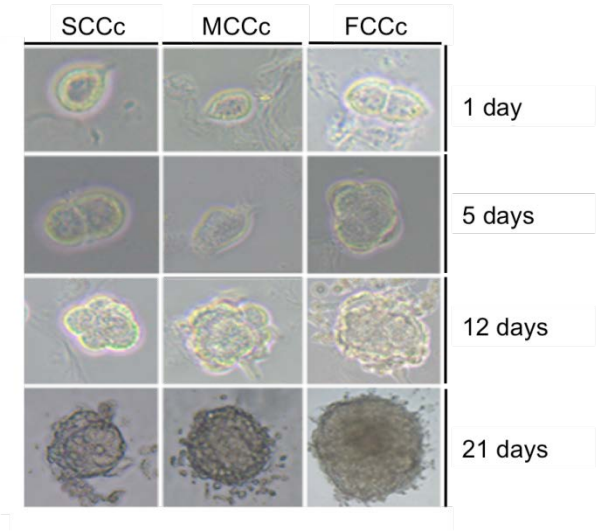

Fig. 42: Sorted single cells derived from fast-, medium- and slowly cycling cells expand *in vitro*. Single cells from all three cycling cell populations were sorted after 10 days of Dox treatment. The presence of the single cells was confirmed via microscopy. The growth of the single cells was monitored at specific time points after the sort (SCCs = slowly cycling cells; MCCs = medium cycling cells; FCCs = fast cycling cells).

After expansion of the sorted single cells, 100.000 cells per population were seeded under serum-free conditions on collagen I coated plates. Eight days later, the cell number was determined (Fig 43.). As already shown in Fig. 33, the single cell derived cell lines showed a similar behavior like the sorted populations. The fast cycling cells grew faster in comparison to the medium- and slowly cycling cell populations.

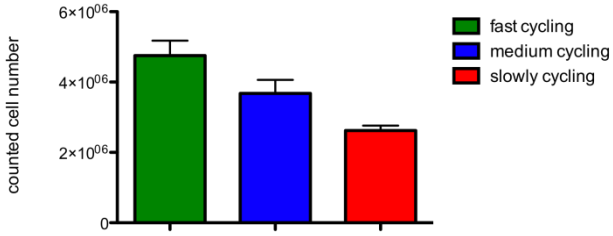

Fig. 43: Single cell derived fast-, medium- and slowly cycling cell lines retain their initial cycling phenotype *in vitro* for eight days. 100.000 cells from each subline generated from single fast-, medium- and slowly cycling cells were seeded on collagen I coated plates and were maintained in serum-free medium. The cell number was determined eight days later (n=3, technical replicates, SEM).

In summary, several independent *in vitro* experiments, such as the Ki-67/Hoechst stainings and the clonogenicity assays have been performed for both cell lines. All of them showed that different cycling cell populations were present in the cultures and their initial cycling phenotype was maintained over several days *in vitro*. Sorted slowly cycling cells were less clonogenic than the fast cycling cells. However, the distinct cycling phenotypes may only be transiently stable as all the three distinct cycling populations were able to expand and to regenerate fast-, medium- and slowly cycling cells, suggesting a dynamic switch between the distinct cell populations.

6.6. The influence of the microenvironment on slowly cycling cells

As shown in the previous sections, cells with different cell cycle rates were detected *in vitro*. The cells retained their cycling behavior over a short period of time *in vitro*. However, after more than 10 days in culture all cells lost their GFP-label and divided. The *in vitro* system enables the study of intrinsic effects on the tumor cells. As a tumor is a complex structure composed of many different cell types like fibroblasts, endothelial- and immune cells (see chapter 4.7.), the interactions between these cells and the tumor cells may influence their cycling behavior. In addition, oxygen- and nutrition deprivation might regulate tumor growth and may maintain tumor cells in a dormant state. Therefore it is crucial to analyze the existence and functionality of LRCs or slowly cycling cells *in vivo*. For the *in vivo* experiments, the G605 cell line was chosen due to its higher tumorigenicity and its ability to metastasize to the lungs and liver, allowing the analysis of the primary tumor and the metastasis at the same time.

Slowly-, medium- and fast cycling cells are able to generate a tumor *in vivo*

In order to determine whether the different cycling cells present in the culture system are functionally different in a xenograft model, the colon cancer cells (G605 H2B-GFP^{+}) were cultured for 10 days with Dox and the fast-, medium- and slowly cycling cells were sorted. Afterwards 50.000 cells (5 mice per group) were injected into the kidney capsule of highly immunocompromised NSG mice (Fig. 44).

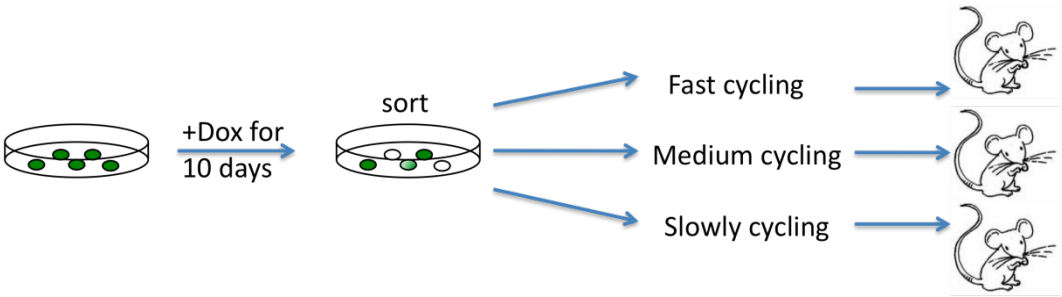

Fig. 44: Experimental set up for the functional analysis of fast-, medium- and slowly cycling cells *in vivo*. Colon cancer cells (G605 H2B-GFP+) were maintained *in vitro* for 10 days with Dox (10 ng/ml). The cells were maintained adherent in serum-free medium. The cells were sorted for fast-, medium and slowly cycling cells and injected into the kidney capsule of NSG-mice. Tumor growth was analyzed after 3 months.

Approximately 3 % of the cells were considered as slowly cycling cells according to the gate of the positive control not treated with Dox (Fig. 45a and b). The lower 15 % of the cell population were regarded as medium cycling and the lowest 46 % as fast cycling cells (Fig. 45b). This separation scheme was established after cell cycle analysis using a human specific anti-Ki-67 antibody and Hoechst. The sorted populations were re-analyzed to assess the purity of the sort. All three populations were properly separated (Fig. 45c).

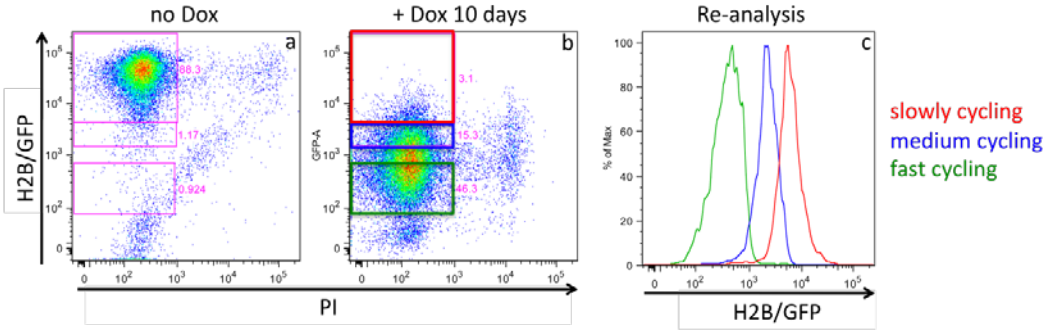

Fig. 45: Sorting scheme of fast-, medium- and slowly cycling cells. Colon cancer cells not treated with Dox were used as a control (a). Colon cancer cells treated for 10 days with Dox were sorted for fast-, medium- and slowly cycling cells according to the three gates (b). A re-analysis was performed after sorting (c). Doublet- and dead cells exclusion (PI) were performed.

Furthermore, the sorted populations were evaluated for their cell cycle status prior to transplantation via Ki-67/Hoechst staining (Fig. 46). The slowly cycling cells were indeed more quiescent with more than 60% of the cells being in G_0 phase (Fig. 46b) in comparison to the fast cycling population with only 38 % of the cells being in G_0 (Fig. 46d).

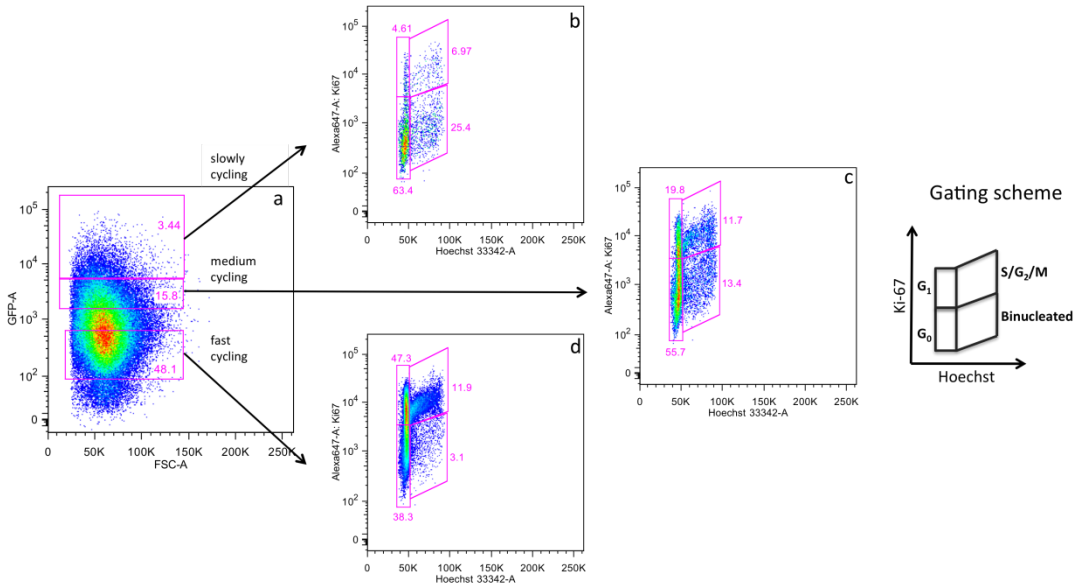

Fig. 46: Slowly cycling sorted and injected colon cancer cells were more quiescent. The sorted cells were stained with a human specific anti-Ki-67 antibody and Hoechst 33342 to verify the quiescent phenotype of the slowly cycling cells. b) Slowly cycling cells were more in G_0 phase (63.4 %) than c) the medium cycling (55.7 %) and d) the fast cycling cells (38.3 %).

Three months after injection of the tumor cells, the mice were euthanized and the tumor growth was evaluated via caliper measurements. Tumors grew in all three groups of mice independent of the initial cell type transplanted. In the fast cycling group two out of six (33%) mice developed tumors, whereas two out of five mice (40%) harbored tumors in the slowly cycling group. One out of five (20%) mice showed a tumor formation in the medium cycling group (Fig. 47).

Interestingly, the mean tumor volume was higher in mice injected with initially slowly cycling cells compared to the medium- or fast cycling population (Fig. 47). However, there was no significant difference between the groups and the variations in each group were too high. Nevertheless, the results show that the slowly cycling cells are able to generate tumors comparable in size to fast cycling cells and thus most likely have the potential to regenerate fast cycling cells.

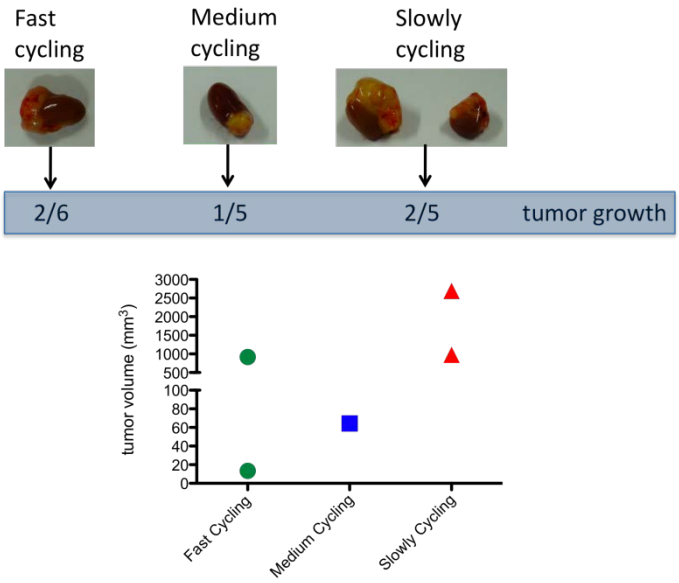

Fig. 47: All different cycling cell types are able to generate tumors *in vivo*. After 10 days of culture with Dox (10 ng/ml), fast-, medium- and slowly cycling cells were sorted. 50.000 cells of the different populations were injected into the kidney capsule of NSG mice. The tumor volume was measured using a caliper 3 months after injection.

Further analyses need to be performed in order to determine whether the onset of tumor growth is different between the distinct cell populations. Moreover, limiting dilution transplantation assays would give more insight into frequency of tumor initiating cells contained in each cell population.

Kinetics of slowly cycling colorectal tumor cells *in vivo*

In all experiments performed so far, the tumor cells were cultured with Dox and sorted afterwards to investigate their functionality either *in vitro* or *in vivo*. The selection of the distinct cycling cell populations was based on this culture system. However, the kinetics of the slowly cycling cells might be changed in the context of a tumor. Probably a specific niche is needed to retain a pool of slowly cycling cells as shown for normal adult stem cells (see chapter 4.9.).

To investigate the role of slowly cycling cells in an established tumor, the bulk of the tumor cells (G605 H2B/GFP^{+}) was injected into the kidney capsule of NSG-mice. The mice were palpated weekly and after detection of a tumor, the mice were treated with Dox (2 g/l) in the drinking water. The tumors were harvested at different time points and digested with collagenase (0.25 %) and DNase for approximately 1 hour at 37°C in order to generate single cell suspensions. The tumor cells were purified via a density gradient using Optiprep™ and the presence of slowly cycling cells was analyzed via flow cytometry (Fig. 48).

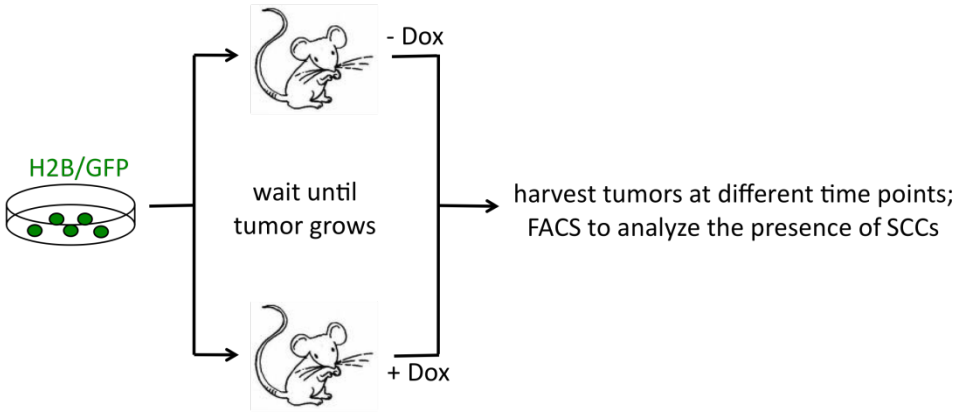

Fig. 48: Experimental set up for the analysis of the kinetics of SCCs *in vivo*. The bulk of the G605 H2B-GFP^{+} tumor cells was injected into the kidney capsule of NSG mice. After palpation of a tumor, the mice were treated with Dox (2 g/l) in the drinking water. The tumors were harvested at different time points and the presence of SCCs was determined via FACS (SCCs = slowly cycling cells).

Prior to the analysis of slowly cycling cells, a doublet-exclusion was performed (Fig. 49b). Additionally, propidium iodide was added to exclude dead cells (Fig. 49c). Some tumor bearing mice were not treated with Dox and were used as controls (Fig. 49d, green curve). The first tumor was harvested after five days of Dox treatment. A small shift in the GFP signal was observed. A small population of the cells divided already several times and lost their label completely (Fig. 49d, yellow curve). After 12 days of Dox treatment, the GFP signal shifted even more towards the left site and became broader (Fig. 49d, blue curve). Fifteen days after Dox treatment, most of the tumor cells divided and only a small population of approximately 7 % retained the high GFP-label and did not divide (Fig. 49d, orange curve). The slowly cycling population was completely lost after 22 days of Dox treatment (Fig. 49d, black curve), indicating that all cells had divided. This result suggests that there are no long-term LRCs present in a tumor or at very low frequencies. However, this is only a snap shot of a tumor at a certain time point. Probably the cells are dynamic and are able to reenter dormancy even though they divide at the beginning. For further experiments, 15 days of Dox treatment was chosen because at this time-point the distribution of the GFP intensity was very broad enabling a proper selection of the fast-, medium- and slowly cycling cells. Nonetheless, this finding needs to be verified in additional primary tumor cell lines.

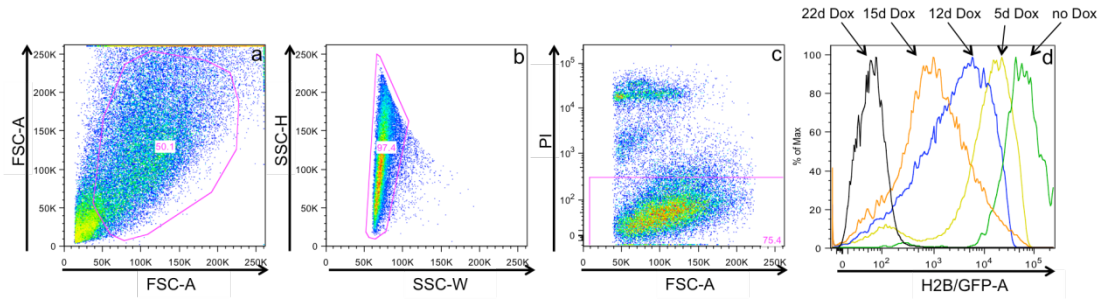

Fig. 49: Kinetics of slowly cycling cells *in vivo*. Tumor bearing mice (injected with G605 H2B-GFP cells) were treated with Dox (2 g/l) in the drinking for different time periods. The tumors were harvested at different time points, dissociated into single cell suspensions and analyzed for the presence of slowly cycling cells (GFP expression) via flow cyctometry (a). Doublet (b)- and dead cell exclusion (c) were performed. Green curve: positive control, tumor without Dox treatment; yellow curve: 5 days of Dox treatment prior to analysis; blue curve: 12 days of Dox treatment prior to analysis; orange curve: 15 days of Dox treatment prior to analysis; black curve: 22 days of Dox treatment prior to analysis (d).

In addition to the flow cytometry analysis, immunohistochemistry stainings using a human specific anti-Ki-67- and anti-GFP antibody were performed. The two stainings were mutually exclusive in specific areas of the tumors (Fig. 50b-d, black arrow: GPF+ and red arrows: Ki-67+) further supporting the findings of the Ki-67/Hoechst stainings of the cell lines. The GFP positive cells do not divide and therefore are negative for Ki-67. Although the same tumor areas were stained in serial sections, one must be aware that these IHC stainings do not allow the analysis of one single cell in both stainings simultaneously, due to the thickness of the cuts. Therefore immunofluorescence stainings would be necessary. However, the stainings show that Ki-67- and GFP positive cells are evenly distributed and located next to each other (Fig. 50c and d, green arrows), indicating that Dox reached all the parts of the tumor equally.

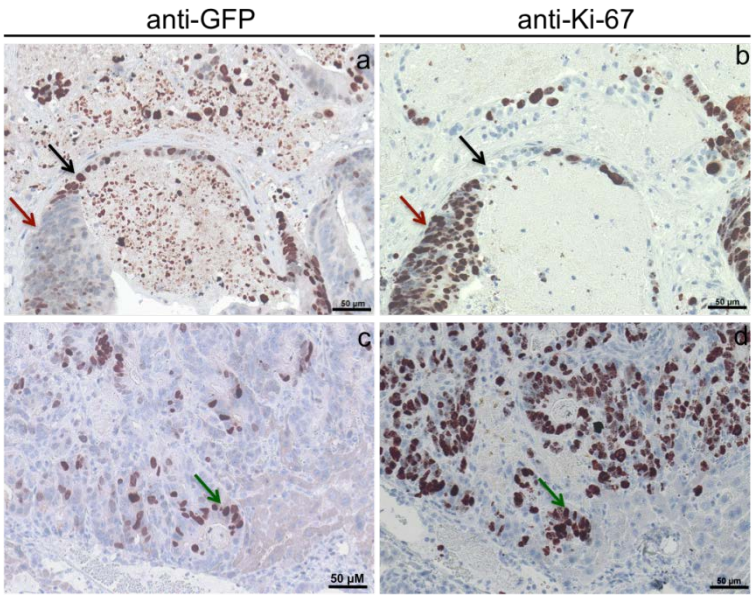

Fig. 50: Slowly cycling cells are present in tumors *in vivo*. Tumor bearing mice were treated with Dox (2 g/l) in the drinking for 15 days. Immunohistochemistry was performed on sections of the paraffin embedded tumor using an anti-GFP antibody (b and d) and a human specific anti-Ki-67 antibody (c and e). The two stainings were mutually exclusive (black arrow: GFP^+ and $Ki\text{-}67^-$; red arrow: GFP^- and $Ki\text{-}67^+$; b and c). The GFP^+ and the $Ki\text{-}67^-$ areas were located next to each other (green arrows, c and d).

Furthermore, the mice developed lung metastasis upon injection of tumor cells into the kidney capsule. The presence of slowly cycling cells in the metastases was analyzed via immunohistochemistry. The lungs were embedded in paraffin, sectioned and stained with an anti-GFP- and a human specific anti-Ki-67 antibody. The lung metastases depicted in Fig. 51 correspond to the primary tumor shown in Fig. 50. The metastasis contained only very few slowly cycling cells (Fig. 51a and c) as indicated by lower GFP intensities and most of the metastatic foci showed no nuclear GFP staining. This result indicates that most of the tumor cells in the lungs divided actively during the time of Dox treatment. The actively dividing state of the cells was confirmed by the Ki-67 staining (Fig. 51b and d). Most of the tumor cells were positive for this marker. Moreover, this result seems to differ from the primary tumor where approximately 7% of label-retaining cells were detected at the same time (Fig. 53e). However, more cases need to be studied and an exact quantification is needed to confirm this observation.

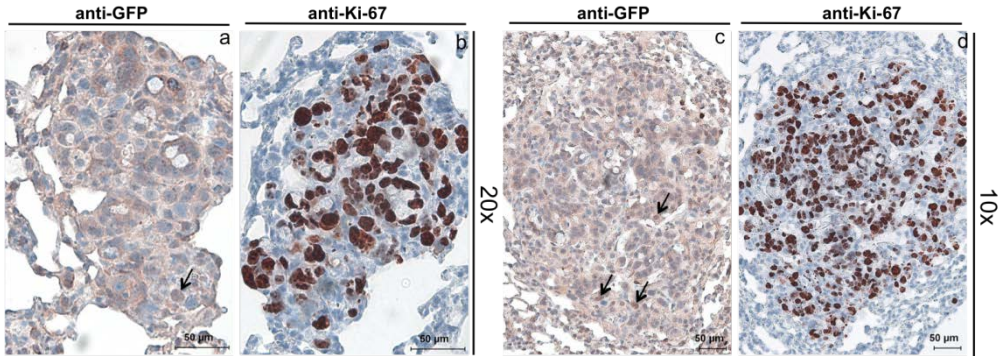

Fig. 51: The frequency of Slowly cycling cells appears to be lower in lung metastasis when compared to the primary tumor. Tumor bearing mice were treated with Dox (2 g/l) in the drinking for 15 days. The lungs were harvested and immunohistochemistry was performed using an anti-GFP antibody (a and c) and a human specific anti-Ki-67 antibody (b and d). Only very few slowly cycling cells were present in the lungs (black arrows). Most of the tumor cells were positive for Ki-67.

Pre-selected slowly-, medium- and fast cycling cells from a tumor regenerate tumors in secondary transplants

The previous experiments demonstrated that the different cycling cell populations preselected *in vitro* developed into a tumor independent of their initial cycling rate. To test whether the distinct cell populations preselected *in vivo* have different functions regarding tumor growth, the following experiment was performed (Fig. 52):

the bulk of the G605-H2B-GFP$^+$ cells was injected into the kidney capsule of NSG mice. After palpation of a tumor, the mice were treated with Dox in the drinking water for 15 days and the tumors were harvested. Moreover, the tumors were digested into single cell suspensions using collagenase and DNase and slowly-, medium- and fast cycling cells were sorted according to their GFP expression. The three different cell populations were transplanted again into secondary recipients (50.000 cells/mouse, 5 mice per group).

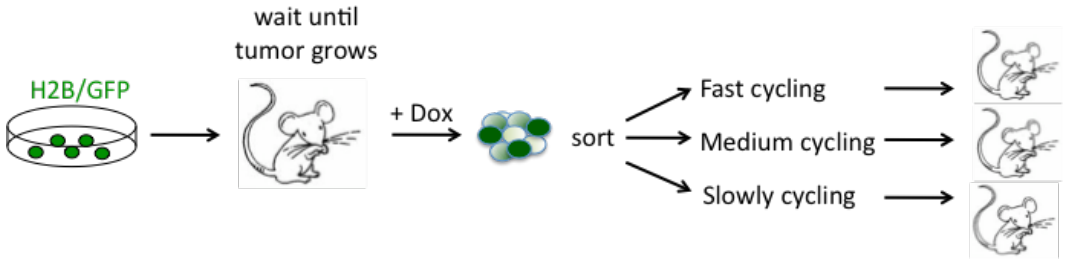

Fig. 52: Experimental set up for functional analysis of slowly-, medium-, and fast cycling cells preselected from a xenograft. The bulk of G605-H2B-GFP$^+$ cells was injected into the kidney capsule of NSG mice. After tumor growth, mice were treated wit Dox (2g/l) for 15 days and the different cycling cell populations were sorted and reinjected into the kidney capsule of secondary recipients in order to analyze their tumor growth capacities.

The tumor harvested for this experiment had a volume of 5.6 cm^3. Prior to the sort, a doublet- and dead cell exclusion (PI) were performed (Fig. 53b and c). In order to select only for human colorectal tumor cells an anti-HLA antibody was included in the analysis. Moreover, the tumor cells were stained with an anti-H2kD antibody to determine the amount of murine cells contained in the tumor (Fig. 53d). More than 80% of the tumor cells were of human origin. Less than 20% of the cells were infiltrating murine cells (Fig. 53d). Afterwards the slowly-, medium- and fast cycling cell populations were sorted according to the gating scheme in Fig. 53e and further transplanted into secondary recipient mice (50.000 cells per mouse; n=5/group). For this tumor, seven percent of the cells did not divide during the 15 days of Dox treatment whereas about nine percent of the tumor cells divided for several times and lost their GFP label completely (Fig. 53e). To ensure that the sort was pure a small aliquot of each sorted cell population was reanalyzed on the same cell sorter. As depicted in Fig. 53f the populations were efficiently separated.

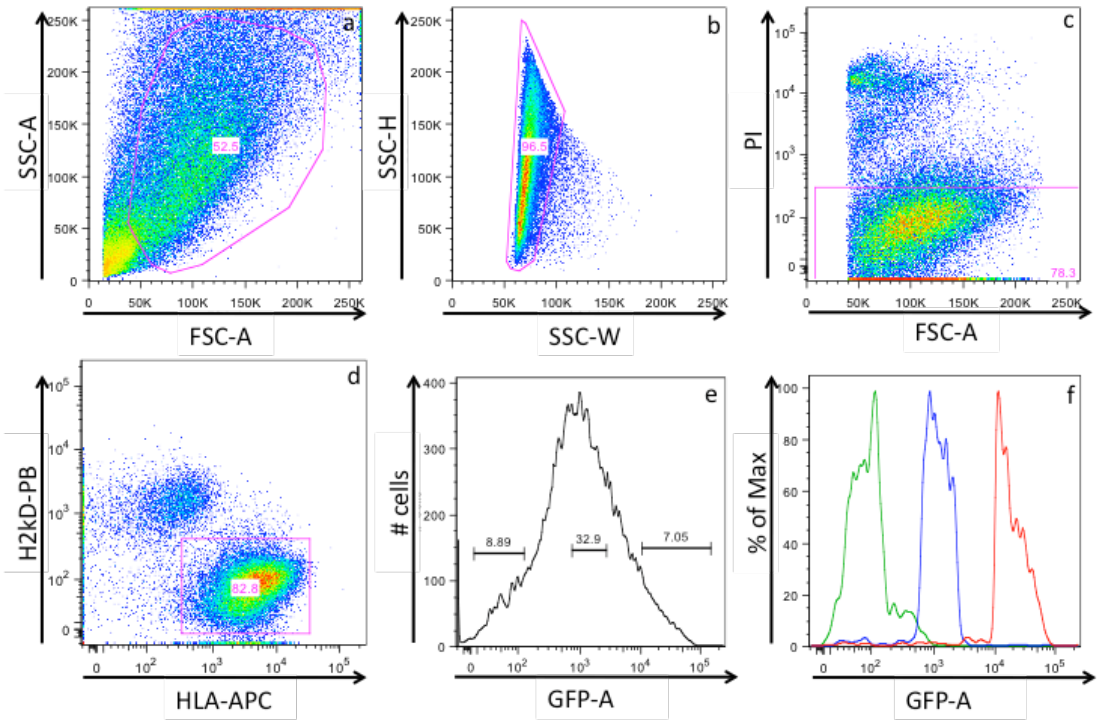

Fig. 53: Gating scheme of a xenograft treated with Dox for 15 days. Doublet- (b) and dead cell exclusion (c) were performed. The cells were stained with anti-mouse H2kD-PB- and anti-human HLA-APC FACS-antibodies (d). Only human cells were included in the analysis. Slowly-, medium- and fast cycling cells were sorted (e). A re-analysis was performed after the sort. All the three populations have been sufficiently separated (green = fast cycling; blue = medium cycling; red = slowly cycling) (f).

The secondary recipients were euthanized after two months and the total tumor volume was evaluated via caliper measurements (Fig. 54a-d). This measurement includes the primary tumor and the lymph node metastases (LN-metastases). All the three sorted cell populations generated tumors in the secondary recipients (Tab. 5). In the fast- and medium cycling cell population, a tumor take rate of 100% was reached whereas the tumor take rate of the slowly cycling cells was 80%. LN-metastases were detected only in the fast- and medium cycling cell population. The tumor volumes were very variable in the different groups with no significant difference between the groups.

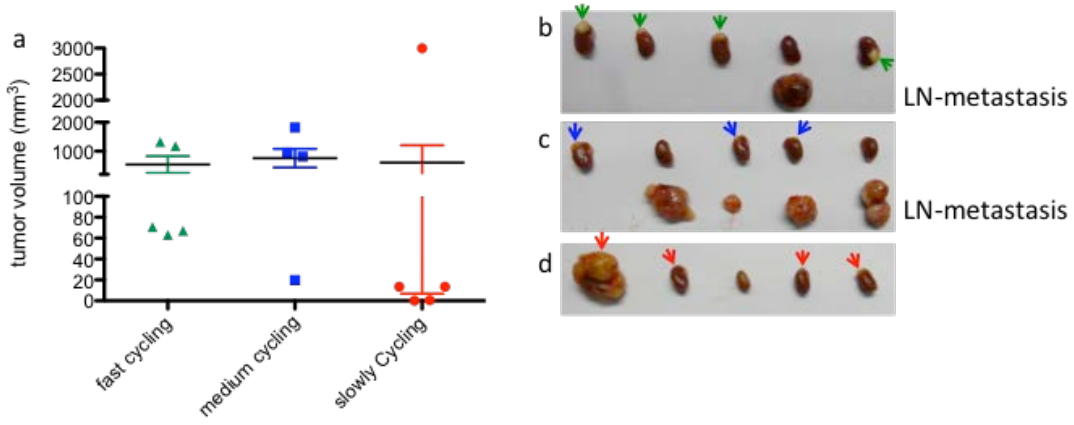

Fig. 54: All different cycling cell types preselected *in vivo* are able to generate a tumor in secondary recipients. Tumor bearing mice were treated for 15 days with Dox and fast-, medium- and slowly cycling cells were sorted. 50.000 cells per population were injected into the kidney capsule of NSG mice. (a) The total tumor volume (primary tumor + LN-metastasis) was measured using a caliper 2 months after injection. Tumors and LN-metastasis grown in the kidneys from (b) fast cycling cells (green arrows), (c) medium cycling cells (blue arrows), (d) slowly cycling cells (red arrows). The tumor volumes were not significantly different between the three groups (ANOVA; p=0.9326).

Tab. 5: Frequency of tumor growth in secondary recipient mice (including LN-metastasis).

Group	Total tumor burden/number of mice
Fast cycling	5/5
Medium cycling	5/5
Slowly cycling	4/5

In order to determine whether the morphology of the tumors generated by the different cell populations was similar, H&E stainings of the tumor sections were performed. Independent of the cell population injected, all the xenografts showed similar morphologies. The tumor cells formed glandular structures (Fig. 55d-f, black arrows) and stromal cells were recruited (Fig. 55a-c)

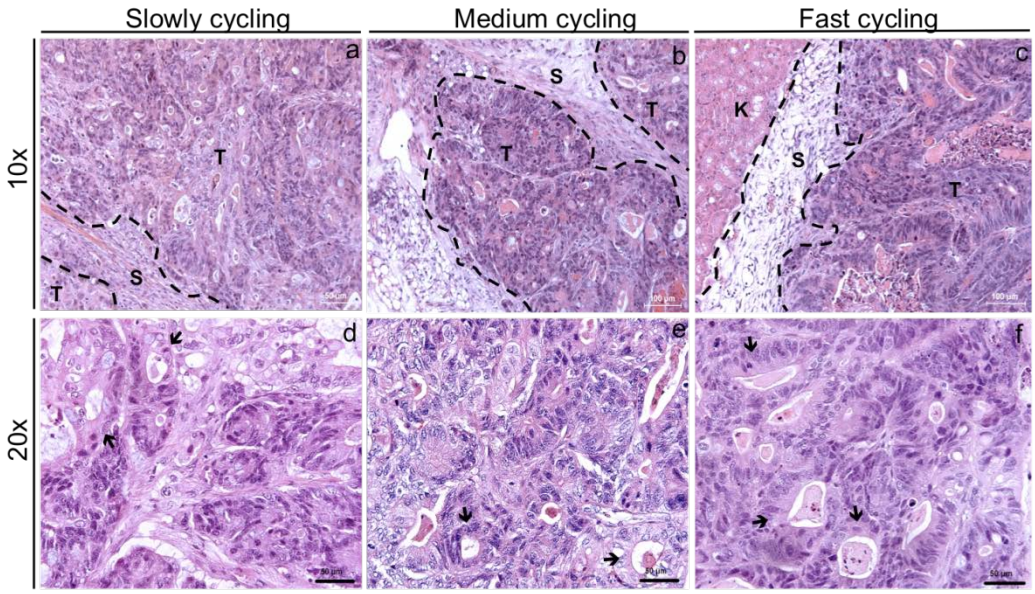

Fig. 55: Tumors derived from fast-, medium- and slowly cycling cells have similar morphologies. H&E staining of xenografts originating from sorted (a and d) slowly-, (b and e) medium- and (c and f) fast cycling cells. All xenografts show a similar morphology. Tumors had glandular structures (d-f arrows) and stromal cells were recruited (S = stromal cells; T = tumor cells; K = kidney).

These data show that all the different cycling cell types were able to form colorectal tumors independent of their initial proliferation rate. This is in line with the *in vitro* studies, which showed that all the cells were able to expand after the sort. However, this result represents only an endpoint analysis. Possibly, the onset of tumor growth may be different. To further investigate the potential role of the different cycling cell populations in the onset of tumor growth, *in vivo* bioluminescence imaging was performed.

Pre-selected slowly-, medium- and fast cycling cells from a xenograft show similar tumor growth kinetics *in vivo*

In order to analyze the tumor growth kinetics of the different cycling cell populations preselected from a xenograft, the transduced tumor cells (G605-H2B-GFP) were modified prior to transplantation using the pTurboGlow lentiviral vector (vector map see Appendix 9.7.). This vector contained luciferase and the fluorescent dye eqFP650 (near-infrared protein). Both proteins were linked via an internal ribosomal entry site (IRES) sequence allowing the simultaneous expression of the two proteins. The cells were selected for H2B-GFP and eqFP650 expression via a FACS sorter. This cell line contained both H2B-GFP to study the cell cycle behavior and luciferase allowing the non-invasive tracking of the cells using the Xenogen system (IVIS® 200 series, Caliper).

The following experimental set up was chosen for the experiment:

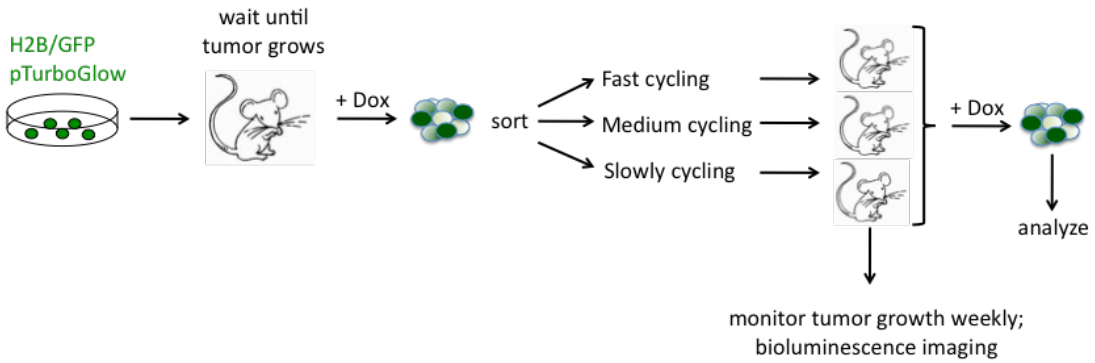

Fig. 56: Experimental set up for the generation of a tumor growth curve of slowly-, medium-, and fast cycling cells preselected from a xenograft. The bulk of G605-H2B-GFP-pTurboGlow cells was injected into the kidney capsule of NSG mice. After tumor growth, mice were treated with Dox (2g/l) for 15 days and the different cycling cell populations were sorted and reinjected into the kidney capsule of secondary recipients. The tumor growth was monitored every week, non-invasively using the Xenogen system and tumor growth curves were generated. After the growth of the tumors in the secondary recipients, the mice were treated with Dox for 15 days to analyze whether all the cells were able to regenerate fast-, medium- and slowly cycling cells.

The bulk of the transduced tumor cells was transplanted into the kidney capsule of NSG mice and tumor growth was monitored every other week. After establishment of a solid tumor, the mice were treated with Dox (2 g/l) in the drinking water for 15 days. The tumor harvested for this experiment had a volume of 529 mm^3 and was digested using collagenase and DNase. A doublet- and dead cell exclusion (7AAD) were performed (Fig. 57b and c). The tumor cells were stained with an anti-human HLA- and anti-mouse-H2kD antibody to distinguish between human and murine cells. 69% of the tumor cells were of human origin (HLA+). Approximately 15% of the cells were infiltrating cells from the mouse host (H2kD+) (Fig. 57d). Slowly-, medium- and fast cycling cells were sorted according to their GFP expression pattern (Fig. 57e). Approximately 20% of the tumor cells were slowly cycling, which was demonstrated by a high GFP expression whereas 14% of the tumor cells divided several times and therefore lost their GFP label completely. The majority of the cells divided only a few times and their GFP label was slowly diluted. These cells showed a moderate GFP expression (Fig. 57e). In order to determine the purity of the sort, the sorted cell populations were reanalyzed at the cell sorter. All sorted populations were successfully separated with minimal overlap (Fig. 57f).

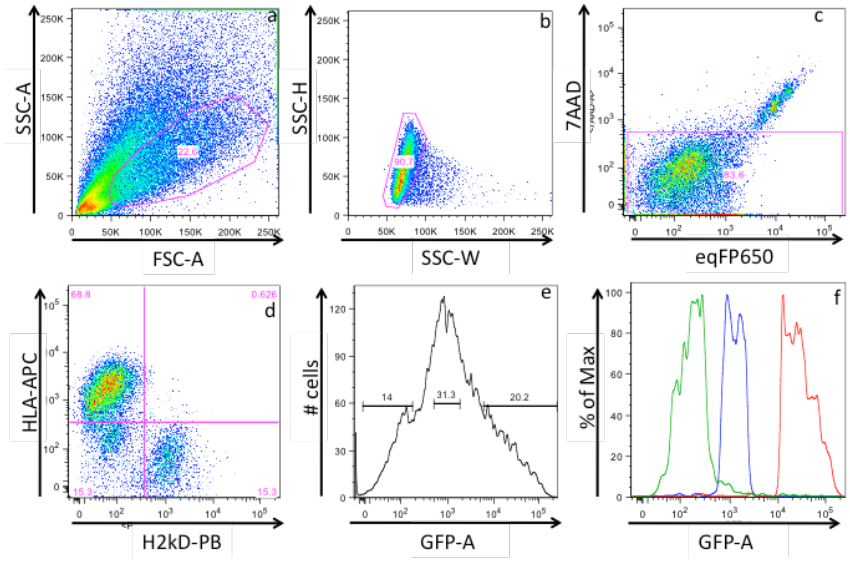

Fig.57: Gating scheme of cells derived from a xenograft treated with Dox for 15 days. Doublet- (b) and dead cell exclusion (c) were performed. The cells were stained with an anti-human HLA and anti-mouse H2kD antibody (d). Only human (HLA positive) cells were included in the analysis. Slowly- (20.2%), medium- (31.3%) and fast cycling cells (14%) were sorted (e). A reanalysis was performed after the sort. All the three populations have been sufficiently separated (green = fast cycling; blue = medium cycling; red = slowly cycling)(f).

25.000 cells of each sorted population were injected into the kidney capsule of secondary recipient mice (5 mice per group). The tumor growth was monitored weekly using the Xenogen system. The total tumor burden of the mice was determined, including metastasis. The first measurement was performed directly after implantation of the tumor cells (Fig. 58). The estimated value of the total flux was used as the baseline for all the following analysis.

The tumor growth was monitored weekly to analyze whether the tumor growth kinetics were different between the distinct cycling cell populations sorted from the primary xenograft. Therefore the mice were injected intra-peritoneally with luciferine (15 mg/ml) at a dose of 10 µl per gram body weight ten minutes prior to analysis.

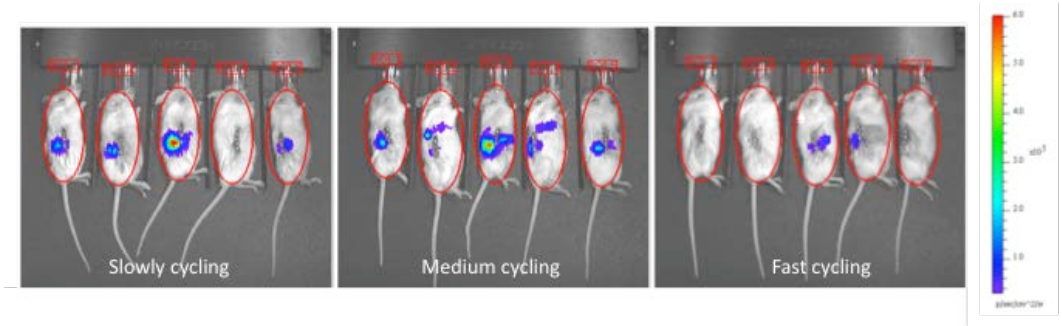

Fig. 58: *In vivo* bioluminescence imaging of NSG mice injected with slowly-, medium- and fast cycling colon tumor cells. 25.000 cells per sorted cell population were injected into the right kidney capsule of secondary recipient mice. The first *in vivo* bioluminescence imaging was performed directly after surgery. The total flux for the region of interest was determined for each mouse (red circles).

The total flux of the region of interest was determined (Fig. 58) and normalized to the values measured at day zero, directly after injection of the cells. The tumor growth curves were not significantly different between the different cycling cell populations. As described in the previous experiment, all the cells were capable of forming a tumor with the same growth kinetics independent of the initial cell cycle state (Fig. 59).

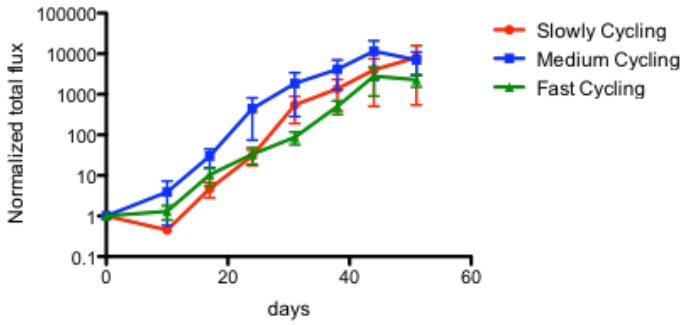

Fig. 59: Slowly-, medium- and fast cycling colorectal tumor cells have similar tumor growth kinetics. 25.000 colorectal tumor cells sorted from a xenograft were reinjected into the kidney capsule of secondary recipient mice. The tumor growth was monitored weekly via the Xenogen system. The first measurement was performed directly after surgery and all the following results were normalized to these values. The growth kinetics of the tumors were similar between the groups (ANOVA, p=0.3014).

The tumor take rate was similar between the three groups. All the mice showed tumor growth. One mouse of the medium- and slowly cycling group was not analyzed because it died prior to the endpoint analysis. However the *in vivo* bioluminescence measurements indicated that these mice developed tumors.

Tab. 6: Frequency of tumor growth in secondary recipient mice.

Group	Tumors/number of mice
Fast cycling	5/5
Medium cycling	4*/5
Slowly cycling	4*/5

* One mouse died before the end of the experiment. The tumor was not analyzed at the endpoint of this experiment.But the values were included in the bioluminescence measurements.

Moreover, the potential of the different cell populations to regenerate fast-, medium- and slowly cycling cells was determined. Therefore, the secondary recipient mice were treated for 15 days with Dox (2g/l) in the drinking water prior to analysis. One tumor that grew out of initially slowly cycling sorted cells was harvested, digested

and stained with an anti-human HLA- and anti-mouse H2kD antibody (Fig. 60d), as described for the primary xenograft. This tumor had a volume of 1.65 cm^3. The initially slowly cycling tumor cells were able to regenerate fast-, medium- and slowly cycling cells. Approximately 3% of the tumor cells retained their slowly cycling phenotye within the 15 days of Dox treatment. The medium cycling population accounted for 57% of the tumor cells and 25% of the cells divided much faster and thus lost their GFP label completely (Fig. 60e and f).

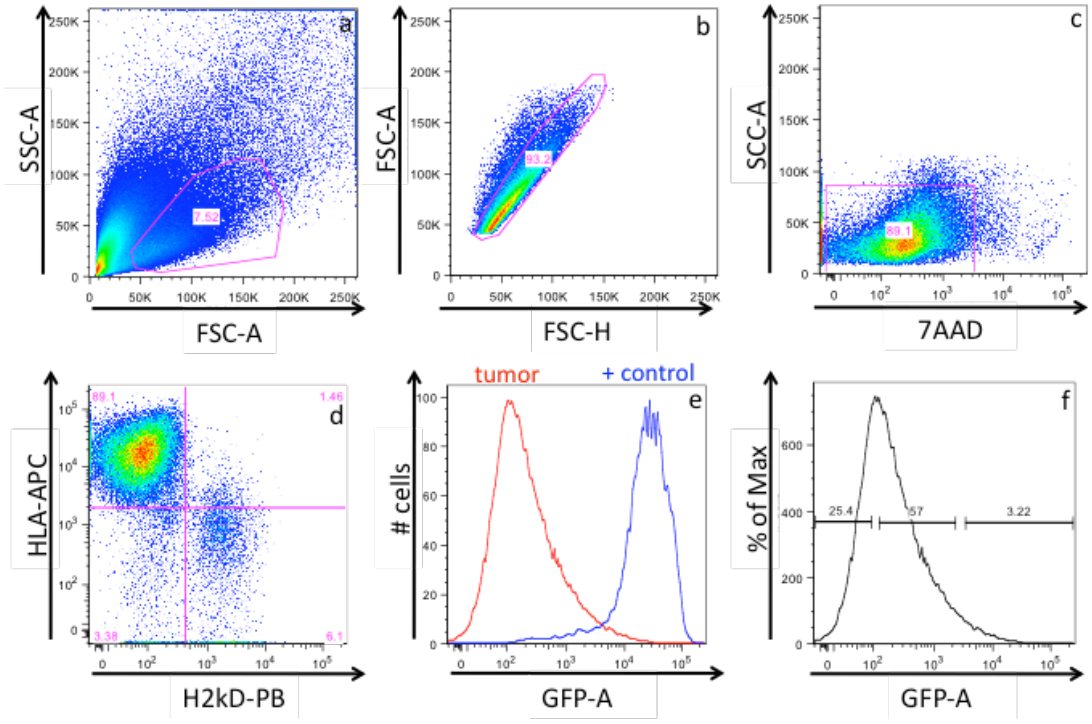

Fig. 60: Slowly cycling cells have the capacity to regenerate all the different cycling cell populations in a secondary recipient *in vivo*. Slowly cycling cells were sorted from a xenograft that was treated for 15 days with Dox and trasplanted into the kidney capsule of secondary recipient mice. These secondary recipients were treated again for 15 days with Dox. Afterwards, the tumors were harvested and analyzed. Doublet- (b) and dead cell exclusion (c) were performed. The cells were stained with an anti-human HLA- and anti-mouse H2kD antibody (d). Only human (HLA positive) cells were included in the analysis. The G605-H2B-GFP cell line was used as a positive control for the GFP expression level (blue curve = control; red curve = tumor) (e). The initially slowly cycling cells were able to regenerate fast- (25.4%), medium- (57%) and slowly cycling cells (3.22%) (e and f).

The morphology of the tumors was analyzed via IHC stainings. The tumor sections were stained with an anti-human Ki-67- and anti-GFP antibody (Fig. 61). The tumor cells in the secondary recipients were able to regenerate fast-, medium- and slowly cycling cells independent of their cell cycle state prior to injection (Fig. 62). GFP positive tumor areas do not stain for Ki-67 and vice versa, further supporting the validity of the system. Cells that do not divide keep the GFP label (Ki-67 negative) and cells that divide loose the GFP label and harbor a Ki-67 positive phenotype.

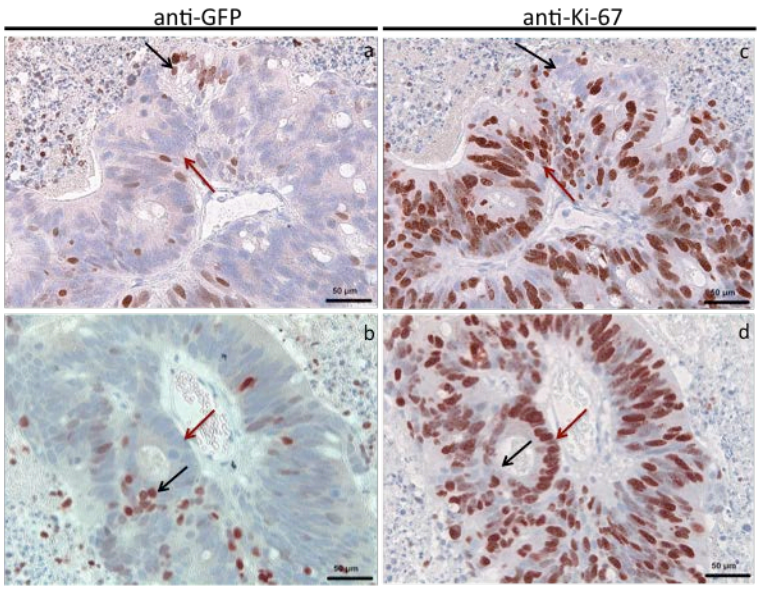

Fig. 61: *In vivo* preselected slowly cycling cells are able to regenerate fast-, medium- and slowly cycling cells in secondary recipient mice. Secondary recipient tumor bearing mice were treated with Dox (2 g/l) in the drinking for 15 days. Immunohistochemistry stainings were performed using an anti-GFP antibody (a and b) and a human specific anti-Ki-67 antibody (c and d). The two stainings were mutually exclusive (black arrow: GFP^+ and $Ki\text{-}67^-$; red arrow: GFP^- and $Ki\text{-}67^+$). Representation of tumor that was generated from sorted slowly cycling cells.

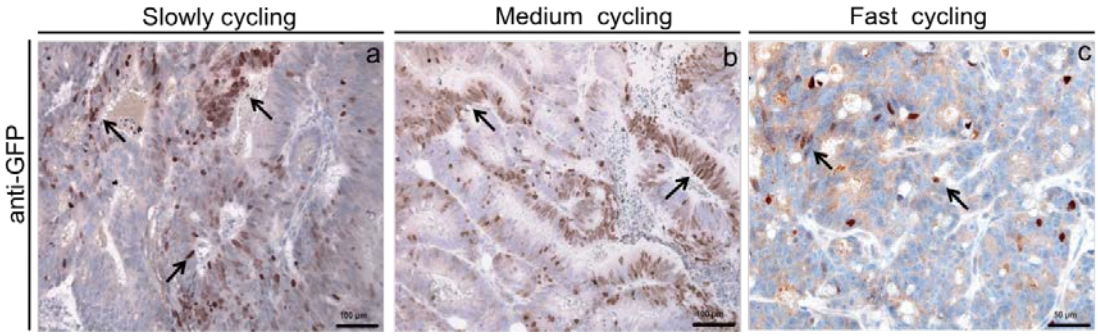

Fig. 62: All sorted different cycling cell populations are able to regenerate fast-, medium- and slowly cycling cells. Secondary recipient tumor bearing mice were treated with Dox (2 g/l) in the drinking for 15 days. Immunohistochemistry stainings were performed using an anti-GFP antibody (examples for GFP+ cells, black arrows).

In summary, these experiments demonstrate that slowly cycling cells are present in a tumor. The immunohistochemistry stainings further support the data of the Ki-67/ Hoechst stainings described in the previous chapter and thereby confirm that the system allows the study of quiescent cells *in vivo*. Nevertheless, after 22 days of Dox treatment all the tumor cells within the xenograft divided and thus lost their H2B-GFP label (Fig. 49). Interestingly, the tumor cells detected in the lungs divided actively and the frequency of the LRCs appeared to be lower in small metastatic foci (Fig. 51) when compared to the corresponding primary tumor (Fig. 50). Furthermore, all the

three different cycling cell populations were tumorigenic independent of their initial cell cycle state (Fig. 54 and 59).

These results do not exclude the possibility that there may be a dynamic process between activation and quiescence. The cells may be activated and probably re-enter dormancy due to stress signals like chemotherapy treatment or lack of nutrition. Moreover, hypoxic areas may serve as a specific niche for dormant tumor cells and therefore might maintain the slowly cycling state of the cells. Initial experiments using oxygen levels of 3% and 0.5% further support this hypothesis. These hypoxic conditions indeed enriched for LRCs compared to standard cell culture conditions where the tumor cells were maintained at an oxygen level of 21% (see Appendix 9.16). Further investigation is required to validate this hypothesis.

6.7. Chemotherapeutics enrich for slowly cycling cells *in vitro*

The effect of 5-Fluorouracil (5-FU) and Oxaliplatin on the cell cycle of the primary colorectal cells *in vitro* was determined. The primary colorectal cancer cell line HD1858-H2B-GFP was treated for 10 days with Dox (to track LRCs) and either Oxaliplatin (0.5 µM) or 5-FU (5 µM). Following treatment, there was a greater proportion of GFP+ cells (Fig. 63a and d, blue square) in comparison to the cells that were not treated with one of the chemotherapeutics (Fig. 63a and d, red square). A cell cycle analysis was also performed using a human specific anti-Ki-67 antibody and Hoechst. The non-treated cells showed a normal cell cycle profile with app. 20-25% in G0-, 50% in G1- and 20% in S-G2-M-phase (Fig. 63c and f). The cell cycle profile of the treated cells showed distinct patterns due to the different mechanisms of the two compounds. Oxaliplatin is a platinum based compound that forms cross-linking DNA adducts and therefore blocks transcription and replication of the DNA. As depicted in Fig. 63b, the cells were blocked in G2-M-phase. In contrast, 5-FU is a nucleoside analog. It prevents the synthesis of thymine nucleosides and thereby impairs DNA replication. As shown in Fig. 63e, the majority of the cells was arrested in G0- to G1-phase.

Two possible mechanisms might explain the enrichment of slowly cycling cells upon chemotherapy treatment: at first, slowly cycling cells were more resistant to chemotherapy and survived the treatment whereas fast cycling cells may have died. Secondly, all the cells were arrested due to the treatment and a slowly cycling phenotype may have been induced to all cells.

In order to study whether slowly cycling cells are more resistant to chemotherapy, the different cycling cell populations were sorted prior to treatment.

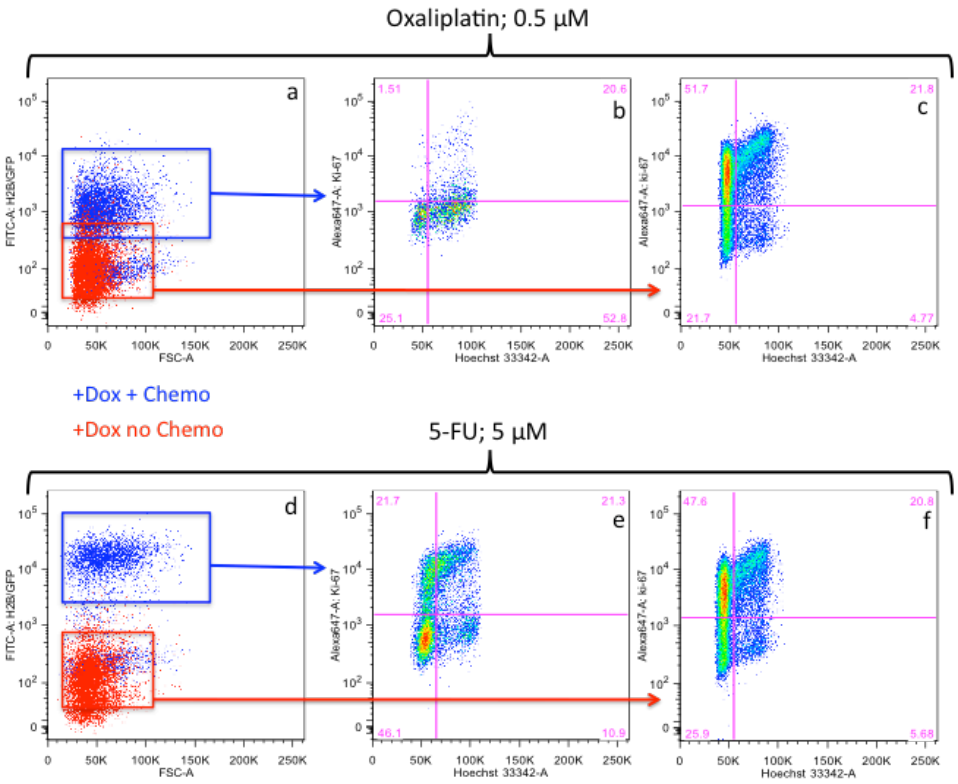

Fig. 63: Chemotherapeutics enrich for slowly cycling cells. The cells were treated for 10 days with Dox and Oxaliplatin or 5-FU (blue square). Cells only treated with Dox were used as control (red square). After treatment, the cells were harvested and the amount of GFP expressing cells was determined (a and d). A Ki-67/Hoechst staining was performed. The chemotherapeutic treated cells showed an altered cell cycle behavior (b and e) in comparison to the non-treated cells (c and f).

Slowly cycling cells are less sensitive to chemotherapy

In order to analyze whether the common chemotherapeutics against colorectal cancer such as 5-FU and Oxaliplatin have a different effect on slowly cycling cells compared to fast cycling cells the following experiment was performed:

Both cell lines, HD1858-H2B-GFP and G605-H2B-GFP, were treated for 10 days with Dox *in vitro*. The cells were sorted prior to chemotherapy treatment for slowly-, medium- and fast cycling cells and seeded in collagen I coated 96-well plates in serum-free medium. The G605 cells were seeded at a density of 5000 cells per well and for the HD1858 cell line 2500 cells per well were seeded. Chemotherapeutics were added in different concentrations to the cells one day after sorting. Four technical replicates (G605) and three technical replicates (HD1858) were analyzed for each condition. Non-treated cells were used as controls. For the dead cell control, 10% of triton was added to the cells 16 hour prior to analysis. Four days after treatment, the CellTiter-Blue® Assay was used to estimate the amount of viable cells per well. Only viable cells are able to reduce the redox dye resazurin into resorufin, a flurescent end product (Promega). The cells were incubated for 4 hours at 37°C with

the CellTiter-Blue® reagent and the fluorescence signal was measured with a plate reader according to the manufacturer's protocol.

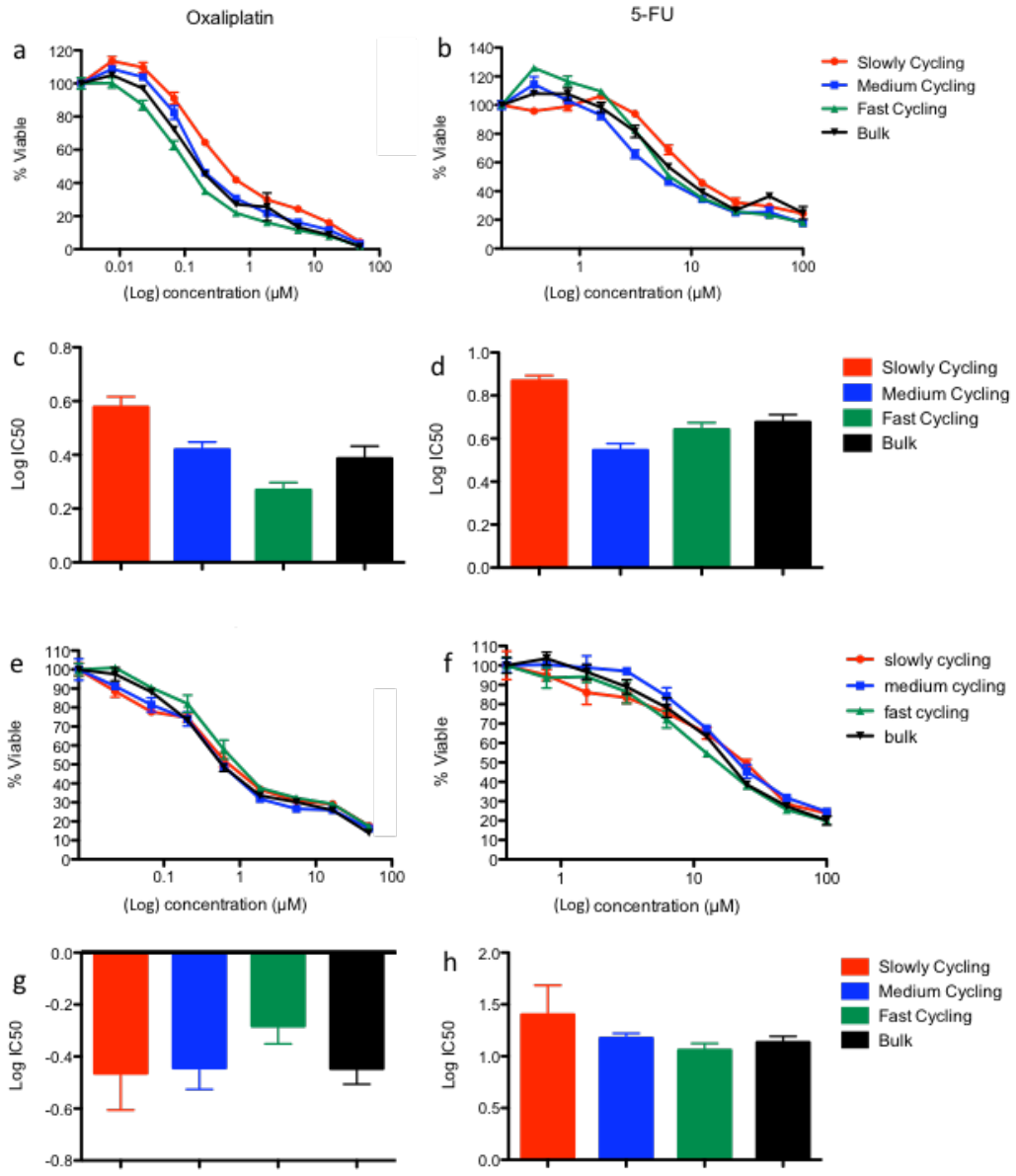

Fig. 64: The effect of Oxaliplatin and 5-FU on different cycling cell populations. Both cell lines (G605-H2B-GFP and HD1858-H2B-GFP) were treated for 10 days with Dox *in vitro*. Slowly-, medium- and fast cycling cells were sorted and treated with different concentrations of Oxaliplatin (a, c, e, g) or 5-FU (b, d, f, h) for 4 days. CellTiter-Blue® was added and the fluorescence signal of viable cells emitted through resorufin was measured in a plate reader. The log IC_{50} was determined for G605-H2B-GFP (c and d) and HD1858-H2B-GFP cells (g and h). The slowly cycling cells had a higher Log IC_{50} than fast cycling cells in G605-H2B-GFP cells (c and d). In HD1858-H2B-GFP cells, no difference in Log IC_{50} between the different cycling cell population was observed upon treatment (g and h).

Tab. 7: IC_{50} of slowly-, medium- and fast cycling G605-H2B-GFP and HD1858-H2B-GFP cells upon chemotherapy treatment. The different cycling cell populatons were sorted and treated for four days with different concentartions of Oxaliplatin and 5-FU. CellTiter-Blue® was added and the IC_{50} was detrmined using GraphPad Prism.

Group	G605-H2B-GFP		HD1858-H2B-GFP	
	IC_{50} Oxaliplatin	IC_{50} 5-FU	IC_{50} Oxaliplatin	IC_{50} 5-FU
Slowly cycling	3.8	7.5	0.3	25.2
Medium cycling	2.6	3.5	0.4	15.0
Fast cycling	1.9	4.4	0.5	11.5
Bulk	2.4	4.7	0.4	13.6

The slowly cycling cells of the G605-H2B-GFP cell line were more resistant to 5-FU and Oxaliplatin than fast cycling-, medium cycling- or bulk cells (Fig. 64a and b). The IC_{50} of the slowly cycling cells was higher when compared to the faster cycling cell populations (Tab. 7). However the cells seemed to be more sensitive to Oxaliplatin than to 5-FU, indicated by higher IC_{50} values for the latter treatment. Furthermore, the Log IC_{50} was calculated using GraphPad Prism®. The Log IC_{50} was higher in the slowly cycling cells compared to medium cycling- and fast cycling cells, upon Oxaliplatin (Fig. 64c) or 5-FU (Fig. 64d) treatment. This suggests that the slowly cycling cells were more resistant to chemotherapy than the faster cycling cells *in vitro*.

In HD1858-H2B-GFP cells, the slowly cycling cells show a higher IC_{50} upon 5-FU treatment in comparison to medium cycling-, fast cycling- or bulk cells (Tab. 7). However, if treated with Oxaliplatin the cells do not show big differences between the different cycling populations (Fig. 64e and g).

Three out of four experimental settings indicate that slowly cycling cells are more resistant to chemotherapy *in vitro*, even though the difference is more pronounced in the G60-H2B-GFP cell line. The two cell lines may behave differently because the experimental setting may not be optimal for both cell lines.

Furthermore, the initial cell number seeded might be critical for the outcome of the experiment. Due to differences in seeding density between the two cell lines, the two experiments cannot be compared to each other and need to be repeated under the same conditions. Also, only technical replicates were analyzed and additional biological replicates of the experiment are necessary to draw a significant conclusion.

Regardless of the effect of the chemotherapeutics on the different cycling cell populations, the fluorescence intensities measured indicate again that the different cycling phenotypes are retained over four days *in vitro* after the sort. The slowly cycling cells grew much slower than the fast cycling cells, in both cell lines. The same cell numbers were seeded for each population but the fluorescence intensities measured for the slowly cycling cells were much lower compared to the fast cycling cells (Fig. 65a and b). However the differences between the fast cycling-, medium cycling- and bulk cells was more pronounced in the HD1858 cell line (Fig. 65b). These results are in line with the clonogenicity experiments performed *in vitro* (see chapter 6.5.).

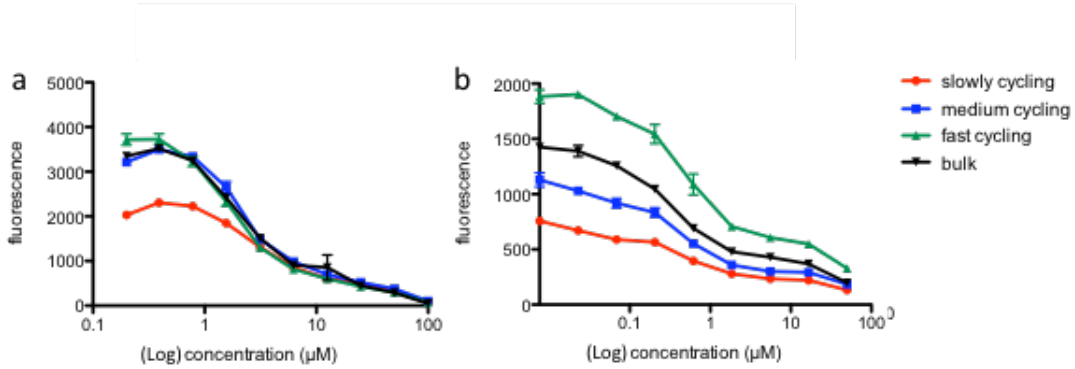

Fig. 65: The different cycling cell populations retain their phenotype over a short period of time *in vitro*. Both cell lines, (a) G605-H2B-GFP and (b) HD1858-H2B-GFP, were treated for 10 days with Dox in vitro. Slowly-, medium- and fast cycling were sorted and treated with different concentrations of Oxaliplatin for 4 days. CellTiter-Blue® was added and the fluorescence signal of viable cells emitted through resorufin was measured in a plate reader. The fluorescence intensity of the slowly cyclig cells was much lower compared to the faster cycling cell populations, indicating that these cells continue to grow slowly.

7. Discussion and Outlook

7.1. Establishment of a suitable *in vivo* system

The goal of this thesis was to study whether different cycling cells are present within colorectal tumors and to phenotypically and functionally characterize the distinct cell populations in regard to tumor initiation, progression and chemotherapy resistance. Therefore a suitable *in vivo* system was needed that fully recapitulates the human disease. To date, several model systems have been described in order to study CRC development. For instance, numerous mouse models have been generated, such as the frequently used $APC^{Min/+}$ model. Similar to FAP patients, these mice harbor heterozygous truncating mutations in the *APC* gene and subsequently develop numerous polyps and adenomas in the intestine (Levy et al., 1994; Moser et al., 1990). Although often used to study CRC this mouse model has some limitiations. In contrast to the human situation where the tumors arise in the duodenum and colon, the adenomas in the $APC^{Min/+}$ mice mainly developed in the small- and large intestine (Moser et al., 1990). As the recently reported Paneth cells, that have been shown to induce Wnt signaling and possibly constitute the niche for the ISCs located at the crypt bottom (Sato et al., 2011), are missing in the colon (Medema and Vermeulen, 2011), the mouse tumors may not fully recapitulate all the aspects colorectal tumors.
To overcome these drawbacks, xenograft models using either conventional human tumor cell lines or primary patient specimen have been established. First, orthotopic transplantation models have been generated in order to provide a beneficial microenvironment for the cancer cells. Although this appears to be a good model, the risk that the injected cancer cells may leak out and thereby influence the reproducibility of the experiments is very high (Tseng et al., 2007). Second, subcutaneous (s.c.) injections of tumor cells or pieces are widely used to expand the tumor material and to study tumor growth (Dalerba et al., 2007; Ricci-Vitiani et al., 2007; Vermeulen et al., 2008b). Although this method allows sufficient tumor growth, the ability of the tumor cells to metastasize to distinct organs is limited due to differences in the microenvironment and lack of vasculature supporting tumor cell dissemination (Heijstek et al., 2005; Kobaek-Larsen et al., 2000). Third, xenograft models using the renal capsule as injection site have been used to study CRC progression (O'Brien et al., 2007). The kidney is a “foreign soil“ for the CRC cells but the organ is interspersed with numerous blood vessels, facilitating nutrition supply for the tumor cells and thereby promoting tumor growth.

This model system enables the study of metastasis development, as cells are able to disseminate in some cases to the liver and the lungs, as shown for the G605 cell line.

The xenograft experiments were carried out in the NSG mouse strain as these mice offer the highest tumor take rate, due to their lack of adaptive immune cells and NK cells. The resulting tumors were analyzed via immunohistochemistry and flow cytometry in order to confirm the human origin of the cells and to compare the morphology with the initial patient tumor. All the tumors preserved the original morphology forming atypical glandular structures, as observed in the patient tumor, suggesting that the model system is suitable for the characterization of the human disease. Interestingly, a small fraction of mouse cells (H2kD+) was detected in the tumors, indicating that some murine cells were successfully recruited to the tumor surrounding (Fig. 15). These murine cells may include stromal- as well as endothelial cells or macrophages but were not characterized in the present study. However, this may indicate that in the patient, tumor cells growing in novel foreign sites such as distant organs might also be able to recruit healthy stromal cells, creating their own niche.

Limitations of xenograft models in highly immunocompromized mice

The method of the xenotransplantation as well as the selection of patient samples can play a critical role in the efficiency of tumor formation. In previous studies, several different immunocompromized mice were used for transplantations of human tissues, such as NOD/SCID mice, nude mice or NSG mice. These mice are genetically modified and harbor defects in important compartments of the immune system. Nude mice for example are athymic and develop only precursors of T-cells that will not fully maturate (Flanagan, 1966). NOD/SCID mice do not have functional T- and B-cells (Bosma and Carroll, 1991) and NSG mice have an additional lack of NK cells (Ito et al., 2002). This immunodeficiency is advantageous for xenotransplants and inhibits graft rejection by the host immune system. Dependent on the mouse strain chosen, the success rate of transplantations can differ. This was demonstrated recently in studies on human melanoma cells. A subpopulation enriched for human malignant-melanoma-initiating cells defined by the expression of the chemoresistance mediator ABCB5 has been identified, occurring at a relatively low frequency in patient specimens (Schatton et al., 2008). Moreover, it has been reported that the use of the highly immunodeficient NSG mice increased the detection of tumorigenic melanoma cells by several orders of magnitude. Co-injections of melanoma cells with Matrigel even further increased tumor growth and

limiting dilution analysis revealed that more tumorigenic melanoma cells were identified, in contrast to cases where tumor cells were injected without Matrigel (Quintana et al., 2008). Importantly, in the latter study, no correlation of tumorigenicity with any of the surface markers tested was observed. However, recently, the neural crest stem cell marker CD271 has been shown to be a putative stem cell marker for melanomas (Boiko et al., 2010). Boiko et al. used a similar transplantation protocol to Quitana et al., however their cohort of patient specimens was different and included primary early-stage melanomas, whereas Quintana et al. obtained samples from patients with late-stage metastasizing disease. Those discrepancies suggest that the ability to detect a distinct CSC population might also depend on the differentiation status of the tumor, and not on the choice of the xenograft model alone. Furthermore, as proposed by Civenni et al. distinct protocols used for the digestion of the primary tumor material might be an additional explanation for the contradicting observations. Unlike Quintana and colleagues who used trypsin for the dissociation of the tumors, which may have proteolytically cleaved the surface epitopes of CD271 and therefore possibly lead to the detection of false-negative cell populations, Boiko et al. used a less harsh digestion method, which may have better preserved the cell surface molecules (Civenni et al., 2011).

Although xenograft models enable the study of the human disease and mirror more closely the tumor heterogeneity found in the patients, they have an important drawback: the murine microenvironment might not be equivalent to the human one, potentially missing some aspects of interactions between tumors and the microenvironment (Richmond and Su, 2008). Indeed, many differences exist between chemokines and chemokine receptors present in mice and in humans (Mestas and Hughes, 2004), which may influence tumor development.

Additionally, the adaptive immune system, which is highly impaired in the immunodeficient mice used for transplantation experiments, has been described to play an important role in tumor progression and metastasis (DeNardo et al., 2009). Thus one must be aware of those limitations and carefully evaluate the impact they have on the interpretation of results obtained.

7.2. Establishment of a suitable *in vitro* system

Even though xenograft models represent a useful method to study human colorectal cancer in a more physiological setting, cell culture systems are indispensable for in-depth studies of numerous cellular processes. Cell culture systems allow manipulations of the cells and enable the testing of different hypotheses in numerous *in vitro* assays prior to their validation in more complex animal models. In order to

establish a primary human colorectal cancer cell line, tumor cells isolated from a freshly resected tumor piece of a CRC patient were maintained as spheres in culture under serum-free conditions (Fig. 17). The culture conditions are of great importance for the genetic stability of the cells. Lee and colleagues compared conventional FCS cultured human glioblastoma cell lines with cultures maintained under serum-free conditions. The authors could show that tumor cells grown in culture medium containing FCS changed genotypically and biologically from the parental tumor. In contrast, tumor cells cultured under serum-free conditions did not undergo such dramatic changes and still retained the gene expression profile and the phenotype of the respective parental tumors (Lee et al., 2006). In transplantation assays, conventional serum cultured cell lines usually form a homogenous tumor mass that morphologically and phenotypically differs from the initial tumor. To date, serum-free cultures are most frequently used for the establishment of tumor cell cultures, including colorectal cancer (Ricci-Vitiani et al., 2007; Todaro et al., 2007; Vermeulen et al., 2008b). This particular method was therefore selected for the culture of the HD1858 and G605 colorectal cancer cell lines.

Characterization of the primary HD1858 colorectal cancer cell line

The generated HD1858 CRC cell line was tumorigenic *in vivo* after maintenance in culture (Fig. 18b). Even sorted single cells were able to generate a heterogeneous tumor cell population *in vitro*, capable of giving rise to an adenocarcinoma after injection into the kidney capsule of NSG mice (Fig. 21). Moreover, the tumors morphologically resembled the original patient tumor (Fig. 18c), suggesting that the cultures maintain so-called cancer stem cells that have the potential to self-renew and to differentiate into all the different cell types.

The expression of nuclear ß-catenin was evaluated in the spheres and the respective xenotransplants. Nuclear ß-catenin is associated with activation of the Wnt signaling pathway, which has been proposed to mark colorectal CSCs (Vermeulen et al., 2010). Fodde and Brabletz reported that the intracellular distribution of ß-catenin is very heterogenous in a tumor with membranous expression in well-differentiated parenchymal cells and nuclear expression in tumor cells located at the invasive front (Brabletz et al., 1998; Fodde and Brabletz, 2007). The CRC spheres as well as the xenografts showed differential expression of nuclear ß-catenin (Fig. 22), indicating that the culture system maintains the heterogeneity of the initial tumor.

CRC cultures differentially express putative CSC markers and cell adhesion molecules

This heterogeneity was further validated via flow cytometry analysis of putative colorectal CSC markers. Both cell lines, HD1858 and G605, differentially expressed the putative CSC markers EpCAM, CD44 and CD166 (Dalerba et al., 2007), indicating that various cell types were present in the cell cultures (Fig. 23). Moreover, the expression of a second reported CSC marker, namely CD133 was analyzed (O'Brien et al., 2009; Ricci-Vitiani et al., 2007). This marker was only expressed in the G605 cell line and not in the HD1858 cells (Fig. 23a an d). However, CD133 is controversially discussed as a stem cell marker for CRC. Shmelkov and colleagues generated knock-in *lacZ* reporter mice for CD133 and discovered that this marker was ubiquitously expressed in differentiated colonic epithelial cells. Moreover, the authors could show that both CD133+ and CD133- cell populations were able to form tumors (LaBarge and Bissell, 2008; Shmelkov et al., 2008). Kemper and colleagues further demonstrated that CD133 is differentially glycosylated in CSCs and differentiated cells. Thereby the binding of the frequently used AC133 antibody to the specific epitope in the differentiated cells is prevented, even though the protein is still expressed. The authors also propose that the AC133 antibody might still be useful for the isolation of CSCs if used in the right conditions (Kemper et al., 2010). Nonetheless, as both CRC cell lines, HD1858 ($CD133^-$) and G605 ($CD133^+$), were able to generate tumors in mice this marker needs to be revised as being a specific CSC marker for CRC.

A similar diversity in marker expression was observed for cell adhesion molecules, such as the different alpha integrins and c-Met (Fig. 24). These molecules are involved in metastasis and have the capacity to bind to different ECM molecules. Possibly, the heterogeneous expression of at least some of these molecules such as integrin alpha 1 (CD49a) and integrin alpha 5 (CD49e), suggests that there might be a subpopulation of CRC cells present with different capacities to metastasize.

Evaluation of CD24 and CD44 as novel CSC marker for CRC

The expression of CD24 in combination with CD44 was analyzed. This marker combination was not yet described as a CSC marker for CRC but has been proposed for several other types of cancer such as pancreatic cancer (Lee et al., 2008) and breast cancer (Al-Hajj et al., 2003a). Interestingly, both cell lines expressed distinct intensities of the two markers, demonstrating again that different cell types were present in the cultures (Fig. 23c and f). In order to test whether

$CD24^{high}/CD44^{high}$ and $CD24^{low}/CD44^{low}$ cells have a different function in terms of tumor initiating capacity and metastasis, the two cell populations were sorted and injected into the kidney capsule of NSG mice. This experiment was only performed with the G605 cell line due to its higher tumorigenicity and ability to generate metastasis in lungs and livers in contrast to the HD1858 cells that did not form any visible metastasis. Both sorted cell populations had tumor initiating capacities, although the mean tumor volume was higher in mice injected with $CD24^{high}/CD44^{high}$ cells compared to mice injected with $CD24^{low}/CD44^{low}$ cells (Fig. 26). However, this result was not significant and needs to be repeated with a bigger cohort of animals. Nonetheless, mice injected with $CD24^{high}/CD44^{high}$ cells formed lung and liver macrometastasis, in contrast to mice injected with $CD24^{low}/CD44^{low}$ cells (Fig. 27; Tab. 2), suggesting that the expression of both or one of the markers may promote the potential of tumor cells to metastasize.

CD24 has been described to play a role in adhesion and tumor cell invasion. Aigner et al. reported that CD24 binds to P-selectin, which is expressed in endothelial cells and activated platelets. The authors suggest that CD24 mediates tumor cell rolling on endothelial monolayers and thereby promotes metastasis (Aigner et al., 1998). Furthermore, CD24 has been found to be involved in the activation of α3ß1 and α4ß1 integrins, mediating cell adhesion to fibronectin, collagen I, IV and laminin, which finally may support extravasation at the distant site (Baumann et al., 2012). These studies indicate that CD24 alone might already be important for the metastatic process, which is in line with our results demonstrating that $CD24^{high}$ bladder cancer cells had in improved binding capacity to the ECM and enhanced metastatic potential to colonize lungs when compared to $CD24^{low}$ cells (Hofner et al., 2012). However, in our hands CD24 does not seem to be a specific CSC marker for CRC as the $CD24^{low}$ population was also able to give rise to tumors (Fig. 26), which is further supported by our finding that both $CD24^{high}$ and $CD24^{low}$ bladder cancer cell populations were able to initiate tumors *in vivo*. Nonetheless, in the bladder cancer model $CD24^{high}$ expressing cells showed a significantly accelerated tumor onset than the $CD24^{low}$ population (Hofner et al., 2012). In order to test this hypothesis for CRC, non-invasive imaging methods are needed to measure the growth kinetics of the tumor cells at various time points. Additionally, the glycoprotein CD44 has been described already as a CSC marker for CRC (Dalerba et al., 2007) and CD24 might even further enrich for more aggressive tumor cells potentiating the metastatic capabilities of these cells.

In conclusion, these results provide a hint that combined expressions of CD24 and CD44 might play an important role in metastasis in CRCs. To further validate this finding, the animal numbers need to be increased. In addition, limiting dilutions will be necessary to analyze whether the two populations have a different tumorigenic capacity and to show that the marker combination indeed enriches for more aggressive CRC cells. For CD44, only low- and high expressing cells were present, making it difficult to draw a conclusion concerning the critical role of this glycoprotein for the metastatic process. In the future, knock-down experiments will allow further conclusions to be drawn on the role of this receptor for metastasis.

7.3. Novel approach to study quiescence as a feature of stem cells in colorectal cancer

To date, various differentially expressed CSC markers have been identified via cell surface screenings in numerous tumor entities, for instance in breast- (Al-Hajj et al., 2003a), pancreas- (Hermann et al., 2007; Li et al., 2007), brain- (Singh et al., 2003; Singh et al., 2004) and prostate cancers (Collins et al., 2005). Using these CSC markers, distinct cell populations were sorted using flow cytometry and subsequently transplanted into immunodeficient mice in order to test their tumorigenic potential. However, CSC marker expression may change dependent on physiological or developmental conditions (Nguyen et al., 2012). Therefore it has been proposed to define CSCs rather via the “cellular state” than by their phenotype alone (Visvader and Lindeman, 2012). Thus, novel approaches are necessary to isolate and characterize tumor cells based on more functional properties.

It has been shown that normal adult stem cells present in the intestine (Potten, 1977; Potten et al., 1974), the skin (Cotsarelis et al., 1990) and the bone marrow (Cheshier et al., 1999; Foudi et al., 2009; Morrison and Weissman, 1994; Passegue et al., 2005; Wilson et al., 2009; Yoshihara et al., 2007) harbor quiescent cell populations. As a parallel, these quiescent cells might also characterize CSC populations. Recently, a lentiviral vector system that mediates the tetracycline-inducible expression of a histone H2B-GFP reporter has been developed, which enables studies of cell cycle kinetics *in vitro* and *in vivo* (Falkowska-Hansen et al., 2010; Kanda et al., 1998). In contrast to BrdU pulse chasing experiments, this novel approach allows the isolation of viable LRCs and thus their functional study.

Slowly cycling cells are present in CRC cultures

We used this lentiviral vector system and identified tumor cell populations with different label-retaining capacites (Fig. 28). For further analysis, these distinct cell populations were termed as slowly-, medium- and fast cycling cells. Although Ki-67/Hoechst stainings confirmed that LRCs had a higher proportion of cells being in G_0 phase when compared to fast cycling cells (Fig. 29), no long-term LRCs were observed upon longer Dox treatment, indicating that these cells still actively divide but less frequently. A similar approach on conventional breast- and colorectal cancer cell lines using CFSE was performed by Moore and colleagues, who identified similar amounts of slowly cycling cells (Moore et al., 2011).

Slowly cycling cells do not express higher levels of putative CSC markers *in vitro*

Differences in cell cycle might indicate that slowly cycling cells share common features with cancer stem cells and therefore express higher levels of CSC markers. To test this hypothesis, the colorectal cancer cell line G605-H2B-GFP was treated for ten days with Dox and the expression of the reported CSC markers, such as CD133 and EpCAM, CD44 and CD166 was analyzed. There was no difference in marker expression, except that there was a greater proportion of CD44 negative cells in the slow and medium cycling populations. (Fig. 30). A similar experiment was performed with the HD1858 cell line. As an alternative, the well-established lipophilic labeling dye PKH-26 was used to identify slowly cycling cells. CD133 was not included in the analysis because this cell line was completely negative for this marker. In correlation with results obtained for the G605-H2B-GFP cell line, no difference in CSC marker expression between fast- and slowly cycling cells was observed (see Appendix 9.4.), suggesting that slowly cycling cells are not enriched for CSCs *in vitro* and the variations in cell cycle behavior may be independent of the CSC model. This result differs from the finding of Dembinski and Kraus who detected an association between slowly cycling pancreatic cancer cells and increased expression of cell surface markers, such as CD133, CD24 and CD44, CD133 and ALDH1 (Dembinski and Krauss, 2009). However, the phenotypic properties of LRCs may vary between distinct tumor entities.

An alternative explanation for this observation is that in our study, CRC cells were cultured under serum-free conditions in medium supplemented with growth factors specifically supporting the growth of CSCs (Lee et al., 2006; Ricci-Vitiani et al., 2007; Vermeulen et al., 2008b). Due to these particular culture conditions, the expression

of the putative CSC markers may already be saturated and differences between the distinct cell populations might be undetectable in an *in vitro* system.

The slowly cycling phenotype is retained over a short period of time *in vitro*

As the stability of the cycling phenotypes was of interest, several independent experiments were carried out, such as cell count (Fig. 33), clonogenicity assays using both crystal violet measurements (Fig. 34) and single cell sorts in 96-well plates (Fig. 35).

In brief, the cycling behavior of the cells was retained over 1 week in culture after sorting (Fig. 35). Moreover, the slowly cycling cells divided less frequent and were less clonogenic than the fast cycling cells (Fig. 33 and 34; Tab. 3). Also single cell-derived cell lines originating from fast-, medium- or slowly cycling cell populations showed similar cycling behaviors over one week in culture (Fig. 42 and 43). However this was only a transient phenotype and all the cells expanded *in vitro* and were able to regenerate fast-, medium- and slowly cycling cells independent of their initial cell cycle status (Fig. 37). Furthermore, this finding indicates that the cycling behavior of the CRC cells is not static and that there might be a dynamic switch between the different cell populations. Fast cycling cells are able to generate slowly cycling cells and more importantly slowly cycling cells are able to generate fast cycling cells in this experimental setting. One could hypothesize that the slowly cycling cells may survive chemotherapy regimens and later on generate fast cycling cells that might be responsible for the relapse of the patients.

However, it is questionable whether the expansion of slowly cycling cells *in vitro* allows the study of quiescent cells. Physiological quiescent tumor cells may have lost their original characteristics under *in vitro* conditions that favor proliferation (Vessella et al., 2007).

The microenvironment plays a crucial role in the maintenance or induction of a quiescent phenotype in the tumor cells. For example, myofibroblasts have been shown to secrete HGF, a ligand of the canonical Wnt signaling pathway (Vermeulen et al., 2010), which in conjunction with other pathways possibly influences the cycling behavior of the ISCs. Recent studies suggested that actively cycling ISCs located at the bottom of the crypt are exposed to high Wnt signaling whereas this signaling pathway may be suppressed in the surrounding microenvironment of the quiescent ISCs at the +4 position (Li and Clevers, 2010). Moreover, the medium used for the cell cultures of this study contained HGF, which induces proliferation and therefore

may have inhibited the quiescent phenotype of some of the tumor cells during *in vitro* experiments.

Additionally, the level of oxygen the tumor cells are exposed to is known to play a critical role. It has been shown that HSCs are located in a specific niche in the bone marrow with low oxygen levels (Cipolleschi et al., 1993; Parmar et al., 2007). Thus hypoxia regulates stem cell function and may induce quiescence (Simon and Keith, 2008). Many hypoxic areas are present in a tumor and might be involved in the balance between quiescent and actively dividing tumor cells.

Therefore *in vivo* studies, which mimic more closely the physiological requirements to maintain or induce quiescence, might yield additional insights into the cell cycle behavior of CRC cells.

All cycling cell populations preselected *in vitro* are able to generate tumors *in vivo*

The colon cancer cell line G605-H2B-GFP was cultured for 10 days with Dox and fast-, medium- and slowly cycling cells were sorted and transplanted into immuno-compromized mice in order to determine their tumorigenic potential. All the populations were able to generate tumors independent of the initial cycling state and the mean tumor volume appeared to be higher in the slowly cycling cell population in comparison to medium- and fast cycling cells (Fig. 47). However the tumor volume was variable even within one group of mice and therefore does not lead to a conclusive result. Nevertheless, it is clear that every tumor cell population independent of their initial cell cycle state is able to engraft in NSG mice. In this experimental set up, the slowly cycling cells generated tumors comparable in size to the fast cycling cells (Fig. 47), indicating that these cells might be able to regenerate fast cycling cells. However, a small contamination of cells not able to switch off the H2B-GFP expression was detected (Fig. 40). These cells may be fast cycling and probably contribute to tumor progression within the slowly cycling population. Nonetheless, additional experiments, where tumors were treated for more than 20 days with Dox and still did not harbor long-term LRCs (Fig. 49), could rule out this hypothesis. Independent of this observation it has been clearly demonstrated that slowly cycling cells are able to regenerate fast cycling cells.

Furthermore, the different cycling cell populations were preselected *in vitro.* These cells might be different from slowly cycling cells that arise in a tumor microenvironment. Therefore additional experiments with different cycling tumor cells preselected *in vivo* were performed.

Xenografts do not harbor long-term LRCs *in vivo*

Xenografts were examined for the presence of slowly cycling cells upon Dox treatment at different time periods. The intensity of the H2B-GFP signal was distributed over several log-shifts upon Dox treatment for more than five days (Fig. 49), confirming that the tumor cells divide at different frequencies. However, after 22 days of Dox treatment all the tumor cells lost their H2B-GFP label indicating that the tumors do not seem to harbor long-term LRCs (Fig. 49, black curve). Several possibilities might explain this observation: first, NSG mice lack functional B-, T- and NK-cells and therefore may be unable to recapitulate all the microenvironmental features required for the establishment of tumor dormancy. However, the impact of the immune system on tumor dormancy has not been shown yet, except for the murine B cell lymphoma, where cytotoxic CD8+ T-cells or anti-idiotypic antibodies against the B-cell receptor are able to arrest tumor cells (Farrar et al., 1999; Rabinovsky et al., 2007).

Second, cancer cells might only switch to a quiescent state when tumors reach a certain size. Bigger tumors often develop hypoxic areas and lack nutrition supply due to poor vascularization, which in the end may influence the cell cycle state of the tumor cells. Probably the tumors analyzed in this study were too small or tumor cells that lost the label already reentered into dormancy and could not be detected anymore at the time point of analysis. In order to visualize a possible reentry from a cycling to a non-cycling state a second labeling method needs to be used at a later time point, such as BrdU.

Furthermore, as described for the *in vitro* preselected tumor cells, all the different cycling cell populations were able to develop into tumors that morphologically resembled each other and more importantly the initial primary tumor (Fig. 55). In addition, there was no significant difference in mean tumor volume between the distinct cell populations, indicating again that there might be a dynamic switch between the different cell populations. The observation that all different cycling cell populations are able to generate a tumor in a xenograft model is in accordance with a recent study from Moore and colleagues who analyzed the function of different cycling cells in conventional breast- and colorectal cancer cell lines. Similarly, the authors showed that slowly cycling cells are able to develop into a tumor (Moore et al., 2011).

Moreover, lung metastases appear to contain less H2B-GFP positive cells in comparison to the matched primary tumor as assessed by IHC (Fig. 51), suggesting that slowly cycling cells that arrive at a distant organ start to proliferate. These

disseminated tumor cells may reenter a quiescent state if a certain tumor size is reached and novel blood vessels and other growth factors are lacking in order to develop into overt macrometastases. Furthermore, a different scenario of angiogenic dormancy could be envisioned. Possibly all tumor cells actively divide but the tumor mass does not increase due to constant balance between proliferation and apoptosis (Aguirre-Ghiso, 2007). As previously discussed, a second labeling technique that allows the tracking of tumor cells that may reenter quiescence at a later time point during tumor progression may give further weight to one hypothesis. This observation needs to be confirmed in more mice and the frequency of LRCs needs to be quantified.

Additionally, all these experiments represent endpoint analyses. In order to determine whether the onset of tumor growth is different between the fast-, medium- and slowly cycling cells an additional labeling with luciferase was performed that enabled a non-invasive analysis of the tumor growth kinetics.

Fast-, medium- and slowly cycling cells preselected *in vivo* induce tumors with similar growth kinetics

In vivo preselected fast-, medium- and slowly cycling cells that express luciferase in addition to H2B-GFP were transplanted into secondary recipient mice and the tumor growth kinetics were estimated weekly via *in vivo* bioluminescence measurements. There was no significant difference between the different cycling cell populations regarding tumor growth (Fig. 59). Furthermore, the secondary recipient mice were treated with Dox for 15 days prior to analysis. IHC stainings of the tumor sections demonstrated that all the sorted cell populations were able to generate fast-, medium- and slowly cycling cells independent of the initial cell cycle state (Fig. 62), indicating again that there might be a dynamic and bidirectional process between the different cycling cell populations. This is in line with recent studies performed in melanoma (Roesch et al., 2010) and pancreatic cancer (Dembinski and Krauss, 2009). Roesch and colleagues demonstrated that JARID1B negative melanoma cells were able to generate slowly cycling JARID1B positive cells similar to the finding of Dembinski and Kraus who reported that DiI negative pancreatic tumor cells could generate DiI positive cells and also vice versa.

The authors suggest that heterogenous tumor cell populations follow rather a dynamic than a hierarchical model.

Even though the distinct cycling cell populations analyzed in this study do not seem to differ in their contribution to tumor progression, these cells may be involved in chemotherapy resistance and relapse.

Slowly cycling cells are more resistant to chemotherapy *in vitro*

In the intestine, quiescent ISCs marked by Bmi1 and mTert have been identified (Cairnie et al., 1965; Montgomery et al., 2011; Potten, 1977; Potten et al., 1974; Yan et al., 2012). These ISCs were resistant to high-dose irradiation and tissue injury and were subsequently able to repopulate the damaged crypts and villi. Furthermore, the quiescent ISC population was capable of giving rise to actively cycling Lgr5+ cells (Montgomery et al., 2011; Yan et al., 2012). Thus quiescent ISCs were able to survive chemotherapy treatments, which might be also true for slowly cycling tumor cells.

In order to test this hypothesis, we exposed our colorectal tumor cell lines to standard chemotherapeutics used to treat metastatic cancer patients, such as 5-FU and Oxaliplatin. Slowly cycling cells were enriched upon either of the two treatments (Fig. 63). This observation might be explained by two possibilities: either slowly cycling cells are more resistant to treatment and have greater survival than fast cycling tumor cells, or simply each tumor cell is arrested and thus retains the H2B-GFP label as a direct consequence of the treatments. In order to exclude the latter possibility, the CRC cells were sorted prior to treatment and the IC_{50} was determined. In three independent experimental settings, slowly cycling cells had a higher IC_{50} compared to faster cycling cell populations (Tab. 7), indicating that these cells were more resistant to chemotherapy. However this result was not observed in the HD1858 cell line treated with Oxaliplatin (Tab. 7). The experimental set up might not have been optimal for both cell lines. Different cell numbers were seeded for HD1858 and G605 cells, which might impact the outcome of the experiment. Furthermore the differences for the IC_{50} observed between the different cycling cell populations were modest (Fig. 64). However, both colorectal tumor cell lines were generated from highly metastatic tumors that disseminated to the liver. The patients were already under treatment and the tumor cells might have adapted to the cytotoxic drugs. This might explain why only minor differences were detected using these two cell lines upon chemotherapy treatment. Nonetheless, future studies will be needed in order to investigate whether this observation holds true *in vivo*.

7.4. Conclusion

In conclusion, this study shows that different cycling tumor cell populations exist in colorectal tumors. Phenotypical characterizations of these distinct cell populations did not reveal an increased expression of the reported CSC markers within the slowly cycling cell population *in vitro*, suggesting that variations in cell cycle might

not depend on the CSC model. All the cells were able to proliferate and to generate adenocarcinomas in xenograft mouse models that morphologically resemble each other and the initial patient tumor. The distinct cycling cell populations were able to regenerate fast-, medium- and slowly cycling cells, indicating that the cells are able to dynamically switch their cycling phenotype, making it difficult to target specifically slowly cycling cells. In addition, slowly cycling cells have an enhanced chemoresistance when compared to the medium- or fast cycling cells. These slowly cycling cells may survive standard chemotherapy treatment and due to their ability to switch to a fast cycling phenotype, upon so far unknown intrinsic or external stimuli may cause relapse in CRC patients. Initially fast cycling cells may acquire a more quiescent phenotype upon treatment and afterwards switch back to a fast cycling phenotype, thereby promoting tumor progression. A more complex and dynamic regulatory network as previously expected may exist between distinct tumor cell populations (Fig. 66). As these populations may be able to switch their cycling behaviors upon intrinsic or external stimuli, this dynamic behavior should be considered when developing novel treatment strategies.

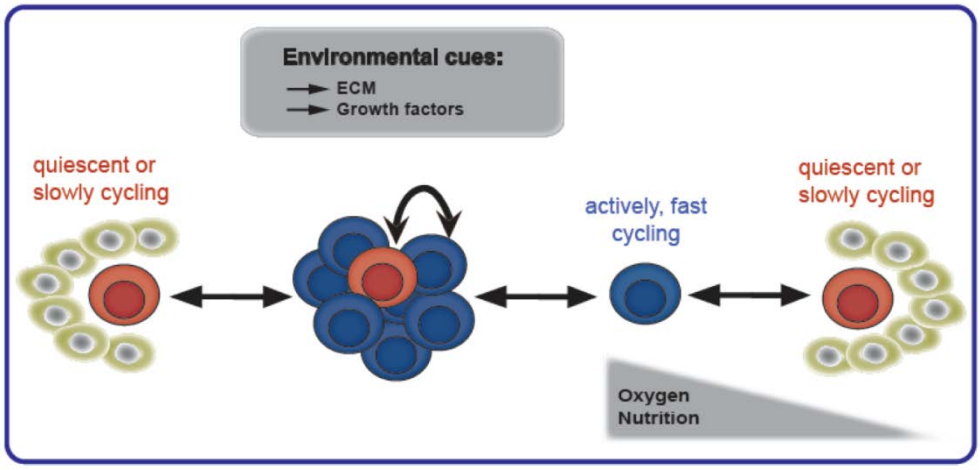

Fig. 66: Model proposing a dynamic interplay between slowly- and fast cycling tumor cells. Tumor cells are able to switch between different cycling phenotypes within the tumor and possibly also at the distant site. This switch may be partially triggered via external stimuli mediated by the microenvironment. Specific niches regulating cellular dormancy either due to low oxygen levels or a lack of nutrition supply may be present in a tumor. Growth factors and ECM could also be involved in the balance between quiescent- and actively dividing cells. Conceivably stress such as chemotherapy may support the release of signals that in turn induces fast cycling cells to arrest in cell cycle and to switch into a more quiescent state. Furthermore, intrinsic mechanisms may also partially determine the cycling phenotype of a tumor cell.

7.5. Outlook

Several clinical observations, such as minimal residual disease with long latency periods between treatment and relapse have led to the concept of tumor cell dormancy, assuming that these dormant cells may be more resistant to therapy (see chapter 4.9.). However, experimental evidence unraveling the exact drug resistance mechanisms in dormant cancer cells is still missing. The experiments performed in this study suggest that slowly cycling cells may be involved in relapse and chemotherapy resistance. Additional studies using *in vivo* models will be necessary to confirm these results. The following experimental setup would provide further insight into the possible role of slowly cycling cells in disease relapse:

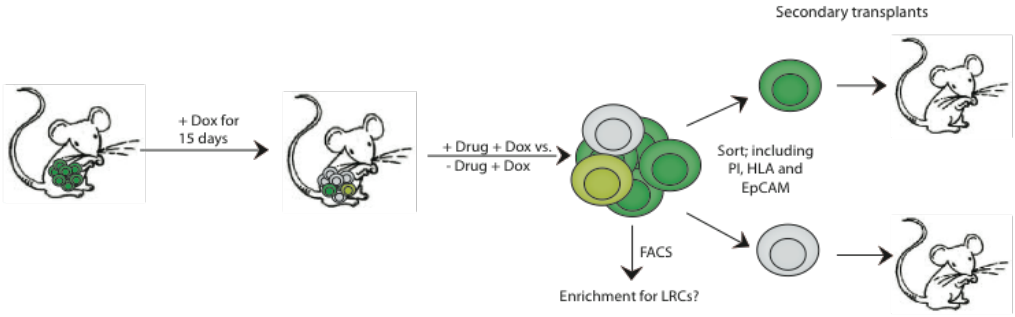

Fig. 67: Experimental set up to test the ability of LRCs to survive chemotherapy treatment *in vivo*. Mice will be injected with H2B-GFP/luciferase expressing colorectal tumor cells. After tumor growth, mice will be treated with Dox for 15 days prior to chemotherapy administration (Dox treatment will continue). Mice not treated with chemotherapy but with Dox will be used as control. The tumors will be harvested and analyzed for the frequency of LRCs. LRCs and non-LRC will be further transplanted into secondary recipients to test their tumor initiating capacity.

Firstly, tet-Off-H2B-GFP and luciferase expressing colorectal tumor cells will be injected into the renal capsule of NSG mice. After establishment of tumors, mice will be treated with Dox in order to mark the different cycling cell populations, according to H2B-GFP label-retention. Initial experiments indicated that after 15 days of Dox treatment a clear distribution of the distinct cycling cell populations could be reached in tumors. Therefore, mice would receive Dox for 15 days. Chemotherapy would then be administered in parallel with continuous Dox treatment. It is likely that the tumors will shrink upon treatment, due to elimination of cycling cells by the chemotherapeutic agent. In order to test whether LRCs are indeed resistant to chemotherapy *in vivo*, the frequency of LRCs will be compared before and after treatment. Viable LRCs and non-LRCs, if present, will be further transplanted into secondary recipients in order to test whether these cells are still able to regenerate a tumor and to compare their tumorigenic potential. For this analysis it is important to carefully exclude dead cells, for instance by using PI (Fig. 67). Moreover, limiting

dilutions will be necessary to determine the frequency of tumor initiating cells. Microarray expression profiling could be performed on the sorted cells in order to get further information about the molecular mechanisms involved in the chemotherapy resistance. Additionally, an intra-splenic metastasis model could be used to test whether the sorted cell populations have different metastasis initiating capacities.

To further investigate whether chemotherapy can induce a quiescent or slowly cycling state in the tumor cells, the following experimental set up would clarify this question:

The primary colorectal tumor cell lines expressing H2B-GFP and luciferase will be injected into the renal capsule of NSG mice. After monitoring of tumor growth, the mice will be treated with Dox for eight days and afterwards chemotherapy will be administered 48 hours prior to BrdU treatment. The mice will be treated with BrdU and Dox until the end of the experiment (Fig. 68a). The exact timing for the treatment with BrdU and the chemotherapy needs to be determined in independent experiments.

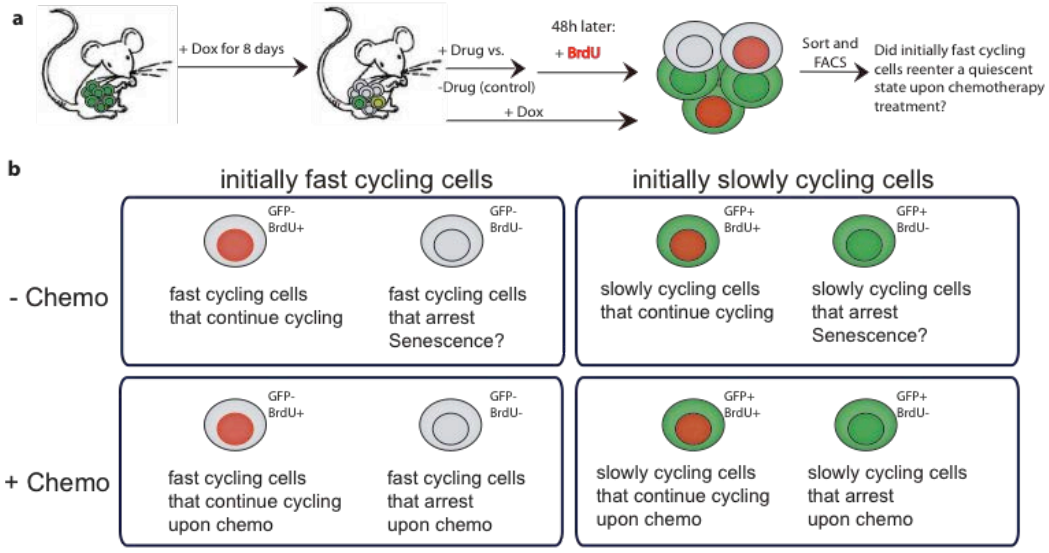

Fig. 68: Experimental set up to test whether chemotherapy can induce cell cycle arrest. a) Mice will be injected with H2B-GFP/luciferase expressing colorectal tumor cells. After tumor growth, mice will be treated with Dox for 15 days prior to chemotherapy administration (Dox treatment will continue). 48h after chemotherapy treatment, BrdU will be administered in order to label cycling cells (BrdU treatment will continue until the end of the experiment). b) Possible outcome of the experiment: Cells that arrest upon chemotherapy treatment will not incorporate BrdU whereas cells that still actively cycle will be BrdU+. Possibly some cells that arrest upon treatment enter senescence.

GFP^+ and GFP^- cell populations will be isolated and subsequently analyzed for their BrdU content and compared with non-treated controls. If the treatment would induce a cell cycle arrest, the initially cycling cells would not incorporate BrdU, in contrast to

resistant cells (Fig. 68b). By determining the frequency of each population it would be possible to analyze the relative effect of the chemotherapy on the distinct cell populations. However, this assay does not allow functional studies because the cells need to be fixed prior to analysis.

8. Material & Methods

Mice

All animal studies were carried out according to the animal protocol approved by GV-Solas (Gesellschaft für Versuchstierkunde). Mice used for all the experiments were NOD.Cg-*Prkdc*^{scid} *Il2rg*^{tm1Wjl}/SzJ (NSG). Authorization numbers G17/12 and G57/10 were obtained from the national authorities for research experiments on animals (Regierungspräsidium, Karlsruhe). Mice were maintained in the DKFZ animal facility in Heidelberg under specific pathogen-free (SPF) conditions and housed in individually ventilated cages (IVC).

Subcutaneous transplantations of primary tumor pieces

Primary tumor pieces from colorectal cancer patients or secondary transplants were minced into small pieces of 1 mm x 1 mm. The mice were anesthetized using xylazin (14.5 mg/kg) and ketamin (90 mg/ml). Ten µl per gram body weight were injected intra-peritoneally (i.p.). The anesthetized mice were kept on a heating pad until they woke up from anesthesia in order to maintain their body temperature. A small incision was made in the flank of the mice with a sterile scissor. The tumor piece was placed under the skin and the incision was closed with wound clips. The wound was disinfected with Betadine and Cicatrex cream was added to facilitate the healing of the wound. Artificial tears were put on the eyes in form of a cream.

Kidney capsule injections of primary tumor cells

Tumors were either digested with collagenase (0.25 %) and DNase to obtain single cell suspensions or cells from cultures were used for the injections. The mice were anesthetized using xylazin (14.5 mg/kg) and ketamin (90 mg/ml). Ten µl per gram body weight were injected i.p.. The anesthetized mice were kept on a heating pad until they woke up from anesthesia in order to maintain their body temperature. Prior to surgery, the mice were shaved at the abdomen and disinfected. A small incision was made in the skin of the mice to expose the kidney. The cells were re-suspended and injected in a volume of 30 µl diluted in PBS (Phosphate buffered saline) via a 29 G syringe. The wound was closed using an absorbable thread and wound clips. The wound was disinfected with Betadine and Cicatrex cream was added to facilitate the healing of the wound. Artificial tears were put on the eyes in form of a cream.

Dox treatment of mice injected with colon tumor cells transduced with tet-Off-H2b-GFP lentivirus

After tumor growth was verified, the mice were treated with Dox (Sigma) in the drinking water at a dose of 2 g/l protected from light.

Dissociation of primary tumors or xenografts

The tumors were washed once with PBS. The PBS was removed and the tumors were minced using sterile scalpels. The minced tumor pieces were resuspended in CO_2-independent medium (Invitrogen) supplemented with BSA (1%) and glutamine. Additionally, collagenase IV (0.25%, Sigma) and DNase I (Roche) were added to the medium. The tumor pieces were further dissociated in the gentleMACS™ dissociator for 30 seconds and incubated at 37°C for 1 hour rotating. Afterwards, the cell suspension was filtered through a 100 µm mesh and washed once with PBS.
In order to purify the tumor cells from erythrocytes and dead cells, an Optiprep™ (Axis-Shield) density gradient was performed at 4°C for 20 minutes at 4000 rpm. The interphase was collected and washed with PBS. The cells were frozen, cultured, analyzed or transplanted dependent on the experiment.

Establishment of primary human tumor cell lines

The tumors were dissociated as described in chapter 9.14. The primary tumor cells were maintained in Advanced DMEM/F12 (Invitrogen) supplemented with glutamine (2 mM, Gibco), N2-supplement (Invitrogen), trace elements A, B and C (Mediatech/Cellgro), heparin (2 mg/ml) (Sigma), glucose (0.6 %) (Sigma), lipid mixture (Sigma), HEPES (5 mM) (Gibco), 2-Mercaptoethanol (100 µM, Invitrogen), BSA (Millipore), basic Fibroblast Growth Factor (bFGF, 50 ng/ml) (Peprotech), Epidermal Growth Factor (EGF, 20 ng/ml) (Peprotech), R3 IGF-I (10 ng/ml, Sigma) and Hepatocyte growth factor (HGF, 50 ng/ml) (Peprotech).
The cells were grown as spheres in hydrophobic suspension culture flasks (Greiner). The cells were cultured short-term adherent on collagen I (30 µg/ml; Gibco) coated cell culture flasks.

Coating of cell culture flasks with collagen I

Cell culture flasks were covered with collagen I (30 µg/ml) diluted in PBS. The flasks were incubated at 37°C for 2 hours and stored at 4°C until usage. Prior to seeding of the cells, the collagen I / PBS mixture was discarded and the surface of the flasks was washed once with PBS.

Clonogenicity assay *in vitro* using crystal violet

Single cell suspensions were generated and 12.000 cells were seeded into one 6-well. The cells were distributed evenly in the wells to avoid cell clumps. The cells were grown on collagen I coated plates in serum-free cancer stem cell medium. The medium was removed and the wells were carefully rinsed with PBS. The PBS was removed and the wells were covered with 0.5% crystal violet containing 6% (v/v) glutaraldehyd and incubated for 30 minutes at room temperature. Afterwards, the crystal violet was removed and the wells were carefully rinsed with tap water. Colonies were counted and colony sizes were determined using the Image J software (particle count). The protocol was adapted from (Franken et al., 2006).

Lentivirus production

For the generation of high titer lentiviruses the Tronolab protocol was used: http://tcf.epfl.ch/site/tcf/page-6764.html. A second generation virus production was performed using psPAX2 as a packaging plasmid and pMD2.G as the plasmid coding for the envelope. For the transgene, the following plasmids were used:

- tet-Off-H2B-GFP (pWPXL-TTT-H2B-GFP) (vector map see chapter 9.5.)
  -> reporters: H2B-GFP
- pV2luc2 (vector map see chapter 9.6)
  -> reporters: luciferase 2 and venus
- pTurboGlow (vector map see chapter 9.7.)
  -> reporters: luviferase 2 and eqFP650 (Evrogen)

The pWPXL-TTT-H2B-GFP plasmid was a kindly provided by Prof. Dr. Boukamp and Prof. Dr. Kirschner (Falkowska-Hansen et al., 2010). Calcium-phosphate was used for the transfection of HEK293T cells. The HEK293T cells were maintained in IMDM (Gibco) supplemented with 10% FCS and 2 mM glutamine. Chloroquine (25 µM) was added to the medium prior to virus production. Virus was harvested 24- and 48 hours after transfection. The supernatant was filtered and spun down to remove cell debris. Afterwards, the viral supernatant was centrifuged at 24000 rpm at 4°C for 2 hours in an ulatracentrifuge. Therefore, 20% sucrose solution (1:10) was covered with the viral supernatant in order to purify the virus. The viral particles were resuspended in PBS/1% BSA and aliquoted.

Transduction of primary colon cancer cell lines

The colon cancer cells were dissociated using StemPro Accutase™ (Invitrogen) and single cell suspensions were seeded on collagen I coated plates. Polybrene (10

µg/ml) was added to the medium prior to transduction. After successful transduction of the colon cancer tumor cells, the cells were sorted for the respective reporter such as GFP, venus or eqFP650. The cells were either transduced with one of the transgene plasmids or a double transduction was performed using pWPXL-TTT-H2B-GFP and pTurboGlow. Therefore, the cells were transduced with one plasmid and sorted prior to the second transduction. Afterwards, the cells were sorted for both transgenes (GFP and eqFP650).

In vivo bioluminescence imaging using the Xenogen system (IVIS-200 Caliper)

Mice were injected intra-peritoneally with D-Luciferine Firefly Potassium salt (15 mg/ml in PBS) at a dose of 10 µl per gram body weight (Biosynth) 10 minutes before imaging. The animals were anesthetized using 4.5% isoflurane in oxygen (0.9 l/min), maintained at 1.5 % isoflurane in oxygen and analyzed in the heated camera chamber. The Living Image software was used according to the manufacturer's instructions (IVIS 200, Caliper).

Slowly cycling cells *in vitro*

The spheroid cultures were dissociated with StemPro Accutase™ (Invitrogen) for 10 minutes at 37°C. A density gradient using OptiPrep™ (Axis-Shield) was performed for 20 minutes at 4000 rpm at 4°C to reduce the amount of dead cells and cell debris. The inter-phase was collected and washed with PBS. The cells were seeded at low densities on collagen I coated tissue culture flasks. One day after seeding, the cells were treated with Dox (10 ng/ml) for 10 days.

PKH-26 staining

The PKH-26 cell linker kit from Sigma was used (catalogue number: PKH26GL). Single cell suspension was washed once with serum-free medium and centrifuged for 5 min at RT with 400 x g. A 2x cell suspension was prepared by adding 1 ml of Diluent C. The cells were gently resuspended. Afterwards, 4 µl of PKH-26 resuspended in 1 ml Diluent C were added to the cells. The cells were incubated for 5 min at RT with periodic mixing. The reaction was stopped by adding 2 ml of protein solution (PBS + 1% BSA) for 1 min. Afterwards 4 ml of medium were added and the cells were centrifuged for 5 min at 400 x g at RT. The cells were washed twice with medium and the viability was determined using trypan blue.

Flow cytometry

All surface stainings were performed in PBS supplemented with 1% BSA and 0.5 M EDTA. 1x 10^6 cells were stained in 100 µl of staining solution for 30 minutes on ice. A complete list of antibodies used for the stainings is provided in chapter 9.1.
For the analysis the following analyzers were used:

- LSR II™ (BD)
- Fortessa™ (BD)
- Cyan ADP™ (Dako, Glostrup, Denmark)

The cell sorting was performed on a FACS Aria Flow Cytometer (Becton Dickinson, San Jose, CA). A 100 µm nozzle was used for the cell sort to ensure that the cells are not destroyed. Data were analyzed with the FlowJo software (Tree Star, Ashland, OR).

Cell cycle analysis via Ki-67/Hoechst staining

The tumor cells were fixed and permeabilized in ice-cold EtOH (70%) for 2 hours at -20°C. Afterwards, the cells were washed twice with PBS and incubated with an anti human Ki-67 antibody (BD Biosciences) at room temperature for 1 hour. Hoechst (Molecular probes) at 20 µg/ml was added for 15 minutes prior to analysis. The analyses were performed on a LSR II or Fortessa (BD Biosciences).

Immunohistochemistry of tumor sections

All histological samples were fixed in 10% neutral buffered formalin solution (Sigma) at room temperature on a rotor. Samples were dehydrated (70%EtOH; 90%EtOH; 100%EtOh), immersed sequentially into xylol and paraffin (Tissue-Tek®VIP®6) and embedded in paraffin (Thermo Scientific, Histo Star®). Embedded tissues were cut at 4 µm, deparaffinized and rehydrated (3x Xylol; 3x EtOH 100%; 1x EtOH 95%; 1x EtOH 80%; distilled (d)H_2O). Sections were stained with hematoxylin and eosin (H&E) for morphological analysis. Additional stainings were performed according to the protocol in chapter 9.8.

Immunohistochemistry of spheres

The spheres were resuspended in Histogel (Thermo Scientific). The mixture of cells and Histogel was added to a cloning cylinder (Corning). The cylinder is sealed to a plate with silicone high vacuum grease to prevent leakage of the fluid. The cells were placed at 4°C until the histogel was solidified. The cloning cylinders were removed from the plate and the cells embedded in the solidified histogel were placed into 10%

neutral buffered formalin solution (Sigma) on a rotor. The spheres were dehydrated (70%EtOH; 90%EtOH; 100%EtOh), immersed sequentially into xylol and paraffin (Tissue-Tek®VIP®6) and embedded in paraffin (Thermo Scientific, Histo Star®). Embedded spheres were cut at 4 µm, deparaffinized and rehydrated (3x Xylol; 3x EtOH 100%; 1x EtOH 95%; 1x EtOH 80%; distilled (d)H_2O). Sections were stained with hematoxylin and eosin (H&E) for morphological analysis. Additionally, stainings with an anti human beta-catenin antibody were performed according to the protocols in chapter 9.8. and 9.9.

Hypoxia induction

The CRC cell lines, G605-H2B-GFP and HD1858-H2B-GFP, were maintained on collagen I coated plates in cancer stem cell medium in hypoxic chambers (BioSpherix) either at oxygen levels of 3% or 0.5% for 10 days prior to analysis.

Image Aquisiton

Light microscopy pictures of the sections were taken via a Leica DM LB2 microscope that contained a Leica DC480 CCD camera or with the Zeiss Axioplan microscope equipped with the AxioCam ICc 3 colour camera.

Statistical Analysis

Statistical significance was determined by T-test (95% confidence interval) or one-way ANOVA at $p \leq 0.05$. For the one-way ANOVA, a post-test was performed using Bonferroni's multiple comparison test. All data are reported as the mean + SE. Statistical significance was considered as * ($P < 0.05$), ** ($P < 0.01$), *** ($P < 0.001$).

9. Appendix

9.1. List of antibodies used for flow cytometry analysis of human cells

ANTIGEN	COMPANY	CAT.#	CLONE	Isotype	Conjugate
CD24	BD	555427	ML5	Mouse IgG2a	FITC
	BD	555428	ML5	Mouse IgG2a	PE
	BioLegend	31106	ML5	Mouse IgG2a	PE
	BioLegend	311118	ML5	Mouse IgG2a	APC
CD44	BioLegend	103020	IM7	Rat IgG2b	Pacific Blue
CD45	BioLegend	304022	HI30	Mouse IgG1	Pacific Blue
	eBioscience	12-0459-42	HI30	Mouse IgG1	PE
	ebioscience	11-0459-73	HI30	Mouse IgG1	FITC
CD49a	BD	559596	SR84	Mouse IgG1	PE
CD49b	BD	555669	12F1	Mouse IgG1	PE
CD49c	BD	556025	C3II.1	Mouse IgG1	PE
CD49d	BD	340296	9F10	Mouse IgG1	PE
CD49e	BD	555617	IIa1	Mouse IgG1	PE
CD49f	BD	555736	GoH3	Mouse IgG1	PE
CD133/1	Milteny	130-090-826	AC133	Mouse IgG1	APC
	Milteny	130-080-801	AC133	Mouse IgG1	PE
CD166	MBL	K0044-4	3A6	Mouse IgG1	FITC
	R&D	FAB6561P	105902	Mouse IgG1	PE
CD326 (EpCAM)	BD	347200	EBA-1	Mouse IgG1	APC
	eBioscience	12.9326-71	1B7	Mouse IgG1	PE
c-Met	eBioscience	13-8858	eBioclone 97	Mouse IgG1	Biotin
	R&D	FAB3582A	95106	Mouse IgG1	APC
HLA-ABC	BD	555552	G46-2.6	Mouse IgG1	FITC
	ebioscience	12-9983	W6/32	Mouse IgG2a	PE
	ebioscience	13-9983	W6/32	Mouse IgG2a	Biotin
	BD	555555	G46-2.6	Mouse IgG1	APC
H2Kd	BioLegend	116612	SF1-1.1	Mouse IgG2a	AF-647
Ki-67	BD	558615	B56	Mouse IgG1	AF-647

9.2. List of reagents used for cell culture

Article	Company	Catalog number
Advanced DMEM/F12	Invitrogen	12634-010
CO_2 Independent Medium	Invitrogen	18045-054
N2 Supplement	Invitrogen	17502048
2-Mercaptoethanol, 50 mM	Invitrogen	31350-010
Glucose 45%	Sigma	G8769
Heparine	Sigma	H-3149-10KU
Lipid Mixture 1	Sigma	L-0288
basic Fibroblast Growth Factor (bFGF)	Preprotec	AF-100-18B
Epidermal Growth Factor	Preprotec	500-P45
LONG®R^3 IGF-I human	Sigma	I1271.1mg
Trace Elements A	Mediatech/Cellgro	MT-99-182-CIc
Trace Elements B	Mediatech/Cellgro	MT-99-175-CIc
Trace Elements C	Mediatech/Cellgro	MT-99-176-CIc

9.3. Flow cytometry analysis of G605 cells

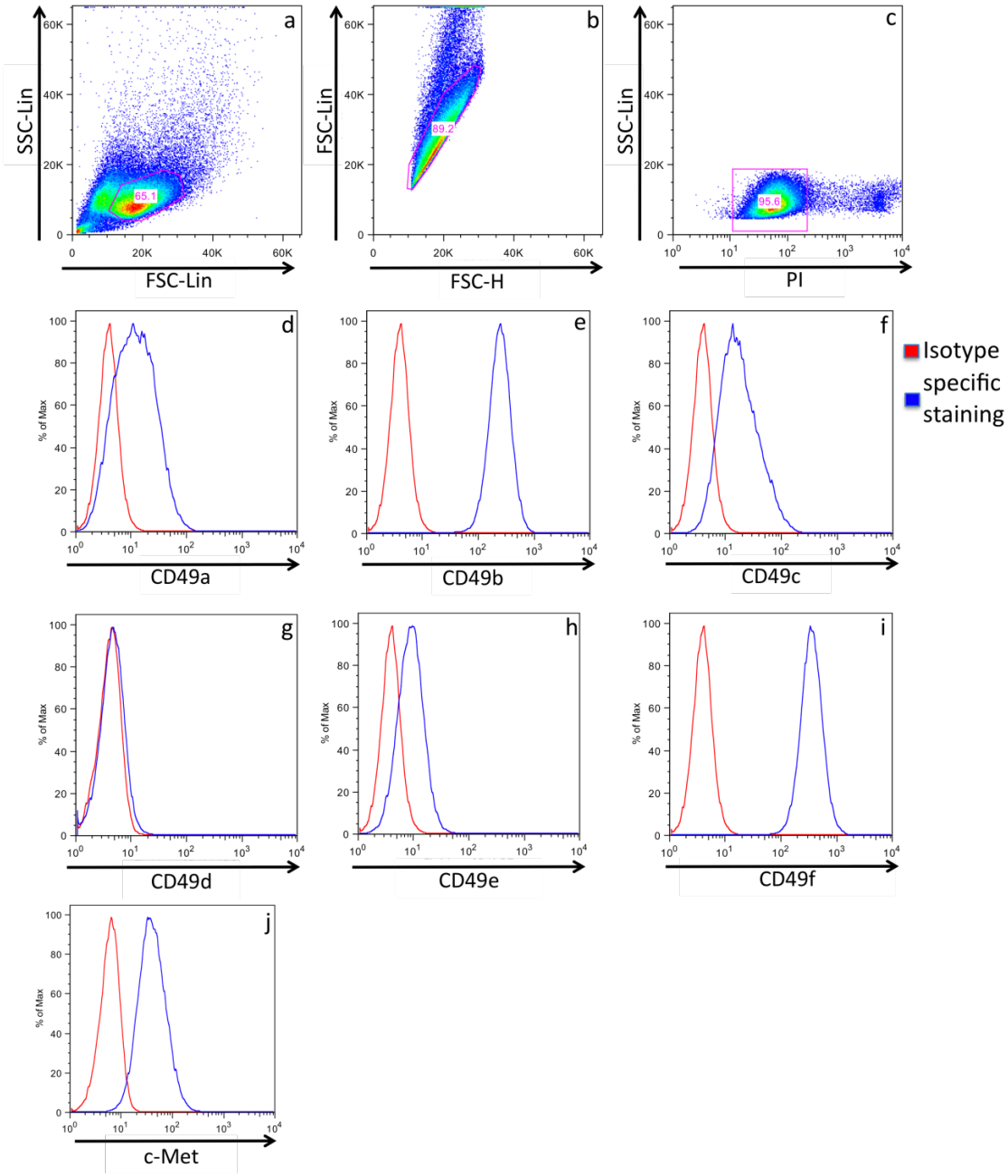

Fig. 69: G605 cells differentially express alpha integrins and c-Met. Doublet- (b) and dead cell exclusion, using PI were performed (c). The cells differentially express CD49a (d), CD49c (f) and CD49e (h). All the cells homogenously express CD49b (e), CD49f (i) and c-Met (j). CD49d is not expressed in G605 cells (g).

9.4. Slowly cycling cells are not enriched for putative CSC markers (HD1858)

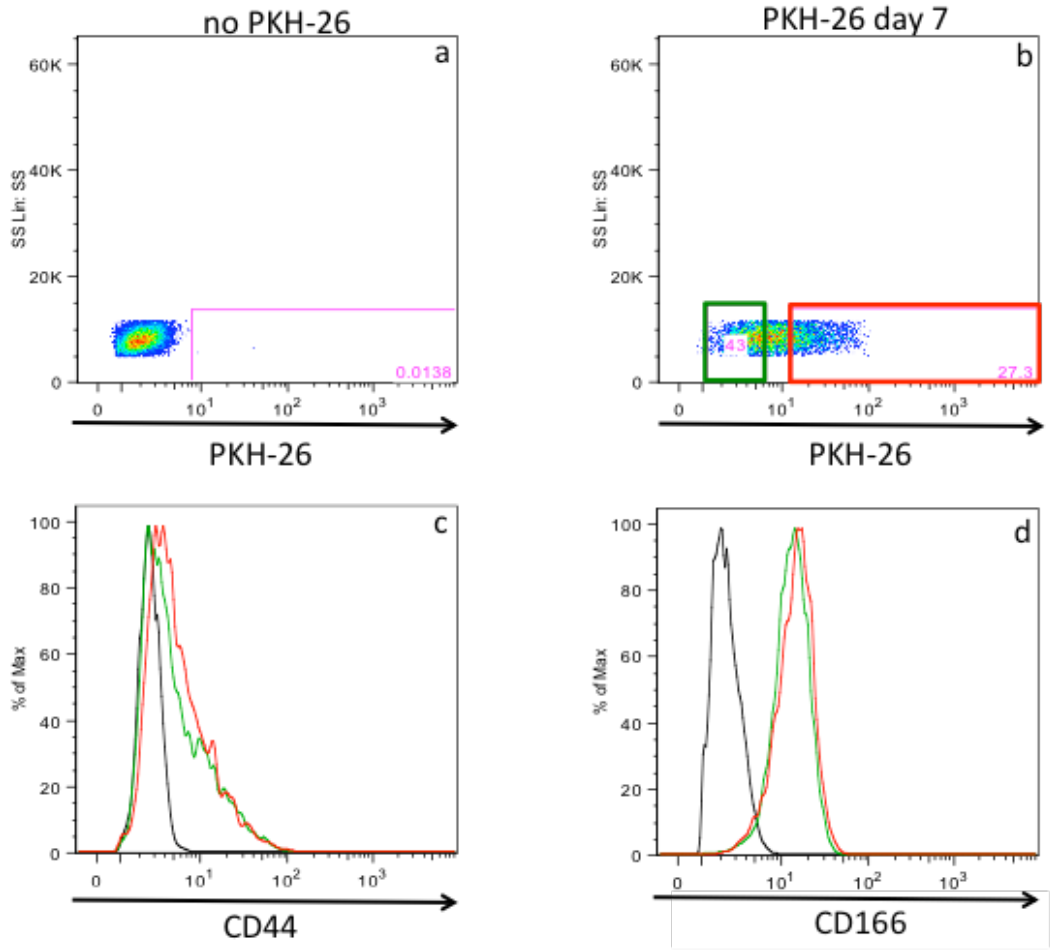

Fig. 70: Slowly cycling HD1858 cells are not enriched for CSC markers. Colon spheres were labeled with PKH-26 and maintained in culture for 7 days. Slowly- (b, red square) and fast cycling cells (b, green square) were classified according to parental cell line not treated with PKH-26 (a). Slowly- and fast cycling cells express the same level of CD44 (c) and CD166 (d) (black curve = isotype control; red curve = slowly cycling cells; green curve = fat cycling cells).

9.5. Vector map pWPXL-TTT-H2B-GFP

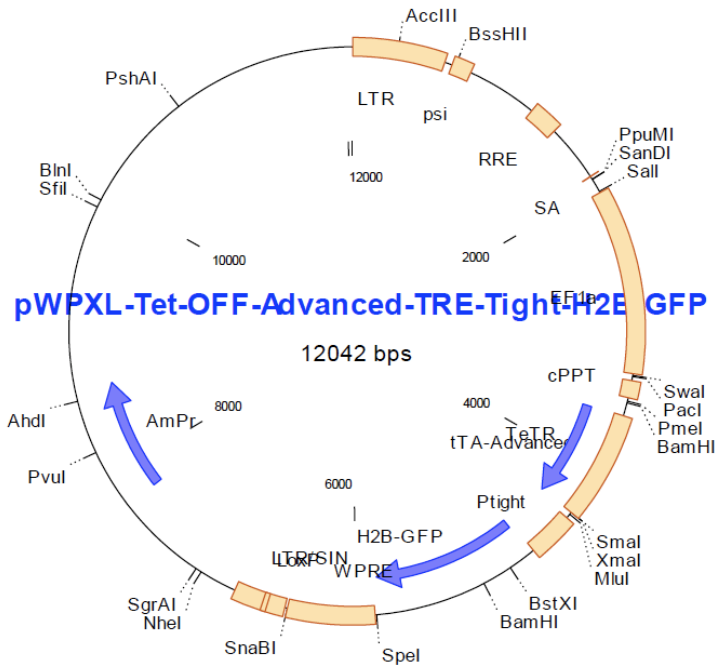


```
Molecule Definition:

Molecule:       pWPXL-Tet-OFF-Advanced-TRE-Tight-H2B-GFP,  12042 bps DNA
Circular
File Name:      pWPXL-Tet-OFF-Advanced-TRE-Tight-H2B-GFP.cm5,  dated 19 Jun
2007

Molecule Features:

Type      Start      End    Name          Description

REGION        2      635    LTR
REGION      687      824    psi           HIV packaging signal
REGION     1311     1515    RRE           Rev responsive element
REGION     1907     1909    SA            3'-splice site
REGION     2034     3297    EF1a
REGION     3345     3462    cPPT
REGION     3588     4334    tTA-Advanced
GENE       3594     4340    TeTR
REGION     4380     4695    Ptight        Tet-responsive promoter
GENE       4724     5836    H2B-GFP
REGION     5868     6465    WPRE          enhancer
REGION     6483     6841    LTR/SIN
REGION     6603     6637    LoxP
GENE       7773     8633    AmPr
```

Generated by (Falkowska-Hansen et al., 2010).

9.6. Vector map pV2luc2

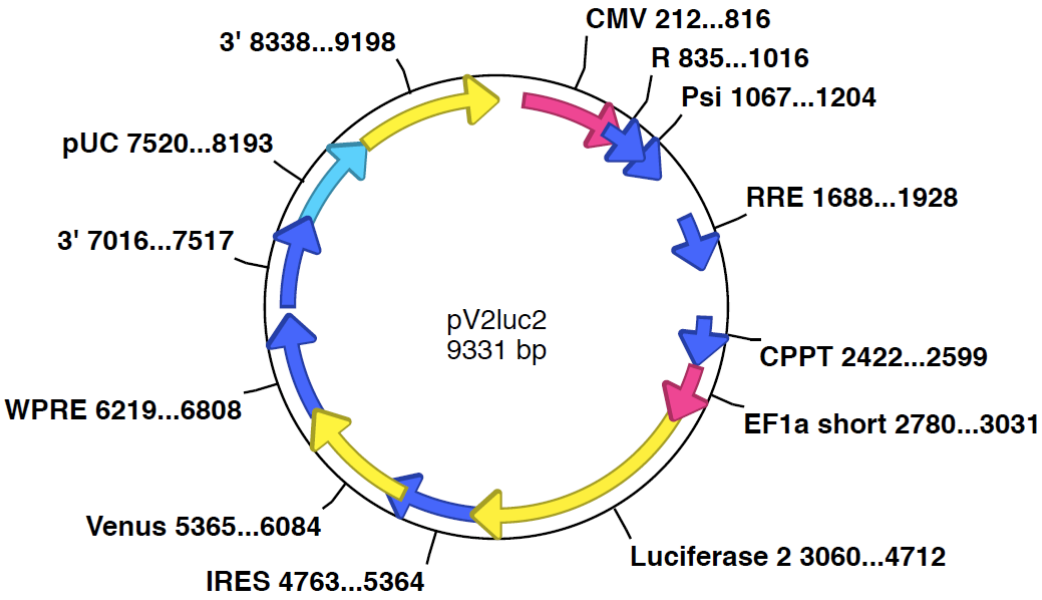

Molecule definition:

Molecule: pV2luc2; 9331 bp
Circular

Molecule Features:

Type	Start	End	Name	Description
Region	212	816	CMV	promotor
Region	1067	1204	Psi	HIV packaging signal
Region	1688	1928	RRE	Rev responsive element
Region	2422	2599	cPPT	central polypurine tract
Region	2780	3031	EF1a short	promotor
Gene	3060	4712	Luciferase 2	reporter for bioluminescence
Region	4763	5364	IRES	Internal ribosome entry site
Gene	5365	6084	Venus	reporter for fluorescence
Region	6219	6808	WPRE	enhancer

Generated by Christian Eisen

9.7. Vector map pTurboGlow

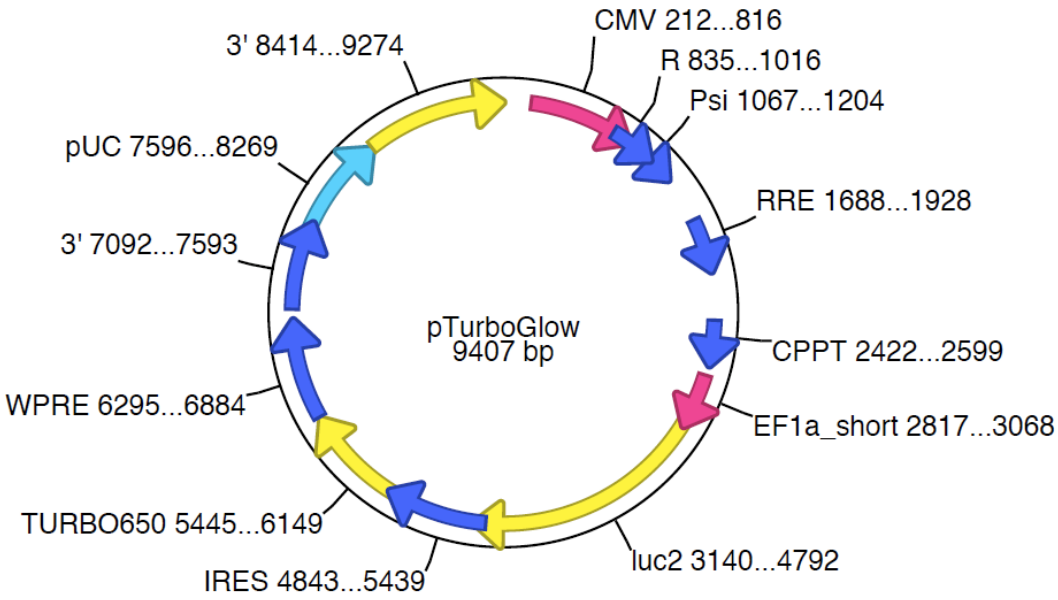

Molecule definition:

Molecule: pTurboGlow; 9407 bp
Circular

Molecule Features:

Type	Start	End	Name	Description
Region	212	816	CMV	promotor
Region	1067	1204	Psi	HIV packaging signal
Region	1688	1928	RRE	Rev responsive element
Region	2422	2599	cPPT	central polypurine tract
Region	2817	3068	EF1a short	promotor
Gene	3140	4792	Luciferase 2	reporter for bioluminescence
Region	4843	5439	IRES	Internal ribosome entry site
Gene	5445	6149	Turbo650	reporter near infrared
Region	6295	6884	WPRE	enhancer

Generated by Christian Eisen

9.8. Immunohistochemistry protocol: mouse anti-human Ki-67 antibody

(established by Department of Pathology, Vanessa Vogel, Prof. Dr. Weichert)
Dako REAL™ Detection System, Peroxidase/AEC, Rabbit/Mouse

Deparaffinize the slides:

- 10 min. Xylol
- 10 min. Xylol
- 5 min. 100% Ethanol
- 5 min. 100% Ethanol
- 5 min. 96% Ethanol
- 5 min. 70% Ethanol
- 5 min. distilled water

Heat-Induced Epitope Retrieval:

Using damp heat in a steam pot with citrate buffer at pH 6.0

- 15 min cooking
- 30 min cooling outside the pot but within the buffer
- Rinse slides in distilled water

Avidin/Biotin Blocking Kit:

- Rinse the slides in PBS Tween buffer
- Apply avidin block for 10 minutes at room temperature
- Rinse the slides in PBS Tween buffer
- Apply biotin block for 10 minutes at room temperature
- Rinse the slides in PBS Tween buffer

Primary Antibody:

- Prepare the primary antibody dilution (total volume 200 µl)
- Incubation with the Primary Antibody for 30 minutes at room temperature
- Rinse the slides in PBS Tween buffer

Secondary Antibody:

- Using the multilink secondary antibody (Goat anti-Rabbit, goat anti-mouse) from Dako Kit bottle A
- Apply 200 µl
- Incubation with the secondary antibody for 20 minutes at room temperature
- Rinse the slides in PBS Tween

H_2O_2:

- Ready to use (not included in the Dako Kit)
- Apply 200 µl
- Incubation for 5 minutes at room temperature
- Rinse the slides in PBS Tween

HRP (Streptavidin Peroxidase):

- HRP using bottle B (Dako Kit)
- Apply 200 µl
- Incubation with HRP for 20 minutes at room temperature
- Rinse the slides in PBS Tween

AEC (reddish), Chromogen:

- AEC using bottle C (Dako Kit)
- Apply 200 µl
- Incubation time will be ascertained microscopically
- Rinse the slides in 2 changes of PBS Tween
- Rinse the slides in distilled water

Counterstain with Hematoxylin:

- 3-5 minutes in hematoxylin
- Rinse the slides in tap water until water is clear
- Coverslip (Aquatex)

9.9. List of antibodies used for immunohistochemistry

Antibody	Company	Catalog #	Clone	Isotype	Conc.	Dilution
ß-catenin	BD	610154	14/Beta-Catenin	mIgG1	250 µg/ml	1:500
Ki-67	DAKO	M7240	MIB-1	IgG1	35 mg/l	1:200
GFP	Abcam	ab290	polyclonal	IgG	n/a	1:500
CD24	Thermo Scientific	MS1279P0	SN3b	IgG	200 µg/ml	1:50
CD44	Sigma	HPA005785	polyclonal	n/a	n/a	1:400

9.10. Reagents used for immunohistochemistry

Reagent	Company	Catalog #
Avidin/Biotin Blocking Kit	Dako	SP-2001
Staining Kit: Dako REAL™ Detection System, Peroxidase/AEC, Rabbit/Mouse	Dako	K5003
Dako Real™Peroxidase Blocking Solution	Dako	S2023
Dako Real™Antibody Diluent	Dako	S2022
Dako Cytomation Target Retrieval Solution Citrate pH 6	Dako	S2369

9.11. Periodic-Acid-Schiff-Reaction (PAS staining)

(established by Department of Pathology, Vanessa Vogel, Prof. Dr. Weichert)

Deparaffinize the slides:

- 10 min. Xylol
- 10 min. Xylol
- 5 min. 100% Ethanol
- 5 min. 100% Ethanol
- 5 min. 96% Ethanol
- 5 min. 70% Ethanol
- 5 min. distilled water

PAS staining:

- Treat with periodic acid for 5 min.
- Rinse quickly with distilled water
- Stain with Schiff's reagent for 5 min.
- Rinse quickly with tap water
- Stain nuclei with haematoxylin for 5 min.
- Rinse with tap water for 5 min.

Dehydrate the slides:

- 2x 70% Ethanol
- 2x 96% Ethanol
- 4x 100% Ethanol
- 4x Xylol

9.12. Hematoxylin & Eosin staining

(established by Department of Pathology, Vanessa Vogel, Prof. Dr. Weichert)

Deparaffinize the slides:

- 2x 5 min. Xylol
- 2x 100% Ethanol (fast)
- 1x 96% Ethanol (fast)
- 1x 70% Ethanol (fast)
- 1x distilled water (fast)

Haematoxylin staining:

- Stain with hematoxylin for 5 min.
- Rinse with tap water for 5 min.

Eosin staining and dehydration:

- Stain with eosin for 1 min.
- Transfer quickly to distilled water containing 2-5 drops of acidic acid
- 2x 70% Ethanol
- 2x 96% Ethanol
- 4x 100% Ethanol
- 4x Xylol

9.13. Dissociation of spheres to single cells and purification using OptiPrep

To prepare in advance:

- OptiPrep 60% (w/v): www.axis-shiel-density-gradient-media.com Prod. No. 1114542

1. Working solution of 40% OptiPrep containg 3x concentration of buffer:

- Mix 2 volumes of OptiPrep with 1 volumes of 3x PBS (or any other buffer solution)
- Example: 66.7 ml OptiPrep + 33.3 ml of 3x PBS

2. Solution to separate epithelial tumor cells

(18% OptiPrep: dilute the Working Solution in 1x PBS; density of 1.1 g/cm^3):

- Example: mix 18 ml of working solution (40%) + 22 ml 1x PBS (=18%)

Dissociation protocol:

- Transfer the medium containing the spheres into a 50 ml Falcon and spin down (1600 rpm, 5 min. at 4°C)
- Discard the supernatant and resuspend the pellet in 1 ml StemPro Accutase™ (Invitrogen)
- Incubate for 2 min. at 37°C
- Pipet up and down 20-50 times using the P1000
- Stop digest and wash cells with PBS in excess
- Spin down and resuspend the pellet in 1 ml PBS/1% BSA/ 2mM EDTA
- Filter the cells through a cell strainer (100 µm)
- Add 9 ml of 18% working solution in a 15 ml Falcon and overlay with 1 or 2 ml of single cell suspension (adapt the volumes according to the amount of cells)
- Spin down at 4000 rpm at 4°C for 20 min.
- Transfer the interphase into a new tube, wash with PBS and spin down (40 ml PBS per 10 ml OptiPrep)
- The cells can be resuspended in medium and seeded or analyzed

9.14. Dissociation of colorectal tumors (primary tumors or xenografts)

CO_2-independent medium:

Add 5 ml of Glutamin and 1% BSA

Optiprep™ density gradient:

See chapter 9.13.

Dissociation protocol:

- Harvest the tumor under the hoot (sterile conditions)
- Keep the tumor in CO_2-independent medium
- Wash the tumor with PBS/1% BSA
- Cut the tumor in small pieces
- Transfer the tumor pieces into a gentleMACS tube
- Add 5 to 10 ml of CO_2-independent medium + 0.25% collagenase + DNase + Y-27632 (5 µM) (Rho-associated kinase (ROCK) inhibitor which reduces dissociation induced apoptosis)
- Dissociate the tumor pieces in the gentle MACS dissociator for 30 sec.
- Incubate for 45 min. at 37°C in a rotator
- Pipette the tumor pieces every 10 min. up and down and check digestion process under the microscope using a small aliquot
- Transfer the tumor cell suspension through a cell strainer (100 µM)
- Wash with PBS/1% BSA
- Resuspend the pellet in an appropriate amount of CO_2-independent medium and perform a density gradient using Optiprep™
- Centrifuge the gradient for 20 min. at 4°C at max. speed (4000 rpm)
- Transfer the interphase into a new falcon tube
- Wash with PBS/1% BSA
- The cell pellet can be used for further processing (injections, flow cytometry)

9.15. Adherent cultures do not change CSC markers but some adhesion molecules compared to spheres

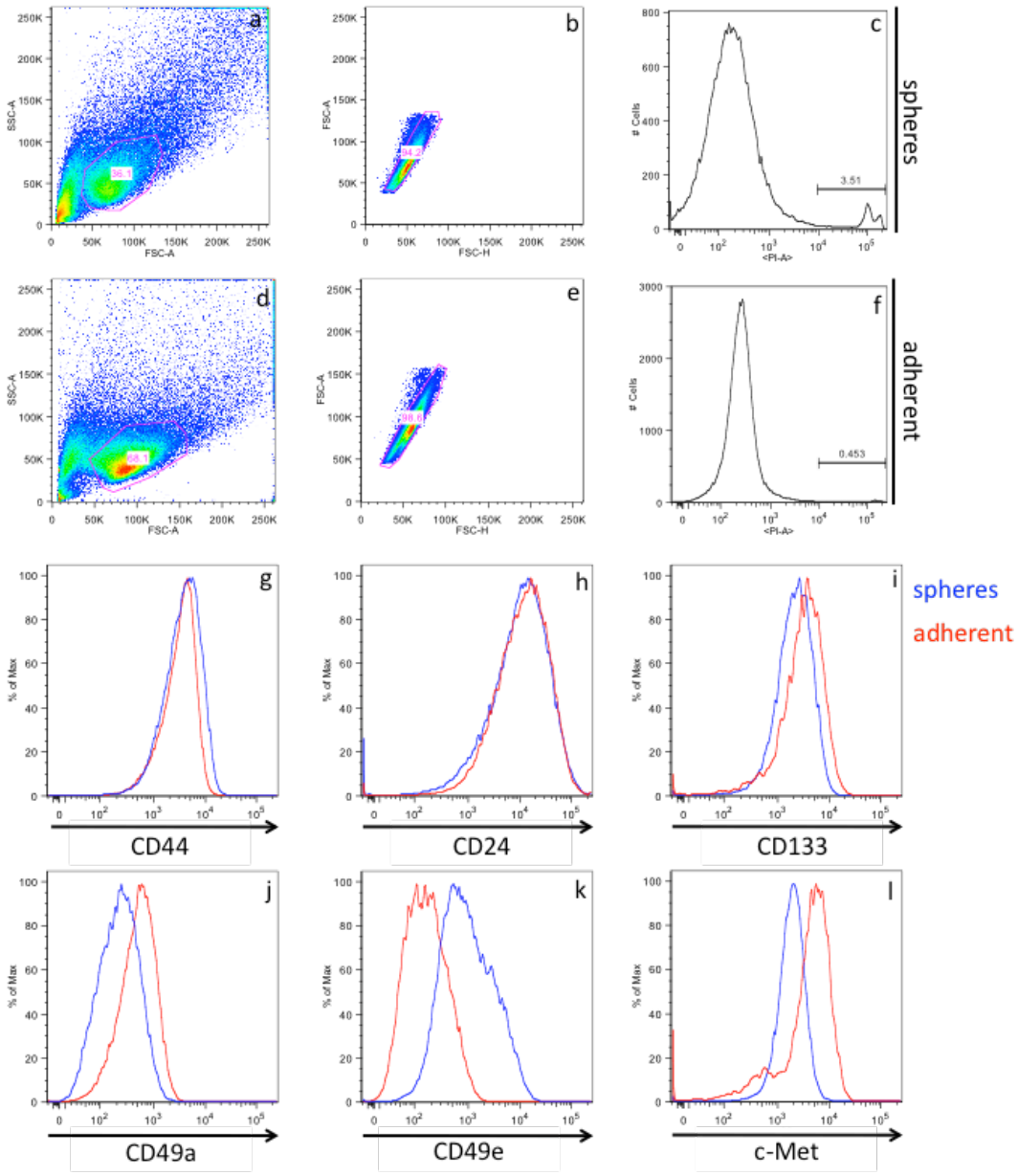

Fig. 71: Spheres vs. adherent cancer stem cell culture. Spheres were dissociated with Accutase and single cell suspensions were either maintained as spheres or seeded in flasks coated with collagen I. The cells were maintained in serum-free cancer stem cell medium. Ten days later the cells were harvested using Accutase and cell surface stainings were performed. Doublet- (b and e) and dead cell exclusion (c and f) were performed prior to analysis. The adherent cultures contain less dead cells and yield a higher amount of cells (d and f) when compared to spheroid cultures (a and c). The reported cancer stem cell markers, CD44 (g) and CD133 (i) were not differentially expressed, as well as CD24 (h). However, the expression of some adhesion molecules was changed. Adherent grown cells expressed higher levels of CD49a (j) and c-Met (l), while spheres expressed higher levels of CD49e (k) (blue = spheres; red = adherent).

9.16. Hypoxia enriches for slowly cycling cells

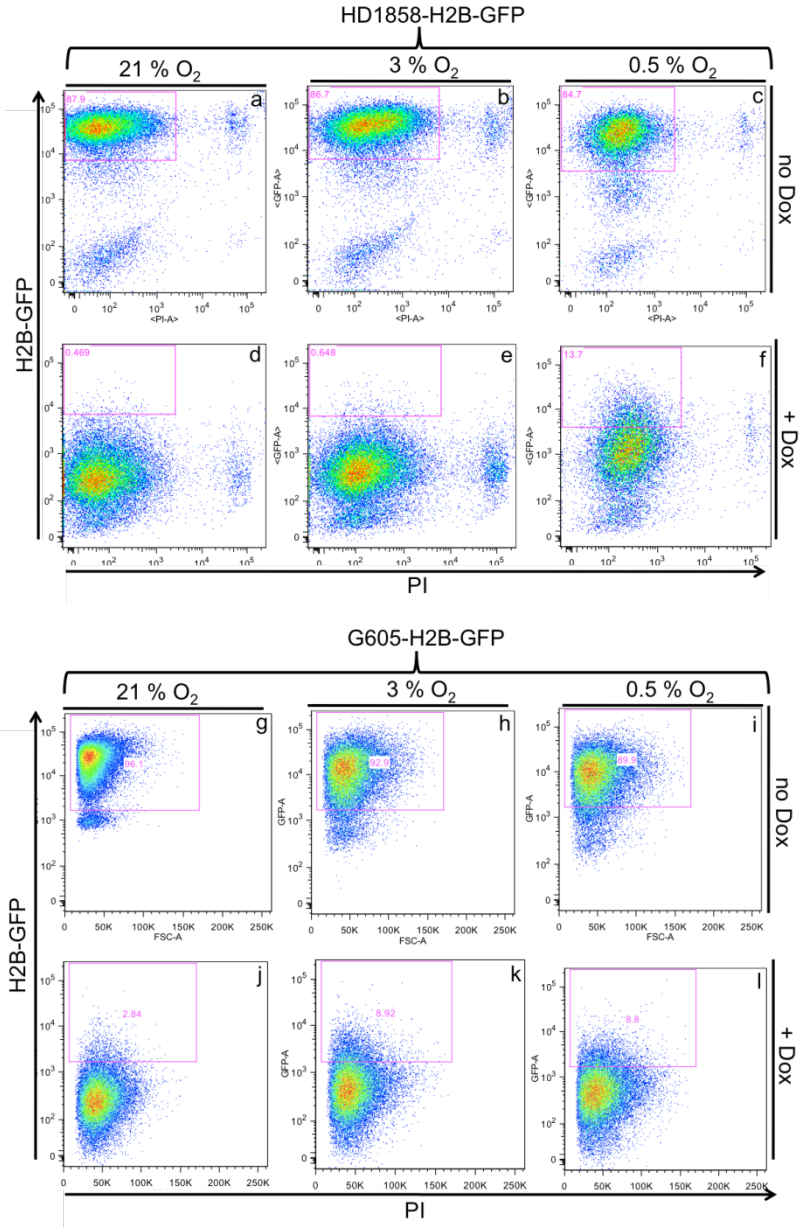

Fig. 72: Hypoxia enriches for slowly cycling cells. Both colon cancer cell lines, G605-H2B-GFP and HD1858-H2B-GFP, were maintained on collagen I coated plates for 10 days either at oxygen levels of 21%, 3% or 0.5%. The cells were treated with Dox (10 ng/ml) for 10 days (d-f and j-l). Non-treated cells were used as controls (a-c and g-i). For the HD1858-H2B-GFP cell line, cells maintained at 21% oxygen levels contained 0.5% of slowly cycling cells (d). The amount of slowly cycling cells increased in 3% oxygen level to 0.6% (e) and in 0.5% oxygen level to 14% (f). The G605-H2B-GFP cell line contained 2.8% of slowly cycling cells in 21% of oxygen level (j), whereas this percentage increased to 8.9% in 3% of oxygen (k) and remained at 8.8% at 0.5% of oxygen (l).

10. Abbreviations

15-PGDH	15-Hydroxyprostaglandin Dehydrogenase
5-FU	5-Fluorouracil
7AAD	7-Amino-Actinomycin D
ACF	Abberant Crypt Foci
AKT/PKB	Protein Kinase B
ALDH1	Aldehyde Dehydrogenase 1
APC	Adenopolyposis Coli
bFGF	basic Fibroblast Growth Factor
BMDC	Bone Marrow-Derived Cells
BMP	Bone Morphogenic Proten
BSA	Bovine Serum Albumin
CAFs	Carcinoma-Associated Fibroblasts
CBCs	Crypt-Based Columnar cells
CBP	CREB-Binding Protein
CCND1	Cyclin D1
CFSE	Carboxyfluorescein Succinimidyl Ester
CGH	Comparative Genomic Hybridization
CIMP	CpG Island Methylator Phenotype
CIN	Chromosomal Instability
CK1α	Casein Kinase 1α
COX-2	Cyclooxygenase-2
CRC	Colorectal Cancer
CSCs	Cancer Stem Cells
CXCL13	C-X-C motif chemokine 13
CXCR4	C-X-C chemokine receptor type 4
CXCR5	C-X-C chemokine receptor type 5
dDlg	human homolog of Drosophila Disc large tumor suppressor gene
DgTCs	Disseminating Tumor Cells
DMEM	Dulbecco's Modified Eagle's Medium
Dox	Doxycyclin
DPC4	Deleted in Pancreatic Carcinoma, locus 4
DVL	Dishevelled
ECM	Extracellular Matrix
EDTA	Ethylenediaminetetraacetic Acid

EGF	Epidermal Growth Factor
EGFR	Epidermal Growth Factor Receptor
EMT	Epithelial-Mesenchymal Transition
EpCAM	Epithelial Cell Adhesion Molecule
ERK	Extracellular signal-Regulated Kinase
FAP	Familial Adenomatous Polyposis
FCS	Fetal Calf Serum
FOLFOX	5-FU / Leucovorin / Oxaliplatin
FOLFRI	5-FU / Leucovorin / Irinotecan
GAP	GTPase-Acitvating Protein
GEF	Guanine nucleotide-Exchange Factor
GFP	Green Fluorescent Protein
GSK3ß	Glycogen Synthase Kinase 3ß
H2kD	murine major histocompatibility complex class I antigen
HEPES	Hydroxyethyl piperazineethanesulfonic acid
HGF	hepatocyte growth factor
HLA	Human Leucocyte Antigen
hNMSCs	human Normal Mammary Stem Cells
HNPCC	Hereditary Nonpolyposis Colorectal Cancer or Lynch syndrome
Hopx	Homeobox gene
HSCs	Hematopoietic Stem Cells
IKK-ß	Inhibitor of nuclear factor Kappa-B Kinase subunit ß
I-Smad	Inhibitory Smad
i.p.	intra peritoneally
IC50	Inhibitory Concentration 50
IMDM	Iscove`s Modified Dulbecco`s Medium
ISCs	Intestinal Stem Cells
IVC	Individually Ventilated Cages
JNK	JUN N-terminal Kinase
LEF	Lymphoid Enhancer Factor
Lgr5	Leucine-rich-repeat containing G-protein-coupled Receptor 5
LN	Lymph Node
LOH	Loss Of Heterozygosity
LRCs	Label Retaining Cells
Lrig1	Leucine-rich repeats and immunoglobulin-like domains 1
LRP5	Low-density lipoprotein-related Receptor Protein 5
LRP6	Low-density lipoprotein-related Receptor Protein 6

mAPC	murine Adenopolyposis Coli
MAPK	Mitogen-Activated Protein Kinase
MCR	Mutation Cluster Region
MH1	Mad Homology 1
MH2	Mad Homology 2
MIN	Multiple Intestinal Neoplasia
MMP	Matrix Metalloproteinase
MMR	Mismatch Repair
MRD	Minimal Residual Disease
MSC	Mesenchymal Stem cells
MSI	Microsatelite Instability
mTERT	mouse Telomerase Reverse Transcriptase
NK	Natural Killer
NOD/SCID	Nonobese diabetic/severe combined immunodeficiency
NSG	NOD/SCID interleukin-2 receptor gamma chain null mice
PAS	Periodic Acid Shiff
PBS	Phosphate Buffered Saline
PI	Propidium Iodide
PI3K	Phosphoinositide 3-Kinase
R-Smad	Receptor-regulated Smad
RTK	Receptor Tyrosine Kinase
s.c.	subcutaneous
SCs	Stem Cells
SDF1	Stromal cell-Derived Factor 1
SMAD4	SMAD family member 4
SPF	Specific Pathogen-Free
SV40	Simian-Virus 40
TA-cells	Transient Amplifying cells
TAMs	Tumor Associated Macrophages
TCF	T-Cell Factor
TEM	TIE2-Expressing Monocytes
TGF-ß	Transforming Growth Factor-ß
TGFßR1	Transforming Growth Factor ß Receptor 1
TGFßR2	Transforming Growth Factor ß Receptor 2
TICs	Tumor Initiating Cells
TMEM	Tumor Microenvironment of Metastasis
TNF a	Tumor Necrosis Factor alpha

TNM	Tumor, Node, Metastasis
TRE	Tet-Responsive Element
uPAR	Urokinase-type Plasminogen Activator
VCAM1	Vascular cell adhesion protein 1
VEGFA	Vascular Endothelial cell Growth Factor A
wt	wild-type

11. List of figures

12. List of tables

13. Contributions

The G605 cell line was kindly provided by Prof. Dr. Giorgio Stassi from the University of Palermo in Italy.

The vector pWXL-TTT-H2B-GFP was kindly provided by Prof. Dr. Petra Boukamp, Dr. Falkowska-Hansen and Prof. Dr. Kirschner.

Corinna Klein performed some of the *in vivo* experiments.

Vanessa Vogel for performed the immunohistochemistry stainings and Prof. Dr. Wilko Weichert and Dr. Albrecht Stenzinger from the Department of Pathology at the University of Heidelberg evaluated them.

Cell sorts were performed by Gelo de la Cruz, Jens Hartwig, Steffen Schmidt and Klaus Hexel at the DKFZ flow cytometry core facility.

Christian Eisen cloned the vectors pV2luc2 and pTurboGlow.

Thanks to Martin, Irène, Hind, Dagmar and Nina for critical review of this thesis. Thanks to Aine for english corrections.

14. Acknowledgement

First of all, I would like to thank **Andreas Trumpp** for giving me the opportunity to do my PhD in such a scientifically stimulating and international environment. It was a great pleasure to see HI-Stem growing and to be a part of it, especially being your first PhD student in Heidelberg. Thanks for all your trust and freedom during my PhD and thereby allowing me to learn how to work independently and to develop my own ideas and projects.

I would like to express my gratitude to **Prof. Dr. Petra Boukamp** for being my second referee and for supporting my work with fruitful discussions during the TAC-meetings. Thank you and **Prof. Dr. Kirschner** and **Dr. Falkowska-Hansen** for providing the vector system for my PhD project. I thank **Prof. Dr. Steinbeisser** for being the chair and **Dr. Hofmann** for being part of my examination committee. I thank **Prof. Dr. von Kalle** for helpful discussions during my TAC committee. Furthermore, I thank **Prof. Dr. Girgio Stassi** for providing the G605 cell line used for my project. Many thanks to **Prof. Dr. Wilko Weichert** und **Dr. Albrecht Stenzel** for the fruitful collaboration with the Pathology in Heidelberg. Many thanks to **Prof. Dr. Weitz** and **Prof. Dr. Büchler** for providing the primary patient material. Thanks to **Prof. Dr. Burwinkel** and **Prof. Dr. Sohn** for the collaboration on the ovarian cancer project. I thank the Hartmut Hoffmann-Berling International Graduate School of Molecular and Cellular Biology (**HBIGS**) for offering an excellent study program and for the great support during my PhD.

I would like to thank **Martin** for joining the Metics group and for bringing a new spirit and new ideas to the group, especially the magic CSC medium ☺ Thanks for your patience, your little lectures (especially about cell culture) and your scientific support during my PhD. I know that it was not always easy to deal with such a bunch of crazy characters.

Special thanks to you, **Irène**. It was a great pleasure to be part of maybe one of the most challenging projects ever, during my first year of PhD ;) Thanks for teaching me all the secrets of CTCs and intra-femoral injections. Thanks for the wonderful friendship and the great time we have spent together. Without you, my PhD would not have been the same. Many thanks for critically reviewing the manuscript. **Corinna**, thank you so much for all your support during the last 4 years. You have done a great job and made a major contribution to all the different projects I worked on. It was a great pleasure to work with you. Without you I would not have come that far. I would like to thank you, **Vanessa**, for doing all the beautiful IHC stainings. I very much appreciate all the work you have done and I will never forget my little

“internship” with you in the pathology ☺. Special thanks to you, **Meli,** for spending many pink moments with me. I very much appreciated to share the desk with you during my first years of PhD and to discuss about science. Thank you for your wonderful friendship and for your Italian spirit. Grazie! Many thanks to you, **Armin**, for being maybe the most patient person in this lab. Thanks for all your help with the cloning at the beginning of my PhD. You always had good advice or a helping hand. It was a great pleasure to have you around in the lab. **Hind**, thanks a lot for your scientific support, helpful discussions and for the nice moments we have spend outside of the lab. Thanks for critically reading my thesis. **Daniel**, thanks for being such a kind and friendly person. I very much appreciated to share the office with you and to have you around. **Nina**, I am very happy that you joined the lab. It is always fun to see such an energetic and smiling person. Stay as you are and don’t forget: Salut i força al canut ☺. Thanks for critically reading the manuscript. **Tom (or better Tombine ☺),** I very much appreciated to work with you, a medical doctor ;). Even though there are many prejudices around in the scientific world, you did a brilliant job and I enjoyed seeing you becoming a crazy scientist. It was always fun to have you around and I will not forget our never-ending mouse experiment. I wish you all the best for the future back in the clinic. **Larissa**, it was a great pleasure to have you in the lab and all the best for your Postdoc. **Dagmar**, it was great to have you in the lab. Keep your good mood and thanks for being such a kind a helpful person. Thanks a lot for reading and critically reviewing my thesis. **Sandra**, the sunshine of the lab. ☺ You really made my day when I met you in the morning. Please stay as you are and keep on smiling. **Simon**, thanks for creating such a nice work atmosphere. All the best for your future. **Steve,** I am very happy that you joined the group and the ovarian cancer project I have started. I don’t know how many hours of my PhD I have spend, sitting next to you in the cell culture, listening to maybe one of your most favorite songs at that time “Welcome to St. Tropez” ☺ I really enjoyed working with you. **Amelie** and **Anja**, I wish you all the best for the rest of your PhD. Thanks for creating a nice atmosphere in the lab. **Christian** thanks for sharing the last 4 years of my PhD with me. All the best for finishing your PhD. **Teresa**, I wish you all the best for the future and for your PhD. Thanks for the scientific support during the Metics meetings. **Jan**, I very much appreciated to have you around in the Metics group. Thanks for taking care of my cells from time to time. I will not forget that you saved my cells once with a huge effort ;) **Stephan**, we started the PhD together and will finish it together. I wish you all the best for the future. **Ines,** thanks for creating a nice work atmosphere with your humor and kindness. **Roberta,** thanks

for bringing the southern Italian spirit to the lab, with a lot of enthusiasm and temper. All the best of your PhD. **Gelo**, thanks so much for all the help, your humor and patience during plenty of sorts. Thanks to **Klaus, Steffen, Jens** and **Tobias** for helping with the sorts. **Andrea K., Andrea T., Katja, Sina, Melanie, Jasmin** and **Maria,** thank you for all the scientific support, including genotyping and especially taking care of diverse animal issues and organizational tasks. Thanks a lot to the animal facility of the DKFZ. **Norma, Michaela, Anja, Theresa, Ute, Stefan** and **all the animal care takers** thanks for all the time and effort you invest. Without your work, many of my experiments would not have been possible. Thanks to **Felix** and **Manuela** at the DKFZ microscope facility for your kind help. **Dr. Frank**, thank you very much for supporting me with the animal applications. **Marina** and **Erika**, thank you very much for your help with all the administration and paper work. I would like to thank **all the members of Mariekes', Christophs'** and **Thodurs group**. Thanks for creating such a nice lab atmosphere and for all your scientific discussions and support. Special thanks to you, **Marieke,** for all the organization in the lab and for taking care and supporting me with the animal applications. **Christoph**, thank you very much for all the interesting techniques you brought to the lab. It was very exciting to see what proteomics can do. **Thodur** and **Mick,** thanks for all your scientific input and for all the great discussions with you. I learned a lot from you. All the best for all of you for the future.
Thanks to all the lab members I did not mention so far. I very much enjoyed my time with you in the lab.
Special thanks to all my friends outside of the lab. Thanks **Jana**, for the long-lasting friendship and all your support since our studies. **Pedro**, thanks for your friendship and your Brazilian spirit. Thanks to **Stefan, Rania, Rafa**, **Andreas, Franzi, Thomas, Micha and Marie** for the great time and thanks to all my friends from the ESBS.

Ευχαριστώ πολύ, Κώστα. Es gibt keine Worte, die auch nur annähernd beschreiben würden, was du für mich in den letzten Jahren getan hast. Ich danke dir und auch deiner ganzen Familie für all die Unterstützung. Danke für deine unendliche Geduld, und nicht zu vergessen, für deine griechische Gelassenheit.
Ich danke meinen Eltern und meinem Bruder, Ingo, für die Unterstützung und Liebe all die Jahre, während meines Studiums und meiner Doktorarbeit. Danke, dass ihr immer an mich geglaubt habt. Ohne euch wäre ich nicht so weit gekommen.
Diese Arbeit möchte ich meinen Eltern widmen.

15. Bibliography

Aaltonen, L.A., Peltomaki, P., Leach, F.S., Sistonen, P., Pylkkanen, L., Mecklin, J.P., Jarvinen, H., Powell, S.M., Jen, J., Hamilton, S.R*., et al.* (1993). Clues to the pathogenesis of familial colorectal cancer. Science *260*, 812-816.

Abkowitz, J.L., Linenberger, M.L., Newton, M.A., Shelton, G.H., Ott, R.L., and Guttorp, P. (1990). Evidence for the maintenance of hematopoiesis in a large animal by the sequential activation of stem-cell clones. Proceedings of the National Academy of Sciences of the United States of America *87*, 9062-9066.

Adrover, E., Maestro, M.L., Sanz-Casla, M.T., del Barco, V., Cerdan, J., Fernandez, C., and Balibrea, J.L. (1999). Expression of high p53 levels in colorectal cancer: a favourable prognostic factor. British journal of cancer *81*, 122-126.

Adson, M.A., van Heerden, J.A., Adson, M.H., Wagner, J.S., and Ilstrup, D.M. (1984). Resection of hepatic metastases from colorectal cancer. Archives of surgery *119*, 647-651.

Afzal, S., Lalani, E.N., Poulsom, R., Stubbs, A., Rowlinson, G., Sato, H., Seiki, M., and Stamp, G.W. (1998). MT1-MMP and MMP-2 mRNA expression in human ovarian tumors: possible implications for the role of desmoplastic fibroblasts. Hum Pathol *29*, 155-165.

Aguirre-Ghiso, J.A. (2007). Models, mechanisms and clinical evidence for cancer dormancy. Nat Rev Cancer *7*, 834-846.

Ahnen, D.J., Feigl, P., Quan, G., Fenoglio-Preiser, C., Lovato, L.C., Bunn, P.A., Jr., Stemmerman, G., Wells, J.D., Macdonald, J.S., and Meyskens, F.L., Jr. (1998). Ki-ras mutation and p53 overexpression predict the clinical behavior of colorectal cancer: a Southwest Oncology Group study. Cancer research *58*, 1149-1158.

Aigner, S., Ramos, C.L., Hafezi-Moghadam, A., Lawrence, M.B., Friederichs, J., Altevogt, P., and Ley, K. (1998). CD24 mediates rolling of breast carcinoma cells on P-selectin. Faseb J *12*, 1241-1251.

Akagi, K., Uchibori, R., Yamaguchi, K., Kurosawa, K., Tanaka, Y., and Kozu, T. (2007). Characterization of a novel oncogenic K-ras mutation in colon cancer. Biochemical and biophysical research communications *352*, 728-732.

Akashi, T., Shirasawa, T., and Hirokawa, K. (1994). Gene expression of CD24 core polypeptide molecule in normal rat tissues and human tumor cell lines. Virchows Arch *425*, 399-406.

Al-Hajj, M., Wicha, M.S., Benito-Hernandez, A., Morrison, S.J., and Clarke, M.F. (2003a). Prospective identification of tumorigenic breast cancer cells. Proc Natl Acad Sci U S A *100*, 3983-3988.

Al-Hajj, M., Wicha, M.S., Benito-Hernandez, A., Morrison, S.J., and Clarke, M.F. (2003b). Prospective identification of tumorigenic breast cancer cells. Proceedings of the National Academy of Sciences of the United States of America *100*, 3983-3988.

Albuquerque, C., Breukel, C., van der Luijt, R., Fidalgo, P., Lage, P., Slors, F.J., Leitao, C.N., Fodde, R., and Smits, R. (2002). The 'just-right' signaling model: APC somatic mutations are selected based on a specific level of activation of the beta-catenin signaling cascade. Human molecular genetics *11*, 1549-1560.

Anderson, K., Lutz, C., van Delft, F.W., Bateman, C.M., Guo, Y., Colman, S.M., Kempski, H., Moorman, A.V., Titley, I., Swansbury, J.*, et al.* (2011). Genetic variegation of clonal architecture and propagating cells in leukaemia. Nature *469*, 356-361.

Annes, J.P., Munger, J.S., and Rifkin, D.B. (2003). Making sense of latent TGFbeta activation. Journal of cell science *116*, 217-224.

Aoki, K., and Taketo, M.M. (2007). Adenomatous polyposis coli (APC): a multi-functional tumor suppressor gene. Journal of cell science *120*, 3327-3335.

Arends, J.W. (2000). Molecular interactions in the Vogelstein model of colorectal carcinoma. J Pathol *190*, 412-416.

Artells, R., Moreno, I., Diaz, T., Martinez, F., Gel, B., Navarro, A., Ibeas, R., Moreno, J., and Monzo, M. (2010). Tumour CD133 mRNA expression and clinical outcome in surgically resected colorectal cancer patients. European journal of cancer *46*, 642-649.

Aruffo, A., Stamenkovic, I., Melnick, M., Underhill, C.B., and Seed, B. (1990). CD44 is the principal cell surface receptor for hyaluronate. Cell *61*, 1303-1313.

Baker, S.J., Fearon, E.R., Nigro, J.M., Hamilton, S.R., Preisinger, A.C., Jessup, J.M., vanTuinen, P., Ledbetter, D.H., Barker, D.F., Nakamura, Y.*, et al.* (1989). Chromosome 17 deletions and p53 gene mutations in colorectal carcinomas. Science *244*, 217-221.

Baker, S.J., Preisinger, A.C., Jessup, J.M., Paraskeva, C., Markowitz, S., Willson, J.K., Hamilton, S., and Vogelstein, B. (1990). p53 gene mutations occur in combination with 17p allelic deletions as late events in colorectal tumorigenesis. Cancer research *50*, 7717-7722.

Balzar, M., Winter, M.J., de Boer, C.J., and Litvinov, S.V. (1999). The biology of the 17-1A antigen (Ep-CAM). J Mol Med (Berl) *77*, 699-712.

Barault, L., Charon-Barra, C., Jooste, V., de la Vega, M.F., Martin, L., Roignot, P., Rat, P., Bouvier, A.M., Laurent-Puig, P., Faivre, J.*, et al.* (2008). Hypermethylator phenotype in sporadic colon cancer: study on a population-based series of 582 cases. Cancer research *68*, 8541-8546.

Barbera-Guillem, E., Nyhus, J.K., Wolford, C.C., Friece, C.R., and Sampsel, J.W. (2002). Vascular endothelial growth factor secretion by tumor-infiltrating macrophages essentially supports tumor angiogenesis, and IgG immune complexes potentiate the process. Cancer research *62*, 7042-7049.

Barker, N., van Es, J.H., Kuipers, J., Kujala, P., van den Born, M., Cozijnsen, M., Haegebarth, A., Korving, J., Begthel, H., Peters, P.J.*, et al.* (2007). Identification of stem cells in small intestine and colon by marker gene Lgr5. Nature *449*, 1003-1007.

Baumann, P., Thiele, W., Cremers, N., Muppala, S., Krachulec, J., Diefenbacher, M., Kassel, O., Mudduluru, G., Allgayer, H., Frame, M.*, et al.* (2012). CD24 interacts with and promotes the activity of c-src within lipid rafts in breast cancer cells, thereby increasing integrin-dependent adhesion. Cell Mol Life Sci *69*, 435-448.

Behrens, J., Jerchow, B.A., Wurtele, M., Grimm, J., Asbrand, C., Wirtz, R., Kuhl, M., Wedlich, D., and Birchmeier, W. (1998). Functional interaction of an axin homolog, conductin, with beta-catenin, APC, and GSK3beta. Science *280*, 596-599.

Behrens, J., von Kries, J.P., Kuhl, M., Bruhn, L., Wedlich, D., Grosschedl, R., and Birchmeier, W. (1996). Functional interaction of beta-catenin with the transcription factor LEF-1. Nature *382*, 638-642.

Belenkaya, T.Y., Han, C., Standley, H.J., Lin, X., Houston, D.W., and Heasman, J. (2002). pygopus Encodes a nuclear protein essential for wingless/Wnt signaling. Development *129*, 4089-4101.

Beroud, C., and Soussi, T. (1996). APC gene: database of germline and somatic mutations in human tumors and cell lines. Nucleic Acids Res *24*, 121-124.

Bhattacharyya, N.P., Skandalis, A., Ganesh, A., Groden, J., and Meuth, M. (1994). Mutator phenotypes in human colorectal carcinoma cell lines. Proceedings of the National Academy of Sciences of the United States of America *91*, 6319-6323.

Bilic, J., Huang, Y.L., Davidson, G., Zimmermann, T., Cruciat, C.M., Bienz, M., and Niehrs, C. (2007). Wnt induces LRP6 signalosomes and promotes dishevelled-dependent LRP6 phosphorylation. Science *316*, 1619-1622.

Bjerknes, M., and Cheng, H. (1999). Clonal analysis of mouse intestinal epithelial progenitors. Gastroenterology *116*, 7-14.

Blandino, G., Levine, A.J., and Oren, M. (1999). Mutant p53 gain of function: differential effects of different p53 mutants on resistance of cultured cells to chemotherapy. Oncogene *18*, 477-485.

Boiko, A.D., Razorenova, O.V., van de Rijn, M., Swetter, S.M., Johnson, D.L., Ly, D.P., Butler, P.D., Yang, G.P., Joshua, B., Kaplan, M.J.*, et al.* (2010). Human melanoma-initiating cells express neural crest nerve growth factor receptor CD271. Nature *466*, 133-137.

Boland, C.R., Koi, M., Chang, D.K., and Carethers, J.M. (2008). The biochemical basis of microsatellite instability and abnormal immunohistochemistry and clinical behavior in Lynch syndrome: from bench to bedside. Fam Cancer *7*, 41-52.

Boland, C.R., Thibodeau, S.N., Hamilton, S.R., Sidransky, D., Eshleman, J.R., Burt, R.W., Meltzer, S.J., Rodriguez-Bigas, M.A., Fodde, R., Ranzani, G.N.*, et al.* (1998). A National Cancer Institute Workshop on Microsatellite Instability for cancer detection and familial predisposition: development of international criteria for the determination of microsatellite instability in colorectal cancer. Cancer research *58*, 5248-5257.

Bonnet, D., and Dick, J.E. (1997). Human acute myeloid leukemia is organized as a hierarchy that originates from a primitive hematopoietic cell. Nat Med *3*, 730-737.

Bos, J.L., Fearon, E.R., Hamilton, S.R., Verlaan-de Vries, M., van Boom, J.H., van der Eb, A.J., and Vogelstein, B. (1987). Prevalence of ras gene mutations in human colorectal cancers. Nature *327*, 293-297.

Bosma, M.J., and Carroll, A.M. (1991). The SCID mouse mutant: definition, characterization, and potential uses. Annu Rev Immunol *9*, 323-350.

Brabletz, T., Jung, A., Dag, S., Hlubek, F., and Kirchner, T. (1999). beta-catenin regulates the expression of the matrix metalloproteinase-7 in human colorectal cancer. The American journal of pathology *155*, 1033-1038.

Brabletz, T., Jung, A., Hermann, K., Gunther, K., Hohenberger, W., and Kirchner, T. (1998). Nuclear overexpression of the oncoprotein beta-catenin in colorectal cancer is localized predominantly at the invasion front. Pathol Res Pract *194*, 701-704.

Brabletz, T., Jung, A., Reu, S., Porzner, M., Hlubek, F., Kunz-Schughart, L.A., Knuechel, R., and Kirchner, T. (2001). Variable beta-catenin expression in colorectal cancers indicates tumor progression driven by the tumor environment. Proceedings of the National Academy of Sciences of the United States of America *98*, 10356-10361.

Braun, S., Pantel, K., Muller, P., Janni, W., Hepp, F., Kentenich, C.R., Gastroph, S., Wischnik, A., Dimpfl, T., Kindermann, G.*, et al.* (2000). Cytokeratin-positive cells in the bone marrow and survival of patients with stage I, II, or III breast cancer. N Engl J Med *342*, 525-533.

Braun, S., Vogl, F.D., Naume, B., Janni, W., Osborne, M.P., Coombes, R.C., Schlimok, G., Diel, I.J., Gerber, B., Gebauer, G.*, et al.* (2005). A pooled analysis of bone marrow micrometastasis in breast cancer. The New England journal of medicine *353*, 793-802.

Brazil, D.P., Yang, Z.Z., and Hemmings, B.A. (2004). Advances in protein kinase B signalling: AKTion on multiple fronts. Trends Biochem Sci *29*, 233-242.

Bronner, C.E., Baker, S.M., Morrison, P.T., Warren, G., Smith, L.G., Lescoe, M.K., Kane, M., Earabino, C., Lipford, J., Lindblom, A.*, et al.* (1994). Mutation in the DNA mismatch repair gene homologue hMLH1 is associated with hereditary non-polyposis colon cancer. Nature *368*, 258-261.

Brosh, R., and Rotter, V. (2009). When mutants gain new powers: news from the mutant p53 field. Nature reviews Cancer *9*, 701-713.

Cairnie, A.B., Lamerton, L.F., and Steel, G.G. (1965). Cell proliferation studies in the intestinal epithelium of the rat. I. Determination of the kinetic parameters. Exp Cell Res *39*, 528-538.

Cannon-Albright, L.A., Skolnick, M.H., Bishop, D.T., Lee, R.G., and Burt, R.W. (1988). Common inheritance of susceptibility to colonic adenomatous polyps and associated colorectal cancers. The New England journal of medicine *319*, 533-537.

Carpenter, G. (1987). Receptors for epidermal growth factor and other polypeptide mitogens. Annual review of biochemistry *56*, 881-914.

Carpenter, G., and Cohen, S. (1990). Epidermal growth factor. The Journal of biological chemistry *265*, 7709-7712.

Cavallo, R.A., Cox, R.T., Moline, M.M., Roose, J., Polevoy, G.A., Clevers, H., Peifer, M., and Bejsovec, A. (1998). Drosophila Tcf and Groucho interact to repress Wingless signalling activity. Nature *395*, 604-608.

Chambers, A.F., Naumov, G.N., Varghese, H.J., Nadkarni, K.V., MacDonald, I.C., and Groom, A.C. (2001). Critical steps in hematogenous metastasis: an overview. Surgical oncology clinics of North America *10*, 243-255, vii.

Chen, C.R., Kang, Y., Siegel, P.M., and Massague, J. (2002). E2F4/5 and p107 as Smad cofactors linking the TGFbeta receptor to c-myc repression. Cell *110*, 19-32.

Chen, K., Ahmed, S., Adeyi, O., Dick, J.E., and Ghanekar, A. (2012). Human solid tumor xenografts in immunodeficient mice are vulnerable to lymphomagenesis associated with epstein-barr virus. PLoS ONE *7*, e39294.

Chen, W.S., Lazar, C.S., Poenie, M., Tsien, R.Y., Gill, G.N., and Rosenfeld, M.G. (1987). Requirement for intrinsic protein tyrosine kinase in the immediate and late actions of the EGF receptor. Nature *328*, 820-823.

Cheng, C., and Sharp, P.A. (2006). Regulation of CD44 alternative splicing by SRm160 and its potential role in tumor cell invasion. Molecular and cellular biology *26*, 362-370.

Cheng, H., and Leblond, C.P. (1974). Origin, differentiation and renewal of the four main epithelial cell types in the mouse small intestine. V. Unitarian Theory of the origin of the four epithelial cell types. Am J Anat *141*, 537-561.

Cheshier, S.H., Morrison, S.J., Liao, X., and Weissman, I.L. (1999). In vivo proliferation and cell cycle kinetics of long-term self-renewing hematopoietic stem cells. Proceedings of the National Academy of Sciences of the United States of America *96*, 3120-3125.

Chu, K.C., Tarone, R.E., Chow, W.H., Hankey, B.F., and Ries, L.A. (1994). Temporal patterns in colorectal cancer incidence, survival, and mortality from 1950 through 1990. Journal of the National Cancer Institute *86*, 997-1006.

Cipolleschi, M.G., Dello Sbarba, P., and Olivotto, M. (1993). The role of hypoxia in the maintenance of hematopoietic stem cells. Blood *82*, 2031-2037.

Civenni, G., Walter, A., Kobert, N., Mihic-Probst, D., Zipser, M., Belloni, B., Seifert, B., Moch, H., Dummer, R., van den Broek, M.*, et al.* (2011). Human CD271-positive melanoma stem cells associated with metastasis establish tumor heterogeneity and long-term growth. Cancer research *71*, 3098-3109.

Clayton, E., Doupe, D.P., Klein, A.M., Winton, D.J., Simons, B.D., and Jones, P.H. (2007). A single type of progenitor cell maintains normal epidermis. Nature *446*, 185-189.

Coller, H.A., Sang, L., and Roberts, J.M. (2006). A new description of cellular quiescence. PLoS Biol *4*, e83.

Collins, A.T., Berry, P.A., Hyde, C., Stower, M.J., and Maitland, N.J. (2005). Prospective identification of tumorigenic prostate cancer stem cells. Cancer research *65*, 10946-10951.

Condeelis, J., and Pollard, J.W. (2006). Macrophages: obligate partners for tumor cell migration, invasion, and metastasis. Cell *124*, 263-266.

Corbeil, D., Roper, K., Fargeas, C.A., Joester, A., and Huttner, W.B. (2001). Prominin: a story of cholesterol, plasma membrane protrusions and human pathology. Traffic *2*, 82-91.

Correa, R.J., Peart, T., Valdes, Y.R., DiMattia, G.E., and Shepherd, T.G. (2012). Modulation of AKT activity is associated with reversible dormancy in ascites-derived epithelial ovarian cancer spheroids. Carcinogenesis *33*, 49-58.

Cotsarelis, G., Sun, T.T., and Lavker, R.M. (1990). Label-retaining cells reside in the bulge area of pilosebaceous unit: implications for follicular stem cells, hair cycle, and skin carcinogenesis. Cell *61*, 1329-1337.

Crawford, H.C., Fingleton, B.M., Rudolph-Owen, L.A., Goss, K.J., Rubinfeld, B., Polakis, P., and Matrisian, L.M. (1999). The metalloproteinase matrilysin is a target of beta-catenin transactivation in intestinal tumors. Oncogene *18*, 2883-2891.

Croce, C.M. (2008). Oncogenes and cancer. The New England journal of medicine *358*, 502-511.

Dai, J.L., Turnacioglu, K.K., Schutte, M., Sugar, A.Y., and Kern, S.E. (1998). Dpc4 transcriptional activation and dysfunction in cancer cells. Cancer research *58*, 4592-4597.

Dalerba, P., Dylla, S.J., Park, I.K., Liu, R., Wang, X., Cho, R.W., Hoey, T., Gurney, A., Huang, E.H., Simeone, D.M.*, et al.* (2007). Phenotypic characterization of human colorectal cancer stem cells. Proc Natl Acad Sci U S A *104*, 10158-10163.

Datta, S.R., Brunet, A., and Greenberg, M.E. (1999). Cellular survival: a play in three Akts. Genes & development *13*, 2905-2927.

Daum, G., Eisenmann-Tappe, I., Fries, H.W., Troppmair, J., and Rapp, U.R. (1994). The ins and outs of Raf kinases. Trends Biochem Sci *19*, 474-480.

Dembinski, J.L., and Krauss, S. (2009). Characterization and functional analysis of a slow cycling stem cell-like subpopulation in pancreas adenocarcinoma. Clin Exp Metastasis *26*, 611-623.

Demicheli, R., Abbattista, A., Miceli, R., Valagussa, P., and Bonadonna, G. (1996). Time distribution of the recurrence risk for breast cancer patients undergoing mastectomy: further support about the concept of tumor dormancy. Breast Cancer Res Treat *41*, 177-185.

Demicheli, R., Terenziani, M., Valagussa, P., Moliterni, A., Zambetti, M., and Bonadonna, G. (1994). Local recurrences following mastectomy: support for the concept of tumor dormancy. J Natl Cancer Inst *86*, 45-48.

DeNardo, D.G., Barreto, J.B., Andreu, P., Vasquez, L., Tawfik, D., Kolhatkar, N., and Coussens, L.M. (2009). CD4(+) T cells regulate pulmonary metastasis of mammary carcinomas by enhancing protumor properties of macrophages. Cancer Cell *16*, 91-102.

Diez, M., Medrano, M., Muguerza, J.M., Ramos, P., Hernandez, P., Villeta, R., Martin, A., Noguerales, F., Ruiz, A., and Granell, J. (2000). Influence of tumor localization on the prognostic value of P53 protein in colorectal adenocarcinomas. Anticancer research *20*, 3907-3912.

Dikovskaya, D., Newton, I.P., and Nathke, I.S. (2004). The adenomatous polyposis coli protein is required for the formation of robust spindles formed in CSF Xenopus extracts. Molecular biology of the cell *15*, 2978-2991.

Dittmer, D., Pati, S., Zambetti, G., Chu, S., Teresky, A.K., Moore, M., Finlay, C., and Levine, A.J. (1993). Gain of function mutations in p53. Nature genetics *4*, 42-46.

Douillard, J.Y., Cunningham, D., Roth, A.D., Navarro, M., James, R.D., Karasek, P., Jandik, P., Iveson, T., Carmichael, J., Alakl, M.*, et al.* (2000). Irinotecan combined with fluorouracil compared with fluorouracil alone as first-line treatment for metastatic colorectal cancer: a multicentre randomised trial. Lancet *355*, 1041-1047.

Downward, J. (2003). Targeting RAS signalling pathways in cancer therapy. Nature reviews Cancer *3*, 11-22.

Duval, A., Rolland, S., Tubacher, E., Bui, H., Thomas, G., and Hamelin, R. (2000). The human T-cell transcription factor-4 gene: structure, extensive characterization of alternative splicings, and mutational analysis in colorectal cancer cell lines. Cancer research *60*, 3872-3879.

Edwards, B.K., Ward, E., Kohler, B.A., Eheman, C., Zauber, A.G., Anderson, R.N., Jemal, A., Schymura, M.J., Lansdorp-Vogelaar, I., Seeff, L.C.*, et al.* (2010). Annual report to the nation on the status of cancer, 1975-2006, featuring colorectal cancer trends and impact of interventions (risk factors, screening, and treatment) to reduce future rates. Cancer *116*, 544-573.

Eshleman, J.R., Lang, E.Z., Bowerfind, G.K., Parsons, R., Vogelstein, B., Willson, J.K., Veigl, M.L., Sedwick, W.D., and Markowitz, S.D. (1995). Increased mutation rate at the hprt locus accompanies microsatellite instability in colon cancer. Oncogene *10*, 33-37.

Essers, M.A., Offner, S., Blanco-Bose, W.E., Waibler, Z., Kalinke, U., Duchosal, M.A., and Trumpp, A. (2009). IFNalpha activates dormant haematopoietic stem cells in vivo. Nature *458*, 904-908.

Fagotto, F., Jho, E., Zeng, L., Kurth, T., Joos, T., Kaufmann, C., and Costantini, F. (1999). Domains of axin involved in protein-protein interactions, Wnt pathway inhibition, and intracellular localization. The Journal of cell biology *145*, 741-756.

Falkowska-Hansen, B., Kollar, J., Gruner, B.M., Schanz, M., Boukamp, P., Siveke, J., Rethwilm, A., and Kirschner, M. (2010). An inducible Tet-Off-H2B-GFP lentiviral reporter vector for detection and in vivo isolation of label-retaining cells. Exp Cell Res *316*, 1885-1895.

Farrar, J.D., Katz, K.H., Windsor, J., Thrush, G., Scheuermann, R.H., Uhr, J.W., and Street, N.E. (1999). Cancer dormancy. VII. A regulatory role for CD8+ T cells and IFN-gamma in establishing and maintaining the tumor-dormant state. Journal of immunology *162*, 2842-2849.

Fearon, E.R. (2011). Molecular genetics of colorectal cancer. Annu Rev Pathol *6*, 479-507.

Fearon, E.R., and Vogelstein, B. (1990). A genetic model for colorectal tumorigenesis. Cell *61*, 759-767.

Feng, X.H., and Derynck, R. (2005). Specificity and versatility in tgf-beta signaling through Smads. Annual review of cell and developmental biology *21*, 659-693.

Feng, X.H., Zhang, Y., Wu, R.Y., and Derynck, R. (1998). The tumor suppressor Smad4/DPC4 and transcriptional adaptor CBP/p300 are coactivators for smad3 in TGF-beta-induced transcriptional activation. Genes & development *12*, 2153-2163.

Ferlay, J., Shin, H.R., Bray, F., Forman, D., Mathers, C., and Parkin, D.M. (2011). Estimates of worldwide burden of cancer in 2008: GLOBOCAN 2008. Int J Cancer *127*, 2893-2917.

Fidler, I.J. (1970). Metastasis: guantitative analysis of distribution and fate of tumor embolilabeled with 125 I-5-iodo-2'-deoxyuridine. Journal of the National Cancer Institute *45*, 773-782.

Fidler, I.J. (1990). Critical factors in the biology of human cancer metastasis: twenty-eighth G.H.A. Clowes memorial award lecture. Cancer research *50*, 6130-6138.

Fidler, I.J. (2002). The organ microenvironment and cancer metastasis. Differentiation *70*, 498-505.

Fidler, I.J. (2003). The pathogenesis of cancer metastasis: the 'seed and soil' hypothesis revisited. Nature reviews Cancer *3*, 453-458.

Fishel, R., and Kolodner, R.D. (1995). Identification of mismatch repair genes and their role in the development of cancer. Current opinion in genetics & development *5*, 382-395.

Fishel, R., Lescoe, M.K., Rao, M.R., Copeland, N.G., Jenkins, N.A., Garber, J., Kane, M., and Kolodner, R. (1993). The human mutator gene homolog MSH2 and its association with hereditary nonpolyposis colon cancer. Cell *75*, 1027-1038.

Flanagan, S.P. (1966). 'Nude', a new hairless gene with pleiotropic effects in the mouse. Genet Res *8*, 295-309.

Fodde, R., and Brabletz, T. (2007). Wnt/beta-catenin signaling in cancer stemness and malignant behavior. Curr Opin Cell Biol *19*, 150-158.

Fodde, R., Smits, R., and Clevers, H. (2001). APC, signal transduction and genetic instability in colorectal cancer. Nature reviews Cancer *1*, 55-67.

Folkman, J., and Kalluri, R. (2004). Cancer without disease. Nature *427*, 787.

Forrester, K., Almoguera, C., Han, K., Grizzle, W.E., and Perucho, M. (1987). Detection of high incidence of K-ras oncogenes during human colon tumorigenesis. Nature *327*, 298-303.

Foudi, A., Hochedlinger, K., Van Buren, D., Schindler, J.W., Jaenisch, R., Carey, V., and Hock, H. (2009). Analysis of histone 2B-GFP retention reveals slowly cycling hematopoietic stem cells. Nat Biotechnol *27*, 84-90.

Franke, T.F., Yang, S.I., Chan, T.O., Datta, K., Kazlauskas, A., Morrison, D.K., Kaplan, D.R., and Tsichlis, P.N. (1995). The protein kinase encoded by the Akt proto-oncogene is a target of the PDGF-activated phosphatidylinositol 3-kinase. Cell *81*, 727-736.

Franken, N.A., Rodermond, H.M., Stap, J., Haveman, J., and van Bree, C. (2006). Clonogenic assay of cells in vitro. Nat Protoc *1*, 2315-2319.

Gao, M.Q., Choi, Y.P., Kang, S., Youn, J.H., and Cho, N.H. (2010). CD24+ cells from hierarchically organized ovarian cancer are enriched in cancer stem cells. Oncogene *29*, 2672-2680.

Giacchetti, S., Perpoint, B., Zidani, R., Le Bail, N., Faggiuolo, R., Focan, C., Chollet, P., Llory, J.F., Letourneau, Y., Coudert, B.*, et al.* (2000). Phase III multicenter randomized trial of oxaliplatin added to chronomodulated fluorouracil-leucovorin as first-line treatment of metastatic colorectal cancer. J Clin Oncol *18*, 136-147.

Gracz, A.D., Ramalingam, S., and Magness, S.T. (2010). Sox9 expression marks a subset of CD24-expressing small intestine epithelial stem cells that form organoids in vitro. Am J Physiol Gastrointest Liver Physiol *298*, G590-600.

Grady, W.M., and Carethers, J.M. (2008). Genomic and epigenetic instability in colorectal cancer pathogenesis. Gastroenterology *135*, 1079-1099.

Greenblatt, M.S., Bennett, W.P., Hollstein, M., and Harris, C.C. (1994). Mutations in the p53 tumor suppressor gene: clues to cancer etiology and molecular pathogenesis. Cancer research *54*, 4855-4878.

Gregorieff, A., and Clevers, H. (2005). Wnt signaling in the intestinal epithelium: from endoderm to cancer. Genes & development *19*, 877-890.

Groden, J., Thliveris, A., Samowitz, W., Carlson, M., Gelbert, L., Albertsen, H., Joslyn, G., Stevens, J., Spirio, L., Robertson, M.*, et al.* (1991). Identification and characterization of the familial adenomatous polyposis coli gene. Cell *66*, 589-600.

Hafner, M., Orosz, P., Kruger, A., and Mannel, D.N. (1996). TNF promotes metastasis by impairing natural killer cell activity. International journal of cancer Journal international du cancer *66*, 388-392.

Hahn, S.A., Schutte, M., Hoque, A.T., Moskaluk, C.A., da Costa, L.T., Rozenblum, E., Weinstein, C.L., Fischer, A., Yeo, C.J., Hruban, R.H.*, et al.* (1996). DPC4, a candidate tumor suppressor gene at human chromosome 18q21.1. Science *271*, 350-353.

Hampel, H., Stephens, J.A., Pukkala, E., Sankila, R., Aaltonen, L.A., Mecklin, J.P., and de la Chapelle, A. (2005). Cancer risk in hereditary nonpolyposis colorectal cancer syndrome: later age of onset. Gastroenterology *129*, 415-421.

Hanahan, D., and Weinberg, R.A. (2000). The hallmarks of cancer. Cell *100*, 57-70.

Hanahan, D., and Weinberg, R.A. (2011). Hallmarks of cancer: the next generation. Cell *144*, 646-674.

Haramis, A.P., Begthel, H., van den Born, M., van Es, J., Jonkheer, S., Offerhaus, G.J., and Clevers, H. (2004). De novo crypt formation and juvenile polyposis on BMP inhibition in mouse intestine. Science *303*, 1684-1686.

Hart, M.J., de los Santos, R., Albert, I.N., Rubinfeld, B., and Polakis, P. (1998). Downregulation of beta-catenin by human Axin and its association with the APC tumor suppressor, beta-catenin and GSK3 beta. Current biology : CB *8*, 573-581.

Hata, A., Lo, R.S., Wotton, D., Lagna, G., and Massague, J. (1997). Mutations increasing autoinhibition inactivate tumour suppressors Smad2 and Smad4. Nature *388*, 82-87.

Haug, J.S., He, X.C., Grindley, J.C., Wunderlich, J.P., Gaudenz, K., Ross, J.T., Paulson, A., Wagner, K.P., Xie, Y., Zhu, R.*, et al.* (2008). N-cadherin expression level distinguishes reserved versus primed states of hematopoietic stem cells. Cell Stem Cell *2*, 367-379.

He, T.C., Sparks, A.B., Rago, C., Hermeking, H., Zawel, L., da Costa, L.T., Morin, P.J., Vogelstein, B., and Kinzler, K.W. (1998). Identification of c-MYC as a target of the APC pathway. Science *281*, 1509-1512.

He, X.C., Zhang, J., Tong, W.G., Tawfik, O., Ross, J., Scoville, D.H., Tian, Q., Zeng, X., He, X., Wiedemann, L.M.*, et al.* (2004). BMP signaling inhibits intestinal stem cell self-renewal through suppression of Wnt-beta-catenin signaling. Nature genetics *36*, 1117-1121.

Hecht, A., Vleminckx, K., Stemmler, M.P., van Roy, F., and Kemler, R. (2000). The p300/CBP acetyltransferases function as transcriptional coactivators of beta-catenin in vertebrates. The EMBO journal *19*, 1839-1850.

Hedley, B.D., and Chambers, A.F. (2009). Tumor dormancy and metastasis. Adv Cancer Res *102*, 67-101.

Heijstek, M.W., Kranenburg, O., and Borel Rinkes, I.H. (2005). Mouse models of colorectal cancer and liver metastases. Digestive surgery *22*, 16-25.

Heldin, C.H., Miyazono, K., and ten Dijke, P. (1997). TGF-beta signalling from cell membrane to nucleus through SMAD proteins. Nature *390*, 465-471.

Hermann, P.C., Huber, S.L., Herrler, T., Aicher, A., Ellwart, J.W., Guba, M., Bruns, C.J., and Heeschen, C. (2007). Distinct populations of cancer stem cells determine tumor growth and metastatic activity in human pancreatic cancer. Cell Stem Cell *1*, 313-323.

Hermiston, M.L., Xu, Z., and Weiss, A. (2003). CD45: a critical regulator of signaling thresholds in immune cells. Annu Rev Immunol *21*, 107-137.

Hiraoka, K., Zenmyo, M., Watari, K., Iguchi, H., Fotovati, A., Kimura, Y.N., Hosoi, F., Shoda, T., Nagata, K., Osada, H.*, et al.* (2008). Inhibition of bone and muscle metastases of lung cancer cells by a decrease in the number of monocytes/macrophages. Cancer Sci *99*, 1595-1602.

Hiratsuka, S., Watanabe, A., Aburatani, H., and Maru, Y. (2006). Tumour-mediated upregulation of chemoattractants and recruitment of myeloid cells predetermines lung metastasis. Nature cell biology *8*, 1369-1375.

Hiratsuka, S., Watanabe, A., Sakurai, Y., Akashi-Takamura, S., Ishibashi, S., Miyake, K., Shibuya, M., Akira, S., Aburatani, H., and Maru, Y. (2008). The S100A8-serum amyloid A3-TLR4 paracrine cascade establishes a pre-metastatic phase. Nature cell biology *10*, 1349-1355.

Hofner, T., Schillert, A., Eisen, C., Wagner, S., Rigo-Watermeier, T., Baccelli, I., Klein, C., Hadaschik, B., Vogel, V., Macher-Goeppinger, S.*, et al.* (2012). CD24 induces early onset of tumor growth and enriches for more adherent, metastatic and chemotherapy resistant bladder cancer cells. submitted.

Hollstein, M., Sidransky, D., Vogelstein, B., and Harris, C.C. (1991). p53 mutations in human cancers. Science *253*, 49-53.

Honegger, A.M., Dull, T.J., Felder, S., Van Obberghen, E., Bellot, F., Szapary, D., Schmidt, A., Ullrich, A., and Schlessinger, J. (1987a). Point mutation at the ATP binding site of EGF receptor abolishes protein-tyrosine kinase activity and alters cellular routing. Cell *51*, 199-209.

Honegger, A.M., Szapary, D., Schmidt, A., Lyall, R., Van Obberghen, E., Dull, T.J., Ullrich, A., and Schlessinger, J. (1987b). A mutant epidermal growth factor receptor with defective protein tyrosine kinase is unable to stimulate proto-oncogene expression and DNA synthesis. Molecular and cellular biology *7*, 4568-4571.

Horst, D., Kriegl, L., Engel, J., Kirchner, T., and Jung, A. (2008). CD133 expression is an independent prognostic marker for low survival in colorectal cancer. British journal of cancer *99*, 1285-1289.

Hsiang, Y.H., Hertzberg, R., Hecht, S., and Liu, L.F. (1985). Camptothecin induces protein-linked DNA breaks via mammalian DNA topoisomerase I. The Journal of biological chemistry *260*, 14873-14878.

Hu, Y., and Smyth, G.K. (2009). ELDA: extreme limiting dilution analysis for comparing depleted and enriched populations in stem cell and other assays. J Immunol Methods *347*, 70-78.

Huang, E.H., Hynes, M.J., Zhang, T., Ginestier, C., Dontu, G., Appelman, H., Fields, J.Z., Wicha, M.S., and Boman, B.M. (2009). Aldehyde dehydrogenase 1 is a marker for normal and malignant human colonic stem cells (SC) and tracks SC overpopulation during colon tumorigenesis. Cancer research *69*, 3382-3389.

Huber, O., Korn, R., McLaughlin, J., Ohsugi, M., Herrmann, B.G., and Kemler, R. (1996). Nuclear localization of beta-catenin by interaction with transcription factor LEF-1. Mechanisms of development *59*, 3-10.

Hughes, K.S., Simon, R., Songhorabodi, S., Adson, M.A., Ilstrup, D.M., Fortner, J.G., Maclean, B.J., Foster, J.H., Daly, J.M., Fitzherbert, D.*, et al.* (1986). Resection of the liver for colorectal carcinoma metastases: a multi-institutional study of patterns of recurrence. Surgery *100*, 278-284.

Hunter, K.W., Crawford, N.P., and Alsarraj, J. (2008). Mechanisms of metastasis. Breast cancer research : BCR *10 Suppl 1*, S2.

Husemann, Y., Geigl, J.B., Schubert, F., Musiani, P., Meyer, M., Burghart, E., Forni, G., Eils, R., Fehm, T., Riethmuller, G.*, et al.* (2008). Systemic spread is an early step in breast cancer. Cancer Cell *13*, 58-68.

Hynes, N.E., and Lane, H.A. (2005). ERBB receptors and cancer: the complexity of targeted inhibitors. Nature reviews Cancer *5*, 341-354.

Ichii, S., Horii, A., Nakatsuru, S., Furuyama, J., Utsunomiya, J., and Nakamura, Y. (1992). Inactivation of both APC alleles in an early stage of colon adenomas in a patient with familial adenomatous polyposis (FAP). Human molecular genetics *1*, 387-390.

Ikeda, S., Kishida, M., Matsuura, Y., Usui, H., and Kikuchi, A. (2000). GSK-3beta-dependent phosphorylation of adenomatous polyposis coli gene product can be modulated by beta-catenin and protein phosphatase 2A complexed with Axin. Oncogene *19*, 537-545.

Ikushima, H., and Miyazono, K. (2010a). Cellular context-dependent "colors" of transforming growth factor-beta signaling. Cancer Sci *101*, 306-312.

Ikushima, H., and Miyazono, K. (2010b). TGFbeta signalling: a complex web in cancer progression. Nature reviews Cancer *10*, 415-424.

Ionov, Y., Peinado, M.A., Malkhosyan, S., Shibata, D., and Perucho, M. (1993). Ubiquitous somatic mutations in simple repeated sequences reveal a new mechanism for colonic carcinogenesis. Nature *363*, 558-561.

Ito, M., Hiramatsu, H., Kobayashi, K., Suzue, K., Kawahata, M., Hioki, K., Ueyama, Y., Koyanagi, Y., Sugamura, K., Tsuji, K.*, et al.* (2002). NOD/SCID/gamma(c)(null) mouse: an excellent recipient mouse model for engraftment of human cells. Blood *100*, 3175-3182.

Itzkovitz, S., Lyubimova, A., Blat, I.C., Maynard, M., van Es, J., Lees, J., Jacks, T., Clevers, H., and van Oudenaarden, A. (2012). Single-molecule transcript counting of stem-cell markers in the mouse intestine. Nature cell biology *14*, 106-114.

Janknecht, R., Wells, N.J., and Hunter, T. (1998). TGF-beta-stimulated cooperation of smad proteins with the coactivators CBP/p300. Genes & development *12*, 2114-2119.

Jemal, A., Bray, F., Center, M.M., Ferlay, J., Ward, E., and Forman, D. (2011). Global cancer statistics. CA Cancer J Clin *61*, 69-90.

Jen, J., Powell, S.M., Papadopoulos, N., Smith, K.J., Hamilton, S.R., Vogelstein, B., and Kinzler, K.W. (1994). Molecular determinants of dysplasia in colorectal lesions. Cancer research *54*, 5523-5526.

Jiang, J., and Struhl, G. (1998). Regulation of the Hedgehog and Wingless signalling pathways by the F-box/WD40-repeat protein Slimb. Nature *391*, 493-496.

Jin, D.K., Shido, K., Kopp, H.G., Petit, I., Shmelkov, S.V., Young, L.M., Hooper, A.T., Amano, H., Avecilla, S.T., Heissig, B*., et al.* (2006). Cytokine-mediated deployment of SDF-1 induces revascularization through recruitment of CXCR4+ hemangiocytes. Nature medicine *12*, 557-567.

Jones, S., Chen, W.D., Parmigiani, G., Diehl, F., Beerenwinkel, N., Antal, T., Traulsen, A., Nowak, M.A., Siegel, C., Velculescu, V.E*., et al.* (2008). Comparative lesion sequencing provides insights into tumor evolution. Proceedings of the National Academy of Sciences of the United States of America *105*, 4283-4288.

Joyce, J.A., and Pollard, J.W. (2009). Microenvironmental regulation of metastasis. Nature reviews Cancer *9*, 239-252.

Kanda, T., Sullivan, K.F., and Wahl, G.M. (1998). Histone-GFP fusion protein enables sensitive analysis of chromosome dynamics in living mammalian cells. Current biology : CB *8*, 377-385.

Kaplan, K.B., Burds, A.A., Swedlow, J.R., Bekir, S.S., Sorger, P.K., and Nathke, I.S. (2001). A role for the Adenomatous Polyposis Coli protein in chromosome segregation. Nature cell biology *3*, 429-432.

Kaplan, R.N., Riba, R.D., Zacharoulis, S., Bramley, A.H., Vincent, L., Costa, C., MacDonald, D.D., Jin, D.K., Shido, K., Kerns, S.A*., et al.* (2005). VEGFR1-positive haematopoietic bone marrow progenitors initiate the pre-metastatic niche. Nature *438*, 820-827.

Kawada, M., Yamagoe, S., Murakami, Y., Suzuki, K., Mizuno, S., and Uehara, Y. (1997). Induction of p27Kip1 degradation and anchorage independence by Ras through the MAP kinase signaling pathway. Oncogene *15*, 629-637.

Kawasaki, Y., Sato, R., and Akiyama, T. (2003). Mutated APC and Asef are involved in the migration of colorectal tumour cells. Nature cell biology *5*, 211-215.

Kawasaki, Y., Senda, T., Ishidate, T., Koyama, R., Morishita, T., Iwayama, Y., Higuchi, O., and Akiyama, T. (2000). Asef, a link between the tumor suppressor APC and G-protein signaling. Science *289*, 1194-1197.

Kemper, K., Sprick, M.R., de Bree, M., Scopelliti, A., Vermeulen, L., Hoek, M., Zeilstra, J., Pals, S.T., Mehmet, H., Stassi, G.*, et al.* (2010). The AC133 epitope, but not the CD133 protein, is lost upon cancer stem cell differentiation. Cancer research *70*, 719-729.

Kerber, R.A., Neklason, D.W., Samowitz, W.S., and Burt, R.W. (2005). Frequency of familial colon cancer and hereditary nonpolyposis colorectal cancer (Lynch syndrome) in a large population database. Fam Cancer *4*, 239-244.

Kim, J., Johnson, K., Chen, H.J., Carroll, S., and Laughon, A. (1997). Drosophila Mad binds to DNA and directly mediates activation of vestigial by Decapentaplegic. Nature *388*, 304-308.

Kim, K., Pang, K.M., Evans, M., and Hay, E.D. (2000). Overexpression of beta-catenin induces apoptosis independent of its transactivation function with LEF-1 or the involvement of major G1 cell cycle regulators. Molecular biology of the cell *11*, 3509-3523.

Kinzler, K.W., Nilbert, M.C., Su, L.K., Vogelstein, B., Bryan, T.M., Levy, D.B., Smith, K.J., Preisinger, A.C., Hedge, P., McKechnie, D.*, et al.* (1991). Identification of FAP locus genes from chromosome 5q21. Science *253*, 661-665.

Kinzler, K.W., and Vogelstein, B. (1996). Lessons from hereditary colorectal cancer. Cell *87*, 159-170.

Kishida, M., Koyama, S., Kishida, S., Matsubara, K., Nakashima, S., Higano, K., Takada, R., Takada, S., and Kikuchi, A. (1999). Axin prevents Wnt-3a-induced accumulation of beta-catenin. Oncogene *18*, 979-985.

Klaus, A., and Birchmeier, W. (2008). Wnt signalling and its impact on development and cancer. Nature reviews Cancer *8*, 387-398.

Klein, C.A. (2009). Parallel progression of primary tumours and metastases. Nature reviews Cancer *9*, 302-312.

Klein, C.A., Blankenstein, T.J., Schmidt-Kittler, O., Petronio, M., Polzer, B., Stoecklein, N.H., and Riethmuller, G. (2002). Genetic heterogeneity of single disseminated tumour cells in minimal residual cancer. Lancet *360*, 683-689.

Klippel, A., Reinhard, C., Kavanaugh, W.M., Apell, G., Escobedo, M.A., and Williams, L.T. (1996). Membrane localization of phosphatidylinositol 3-kinase is sufficient to activate multiple signal-transducing kinase pathways. Molecular and cellular biology *16*, 4117-4127.

Kobaek-Larsen, M., Thorup, I., Diederichsen, A., Fenger, C., and Hoitinga, M.R. (2000). Review of colorectal cancer and its metastases in rodent models: comparative aspects with those in humans. Comp Med *50*, 16-26.

Kobayashi, H., Mochizuki, H., Sugihara, K., Morita, T., Kotake, K., Teramoto, T., Kameoka, S., Saito, Y., Takahashi, K., Hase, K.*, et al.* (2007). Characteristics of recurrence and surveillance tools after curative resection for colorectal cancer: a multicenter study. Surgery *141*, 67-75.

Korinek, V., Barker, N., Morin, P.J., van Wichen, D., de Weger, R., Kinzler, K.W., Vogelstein, B., and Clevers, H. (1997). Constitutive transcriptional activation by a beta-catenin-Tcf complex in APC-/- colon carcinoma. Science *275*, 1784-1787.

Kosinski, C., Li, V.S., Chan, A.S., Zhang, J., Ho, C., Tsui, W.Y., Chan, T.L., Mifflin, R.C., Powell, D.W., Yuen, S.T.*, et al.* (2007). Gene expression patterns of human colon tops and basal crypts and BMP antagonists as intestinal stem cell niche factors. Proceedings of the National Academy of Sciences of the United States of America *104*, 15418-15423.

Koyama, M., Ito, M., Nagai, H., Emi, M., and Moriyama, Y. (1999). Inactivation of both alleles of the DPC4/SMAD4 gene in advanced colorectal cancers: identification of seven novel somatic mutations in tumors from Japanese patients. Mutation research *406*, 71-77.

Kramps, T., Peter, O., Brunner, E., Nellen, D., Froesch, B., Chatterjee, S., Murone, M., Zullig, S., and Basler, K. (2002). Wnt/wingless signaling requires BCL9/legless-mediated recruitment of pygopus to the nuclear beta-catenin-TCF complex. Cell *109*, 47-60.

LaBarge, M.A., and Bissell, M.J. (2008). Is CD133 a marker of metastatic colon cancer stem cells? The Journal of clinical investigation *118*, 2021-2024.

Laederich, M.B., Funes-Duran, M., Yen, L., Ingalla, E., Wu, X., Carraway, K.L., 3rd, and Sweeney, C. (2004). The leucine-rich repeat protein LRIG1 is a negative regulator of ErbB family receptor tyrosine kinases. The Journal of biological chemistry *279*, 47050-47056.

Lee, C.J., Dosch, J., and Simeone, D.M. (2008). Pancreatic cancer stem cells. Journal of clinical oncology : official journal of the American Society of Clinical Oncology *26*, 2806-2812.

Lee, J., Kotliarova, S., Kotliarov, Y., Li, A., Su, Q., Donin, N.M., Pastorino, S., Purow, B.W., Christopher, N., Zhang, W*., et al.* (2006). Tumor stem cells derived from glioblastomas cultured in bFGF and EGF more closely mirror the phenotype and genotype of primary tumors than do serum-cultured cell lines. Cancer Cell *9*, 391-403.

Leevers, S.J., Paterson, H.F., and Marshall, C.J. (1994). Requirement for Ras in Raf activation is overcome by targeting Raf to the plasma membrane. Nature *369*, 411-414.

Leinung, S., Wurl, P., Weiss, C.L., Roder, I., and Schonfelder, M. (2000). Cytokeratin-positive cells in bone marrow in comparison with other prognostic factors in colon carcinoma. Langenbeck's archives of surgery / Deutsche Gesellschaft fur Chirurgie *385*, 337-343.

Lengauer, C., Kinzler, K.W., and Vogelstein, B. (1998). Genetic instabilities in human cancers. Nature *396*, 643-649.

Leong, K.G., Wang, B.E., Johnson, L., and Gao, W.Q. (2008). Generation of a prostate from a single adult stem cell. Nature *456*, 804-808.

Levin, T.G., Powell, A.E., Davies, P.S., Silk, A.D., Dismuke, A.D., Anderson, E.C., Swain, J.R., and Wong, M.H. (2010). Characterization of the intestinal cancer stem

cell marker CD166 in the human and mouse gastrointestinal tract. Gastroenterology *139*, 2072-2082 e2075.

Levy, D.B., Smith, K.J., Beazer-Barclay, Y., Hamilton, S.R., Vogelstein, B., and Kinzler, K.W. (1994). Inactivation of both APC alleles in human and mouse tumors. Cancer research *54*, 5953-5958.

Li, C., Heidt, D.G., Dalerba, P., Burant, C.F., Zhang, L., Adsay, V., Wicha, M., Clarke, M.F., and Simeone, D.M. (2007). Identification of pancreatic cancer stem cells. Cancer Res *67*, 1030-1037.

Li, F.P., and Fraumeni, J.F., Jr. (1969a). Rhabdomyosarcoma in children: epidemiologic study and identification of a familial cancer syndrome. Journal of the National Cancer Institute *43*, 1365-1373.

Li, F.P., and Fraumeni, J.F., Jr. (1969b). Soft-tissue sarcomas, breast cancer, and other neoplasms. A familial syndrome? Ann Intern Med *71*, 747-752.

Li, L., and Clevers, H. (2010). Coexistence of quiescent and active adult stem cells in mammals. Science *327*, 542-545.

Li, R., Sutphin, P.D., Schwartz, D., Matas, D., Almog, N., Wolkowicz, R., Goldfinger, N., Pei, H., Prokocimer, M., and Rotter, V. (1998). Mutant p53 protein expression interferes with p53-independent apoptotic pathways. Oncogene *16*, 3269-3277.

Lievre, A., Bachet, J.B., Boige, V., Cayre, A., Le Corre, D., Buc, E., Ychou, M., Bouche, O., Landi, B., Louvet, C*., et al.* (2008). KRAS mutations as an independent prognostic factor in patients with advanced colorectal cancer treated with cetuximab. Journal of clinical oncology : official journal of the American Society of Clinical Oncology *26*, 374-379.

Lin, E.Y., Li, J.F., Gnatovskiy, L., Deng, Y., Zhu, L., Grzesik, D.A., Qian, H., Xue, X.N., and Pollard, J.W. (2006). Macrophages regulate the angiogenic switch in a mouse model of breast cancer. Cancer research *66*, 11238-11246.

Lin, E.Y., Nguyen, A.V., Russell, R.G., and Pollard, J.W. (2001). Colony-stimulating factor 1 promotes progression of mammary tumors to malignancy. J Exp Med *193*, 727-740.

Lindemann, F., Schlimok, G., Dirschedl, P., Witte, J., and Riethmuller, G. (1992). Prognostic significance of micrometastatic tumour cells in bone marrow of colorectal cancer patients. Lancet *340*, 685-689.

Litvinov, S.V., Balzar, M., Winter, M.J., Bakker, H.A., Briaire-de Bruijn, I.H., Prins, F., Fleuren, G.J., and Warnaar, S.O. (1997). Epithelial cell adhesion molecule (Ep-CAM) modulates cell-cell interactions mediated by classic cadherins. The Journal of cell biology *139*, 1337-1348.

Litvinov, S.V., Velders, M.P., Bakker, H.A., Fleuren, G.J., and Warnaar, S.O. (1994). Ep-CAM: a human epithelial antigen is a homophilic cell-cell adhesion molecule. The Journal of cell biology *125*, 437-446.

Liu, F., Hata, A., Baker, J.C., Doody, J., Carcamo, J., Harland, R.M., and Massague, J. (1996). A human Mad protein acting as a BMP-regulated transcriptional activator. Nature *381*, 620-623.

Liu, W., Dong, X., Mai, M., Seelan, R.S., Taniguchi, K., Krishnadath, K.K., Halling, K.C., Cunningham, J.M., Boardman, L.A., Qian, C.*, et al.* (2000). Mutations in AXIN2 cause colorectal cancer with defective mismatch repair by activating beta-catenin/TCF signalling. Nature genetics *26*, 146-147.

Lobo, N.A., Shimono, Y., Qian, D., and Clarke, M.F. (2007). The biology of cancer stem cells. Annu Rev Cell Dev Biol *23*, 675-699.

Loda, M., Cukor, B., Tam, S.W., Lavin, P., Fiorentino, M., Draetta, G.F., Jessup, J.M., and Pagano, M. (1997). Increased proteasome-dependent degradation of the cyclin-dependent kinase inhibitor p27 in aggressive colorectal carcinomas. Nature medicine *3*, 231-234.

Louie, R.K., Bahmanyar, S., Siemers, K.A., Votin, V., Chang, P., Stearns, T., Nelson, W.J., and Barth, A.I. (2004). Adenomatous polyposis coli and EB1 localize in close proximity of the mother centriole and EB1 is a functional component of centrosomes. Journal of cell science *117*, 1117-1128.

Luongo, C., Moser, A.R., Gledhill, S., and Dove, W.F. (1994). Loss of Apc+ in intestinal adenomas from Min mice. Cancer research *54*, 5947-5952.

Lyle, S., Christofidou-Solomidou, M., Liu, Y., Elder, D.E., Albelda, S., and Cotsarelis, G. (1998). The C8/144B monoclonal antibody recognizes cytokeratin 15 and defines the location of human hair follicle stem cells. J Cell Sci *111 (Pt 21)*, 3179-3188.

Lynch, H.T., Lynch, J.F., Lynch, P.M., and Attard, T. (2008). Hereditary colorectal cancer syndromes: molecular genetics, genetic counseling, diagnosis and management. Fam Cancer *7*, 27-39.

Lynch, H.T., Smyrk, T., and Lynch, J.F. (1996). Overview of natural history, pathology, molecular genetics and management of HNPCC (Lynch Syndrome). International journal of cancer Journal international du cancer *69*, 38-43.

MacGrogan, D., Pegram, M., Slamon, D., and Bookstein, R. (1997). Comparative mutational analysis of DPC4 (Smad4) in prostatic and colorectal carcinomas. Oncogene *15*, 1111-1114.

Maitra, A., Molberg, K., Albores-Saavedra, J., and Lindberg, G. (2000). Loss of Dpc4 expression in colonic adenocarcinomas correlates with the presence of metastatic disease. The American journal of pathology *157*, 1105-1111.

Malumbres, M., and Barbacid, M. (2003). RAS oncogenes: the first 30 years. Nature reviews Cancer *3*, 459-465.

Mann, B., Gelos, M., Siedow, A., Hanski, M.L., Gratchev, A., Ilyas, M., Bodmer, W.F., Moyer, M.P., Riecken, E.O., Buhr, H.J.*, et al.* (1999). Target genes of beta-catenin-T cell-factor/lymphoid-enhancer-factor signaling in human colorectal carcinomas. Proceedings of the National Academy of Sciences of the United States of America *96*, 1603-1608.

Manne, U., Weiss, H.L., Myers, R.B., Danner, O.K., Moron, C., Srivastava, S., and Grizzle, W.E. (1998). Nuclear accumulation of p53 in colorectal adenocarcinoma: prognostic importance differs with race and location of the tumor. Cancer *83*, 2456-2467.

Mannel, D.N., Orosz, P., Hafner, M., and Falk, W. (1994). Mechanisms involved in metastasis enhanced by inflammatory mediators. Circ Shock *44*, 9-13.

Marais, R., Light, Y., Paterson, H.F., and Marshall, C.J. (1995). Ras recruits Raf-1 to the plasma membrane for activation by tyrosine phosphorylation. The EMBO journal *14*, 3136-3145.

Marches, R., Scheuermann, R., and Uhr, J. (2006). Cancer dormancy: from mice to man. Cell Cycle *5*, 1772-1778.

Marikawa, Y., and Elinson, R.P. (1998). beta-TrCP is a negative regulator of Wnt/beta-catenin signaling pathway and dorsal axis formation in Xenopus embryos. Mechanisms of development *77*, 75-80.

Markowitz, S.D., and Bertagnolli, M.M. (2009). Molecular origins of cancer: Molecular basis of colorectal cancer. The New England journal of medicine *361*, 2449-2460.

Massarelli, E., Varella-Garcia, M., Tang, X., Xavier, A.C., Ozburn, N.C., Liu, D.D., Bekele, B.N., Herbst, R.S., and Wistuba, II (2007). KRAS mutation is an important predictor of resistance to therapy with epidermal growth factor receptor tyrosine kinase inhibitors in non-small-cell lung cancer. Clinical cancer research : an official journal of the American Association for Cancer Research *13*, 2890-2896.

Massberg, S., Konrad, I., Schurzinger, K., Lorenz, M., Schneider, S., Zohlnhoefer, D., Hoppe, K., Schiemann, M., Kennerknecht, E., Sauer, S*., et al.* (2006). Platelets secrete stromal cell-derived factor 1alpha and recruit bone marrow-derived progenitor cells to arterial thrombi in vivo. J Exp Med *203*, 1221-1233.

Matsumine, A., Ogai, A., Senda, T., Okumura, N., Satoh, K., Baeg, G.H., Kawahara, T., Kobayashi, S., Okada, M., Toyoshima, K*., et al.* (1996). Binding of APC to the human homolog of the Drosophila discs large tumor suppressor protein. Science *272*, 1020-1023.

Matsuzaki, K., Deng, G., Tanaka, H., Kakar, S., Miura, S., and Kim, Y.S. (2005). The relationship between global methylation level, loss of heterozygosity, and microsatellite instability in sporadic colorectal cancer. Clinical cancer research : an official journal of the American Association for Cancer Research *11*, 8564-8569.

Medema, J.P., and Vermeulen, L. (2011). Microenvironmental regulation of stem cells in intestinal homeostasis and cancer. Nature *474*, 318-326.

Mehlen, P., and Puisieux, A. (2006). Metastasis: a question of life or death. Nature reviews Cancer *6*, 449-458.

Meijer, J., Zeelenberg, I.S., Sipos, B., and Roos, E. (2006). The CXCR5 chemokine receptor is expressed by carcinoma cells and promotes growth of colon carcinoma in the liver. Cancer research *66*, 9576-9582.

Meltzer, A. (1990). Dormancy and breast cancer. J Surg Oncol *43*, 181-188.

Mestas, J., and Hughes, C.C. (2004). Of mice and not men: differences between mouse and human immunology. J Immunol *172*, 2731-2738.

Milner, J., and Medcalf, E.A. (1991). Cotranslation of activated mutant p53 with wild type drives the wild-type p53 protein into the mutant conformation. Cell *65*, 765-774.

Milner, J., Medcalf, E.A., and Cook, A.C. (1991). Tumor suppressor p53: analysis of wild-type and mutant p53 complexes. Molecular and cellular biology *11*, 12-19.

Miselis, N.R., Wu, Z.J., Van Rooijen, N., and Kane, A.B. (2008). Targeting tumor-associated macrophages in an orthotopic murine model of diffuse malignant mesothelioma. Molecular cancer therapeutics *7*, 788-799.

Mitry, E., Bouvier, A.M., Esteve, J., and Faivre, J. (2002). Benefit of operative mortality reduction on colorectal cancer survival. The British journal of surgery *89*, 1557-1562.

Miyaki, M., Iijima, T., Konishi, M., Sakai, K., Ishii, A., Yasuno, M., Hishima, T., Koike, M., Shitara, N., Iwama, T.*, et al.* (1999). Higher frequency of Smad4 gene mutation in human colorectal cancer with distant metastasis. Oncogene *18*, 3098-3103.

Miyakura, Y., Sugano, K., Fukayama, N., Konishi, F., and Nagai, H. (2002). Concurrent mutations of K-ras oncogene at codons 12 and 22 in colon cancer. Jpn J Clin Oncol *32*, 219-221.

Miyazaki, M., Furuya, T., Shiraki, A., Sato, T., Oga, A., and Sasaki, K. (1999). The relationship of DNA ploidy to chromosomal instability in primary human colorectal cancers. Cancer research *59*, 5283-5285.

Miyoshi, Y., Nagase, H., Ando, H., Horii, A., Ichii, S., Nakatsuru, S., Aoki, T., Miki, Y., Mori, T., and Nakamura, Y. (1992). Somatic mutations of the APC gene in colorectal tumors: mutation cluster region in the APC gene. Human molecular genetics *1*, 229-233.

Molenaar, M., van de Wetering, M., Oosterwegel, M., Peterson-Maduro, J., Godsave, S., Korinek, V., Roose, J., Destree, O., and Clevers, H. (1996). XTcf-3 transcription factor mediates beta-catenin-induced axis formation in Xenopus embryos. Cell *86*, 391-399.

Montgomery, R.K., Carlone, D.L., Richmond, C.A., Farilla, L., Kranendonk, M.E., Henderson, D.E., Baffour-Awuah, N.Y., Ambruzs, D.M., Fogli, L.K., Algra, S.*, et al.* (2011). Mouse telomerase reverse transcriptase (mTert) expression marks slowly cycling intestinal stem cells. Proceedings of the National Academy of Sciences of the United States of America *108*, 179-184.

Moore, N., Houghton, J., and Lyle, S. (2011). Slow-Cycling Therapy-Resistant Cancer Cells. Stem cells and development.

Morgan, T.M., Lange, P.H., Porter, M.P., Lin, D.W., Ellis, W.J., Gallaher, I.S., and Vessella, R.L. (2009). Disseminated tumor cells in prostate cancer patients after radical prostatectomy and without evidence of disease predicts biochemical recurrence. Clin Cancer Res *15*, 677-683.

Morin, P.J., Sparks, A.B., Korinek, V., Barker, N., Clevers, H., Vogelstein, B., and Kinzler, K.W. (1997). Activation of beta-catenin-Tcf signaling in colon cancer by mutations in beta-catenin or APC. Science *275*, 1787-1790.

Morrison, S.J., and Weissman, I.L. (1994). The long-term repopulating subset of hematopoietic stem cells is deterministic and isolatable by phenotype. Immunity *1*, 661-673.

Morton, C.L., and Houghton, P.J. (2007). Establishment of human tumor xenografts in immunodeficient mice. Nature protocols *2*, 247-250.

Moser, A.R., Pitot, H.C., and Dove, W.F. (1990). A dominant mutation that predisposes to multiple intestinal neoplasia in the mouse. Science *247*, 322-324.

Mosimann, C., Hausmann, G., and Basler, K. (2006). Parafibromin/Hyrax activates Wnt/Wg target gene transcription by direct association with beta-catenin/Armadillo. Cell *125*, 327-341.

Moustakas, A., and Heldin, C.H. (2005). Non-Smad TGF-beta signals. Journal of cell science *118*, 3573-3584.

Muller, A., Homey, B., Soto, H., Ge, N., Catron, D., Buchanan, M.E., McClanahan, T., Murphy, E., Yuan, W., Wagner, S.N.*, et al.* (2001). Involvement of chemokine receptors in breast cancer metastasis. Nature *410*, 50-56.

Munemitsu, S., Albert, I., Souza, B., Rubinfeld, B., and Polakis, P. (1995). Regulation of intracellular beta-catenin levels by the adenomatous polyposis coli (APC) tumor-suppressor protein. Proceedings of the National Academy of Sciences of the United States of America *92*, 3046-3050.

Munemitsu, S., Souza, B., Muller, O., Albert, I., Rubinfeld, B., and Polakis, P. (1994). The APC gene product associates with microtubules in vivo and promotes their assembly in vitro. Cancer research *54*, 3676-3681.

Munz, M., Kieu, C., Mack, B., Schmitt, B., Zeidler, R., and Gires, O. (2004). The carcinoma-associated antigen EpCAM upregulates c-myc and induces cell proliferation. Oncogene *23*, 5748-5758.

Nagano, O., and Saya, H. (2004). Mechanism and biological significance of CD44 cleavage. Cancer Sci *95*, 930-935.

Nagase, H., and Nakamura, Y. (1993). Mutations of the APC (adenomatous polyposis coli) gene. Human mutation *2*, 425-434.

Nakamura, Y. (1993). The role of the adenomatous polyposis coli (APC) gene in human cancers. Advances in cancer research *62*, 65-87.

Nakao, A., Roijer, E., Imamura, T., Souchelnytskyi, S., Stenman, G., Heldin, C.H., and ten Dijke, P. (1997). Identification of Smad2, a human Mad-related protein in the transforming growth factor beta signaling pathway. The Journal of biological chemistry *272*, 2896-2900.

Naumov, G.N., Townson, J.L., MacDonald, I.C., Wilson, S.M., Bramwell, V.H., Groom, A.C., and Chambers, A.F. (2003). Ineffectiveness of doxorubicin treatment on solitary dormant mammary carcinoma cells or late-developing metastases. Breast Cancer Res Treat *82*, 199-206.

Nguyen, L.V., Vanner, R., Dirks, P., and Eaves, C.J. (2012). Cancer stem cells: an evolving concept. Nature reviews Cancer *12*, 133-143.

Nigro, J.M., Baker, S.J., Preisinger, A.C., Jessup, J.M., Hostetter, R., Cleary, K., Bigner, S.H., Davidson, N., Baylin, S., Devilee, P.*, et al.* (1989). Mutations in the p53 gene occur in diverse human tumour types. Nature *342*, 705-708.

Noel, A., Hajitou, A., L'Hoir, C., Maquoi, E., Baramova, E., Lewalle, J.M., Remacle, A., Kebers, F., Brown, P., Calberg-Bacq, C.M.*, et al.* (1998). Inhibition of stromal matrix metalloproteases: effects on breast-tumor promotion by fibroblasts. International journal of cancer Journal international du cancer *76*, 267-273.

Notta, F., Mullighan, C.G., Wang, J.C., Poeppl, A., Doulatov, S., Phillips, L.A., Ma, J., Minden, M.D., Downing, J.R., and Dick, J.E. (2011). Evolution of human BCR-ABL1 lymphoblastic leukaemia-initiating cells. Nature *469*, 362-367.

O'Brien, C.A., Kreso, A., and Dick, J.E. (2009). Cancer stem cells in solid tumors: an overview. Semin Radiat Oncol *19*, 71-77.

O'Brien, C.A., Pollett, A., Gallinger, S., and Dick, J.E. (2007). A human colon cancer cell capable of initiating tumour growth in immunodeficient mice. Nature *445*, 106-110.

Olivier, M., Eeles, R., Hollstein, M., Khan, M.A., Harris, C.C., and Hainaut, P. (2002). The IARC TP53 database: new online mutation analysis and recommendations to users. Human mutation *19*, 607-614.

Olmeda, D., Castel, S., Vilaro, S., and Cano, A. (2003). Beta-catenin regulation during the cell cycle: implications in G2/M and apoptosis. Molecular biology of the cell *14*, 2844-2860.

Orford, K.W., and Scadden, D.T. (2008). Deconstructing stem cell self-renewal: genetic insights into cell-cycle regulation. Nat Rev Genet *9*, 115-128.

Orita, S., Higashi, T., Kawasaki, Y., Harada, A., Igarashi, H., Monden, T., Morimoto, H., Shimano, T., Mori, T., and Miyoshi, J. (1991). A novel point mutation at codon 146 of the K-ras gene in a human colorectal cancer identified by the polymerase chain reaction. Virus Genes *5*, 75-79.

Osawa, M., Hanada, K., Hamada, H., and Nakauchi, H. (1996). Long-term lymphohematopoietic reconstitution by a single CD34-low/negative hematopoietic stem cell. Science *273*, 242-245.

Paget, S. (1989). The distribution of secondary growths in cancer of the breast. 1889. Cancer Metastasis Rev *8*, 98-101.

Pantel, K., Izbicki, J., Passlick, B., Angstwurm, M., Haussinger, K., Thetter, O., and Riethmuller, G. (1996). Frequency and prognostic significance of isolated tumour cells in bone marrow of patients with non-small-cell lung cancer without overt metastases. Lancet *347*, 649-653.

Pantel, K., Schlimok, G., Braun, S., Kutter, D., Lindemann, F., Schaller, G., Funke, I., Izbicki, J.R., and Riethmuller, G. (1993). Differential expression of proliferation-associated molecules in individual micrometastatic carcinoma cells. Journal of the National Cancer Institute *85*, 1419-1424.

Pantel, K., and Woelfle, U. (2005). Detection and molecular characterisation of disseminated tumour cells: implications for anti-cancer therapy. Biochim Biophys Acta *1756*, 53-64.

Park, Y., and Gerson, S.L. (2005). DNA repair defects in stem cell function and aging. Annu Rev Med *56*, 495-508.

Parmar, K., Mauch, P., Vergilio, J.A., Sackstein, R., and Down, J.D. (2007). Distribution of hematopoietic stem cells in the bone marrow according to regional hypoxia. Proceedings of the National Academy of Sciences of the United States of America *104*, 5431-5436.

Pasetto, L.M., Jirillo, A., Iadicicco, G., Rossi, E., Paris, M.K., and Monfardini, S. (2005). FOLFOX versus FOLFIRI: a comparison of regimens in the treatment of colorectal cancer metastases. Anticancer research *25*, 563-576.

Passegue, E., Wagers, A.J., Giuriato, S., Anderson, W.C., and Weissman, I.L. (2005). Global analysis of proliferation and cell cycle gene expression in the regulation of hematopoietic stem and progenitor cell fates. J Exp Med *202*, 1599-1611.

Patrawala, L., Calhoun, T., Schneider-Broussard, R., Li, H., Bhatia, B., Tang, S., Reilly, J.G., Chandra, D., Zhou, J., Claypool, K.*, et al.* (2006). Highly purified CD44+ prostate cancer cells from xenograft human tumors are enriched in tumorigenic and metastatic progenitor cells. Oncogene *25*, 1696-1708.

Pece, S., Tosoni, D., Confalonieri, S., Mazzarol, G., Vecchi, M., Ronzoni, S., Bernard, L., Viale, G., Pelicci, P.G., and Di Fiore, P.P. (2010). Biological and molecular heterogeneity of breast cancers correlates with their cancer stem cell content. Cell *140*, 62-73.

Polakis, P. (2000). Wnt signaling and cancer. Genes & development *14*, 1837-1851.

Polakis, P. (2007). The many ways of Wnt in cancer. Current opinion in genetics & development *17*, 45-51.

Popat, S., and Houlston, R.S. (2005). A systematic review and meta-analysis of the relationship between chromosome 18q genotype, DCC status and colorectal cancer prognosis. European journal of cancer *41*, 2060-2070.

Popat, S., Hubner, R., and Houlston, R.S. (2005). Systematic review of microsatellite instability and colorectal cancer prognosis. Journal of clinical oncology : official journal of the American Society of Clinical Oncology *23*, 609-618.

Poste, G., and Fidler, I.J. (1980). The pathogenesis of cancer metastasis. Nature *283*, 139-146.

Potten, C.S. (1977). Extreme sensitivity of some intestinal crypt cells to X and gamma irradiation. Nature *269*, 518-521.

Potten, C.S., Kellett, M., Roberts, S.A., Rew, D.A., and Wilson, G.D. (1992). Measurement of in vivo proliferation in human colorectal mucosa using bromodeoxyuridine. Gut *33*, 71-78.

Potten, C.S., Kovacs, L., and Hamilton, E. (1974). Continuous labelling studies on mouse skin and intestine. Cell Tissue Kinet *7*, 271-283.

Powell, A.E., Wang, Y., Li, Y., Poulin, E.J., Means, A.L., Washington, M.K., Higginbotham, J.N., Juchheim, A., Prasad, N., Levy, S.E.*, et al.* (2012). The Pan-ErbB Negative Regulator Lrig1 Is an Intestinal Stem Cell Marker that Functions as a Tumor Suppressor. Cell *149*, 146-158.

Powell, S.M., Zilz, N., Beazer-Barclay, Y., Bryan, T.M., Hamilton, S.R., Thibodeau, S.N., Vogelstein, B., and Kinzler, K.W. (1992). APC mutations occur early during colorectal tumorigenesis. Nature *359*, 235-237.

Pritchard, C.C., and Grady, W.M. (2011). Colorectal cancer molecular biology moves into clinical practice. Gut *60*, 116-129.

Quintana, E., Shackleton, M., Sabel, M.S., Fullen, D.R., Johnson, T.M., and Morrison, S.J. (2008). Efficient tumour formation by single human melanoma cells. Nature *456*, 593-598.

Rabinovitz, I., and Mercurio, A.M. (1997). The integrin alpha6beta4 functions in carcinoma cell migration on laminin-1 by mediating the formation and stabilization of actin-containing motility structures. The Journal of cell biology *139*, 1873-1884.

Rabinovsky, R., Uhr, J.W., Vitetta, E.S., and Yefenof, E. (2007). Cancer dormancy: lessons from a B cell lymphoma and adenocarcinoma of the prostate. Advances in cancer research *97*, 189-202.

Raymond, E., Chaney, S.G., Taamma, A., and Cvitkovic, E. (1998). Oxaliplatin: a review of preclinical and clinical studies. Annals of oncology : official journal of the European Society for Medical Oncology / ESMO *9*, 1053-1071.

Reya, T., Morrison, S.J., Clarke, M.F., and Weissman, I.L. (2001). Stem cells, cancer, and cancer stem cells. Nature *414*, 105-111.

Ricci-Vitiani, L., Lombardi, D.G., Pilozzi, E., Biffoni, M., Todaro, M., Peschle, C., and De Maria, R. (2007). Identification and expansion of human colon-cancer-initiating cells. Nature *445*, 111-115.

Richmond, A., and Su, Y. (2008). Mouse xenograft models vs GEM models for human cancer therapeutics. Dis Model Mech *1*, 78-82.

Robinson, B.D., Sica, G.L., Liu, Y.F., Rohan, T.E., Gertler, F.B., Condeelis, J.S., and Jones, J.G. (2009). Tumor microenvironment of metastasis in human breast carcinoma: a potential prognostic marker linked to hematogenous dissemination. Clinical cancer research : an official journal of the American Association for Cancer Research *15*, 2433-2441.

Rodriguez, J., Frigola, J., Vendrell, E., Risques, R.A., Fraga, M.F., Morales, C., Moreno, V., Esteller, M., Capella, G., Ribas, M.*, et al.* (2006). Chromosomal instability correlates with genome-wide DNA demethylation in human primary colorectal cancers. Cancer research *66*, 8462-9468.

Roesch, A., Fukunaga-Kalabis, M., Schmidt, E.C., Zabierowski, S.E., Brafford, P.A., Vultur, A., Basu, D., Gimotty, P., Vogt, T., and Herlyn, M. (2010). A temporarily distinct subpopulation of slow-cycling melanoma cells is required for continuous tumor growth. Cell *141*, 583-594.

Roijer, E., Moren, A., ten Dijke, P., and Stenman, G. (1998). Assignment1 of the Smad7 gene (MADH7) to human chromosome 18q21.1 by fluorescence in situ hybridization. Cytogenet Cell Genet *81*, 189-190.

Roose, J., Molenaar, M., Peterson, J., Hurenkamp, J., Brantjes, H., Moerer, P., van de Wetering, M., Destree, O., and Clevers, H. (1998). The Xenopus Wnt effector XTcf-3 interacts with Groucho-related transcriptional repressors. Nature *395*, 608-612.

Rothbarth, J., and van de Velde, C.J. (2005). Treatment of liver metastases of colorectal cancer. Annals of oncology : official journal of the European Society for Medical Oncology / ESMO *16 Suppl 2*, ii144-149.

Rubinfeld, B., Souza, B., Albert, I., Muller, O., Chamberlain, S.H., Masiarz, F.R., Munemitsu, S., and Polakis, P. (1993). Association of the APC gene product with beta-catenin. Science *262*, 1731-1734.

Samak, R., and Israel, L. (1982). [Extraction and identification of circulating immune complexes from the serum of cancer patient by affinity chromatography followed by high pressure steric exclusion chromatography. Demonstration of their effect on the mitogenesis of normal lymphocytes]. Ann Med Interne (Paris) *133*, 362-366.

Samowitz, W.S., Curtin, K., Ma, K.N., Edwards, S., Schaffer, D., Leppert, M.F., and Slattery, M.L. (2002). Prognostic significance of p53 mutations in colon cancer at the population level. International journal of cancer Journal international du cancer *99*, 597-602.

Sang, L., Coller, H.A., and Roberts, J.M. (2008). Control of the reversibility of cellular quiescence by the transcriptional repressor HES1. Science *321*, 1095-1100.

Sangiorgi, E., and Capecchi, M.R. (2008). Bmi1 is expressed in vivo in intestinal stem cells. Nat Genet *40*, 915-920.

Sant, M., Capocaccia, R., Coleman, M.P., Berrino, F., Gatta, G., Micheli, A., Verdecchia, A., Faivre, J., Hakulinen, T., Coebergh, J.W*., et al.* (2001). Cancer survival increases in Europe, but international differences remain wide. European journal of cancer *37*, 1659-1667.

Sato, T., van Es, J.H., Snippert, H.J., Stange, D.E., Vries, R.G., van den Born, M., Barker, N., Shroyer, N.F., van de Wetering, M., and Clevers, H. (2011). Paneth cells constitute the niche for Lgr5 stem cells in intestinal crypts. Nature *469*, 415-418.

Schatton, T., Murphy, G.F., Frank, N.Y., Yamaura, K., Waaga-Gasser, A.M., Gasser, M., Zhan, Q., Jordan, S., Duncan, L.M., Weishaupt, C.*, et al.* (2008). Identification of cells initiating human melanomas. Nature *451*, 345-349.

Scheel, C., Onder, T., Karnoub, A., and Weinberg, R.A. (2007). Adaptation versus selection: the origins of metastatic behavior. Cancer research *67*, 11476-11479; discussion 11479-11480.

Scheele, J., Stang, R., Altendorf-Hofmann, A., and Paul, M. (1995). Resection of colorectal liver metastases. World journal of surgery *19*, 59-71.

Schmidt-Kittler, O., Ragg, T., Daskalakis, A., Granzow, M., Ahr, A., Blankenstein, T.J., Kaufmann, M., Diebold, J., Arnholdt, H., Muller, P.*, et al.* (2003). From latent disseminated cells to overt metastasis: genetic analysis of systemic breast cancer progression. Proceedings of the National Academy of Sciences of the United States of America *100*, 7737-7742.

Schwarz-Romond, T., Fiedler, M., Shibata, N., Butler, P.J., Kikuchi, A., Higuchi, Y., and Bienz, M. (2007). The DIX domain of Dishevelled confers Wnt signaling by dynamic polymerization. Nat Struct Mol Biol *14*, 484-492.

Scoville, D.H., Sato, T., He, X.C., and Li, L. (2008). Current view: intestinal stem cells and signaling. Gastroenterology *134*, 849-864.

Segal, N.H., and Saltz, L.B. (2009). Evolving treatment of advanced colon cancer. Annual review of medicine *60*, 207-219.

Shackleton, M., Vaillant, F., Simpson, K.J., Stingl, J., Smyth, G.K., Asselin-Labat, M.L., Wu, L., Lindeman, G.J., and Visvader, J.E. (2006). Generation of a functional mammary gland from a single stem cell. Nature *439*, 84-88.

Sharma, S.V., Lee, D.Y., Li, B., Quinlan, M.P., Takahashi, F., Maheswaran, S., McDermott, U., Azizian, N., Zou, L., Fischbach, M.A.*, et al.* (2010). A chromatin-mediated reversible drug-tolerant state in cancer cell subpopulations. Cell *141*, 69-80.

Shi, Y., Hata, A., Lo, R.S., Massague, J., and Pavletich, N.P. (1997). A structural basis for mutational inactivation of the tumour suppressor Smad4. Nature *388*, 87-93.

Shi, Y., and Massague, J. (2003). Mechanisms of TGF-beta signaling from cell membrane to the nucleus. Cell *113*, 685-700.

Shibata, D., Peinado, M.A., Ionov, Y., Malkhosyan, S., and Perucho, M. (1994). Genomic instability in repeated sequences is an early somatic event in colorectal tumorigenesis that persists after transformation. Nature genetics *6*, 273-281.

Shields, J.M., Pruitt, K., McFall, A., Shaub, A., and Der, C.J. (2000). Understanding Ras: 'it ain't over 'til it's over'. Trends in cell biology *10*, 147-154.

Shmelkov, S.V., Butler, J.M., Hooper, A.T., Hormigo, A., Kushner, J., Milde, T., St Clair, R., Baljevic, M., White, I., Jin, D.K.*, et al.* (2008). CD133 expression is not restricted to stem cells, and both CD133+ and CD133- metastatic colon cancer cells initiate tumors. The Journal of clinical investigation *118*, 2111-2120.

Shtutman, M., Zhurinsky, J., Simcha, I., Albanese, C., D'Amico, M., Pestell, R., and Ben-Ze'ev, A. (1999). The cyclin D1 gene is a target of the beta-catenin/LEF-1 pathway. Proceedings of the National Academy of Sciences of the United States of America *96*, 5522-5527.

Sigal, A., and Rotter, V. (2000). Oncogenic mutations of the p53 tumor suppressor: the demons of the guardian of the genome. Cancer research *60*, 6788-6793.

Simmonds, P.C. (2000). Palliative chemotherapy for advanced colorectal cancer: systematic review and meta-analysis. Colorectal Cancer Collaborative Group. BMJ *321*, 531-535.

Simon, M.C., and Keith, B. (2008). The role of oxygen availability in embryonic development and stem cell function. Nature reviews Molecular cell biology *9*, 285-296.

Simpson-Abelson, M.R., Sonnenberg, G.F., Takita, H., Yokota, S.J., Conway, T.F., Jr., Kelleher, R.J., Jr., Shultz, L.D., Barcos, M., and Bankert, R.B. (2008). Long-term engraftment and expansion of tumor-derived memory T cells following the implantation of non-disrupted pieces of human lung tumor into NOD-scid IL2Rgamma(null) mice. Journal of immunology *180*, 7009-7018.

Singh, S.K., Clarke, I.D., Terasaki, M., Bonn, V.E., Hawkins, C., Squire, J., and Dirks, P.B. (2003). Identification of a cancer stem cell in human brain tumors. Cancer research *63*, 5821-5828.

Singh, S.K., Hawkins, C., Clarke, I.D., Squire, J.A., Bayani, J., Hide, T., Henkelman, R.M., Cusimano, M.D., and Dirks, P.B. (2004). Identification of human brain tumour initiating cells. Nature *432*, 396-401.

Slade, M.J., and Coombes, R.C. (2007). The clinical significance of disseminated tumor cells in breast cancer. Nature clinical practice Oncology *4*, 30-41.

Smith, A.J., Stern, H.S., Penner, M., Hay, K., Mitri, A., Bapat, B.V., and Gallinger, S. (1994a). Somatic APC and K-ras codon 12 mutations in aberrant crypt foci from human colons. Cancer research *54*, 5527-5530.

Smith, G., Bounds, R., Wolf, H., Steele, R.J., Carey, F.A., and Wolf, C.R. (2010). Activating K-Ras mutations outwith 'hotspot' codons in sporadic colorectal tumours - implications for personalised cancer medicine. British journal of cancer *102*, 693-703.

Smith, K.J., Johnson, K.A., Bryan, T.M., Hill, D.E., Markowitz, S., Willson, J.K., Paraskeva, C., Petersen, G.M., Hamilton, S.R., Vogelstein, B.*, et al.* (1993). The APC gene product in normal and tumor cells. Proceedings of the National Academy of Sciences of the United States of America *90*, 2846-2850.

Smith, K.J., Levy, D.B., Maupin, P., Pollard, T.D., Vogelstein, B., and Kinzler, K.W. (1994b). Wild-type but not mutant APC associates with the microtubule cytoskeleton. Cancer research *54*, 3672-3675.

Smits, R., Hofland, N., Edelmann, W., Geugien, M., Jagmohan-Changur, S., Albuquerque, C., Breukel, C., Kucherlapati, R., Kielman, M.F., and Fodde, R. (2000). Somatic Apc mutations are selected upon their capacity to inactivate the beta-catenin downregulating activity. Genes, chromosomes & cancer *29*, 229-239.

Smits, R., Kielman, M.F., Breukel, C., Zurcher, C., Neufeld, K., Jagmohan-Changur, S., Hofland, N., van Dijk, J., White, R., Edelmann, W.*, et al.* (1999). Apc1638T: a mouse model delineating critical domains of the adenomatous polyposis coli protein involved in tumorigenesis and development. Genes & development *13*, 1309-1321.

Snippert, H.J., Haegebarth, A., Kasper, M., Jaks, V., van Es, J.H., Barker, N., van de Wetering, M., van den Born, M., Begthel, H., Vries, R.G.*, et al.* (2010). Lgr6 marks stem cells in the hair follicle that generate all cell lineages of the skin. Science *327*, 1385-1389.

Soong, R., Grieu, F., Robbins, P., Dix, B., Chen, D., Parsons, R., House, A., and Iacopetta, B. (1997). p53 alterations are associated with improved prognosis in distal colonic carcinomas. Clinical cancer research : an official journal of the American Association for Cancer Research *3*, 1405-1411.

Soong, R., Powell, B., Elsaleh, H., Gnanasampanthan, G., Smith, D.R., Goh, H.S., Joseph, D., and Iacopetta, B. (2000). Prognostic significance of TP53 gene mutation in 995 cases of colorectal carcinoma. Influence of tumour site, stage, adjuvant chemotherapy and type of mutation. European journal of cancer *36*, 2053-2060.

Soussi, T., and Beroud, C. (2001). Assessing TP53 status in human tumours to evaluate clinical outcome. Nature reviews Cancer *1*, 233-240.

Spano, J.P., Lagorce, C., Atlan, D., Milano, G., Domont, J., Benamouzig, R., Attar, A., Benichou, J., Martin, A., Morere, J.F.*, et al.* (2005). Impact of EGFR expression on colorectal cancer patient prognosis and survival. Annals of oncology : official journal of the European Society for Medical Oncology / ESMO *16*, 102-108.

Sparks, A.B., Morin, P.J., Vogelstein, B., and Kinzler, K.W. (1998). Mutational analysis of the APC/beta-catenin/Tcf pathway in colorectal cancer. Cancer research *58*, 1130-1134.

Steinmetz, M., and Hood, L. (1983). Genes of the major histocompatibility complex in mouse and man. Science *222*, 727-733.

Stoelcker, B., Hafner, M., Orosz, P., Nieswandt, B., and Mannel, D.N. (1995). Role of adhesion molecules and platelets in TNF-induced adhesion of tumor cells to endothelial cells: implications for experimental metastasis. J Inflamm *46*, 155-167.

Su, L.K., Burrell, M., Hill, D.E., Gyuris, J., Brent, R., Wiltshire, R., Trent, J., Vogelstein, B., and Kinzler, K.W. (1995). APC binds to the novel protein EB1. Cancer research *55*, 2972-2977.

Su, L.K., Vogelstein, B., and Kinzler, K.W. (1993). Association of the APC tumor suppressor protein with catenins. Science *262*, 1734-1737.

Sun, X.F., Carstensen, J.M., Zhang, H., Arbman, G., and Nordenskjold, B. (1996). Prognostic significance of p53 nuclear and cytoplasmic overexpression in right and left colorectal adenocarcinomas. European journal of cancer *32A*, 1963-1967.

Takagi, Y., Kohmura, H., Futamura, M., Kida, H., Tanemura, H., Shimokawa, K., and Saji, S. (1996). Somatic alterations of the DPC4 gene in human colorectal cancers in vivo. Gastroenterology *111*, 1369-1372.

Takeda, N., Jain, R., LeBoeuf, M.R., Wang, Q., Lu, M.M., and Epstein, J.A. (2011). Interconversion between intestinal stem cell populations in distinct niches. Science *334*, 1420-1424.

Taylor, D.P., Burt, R.W., Williams, M.S., Haug, P.J., and Cannon-Albright, L.A. (2010). Population-based family history-specific risks for colorectal cancer: a constellation approach. Gastroenterology *138*, 877-885.

Tetsu, O., and McCormick, F. (1999). Beta-catenin regulates expression of cyclin D1 in colon carcinoma cells. Nature *398*, 422-426.

Thibodeau, S.N., Bren, G., and Schaid, D. (1993). Microsatellite instability in cancer of the proximal colon. Science *260*, 816-819.

Tian, H., Biehs, B., Warming, S., Leong, K.G., Rangell, L., Klein, O.D., and de Sauvage, F.J. (2011). A reserve stem cell population in small intestine renders Lgr5-positive cells dispensable. Nature *478*, 255-259.

Todaro, M., Alea, M.P., Di Stefano, A.B., Cammareri, P., Vermeulen, L., Iovino, F., Tripodo, C., Russo, A., Gulotta, G., Medema, J.P.*, et al.* (2007). Colon cancer stem cells dictate tumor growth and resist cell death by production of interleukin-4. Cell Stem Cell *1*, 389-402.

Trumpp, A., and Wiestler, O.D. (2008). Mechanisms of Disease: cancer stem cells--targeting the evil twin. Nat Clin Pract Oncol *5*, 337-347.

Tseng, W., Leong, X., and Engleman, E. (2007). Orthotopic mouse model of colorectal cancer. J Vis Exp, 484.

Uberall, I., Kolar, Z., Trojanec, R., Berkovcova, J., and Hajduch, M. (2008). The status and role of ErbB receptors in human cancer. Exp Mol Pathol *84*, 79-89.

Uchida, N., Buck, D.W., He, D., Reitsma, M.J., Masek, M., Phan, T.V., Tsukamoto, A.S., Gage, F.H., and Weissman, I.L. (2000). Direct isolation of human central nervous system stem cells. Proc Natl Acad Sci U S A *97*, 14720-14725.

van Kempen, L.C., van den Oord, J.J., van Muijen, G.N., Weidle, U.H., Bloemers, H.P., and Swart, G.W. (2000). Activated leukocyte cell adhesion molecule/CD166, a marker of tumor progression in primary malignant melanoma of the skin. The American journal of pathology *156*, 769-774.

Vermeulen, L., De Sousa, E.M.F., van der Heijden, M., Cameron, K., de Jong, J.H., Borovski, T., Tuynman, J.B., Todaro, M., Merz, C., Rodermond, H.*, et al.* (2010). Wnt activity defines colon cancer stem cells and is regulated by the microenvironment. Nat Cell Biol *12*, 468-476.

Vermeulen, L., Sprick, M.R., Kemper, K., Stassi, G., and Medema, J.P. (2008a). Cancer stem cells--old concepts, new insights. Cell Death Differ *15*, 947-958.

Vermeulen, L., Todaro, M., de Sousa Mello, F., Sprick, M.R., Kemper, K., Perez Alea, M., Richel, D.J., Stassi, G., and Medema, J.P. (2008b). Single-cell cloning of colon cancer stem cells reveals a multi-lineage differentiation capacity. Proc Natl Acad Sci U S A *105*, 13427-13432.

Vessella, R.L., Pantel, K., and Mohla, S. (2007). Tumor cell dormancy: an NCI workshop report. Cancer Biol Ther *6*, 1496-1504.

Viatour, P., Somervaille, T.C., Venkatasubrahmanyam, S., Kogan, S., McLaughlin, M.E., Weissman, I.L., Butte, A.J., Passegue, E., and Sage, J. (2008). Hematopoietic stem cell quiescence is maintained by compound contributions of the retinoblastoma gene family. Cell Stem Cell *3*, 416-428.

Vigetti, D., Viola, M., Karousou, E., Rizzi, M., Moretto, P., Genasetti, A., Clerici, M., Hascall, V.C., De Luca, G., and Passi, A. (2008). Hyaluronan-CD44-ERK1/2 regulate human aortic smooth muscle cell motility during aging. The Journal of biological chemistry *283*, 4448-4458.

Visvader, J.E., and Lindeman, G.J. (2012). Cancer stem cells: current status and evolving complexities. Cell Stem Cell *10*, 717-728.

Vogelstein, B. (1990). Cancer. A deadly inheritance. Nature *348*, 681-682.

Vogelstein, B., Fearon, E.R., Hamilton, S.R., Kern, S.E., Preisinger, A.C., Leppert, M., Nakamura, Y., White, R., Smits, A.M., and Bos, J.L. (1988). Genetic alterations during colorectal-tumor development. The New England journal of medicine *319*, 525-532.

von Furstenberg, R.J., Gulati, A.S., Baxi, A., Doherty, J.M., Stappenbeck, T.S., Gracz, A.D., Magness, S.T., and Henning, S.J. (2011). Sorting mouse jejunal epithelial cells with CD24 yields a population with characteristics of intestinal stem cells. Am J Physiol Gastrointest Liver Physiol *300*, G409-417.

Vousden, K.H., and Prives, C. (2009). Blinded by the Light: The Growing Complexity of p53. Cell *137*, 413-431.

Walther, A., Houlston, R., and Tomlinson, I. (2008). Association between chromosomal instability and prognosis in colorectal cancer: a meta-analysis. Gut *57*, 941-950.

Wanebo, H.J., Semoglou, C., Attiyeh, F., and Stearns, M.J., Jr. (1978). Surgical management of patients with primary operable colorectal cancer and synchronous liver metastases. American journal of surgery *135*, 81-85.

Wang, J.C., and Dick, J.E. (2005). Cancer stem cells: lessons from leukemia. Trends Cell Biol *15*, 494-501.

Weichert, W., Knosel, T., Bellach, J., Dietel, M., and Kristiansen, G. (2004). ALCAM/CD166 is overexpressed in colorectal carcinoma and correlates with shortened patient survival. J Clin Pathol *57*, 1160-1164.

Weinberg, R.A. (2008). Mechanisms of malignant progression. Carcinogenesis *29*, 1092-1095.

Weisenberger, D.J., Siegmund, K.D., Campan, M., Young, J., Long, T.I., Faasse, M.A., Kang, G.H., Widschwendter, M., Weener, D., Buchanan, D.*, et al.* (2006). CpG island methylator phenotype underlies sporadic microsatellite instability and is tightly associated with BRAF mutation in colorectal cancer. Nature genetics *38*, 787-793.

Weiss, L. (1990). Metastatic inefficiency. Advances in cancer research *54*, 159-211.

Weiss, L., Grundmann, E., Torhorst, J., Hartveit, F., Moberg, I., Eder, M., Fenoglio-Preiser, C.M., Napier, J., Horne, C.H., Lopez, M.J.*, et al.* (1986). Haematogenous

metastatic patterns in colonic carcinoma: an analysis of 1541 necropsies. J Pathol *150*, 195-203.

Weiss, L., Nannmark, U., Johansson, B.R., and Bagge, U. (1992). Lethal deformation of cancer cells in the microcirculation: a potential rate regulator of hematogenous metastasis. International journal of cancer Journal international du cancer *50*, 103-107.

Weissman, I.L. (2000). Stem cells: units of development, units of regeneration, and units in evolution. Cell *100*, 157-168.

Welch, D.R. (2006). Do we need to redefine a cancer metastasis and staging definitions? Breast disease *26*, 3-12.

Welch, J.P., and Donaldson, G.A. (1979). The clinical correlation of an autopsy study of recurrent colorectal cancer. Annals of surgery *189*, 496-502.

Welm, B.E., Tepera, S.B., Venezia, T., Graubert, T.A., Rosen, J.M., and Goodell, M.A. (2002). Sca-1(pos) cells in the mouse mammary gland represent an enriched progenitor cell population. Dev Biol *245*, 42-56.

Wennerberg, K., Rossman, K.L., and Der, C.J. (2005). The Ras superfamily at a glance. Journal of cell science *118*, 843-846.

Wielenga, V.J., Smits, R., Korinek, V., Smit, L., Kielman, M., Fodde, R., Clevers, H., and Pals, S.T. (1999). Expression of CD44 in Apc and Tcf mutant mice implies regulation by the WNT pathway. The American journal of pathology *154*, 515-523.

Wilson, A., Laurenti, E., Oser, G., van der Wath, R.C., Blanco-Bose, W., Jaworski, M., Offner, S., Dunant, C.F., Eshkind, L., Bockamp, E.*, et al.* (2008). Hematopoietic stem cells reversibly switch from dormancy to self-renewal during homeostasis and repair. Cell *135*, 1118-1129.

Wilson, A., Laurenti, E., and Trumpp, A. (2009). Balancing dormant and self-renewing hematopoietic stem cells. Curr Opin Genet Dev *19*, 461-468.

Wimberger, P., Heubner, M., Otterbach, F., Fehm, T., Kimmig, R., and Kasimir-Bauer, S. (2007). Influence of platinum-based chemotherapy on disseminated tumor cells in blood and bone marrow of patients with ovarian cancer. Gynecol Oncol *107*, 331-338.

Wolf, D., Harris, N., and Rotter, V. (1984). Reconstitution of p53 expression in a nonproducer Ab-MuLV-transformed cell line by transfection of a functional p53 gene. Cell *38*, 119-126.

Wong, P., Verselis, S.J., Garber, J.E., Schneider, K., DiGianni, L., Stockwell, D.H., Li, F.P., and Syngal, S. (2006). Prevalence of early onset colorectal cancer in 397 patients with classic Li-Fraumeni syndrome. Gastroenterology *130*, 73-79.

Woynarowski, J.M., Chapman, W.G., Napier, C., Herzig, M.C., and Juniewicz, P. (1998). Sequence- and region-specificity of oxaliplatin adducts in naked and cellular DNA. Mol Pharmacol *54*, 770-777.

Wrana, J.L., Attisano, L., Wieser, R., Ventura, F., and Massague, J. (1994). Mechanism of activation of the TGF-beta receptor. Nature *370*, 341-347.

Yachida, S., Jones, S., Bozic, I., Antal, T., Leary, R., Fu, B., Kamiyama, M., Hruban, R.H., Eshleman, J.R., Nowak, M.A.*, et al.* (2010). Distant metastasis occurs late during the genetic evolution of pancreatic cancer. Nature *467*, 1114-1117.

Yan, K.S., Chia, L.A., Li, X., Ootani, A., Su, J., Lee, J.Y., Su, N., Luo, Y., Heilshorn, S.C., Amieva, M.R.*, et al.* (2012). The intestinal stem cell markers Bmi1 and Lgr5 identify two functionally distinct populations. Proceedings of the National Academy of Sciences of the United States of America *109*, 466-471.

Yin, A.H., Miraglia, S., Zanjani, E.D., Almeida-Porada, G., Ogawa, M., Leary, A.G., Olweus, J., Kearney, J., and Buck, D.W. (1997). AC133, a novel marker for human hematopoietic stem and progenitor cells. Blood *90*, 5002-5012.

Yoshihara, H., Arai, F., Hosokawa, K., Hagiwara, T., Takubo, K., Nakamura, Y., Gomei, Y., Iwasaki, H., Matsuoka, S., Miyamoto, K.*, et al.* (2007). Thrombopoietin/MPL signaling regulates hematopoietic stem cell quiescence and interaction with the osteoblastic niche. Cell Stem Cell *1*, 685-697.

Zawel, L., Dai, J.L., Buckhaults, P., Zhou, S., Kinzler, K.W., Vogelstein, B., and Kern, S.E. (1998). Human Smad3 and Smad4 are sequence-specific transcription activators. Molecular cell *1*, 611-617.

Zeisberger, S.M., Odermatt, B., Marty, C., Zehnder-Fjallman, A.H., Ballmer-Hofer, K., and Schwendener, R.A. (2006). Clodronate-liposome-mediated depletion of

tumour-associated macrophages: a new and highly effective antiangiogenic therapy approach. British journal of cancer *95*, 272-281.

Zhang, C., Li, C., He, F., Cai, Y., and Yang, H. (2011). Identification of CD44+CD24+ gastric cancer stem cells. J Cancer Res Clin Oncol *137*, 1679-1686.

Zhang, Y.E. (2009). Non-Smad pathways in TGF-beta signaling. Cell research *19*, 128-139.

The schematic mouse picture in figures 44, 48, 52, 56, 67 and 68 was adapted from: http://mousetales.wordpress.com/